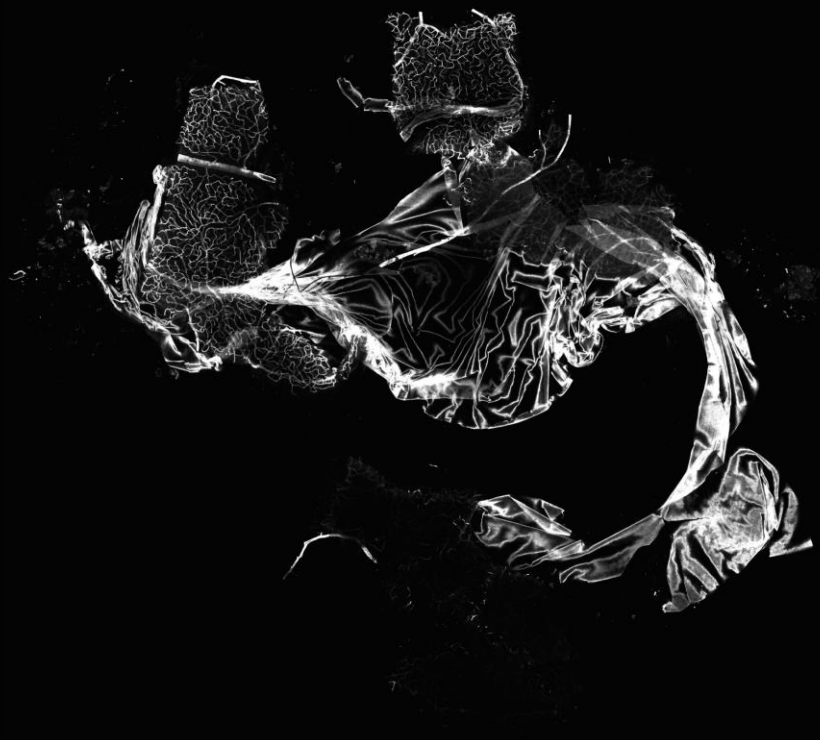

The prevention and pathogenesis of retinal detachment

Gregory Scott Fincham

Thesis submitted for the degree of MD(Res)

UCL

Declaration

'I, Gregory Scott Fincham, confirm that the work presented in this thesis is my own. Where information has been derived from other sources, I confirm that this has been indicated in the thesis.'

In memory of John D. Scott

4th June 1936 – 10th January 2013

Abstract

The prevention and pathogenesis of retinal detachment

Retinal detachment contributes to nearly 500 new blind registrations in the United Kingdom each year. In contrast to other retinal blinding disorders, blindness from retinal detachment is potentially avoidable with a better understanding of the mechanisms defining sub-groups at risk of the event.

The majority of retinal detachments are rhegmatogenous, resulting from retinal tears that occur during the process of posterior vitreous detachment. Posterior vitreous detachment is generally considered to be a common, age-related synchitic and syneretic degeneration of the vitreous gel. However, this current understanding fails to explain the significant number of elderly individuals who never undergo posterior vitreous detachment, or the number of young patients with co-existing intraocular pathology who do.

Furthermore, the factors distinguishing the majority of patients who undergo 'physiological' posterior vitreous detachment (with no associated retinal tears or detachment) from the minority of patients who suffer 'pathological' posterior vitreous detachment (associated with retinal tears and/or detachment), remain poorly understood.

The objectives of this research project were two-fold:

Firstly, to investigate the hypothesis that appropriate prophylactic intervention could reduce blindness from retinal detachment if a high-risk sub-group of individuals were defined. This clinical study retrospectively evaluated a group of molecularly confirmed type 1 Stickler syndrome patients, a homogenous cohort who have been identified to carry the greatest risk of inherited retinal detachment at the time of their posterior vitreous detachment. Multiple analyses comparing patients and eyes that received prophylactic intervention with appropriate controls, consistently demonstrated that the Cambridge Prophylactic Cryotherapy protocol is safe and markedly reduces the risk of retinal detachment in type 1 Stickler syndrome.

Secondly, to investigate the anatomical and cellular mechanisms of posterior vitreous detachment in the wider population. This laboratory study sought to isolate and immunohistochemically phenotype posterior hyaloid membranes and associated laminocytes from donor human globes that had undergone ‘physiological’ posterior vitreous detachment. The isolated posterior hyaloid membranes were demonsatrated to be distinct basement membranes composed of type IV collagen and laminin, and morphologically correlated with posterior hyaloid membranes observed clinically in patietns presenting with posterior vitrous detachment. Furthermore, the laminocyte cell population adherent to the vitreal aspect of the posterior hyaloid membrane, was identified to express macrophage cell markers.

Preface/acknowledgements

Although the content presented in the following 242 pages, which includes 342 images compiled in 78 figures, has been completed by myself for the submission of the research degree MD(Res), I am indebted to so many who have volunteered their knowledge, skill, expertise and time; without their support and guidance I would not have been able to report the current findings investigating the prevention and pathogenesis of retinal detachment.

The list of all those incredible people who have helped me so much over the last two and a half years is tabulated on the following page, but additional thanks and acknowledgement need to be paid to the following individuals who have given me so much of their valuable time:

Dr Carl Spickett, the post-doctoral scientist who was tasked with supervising me in the laboratory; I do not think Carl fully appreciated how onerous it was going to be to have to guide someone as novice as me into the world of research, but his resolve has been heroic. Carl has patiently taught and re-taught me how to pipette, dilute, reconstitute, order, extract, amplify, quantify, design, record, validate, analyse and interpret what I have done in the laboratory, in addition to teaching me countless word processing and graphic design skills. He has always been eager and available (at any hour of any day) to answer the tens of thousands of questions I must have asked.

In order to ensure the validity of the results of prophylactic cryotherapy in Stickler syndrome, a finding that has immediate clinical importance to all type 1 Stickler syndrome patients who are at such a high risk of retinal detachment and subsequent visual loss, it was decided that the statistical analysis would be completed independently by the Centre for Applied Medical Statistics, University of Cambridge. Laura Pasea was tasked with this enormously complicated part of the project that required repeated analysis on multiple subgroups to prove the efficacy of the treatment. Her dedication and enthusiasm have been incredible.

My new found talent of preparing human tissue for immunohistochemical interrogation is attributed entirely to Sean James from the Tissue Bank at University Hospital, Coventry. Sean has been invaluable in helping to obtain and register all

the human tissues used in the investigations into the posterior hyaloid membrane and its associated laminocytes, in addition to teaching me how to design, fix, process, freeze, cut, stain, plate, coverslip, mount, control and interpret histological experiments; Sean was always available to help enthusiastically with any request or questions despite his inordinate workload.

Dr Christopher Thrashivoulou from the Research Department of Cell and Developmental Biology, UCL and Dr Michael Hollingshead from the Department of Pathology, University of Cambridge for the hours they spent with me in front of their respective confocal microscopes searching for invisible cells on an invisible membrane in invisible gel; Chris and Mike, thank you for your invaluable and constant advice and teaching me how to drive a confocal microscope.

A special thanks needs to be paid to Professor Eamonn Maher and Dr Dick Sanford who kindly agreed to let me work alongside their teams in the Medical Genetics Laboratory; thank you for providing me with the bench space and facilities that was so crucial to this project.

To Specialist Sister Annie McNinch who has mothered me through my MD, providing cakes, sweets, countless lifts, and even sorting out my wedding planning duties (in addition to growing flowers for the event), Wiesia Johnson our amazing secretary who has gone above and beyond her job description and had to put up with sitting next to me for over two years (sorry for teaching you how to swear at your computer), and Dr Howard Martin, one of the cleverest men I know and my ‘adopted supervisor' (and a man with the most unbecoming sense of humour), thank you all for the most fun a man can have in a Stickler Office; the last two years have been fantastic. I can only apologise for eating more than my fair share of the cake.

My UCL supervisors, Professor Astrid Limb and Mr Hari Jayaram from the Institute of Ophthalmology, thank you for all of your help, advice and supervision. In addition to all of her knowledgeable insights and suggestions which have made this project so successful, I need to pay a special thank you to Astrid for all of her assistance in dealing with the administrational aspects of her student doing a higher degree in London, whilst working in Cambridge and Coventry; the fact that the whole process was so seamless is a testament to all of the hard work that she must have been doing behind the scenes.

My histopathology supervisor, Dr David Snead from the Department of Pathology, University Hospital Coventry, thank you for your advice and suggestions, and help with administrating the laminocyte project; you have been very kind about my complete lack of knowledge in your chosen field and for this I am greatly appreciative.

My laboratory supervisor, Dr Allan Richards from the Department of Pathology, University of Cambridge, thank you for all of your help and sensible advice; being the supervisor who was closest at hand, you have had to answer an unfair share of the inane and ridiculous questions (I think you were right to go with 'cashew' instead of 'testicular' in describing the nuclear phenotype of laminocytes).

My greatest thanks goes to Mr Martin Snead. I do not know where to begin, but as there is a fifty thousand word limit to this thesis, I will have to give the abridged version; thank you for giving me the opportunity to work for you and your incredible team. Apart from being an inspirational supervisor, a consultant surgeon within the National Health Service, a research group leader, an accomplished athlete, a dedicated charity fundraiser, a promising wedding chauffeur and the world authority on Stickler syndrome, you are one of the kindest, fairest, funniest and most generous people I have met. The Cambridge University Vitreoretinal Service and the Stickler National Diagnostic Service at Addenbrooke's Hospital Cambridge are amazing institutions that benefit so many, and both are testament to all the hard work you do. It has been an honour to have been entrusted with this opportunity and is an experience that I will always remember fondly. Thank you.

Finally, to my beautiful wife, thank you for putting up with me in spite of myself; your sacrifices and support have been immensely appreciated and I could have not done this without you.

Cambridge University Teaching Hospital Vitreoretinal Service
Mr Martin Snead
Dr Allan Richards
Dr Carl Spickett
Sister Annie McNinch
Wiesia Johnson
Linda Godden
Dr Laura Towns
Sue Fellows
Kim Royle

University Hospitals Coventry and Warwickshire NHS Trust
Dr David Snead
Sean James
Dr Andrew White
Adrian Frisk
Parmjit Dahaley

Centre for Applied Medical Statistics, University of Cambridge
Laura Pasea
Dr Christopher Palmer

Department of Pathology, University of Cambridge
Dr Michael Hollingshead
Alan Kirby
Sue Reason
Irene Piper
Dr Emily Clemente
Marta Almeida

Corneal Transplant Service Eye Bank, University of Bristol
Prof John Armitage
Paul Bowerman
Tony Woodward
Angela Chapman
Hanna Pod
Val Smith

Department of Medical Genetics, University of Cambridge
Professor Eamonn Maher
Linda Smith
Dr Cassie Ragnaught

Medical Genetics, Cambridge University Hospitals NHS Foundation Trust
Dr Howard Martin
Dr Kim Brugger
Ruth Littleboy
Fay Roger
Dr Richard Sanford

Department of Pure Mathematics and Mathematical Statistics, University of Cambridge
Professor Richard Samworth

Department of Oncology, Public Health and Primary Care, University of Cambridge
Professor Douglas Easton

Department of Epidemiology and Medical Statistics, Cancer Research UK & UCL
Professor Alan Hackshaw

Institute of Ophthalmology, UCL
Professor Astrid Limb
Mr Hari Jayaram

Research Department of Cell and Developmental Biology, UCL
Dr Christopher Thrashivoulou
Dr Daniel Ciantar
Jane Pendjiky

School of Health and Related Research, University of Sheffield
Dr Christopher Carroll

Clinical Governance, Cambridge University Hospitals NHS Foundation Trust
Roosmarij Eichenberger
Lizzie Hart
Melissa King
Mr Tony Vivian

Department of Ophthalmology, Cambridge University Hospitals NHS Foundation Trust
Ms Arabella Poulson
Dr Paul Meyer
Mr Douglas Newman
Mr Jon Ong
Theatre 10 Staff
Theatre 41 Staff

Department of Histology, Cambridge University Hospitals NHS Foundation Trust
Nicola Johnson

Oxford Eye Hospital Imaging Department, Oxford University Hospitals NHS Trust
Mr CK Patel

Programme Director, The Royal College of Ophthalmologists
Mr Andrew Waldock

Table of contents

Table of tables

Table of figures

Video appendix

Video Appendex 1.1 The Cambridge Prophylactic Cryotherapy protocol

Video Appendix 1.2 Matching protocol explanation

Video Appendix 1.3 The clinical appearance of the posterior hyaloid membrane

1 Introduction

1.1 Retinal detachment

The retina is a multi-layered, light-sensitive neural tissue lining the inner aspect of the posterior segment of the eye; rhegmatogenous retinal detachment refers to the disorder in which a break in the retina, commonly caused by the process of posterior vitreous detachment, permits fluid from the vitreous cavity to gain access to the potential subretinal space between the neural retina and the retinal pigment epithelium, and peels the retina off its underlying support tissue.

In contrast to other ophthalmic disorders, such as cataract, until the turn of the 20th century retinal detachment was considered an untreatable blinding disorder. However, Joules Gonin, a Professor of Ophthalmology from the University of Lausanne, Switzerland, had the insight that retinal breaks were the cause and not the consequence of retinal detachment, challenging the *Zeitgeist* of the time (Wolfensberger, 2003); from 1902 to 1921, Gonin championed the doctrine that successful surgical management of retinal detachment had to comprise of the closure of causative retinal breaks at all costs (Gonin, 1904, 1931, 1934).

For the first time it became possible to manage retinal detachments surgically. Gonin reported retinal reattachment rates of up to 40% using an ignipuncture technique (a thermocautery induced chorioretinal scar used to seal retinal breaks) (Gonin, 1923; Thilges and Gonin, 1970). Conceptual advances in the field of vitreoretinal surgery over the following century, such as intraocular air injection introduced by Bengt Rosengren (Rosengren, 1938), scleral buckling popularised by Ernst Custodis (Custodis, 1952, 1953, 1956) and closed vitrectomy techniques pioneered by Robert Machemer (Machemer et al., 1971), in addition to innumerable modifications of these surgical techniques, equipment and tamponades, have improved the rates of retinal reattachment surgery to approximately 90% (Chignell et al., 1973; Rachal and Burton, 1979; Tani et al., 1981; Sharma et al., 1994; Lincoff and Kreissig, 2000; Pastor et al., 2008).

However, permanent functional damage to visual acuity is a recognised consequence in many patients suffering retinal detachment, despite the greatly improved postoperative anatomical success rates (Burton, 1982; Diederen et al.,

2007; Hassan et al., 2002; Lewis et al., 2004; Machemer, 1968; Mervin et al., 1999; Mitry et al., 2013; Ozgür and Esgin, 2007; van de Put et al., 2014; Ross and Kozy, 1998).

Although unprecedented progress in vitreoretinal surgery has improved anatomical outcomes, in order to improve functional outcomes we need to develop a deeper understanding of the process of posterior vitreous detachment, the preceding event for the vast majority of rhegmatogenous retinal detachments. This could ultimately provide an insight into preventing this sight threatening event.

In order to fully understand the aetiology of retinal detachment we should consider the prophetic words Gonin wrote for the fourth volume of the French Encyclopaedia of Ophthalmology in 1906:

> *"…to effectively fight a pathological process, we must know its nature and anatomic conditions. Only the study of pathogenesis of spontaneous detachment, based on facts and not on hypotheses, will make it possible to find the treatment of this disease".* (Gonin, 1906)

1.2 Objectives

The objectives of this research project were two-fold:

Firstly, to undertake a retrospective clinical study in a group of type 1 Stickler syndrome patients, to investigate if an appropriately designed prophylactic intervention could reduce visual loss from retinal detachment in these individuals. Type 1 Stickler syndrome patients constitute a homogeneous cohort who have been identified to carry the greatest risk of inherited retinal detachment associated with posterior vitreous detachment.

Secondly, to investigate the anatomical and cellular mechanisms of posterior vitreous detachment in a wider population. This laboratory study sought to isolate and immunohistochemically phenotype posterior hyaloid membranes and associated laminocytes from donor human globes that had undergone ‘physiological’ posterior vitreous detachment.

2 Prevention: Retinal detachment prophylaxis in type 1 Stickler syndrome

2.1 Background

2.1.1 Non-syndromic retinal detachment prophylaxis

The hypothesis that prophylactic retinopexy could prevent retinal detachment is an attractive concept for vitreoretinal practitioners and patients at risk of retinal detachment. To date however, no prospective randomised trial has been conducted into the prevention of retinal detachment (Ang et al., 2012; Wilkinson, 2012).

Best current clinical practice guidelines regarding retinal detachment prophylaxis are founded on amalgamated historical cohort and case-control series (American Academy of Ophthalmology Retina Panel, 2008). These non-randomised studies are often incomplete and difficult to compare, with assumptions often based on comparisons between heterogeneous patient groups with variable follow-up (Folk et al., 1989). Furthermore, known risk factors for retinal detachment, such as refractive error, type of retinal break, vitreous status, fellow eye retinal status, previous ocular surgery, lens status, family history of retinal detachment, extent of lattice degeneration and presenting symptoms are often lacking (Chauhan et al., 2006). Currently, no prospective or retrospective trial scrutinising prophylactic intervention has stratified study patients for the presence or absence of posterior vitreous detachment, despite good prospective evidence demonstrating posterior vitreous detachment increases the risk of retinal detachment tenfold in certain groups (Hovland, 1978).

Symptomatic retinal breaks refer to the classic horseshoe retinal tears, typically found on fundal examination after patients present with new onset floaters and temporal photopsia at the time of posterior vitreous detachment; symptomatic retinal breaks are recognised as a significant precursor to retinal detachment. Prompt retinopexy, to create a chorioretinal adhesion around these breaks, reduces the risk of retinal detachment to less than 5% (Pollak and Oliver, 1981; Robertson and Norton, 1973; Smiddy et al., 1991), whereas at least half of untreated breaks will progress to retinal detachment (spontaneous reattachment is exceedingly uncommon) (Colyear and Pishel, 1960; Davis, 1974; Shea et al., 1974). Treating

symptomatic breaks before a significant retinal detachment has occurred usually prevents progression, preserves vision, and is generally associated with few or no complications. It is accepted that there is sufficient published evidence and clinical experience to support an evidence-based recommendation to treat symptomatic retinal breaks (American Academy of Ophthalmology Retina Panel, 2008).

However, asymptomatic retinal breaks, classified as operculated holes and atrophic round holes, very rarely progress to retinal detachment (Byer, 1998; Davis, 1974). Similarly, atrophic round holes associated with lattice degeneration only occasionally progress to retinal detachment; lattice-associated retinal detachment usually occurs when a horseshoe tear develops at the time of posterior vitreous detachment (Byer, 1989). In addition, prophylactic treatment is recognised to prevent retinal tear formation within treated areas, but does not preclude, nor predict, tears occurring elsewhere in the retina (Chauhan et al., 2006). Evidence informing current clinical practice does not support treating asymptomatic retinal breaks or lattice degeneration (American Academy of Ophthalmology Retina Panel, 2008; Wilkinson, 2012).

Although the cited evidence which supports current clinical recommendations are not randomised controlled trials, they are the best and only available evidence and are considered to be sufficiently rigorous (American Academy of Ophthalmology Retina Panel, 2008).

Review of the literature reiterates the clinical sentiment that no prophylactic intervention is suitable for all patients. Appropriate retinal detachment prophylaxis is difficult to achieve because of the heterogenous nature of non-syndromic rhegmatogenous retinal detachment group populations, in addition to the observation that aetiological breaks may occur in almost any fundal location (prohibiting precise preventative retinopexy application). In order to design a successful retinal detachment prophylaxis strategy, one would require a defined homogenous sub-group of individuals at high-risk of retinal detachment, who were predisposed to retinal breaks at a predictable fundal location.

2.1.2 Retinal detachment prophylaxis in Stickler syndrome

The original Stickler family

In June 1965, Gunnar Stickler, a paediatrician working at the Mayo Clinic in Rochester, Minnesota, USA, published the first description of hereditary progressive arthro-ophthalmopathy (Stickler et al., 1965). Eleven affected family members were traced through a five-generation family pedigree, after an initial examination of a visually impaired 12-year-old male proband with marked joint bony prominences, who attended the clinic with his blind mother in 1960.

Reported ocular features of the family pedigree included congenital high myopia and total rhegmatogenous retinal detachment arising from “very large retinal disinsertions”. Retinal detachments tended to be bilateral and occurred in the first decade of life. Reported systemic features included premature degenerative arthropathy characterised by joint hypermobility and pain; there was destruction of articular cartilage surfaces, with wide joint spaces and broadening of metatarsal and metacarpal heads. The syndrome exhibited an autosomal dominant inheritance pattern.

Two years later, a follow-up paper reported associated degenerative arthropathy of the thoracolumbar spine and sensorineural hearing loss in the proband and his mother (Stickler and Pugh, 1967). Although not mentioned in the original reports, published photographs demonstrated a patient with a facial profile that suggested a flattened malar region and a short nose with a depressed nasal bridge and anteverted nares (Snead, 1996) (Figure 2-1).

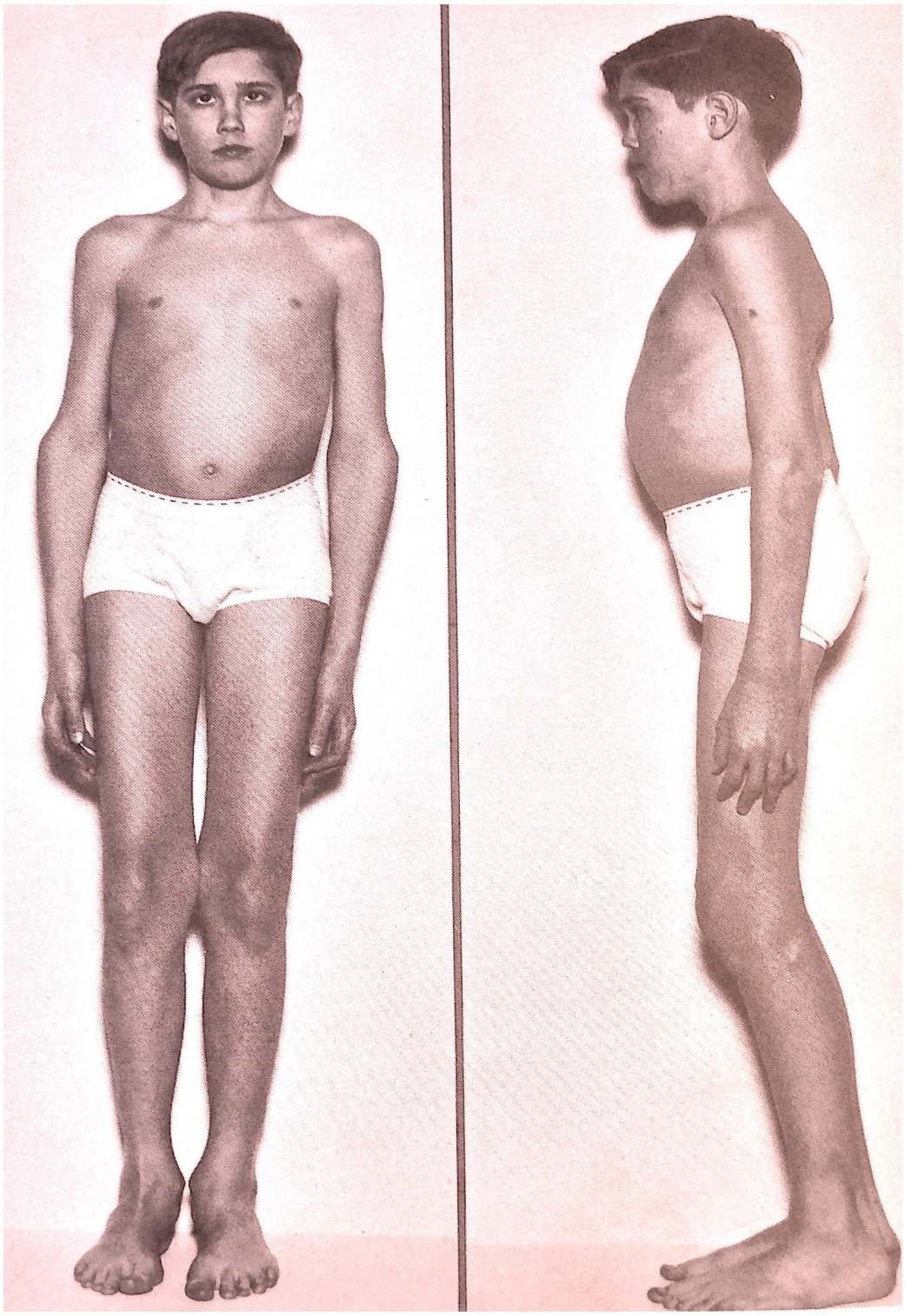

Figure 2-1 The original Stickler syndrome proband

Photograph demonstrating the bony joint prominences and kyphoscoliosis in the original Stickler proband. Note classic facial features of Stickler syndrome not described in original reports.

Reproduced with permission from Elsevier publishers (Stickler and Pugh, 1967).

Genetic classification of the Stickler syndromes

Originally considered a single gene disorder, at least eight sub-groups of Stickler syndrome are now recognised according to genetic abnormalities of type II, IX and XI collagen (Figure 2-1), suggesting the condition may be more precisely referred to as the Stickler syndromes (Snead et al., 2011). As the collagen structural proteins are principally and collectively expressed in the eye and in articular and hyaline cartilage, affected patients unsurprisingly present with premature arthropathy and classic orofacial, auditory and ocular features (Poulson et al., 2004; Snead and Yates, 1999; Stickler and Pugh, 1967; Stickler et al., 1965).

The Stickler syndromes are one of the most frequently inherited connective tissue disorders (Herrmann et al., 1975), and are recognised as the most common cause of inherited and childhood retinal detachment (Carroll et al., 2011; Snead and Yates, 1999). Although there are no available prevalence studies for the Stickler syndromes, an approximate incidence of 1:7500 live births has been estimated based on the known incidence of the disorder among neonates born with Pierre Robin sequence (Printzlau and Andersen, 2004). This equates to approximately eight and a half thousand affected individuals in the United Kingdom and nearly one million affected individuals worldwide.

Table 2-1 Molecular classification of Stickler syndrome

Type	Gene (Locus)	Inheritance	Ocular features	Systemic features	MIM No.	Ref.
Type 1	COL2A1 (12q13.11)	Autosomal dominant	• Congenital membranous type 1 vitreous anomaly • Congenital megalophthalmos • Congenital myopia • Retinal detachment • Paravascular lattice degeneration • Cataracts	• Arthropathy • Hearing loss • Midline clefting • Facial dysmorphia	#108300	1-3
Ocular only	COL2A1 (12q13.11)	Autosomal dominant	• Congenital membranous type 1 vitreous anomaly (majority) • Congenital megalophthalmos • Congenital myopia • Retinal detachment • Paravascular lattice degeneration • Cataracts	• No systemic features	#609508	4-8
Type 2	COL11A1 (1p21.1)	Autosomal dominant	• Congenital beaded type 2 vitreous anomaly • Congenital megalophthalmos • Congenital myopia • Retinal detachment • Paravascular lattice degeneration • Cataracts	• Arthropathy • Midline clefting • Hearing loss • Facial dysmorphia	#604841	9-13
Type 2	COL11A1 (1p21.1)	Autosomal recessive	• Congenital hypoplastic/ beaded type 2 vitreous anomaly • Congenital megalophthalmos • Congenital myopia (majority)	• Congenital profound sensorineural deafness • Midline clefting	Awaiting	14
Type 3	COL11A2 (6p21.32)	Autosomal dominant	• Normal vitreous phenotype • Normal ocular phenotype	• Arthropathy • Midline clefting • Hearing loss • Facial dysmorphia	#184840	15-18
Type 4	COL9A1 (6q13)	Autosomal recessive	• Syneretic empty vitreous • Myopia • Vitreoretinal degeneration	• Epiphyseal dysplasia • Sensorineural hearing loss	#614134	19
Type 5	COL9A2 (1p34.2)	Autosomal recessive	• Anomalous vitreous • Myopia • Vitreoretinal degeneration • Retinal detachment	• Sensorineural hearing loss • Short stature • Facial dysmorphia	#614284	20
Other	Unknown	Autosomal dominant	• Hypoplastic vitreous • Retinal detachment	• Arthropathy • Midline clefting • Hearing loss		21-22

1-3 (Ahmad et al., 1991; Snead and Yates, 1999; Williams et al., 1996)

4-8 (Go et al., 2003; Körkkö et al., 1993; McAlinden et al., 2008; Richards et al., 2005, 2006)

9-13 (Annunen et al., 1999; Majava et al., 2007; Martin et al., 1999; Poulson et al., 2004; Richards et al., 1996)

14 (Richards et al., 2013)

15-18 (Brunner et al., 1994; Sirko-Osadsa et al., 1998; Vikkula et al., 1995; Vuoristo et al., 2004)

19 (Van Camp et al., 2006)

20 (Baker et al., 2011)

21-22 (Martin et al., 1999; Wilkin et al., 1998)

Clinical features of type 1 Stickler syndrome

Over 80% of affected individuals have type 1 Stickler syndrome (OMIM#108300), a type II collagenopathy typically characterised by an autosomal dominant mutation in the COL2A1 gene (Ahmad et al., 1991); the majority are premature termination codon or frameshift mutations and result in haploinsufficiency of type II procollagen.

On slit lamp biomicroscopic examination type 1 Stickler syndrome patients have a pathognomic vitreous phenotype with the appearance of a vestigial retrolenticular congenital membranous anomaly (Figure 2-2) (Snead et al., 1994a, 1996).

Additional ocular features include megalophthalmos and high myopia that is typically congenital and non-progressive, congenital quadrantic lamellar cataract and early onset nuclear sclerosis (Scott, 1989; Seery et al., 1990), radial paravascular pigmented lattice degeneration (Parma et al., 2002; Vu et al., 2003) and a high risk of retinal detachment, the majority of which are bilateral, most frequently arising from giant retinal tears at the pars plana (Snead and Yates, 1999) (Figure 2-3). Developmental anterior chamber drainage angle abnormalities may predispose patients to glaucoma (Nielsen, 1981), but are relatively uncommon in patients who have not undergone previous intraocular surgery.

The systemic features of type 1 Stickler syndrome include a characteristic orofacial phenotype (Temple, 1989), midline palatal clefting (Hoornaert et al., 2010; Snead and Yates, 1999) and spondyloepiphyseal dysplasia (Liberfarb and Hirose, 1982; Rai et al., 1994; Rose et al., 2001) (Figure 2-4, Figure 2-5 and Figure 2-6 respectively). In addition, conductive and/or sensorineural hearing loss is a recognised systemic feature (Cho et al., 1991; Snead and Yates, 1999; Temple, 1989); conductive hearing loss being associated with eustation tube dysfunction related to midline clefting and sensorineural hearing loss related to the observation of that type II collagen is expressed within the cochlea (Slepecky et al., 1992; Thalmann, 1993).

Communication difficulties due to speech and language impairment resulting from palatal abnormalities, hearing impairment and blindness resulting from retinal detachment, coupled with mobility difficulties from premature arthropathy, can result in severe reduction in the quality of life in patients with Stickler syndrome.

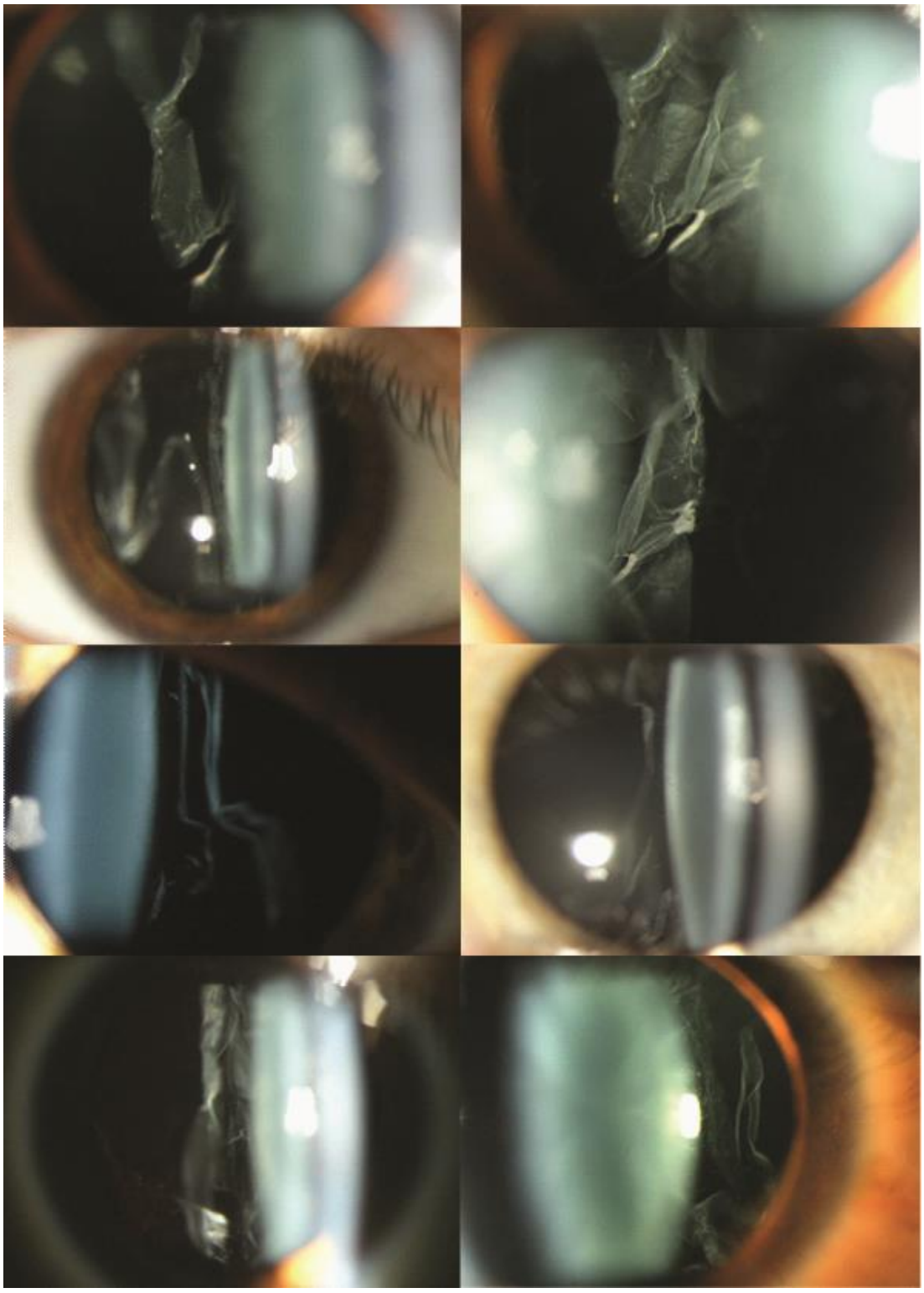

Figure 2-2 The type 1 membranous anomaly

Anterior segment colour photographs illustrating the pathognomonic retrolenticular congenital type 1 anomaly that appears clinically as a folded membrane over the posterior aspect of a vestigial secondary vitreous on slit-lamp biomicroscopy.

Photographs courtesy of Mr Martin Snead.

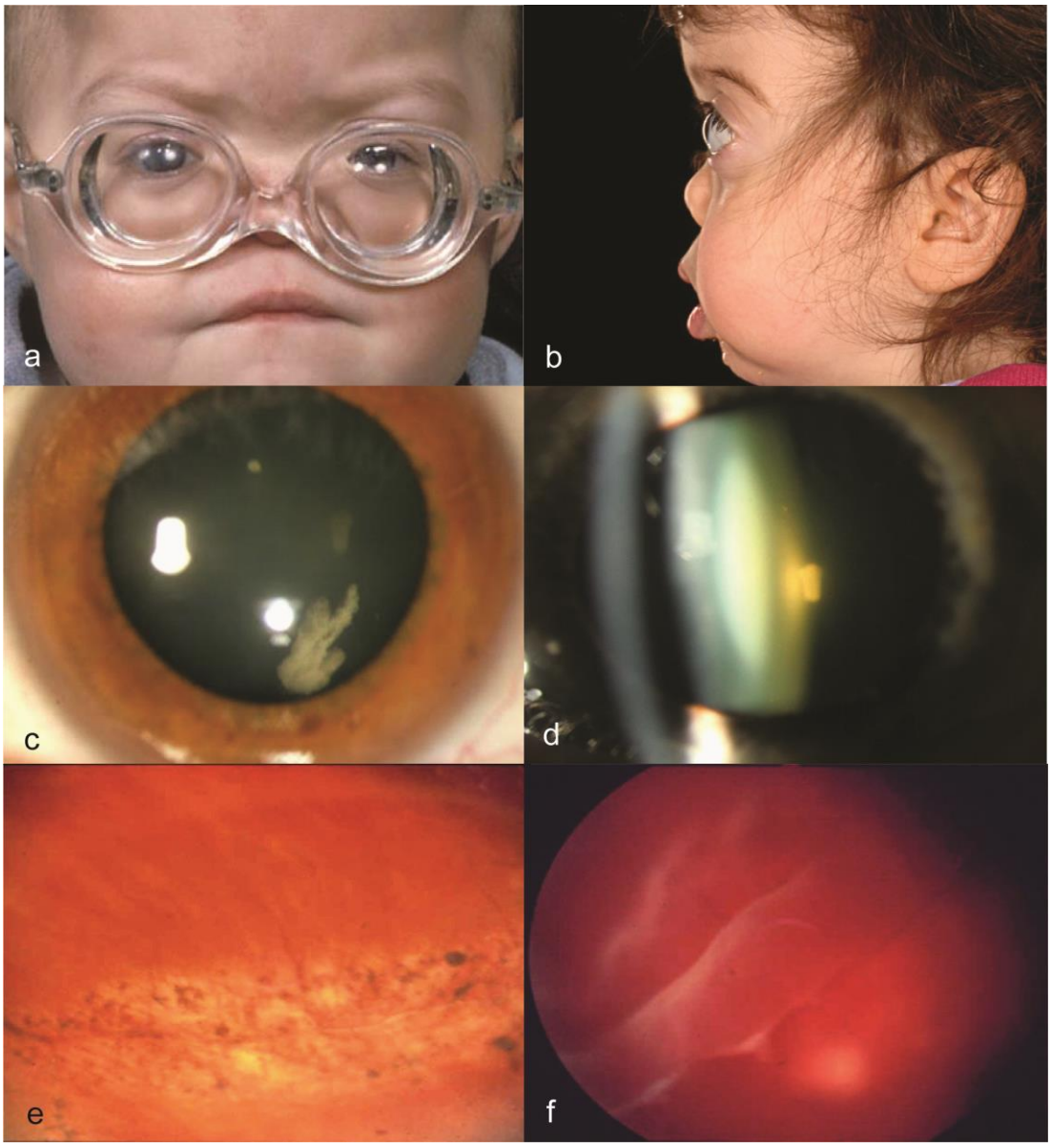

Figure 2-3 The ocular features of Stickler syndrome

Colour photographs demonstrating (a) congenital, non-progressive high myopia, (b) megalophalmos, (c) quadrantic lamellar and (d) nuclear sclerotic cataracts, (e) radial paravascular lattice degeneration, (f) oral giant retinal tear.

Photographs courtesy of Mr Martin Snead.

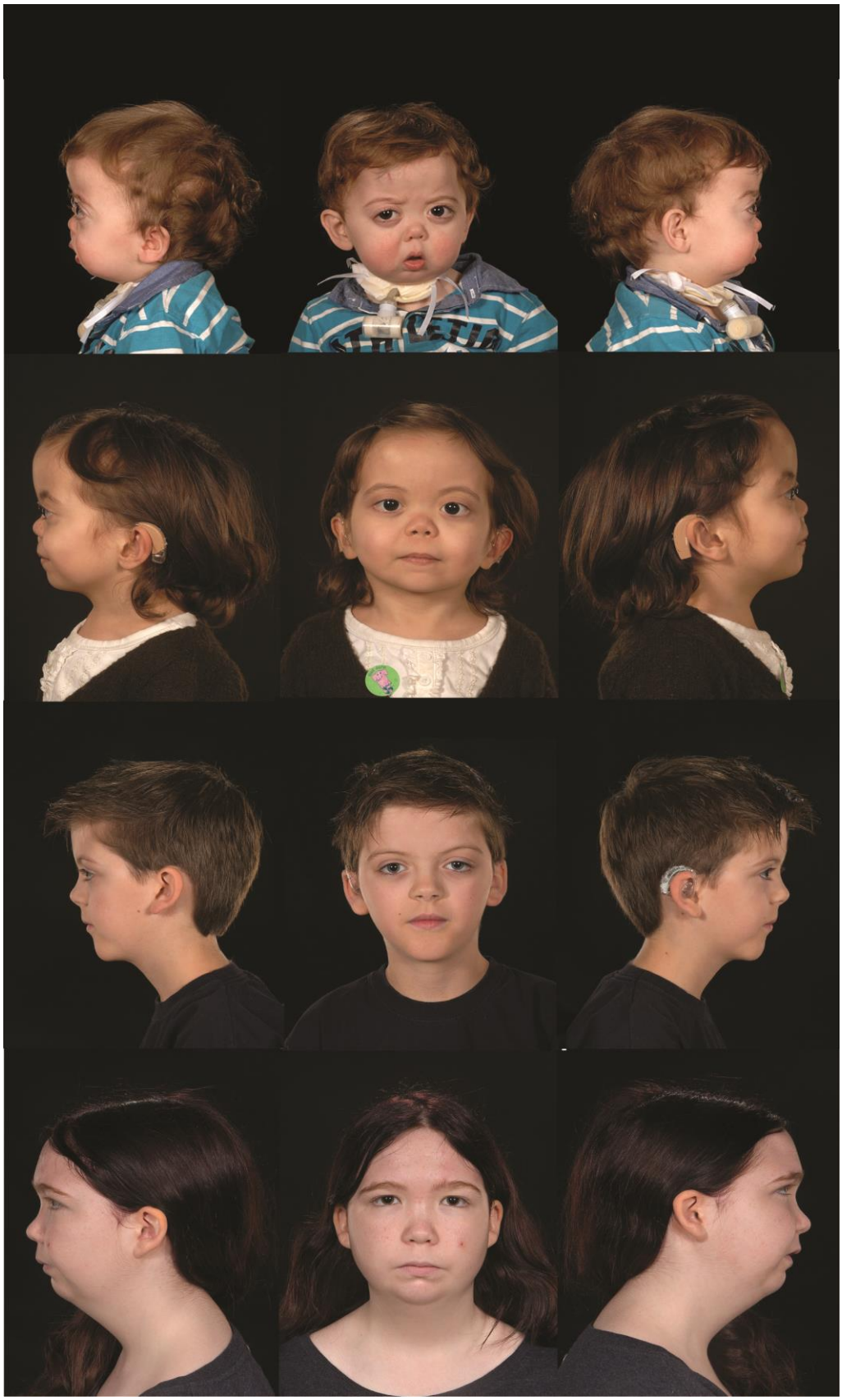

Figure 2-4 The Stickler syndrome facial phenotype

Please turn over for figure legend

Figure 2-4 The Stickler syndrome facial phenotype

Colour photographs demonstrating the facial features associated with Stickler syndrome, these include micrognathia long philtrum, anteverte nares, depressed nasal bridge, low set ears, flattened malar regions and megalophthalmos. Note clinical observations suggest the facial phenotype in Stickler syndrome becomes less pronounced with age. A possible explaination of this observation may be that the majority of type II collagen mutations result in haploinsufficiency; this relative shortage in structural collagen may be most apparent during the rapid facial development that occurs during embryological development, resulting in a more pronounced facial phenotype in youth that gradually reduce as patients age.

Photographs courtesy of Mr Martin Snead.

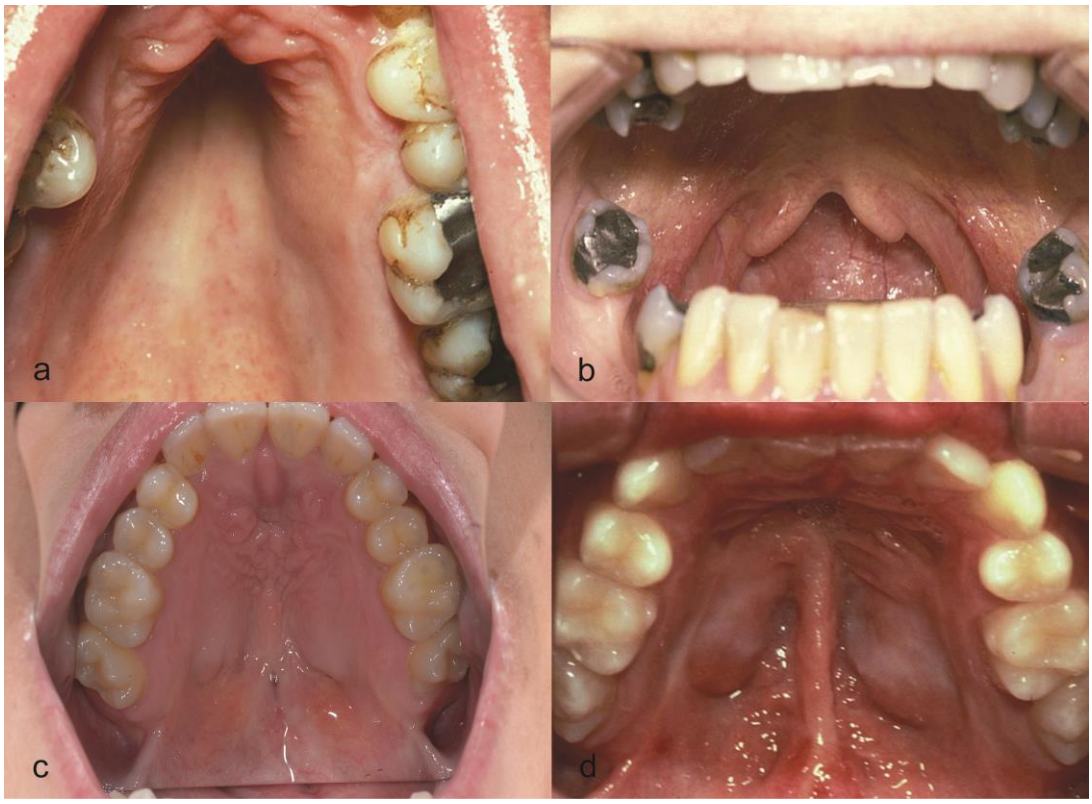

Figure 2-5 The spectrum of midline clefting in Stickler syndrome

Colour photographs demonstrating (a) high-arched palate, (b) bifid uvula, (c) submucosal cleft of the soft and hard palate, (d) palatal cleft.

Photographs courtesy of Mr Martin Snead.

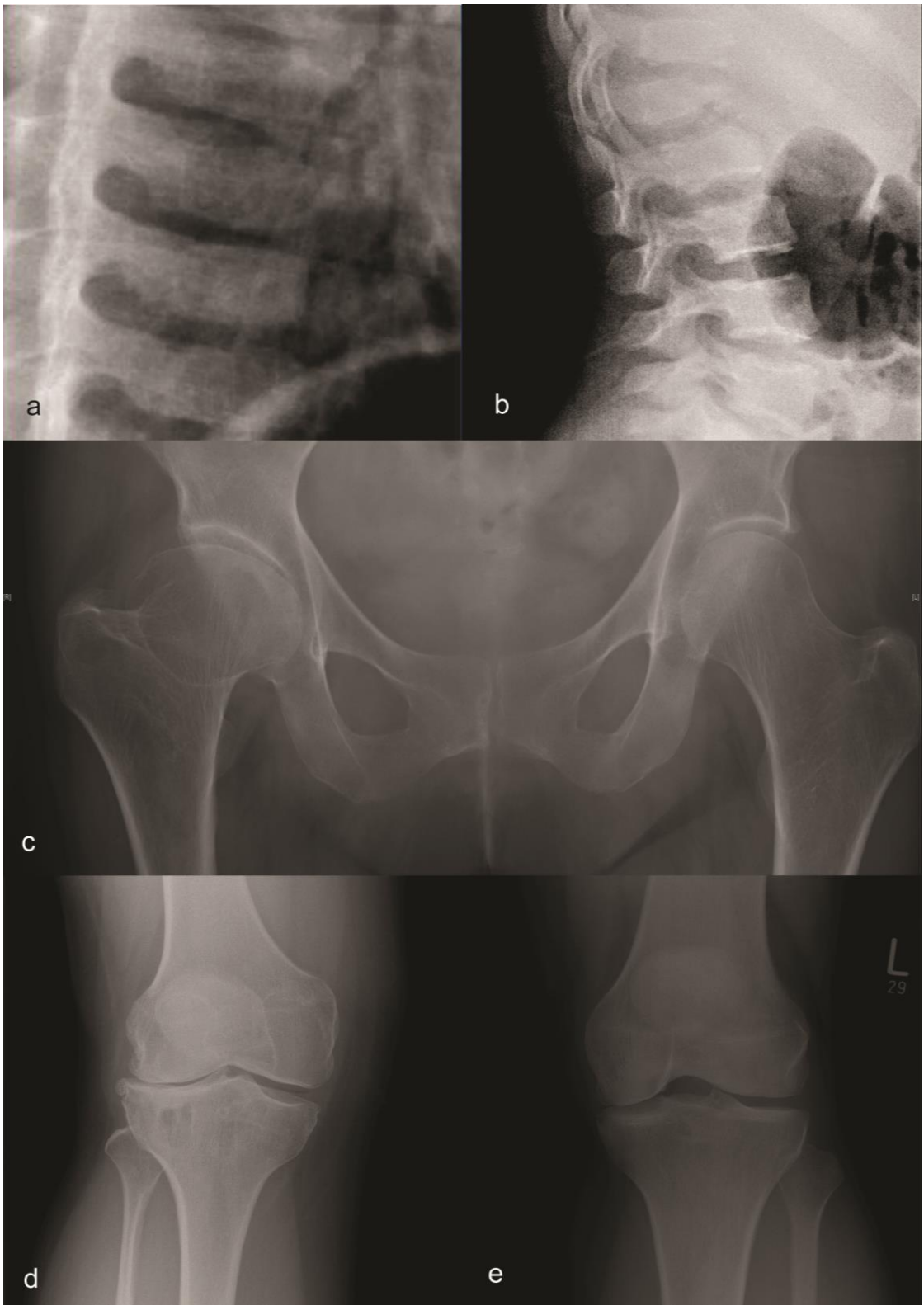

Figure 2-6 Radiological features of Stickler syndrome arthropathy

Please turn over for figure legend

Figure 2-6 Radiological features of Stickler syndrome arthropathy

X-ray radiographs demonstrating (a) axial skeleton vertebral body flattening (platyspondyly), (b) L1 anterior vertebral body beaking in a three year old girl, (c) right widened and flattened femoral head deformity (initially incorrectly diagnosed as Perthes disease in this case) and left sclerotic hip joint with narrowed joint space, (d) right knee premature osteoarthropathy with lateral subchondral cystic degeneration and osteophyte formation, (e) left knee medial joint space narrowing.

Radiographs courtesy of Mr Martin Snead.

Current prophylactic practice in Stickler syndrome

Existing service provision, with regards to retinal detachment prophylaxis in Stickler syndrome populations, consists of either no treatment (with or without monitoring), laser retinopexy prophylaxis or retinal cryotherapy prophylaxis (Carroll et al., 2011); retinal laser and cryotherapy prophylaxis has been reported to be applied focally or circumferentially to the retina (at various positions anterior to the retinal equator), or specifically to areas of paravascular lattice (Haut et al., 1987; Leiba et al., 1996; Monin et al., 1994). There is widespread uncertainty regarding best practice and no agreed guidelines in the United Kingdom or elsewhere. The absence of robust and accepted evidence has divided opinion in vitreoretinal communities, and this disparity has created confusion and anxiety amongst patients, who often receive conflicting advice.

In the United Kingdom, the lack of consensus prompted the Secretary of State for Health to commission the National Institute for Health Research to generate a Health Technology Assessment report into the clinical effectiveness and safety of prophylactic retinal interventions in reducing the risk of retinal detachment and subsequent visual loss in adults and children with Stickler syndrome. Under the terms of a commissioning contract, the School of Health and Related Research at the University of Sheffield published the findings of a systematic review in April 2011 (Carroll et al., 2011). Of the 1444 unique citations identified by the literature search, two retrospective cohort studies with control groups satisfied the inclusion criteria as principal studies.

The review established that both studies found a statistically significant reduction in the risk of retinal detachment after prophylaxis, however, the reported data did not permit a reliable estimate of the effect of cryotherapy or laser therapy compared to no prophylaxis. Due to the potential risk of bias in both studies, it was concluded that the efficacy of retinal prophylaxis remained uncertain in type 1 Stickler syndrome, and no recommendation regarding intervention could be supported.

In the first principal study by Ang and colleagues (Ang et al., 2008), the efficacy of 360° prophylactic cryotherapy to the post-oral retina was evaluated in a cohort of 204 patients with type 1 Stickler syndrome. The rate of retinal detachment in 111 control patients (who had received no prophylaxis) was compared to the rate of prophylaxis failure (defined as the development of retinal detachment or retinal tears

requiring further retinopexy) in 62 patients who underwent bilateral prophylactic cryotherapy and 31 patients who underwent unilateral prophylactic cryotherapy (after suffering a previous retinal detachment in their fellow eye). The results indicated a statistically significant benefit to 360° prophylactic cryotherapy, with the rate of unilateral retinal detachment in the control group being 73% (81/111) compared to 8% (5/62) in the bilateral and 10% (3/31) in the unilateral prophylactic cryotherapy groups. The rate of bilateral retinal detachment in the control group was 48% (53/111) compared to no cases of bilateral prophylactic failure in the bilateral prophylactic cryotherapy group.

However, the principal source of bias affecting the validity of these findings was deemed to be a discrepancy in the ages of the compared groups; the mean age of the control group was 49 years compared to a mean age of 21 years in the bilateral and 36 years in the unilateral prophylactic cryotherapy groups. As the risk of retinal detachment is known to be life-long in Stickler syndrome, the older controls were considered more likely to have experienced the primary outcome of retinal detachment. This lack of comparability between the groups introduced bias weighted in favour of prophylactic intervention (Aylward et al., 2008; Carroll et al., 2011).

In the second principal study by Leiba and colleagues (Leiba et al., 1996), the efficacy of focal and 360° prophylactic laser retinopexy was evaluated in a single family pedigree consisting of 22 members with type 1 Stickler syndrome. The incidence of retinal detachment was 44% (15/34) in the untreated eyes compared to 10% (1/10) in those eyes that underwent laser retinal prophylaxis (four eyes received 360° circumferential laser retinopexy at the borders of extensive lattice degeneration, and six eyes received focal laser retinopexy).

Although the results were reported as statistically significant, the study suffered from the same major potential confounding factor of discrepancy between control and treatment groups; mean age differences were not reported and the series was considered to be too small to generate a reliable estimate of efficacy (Carroll et al., 2011).

As evidence-based medicine becomes increasingly important to ensure contemporary practice delivers and maintains quality and consistency in the context of funding constraints, prophylactic therapies require robust scrutiny before being

accepted into clinical practice. However, the corollary to this approach has the potential to produce a contradictory situation, where the best available evidence may indicate a seemingly obvious benefit, but however likely, is ignored in favour of waiting for concrete evidence.

2.2 Hypothesis

In order to evaluate the efficacy and safety of retinal prophylaxis in preventing retinal detachment, it is essential to identify a homogenous cohort of patients who are predisposed to a defined retinal detachment aetiology (recognising who is at risk and what it is they are at risk of). In addition, accurate assessment of intervention requires eliminating variables that may confound the results.

Patients with type 1 Stickler syndrome are at an increased risk of retinal detachment, typically arising after a pathological anterior extension of a posterior vitreous detachment with subsequent circumferential oral giant retinal tear formation.

Knowing this predisposition to anterior oral giant retinal tears, it is conceivable that applying primary 360° prophylactic cryotherapy to the junction of the post-oral retina with the pars plana in patients with type 1 Stickler syndrome would result in a chorioretinal adhesion between the anterior neurosensory retina and the retinal pigment epithelium before the development of a retinal break at that position, and thereby reduce the likelihood of retinal tears forming and progressing to retinal detachment.

Furthermore, a second outcome measure assessing the long-term side effect profile of primary 360° prophylactic cryotherapy would be essential to determine if the benefit of prophylactic intervention outweighed any associated adverse side effects.

2.3 Material and methods

2.3.1 Ethical approval

Following local Research Governance Coordinator and Cambridge Research and Ethics Committee review, it was decided the project would be registered as a Service Evaluation under the Cambridge University Hospitals NHS Foundation Trust's Audit Department.

2.3.2 Patients and study design

To assess the efficacy and safety of primary 360° prophylactic cryotherapy in preventing retinal detachment in Stickler syndrome, a retrospective observational analysis was conducted. Type 1 Stickler syndrome patients (OMIM#108300) were selected as they are the most common subgroup of the disorder and have the highest risk of retinal detachment, typically arising from oral giant retinal tears (Snead and Yates, 1999). Study patients were identified from the Vitreoretinal Research Unit electronic database at Addenbrooke's Hospital (nationally commissioned Multidisciplinary Stickler Diagnostic Service). Retrospective data from clinical records and research pedigree files were collected and anonymised before analysis.

The clinical diagnosis of type 1 Stickler syndrome was made according to published criteria (Snead and Yates, 1999); this required the presence of the congenital vitreous membranous anomaly, pathognomonic of type 1 Stickler syndrome, in addition to any three of the following clinical features:

1. Myopia, with onset before six years of age.
2. Rhegmatogenous retinal detachment and/or paravascular pigmented lattice degeneration.
3. Joint hypermobility with an abnormal Beighton score, with or without radiological evidence of joint degeneration.
4. Audiometric confirmation of a sensorineural hearing defect.
5. Midline clefting (including high-arched palate, bifid uvula, submucosal cleft or cleft palate).

Mutational analysis was performed in the majority of cases and in every case where vitreous phenotyping was not possible due to previous bilateral vitrectomy surgery.

2.3.3 Exclusion criteria

All eyes that received any form of non-standard prophylaxis were excluded; this included any previous focal laser or cryotherapy to identified retinal breaks or areas of lattice degeneration, previous 360° prophylactic laser retinopexy, previous prophylactic scleral buckling, and previous 360° prophylactic cryotherapy applied equatorially or posteriorly to the oral retina (undertaken in other eye units). In addition, all eyes without the required study details available in the clinical notes and research pedigree files were excluded from analysis.

2.3.4 Primary outcome measures

1. Time to retinal detachment (this included any post prophylactic cryotherapy case requiring further retinopexy, even those without formal retinal detachment repair in the treatment group).

2. Side effects resulting from prophylactic treatment.

2.3.5 The Cambridge Prophylactic Cryotherapy Protocol

The Cambridge Prophylactic Cryotherapy Protocol is performed under general anaesthesia following informed patient consent. The consent process reiterates that the rationale of the procedure is to reduce the risk of retinal detachment arising from giant retinal tears, but is not intended or expected to prevent rhegmatogenous retinal detachments occurring from more posteriorly located horseshoe tears.

The protocol begins with bilateral indirect indentation ophthalmoscopic examination under anaesthetic. Previously unidentified retinal breaks or detachments are treated accordingly, either by inclusion into the planned 360° cryotherapy treatment or by formal retinal detachment repair, depending on their location and extent.

Under direct visualisation, carefully monitored 360° transconjunctival prophylactic cryotherapy is applied in a contiguous ribbon at the junction of the post-oral retina with the pars plana; the cryotherapy applications are deployed so they touch shoulder to shoulder, ensuring no gaps are left in the prophylactic treatment, whilst at the same time avoiding any areas of retreatment. The final application connects the penultimate cryotherapy application with the first to ensure a continuous barrier at the far anterior limit of the retina (Figure 2-7 Video Appendix 1.1).

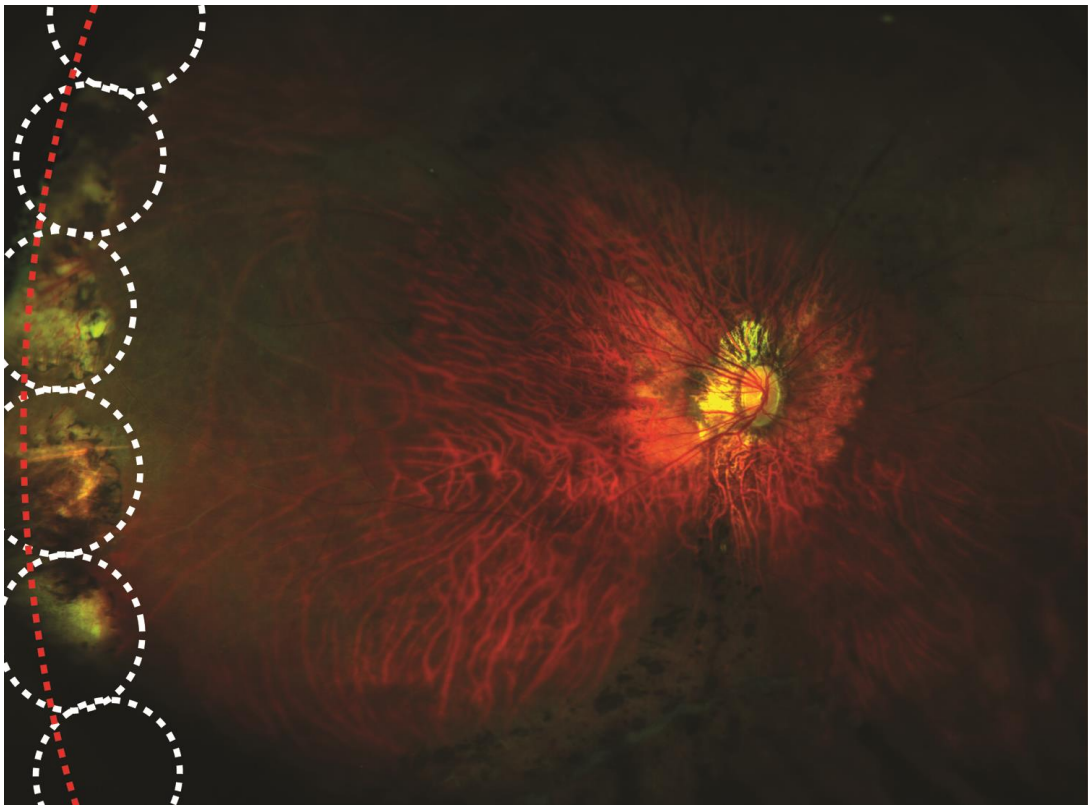

Figure 2-7 Fundal photograph illustrating the positioning of cryotherapy application in the Cambridge Prophylactic Cryotherapy protocol.

Noncontact, high resolution ultrawide-field colour fundal photograph annotated to demonstrate the standardised anterior positioning of retinal cryopexy applied during the Cambridge Prophylactic Cryotherapy protocol. Individual cryotherapy applications (white dotted circles) touch shoulder to shoulder and include the ora serrata (dotted red line). Note classic paravascular lattice degeneration inferior to optic disc.

Original photograph courtesy of Mr C.K. Patel and the Oxford Eye Hospital Imaging Department.

2.3.6 Statistical analysis

No single statistical method could unequivocally address the complex, heterogeneous dataset, which included patients of different ages, who had prophylactic interventions at different times, with the possibility of multiple events (retinal detachment in both eyes), and then compare the differences in primary outcome to an appropriate control.

To ensure a robust systematic approach, a network of several analytical methods was devised to be performed on multiple data-subsets, with the hypothesis that should prophylactic intervention be efficacious, there would be consistency of the results between various methods.

The devised analytical methodology was validated by independent external methodologists and statisticians. These individuals included: Dr Christopher Carroll, School of Health and Related Research, University of Sheffield (primary investigator of the commissioned Health Technology Assessment report (Carroll et al., 2011)); Professor Alan Hackshaw, Department of Epidemiology and Medical Statistics, Cancer Research UK and UCL Cancer Trial Centre; Professor Richard Samworth, Department of Pure Mathematics and Mathematical Statistics, University of Cambridge; Professor Douglas Easton, Department of Oncology, Public Health and Primary Care, University of Cambridge and Dr Christopher, Centre for Applied Medical Statistics, University of Cambridge.

All statistical analysis was completed by an independent external statistician (Laura Pasea, Centre for Applied Medical Statistics, University of Cambridge). All statistical tests were two-sided and used a 5% significance level; analyses were completed using SPSS software version 21.0 (IBM Corp., Armonk, NY).

Collected data were analysed separately as patient and single eye datasets.

2.3.7 Patient dataset analysis

Patient dataset analysis included only those participants who had both eyes available for study. Patients were divided into the following groups for comparison:

1. **Bilateral prophylaxis group**. Patients who had suffered no previous retinal detachment and had undergone the Cambridge Prophylactic Cryotherapy protocol in both eyes.

2. **Bilateral control group**. Patients who had not undergone the prophylactic protocol (patients may have suffered unilateral, bilateral or no previous retinal detachment).

3. **Unilateral prophylaxis group**. Patients who had undergone the Cambridge Prophylactic Cryotherapy protocol to one eye following retinal detachment in their fellow eye.

4. **Unilateral control group**. Patients who had not undergone the prophylactic protocol and suffered previous unilateral or bilateral retinal detachment (a subgroup of the bilateral control group).

Outcomes between groups receiving the Cambridge Prophylactic Cryotherapy protocol and their respective controls were compared. A risk ratio was estimated from patients having a retinal detachment event in at least one eye for the bilateral prophylaxis and bilateral control groups, and for a second eye retinal detachment event for the unilateral prophylaxis and unilateral control groups. Survival analysis was then made to compare the time to event outcomes amongst the groups. For the bilateral prophylaxis and control group, this was time from birth until first retinal detachment or the end of follow-up; for the unilateral prophylaxis and control groups, this was time from first to second eye retinal detachment or the end of follow-up. Survival analysis was completed using Kaplan Meier plots, log rank tests and a Cox regression model to estimate hazard ratios and 95% confidence intervals. Covariate analysis using Cox proportional hazards models was performed to adjust for gender.

To specifically address previous concerns regarding differences in age and follow-up duration between controls and patients receiving prophylaxis, and to ensure control patients did not sustain a retinal detachment event prior to the prophylaxis

group receiving cryotherapy, a novel individual patient matching protocol was developed to compare the bilateral prophylaxis and bilateral control groups, and the unilateral prophylaxis and unilateral control groups. To facilitate equal age at last review between matched pairs, a control group follow-up 'cropping' step was implemented; any retinal detachment that occurred during this 'cropped' period was discarded, as it did not occur during the matched follow-up time. After matching and control group 'cropping', comparison groups were exactly equal in number, age and follow-up duration, and patients who received prophylaxis did so prior to any retinal detachment event in their individually matched control.

Outcomes between individually matched groups receiving prophylaxis and their respective matched controls were then compared. The matched data were analysed using paired tables, and the Mantel-Haenszel method for stratified data (that takes matching into account) was used to estimate the risk ratio. McNemar's test was used to test the association between prophylaxis groups and retinal detachment events. Survival analysis was completed using Kaplan Meier plots and log rank tests to investigate and compare time to event outcomes between the matched groups. Since the pairs were matched to ensure that neither the prophylaxis case nor the control in a pair had had a retinal detachment event before the prophylaxis case subject had cryotherapy, a Cox proportional hazards model was used to estimate an adjusted hazard ratio at a 95% confidence interval. The time of origin for the matched bilateral prophylaxis and control group was the time from prophylaxis (or the corresponding time point in the matched control) to first retinal detachment or the end of follow-up, and for the matched unilateral prophylaxis and control groups was the time from prophylaxis (or the corresponding time point in the matched control) to second eye retinal detachment or the end of follow-up. The proportional hazards assumption of the Cox models was verified using residual and log-log plots.

2.3.8 Patient dataset matching protocols

See video appendix 1.2 for matching protocol explanation.

Bilateral prophylaxis group versus bilateral control group

1. All bilateral prophylaxis group patients with both eyes available for analysis were included for matching.
2. Observers were blinded to prophylactic cryotherapy failure status.
3. All bilateral prophylaxis group patients were arranged in descending order of length of follow-up after prophylactic cryotherapy. Those patients with less than one year of post-prophylactic cryotherapy follow-up were excluded from further analysis.
4. The individual bilateral prophylaxis group patient with the longest follow-up after prophylactic cryotherapy was selected for matching. The age at which this patient underwent prophylactic cryotherapy and their age at last review were noted for subsequent control matching.
5. All bilateral control group patients with both eyes available for analysis were included for matching.
6. From the bilateral control group, all patients who had their first retinal detachment at an age equal to or less than the age at which the selected bilateral prophylaxis group patient had their prophylactic cryotherapy were excluded from the current round of matching (but returned to the bilateral control group for subsequent rounds of matching).
7. Observers were blinded to the retinal detachment status in the selected subgroup of bilateral control group patients available for the current round of matching.
8. From this subgroup, the patient with an equal or next closest (but older) age at last review was selected to be matched to the selected bilateral prophylaxis group patient (if no control group patient had an equal or older age at last review, the selected prophylaxis group patient was considered unmatched and excluded from further matching analysis; analysis would then restart from step 4).
9. Once matched, these patients were removed from their respective bilateral prophylaxis and bilateral control groups and made unavailable for further matching.

10. Steps 4 through 9 were repeated, using the bilateral prophylaxis group patient with the next longest follow-up after prophylactic cryotherapy as the next selected case for matching.
11. Matching continued until all bilateral prophylaxis group patients had been matched to an appropriate bilateral control or were excluded from matching.
12. The matched bilateral prophylaxis and bilateral control group patients were unmasked with regards to prophylactic cryotherapy failure and retinal detachment status respectively.
13. Individual patient ages at last review in the matched bilateral control group (purposely selected to be equal or older) were compared with the individual patient ages at last review in the corresponding matched bilateral prophylaxis group and 'cropped' accordingly to equal the age at last review of their match. Any retinal detachment events that occurred in the matched bilateral control group patients during this 'cropped' period were excluded from further analysis.
14. Prevalence of retinal detachment was then compared between the matched bilateral prophylaxis and 'cropped' matched bilateral control groups.

Unilateral prophylaxis group versus unilateral control group

1. All unilateral prophylaxis group patients with both eyes available for analysis were included for matching.
2. Observers were blinded to prophylactic cryotherapy failure status.
3. All unilateral prophylaxis group patients were arranged in descending order of length of follow-up after prophylactic cryotherapy. Those patients with less than one year of post-prophylactic cryotherapy follow-up were excluded from further analysis.
4. The unilateral prophylaxis group patient with the longest follow-up after prophylactic cryotherapy was selected for matching. The age at which this patient suffered their first retinal detachment (untreated eye), the age at which they underwent prophylactic cryotherapy (treated eye), and their age at last review were noted for subsequent control matching.
5. All unilateral control group patients with both eyes available for analysis were included for matching.
6. Observers were blinded to the retinal detachment status in the second eye.
7. The unilateral control group patient with an age of first retinal detachment closest to that of the selected unilateral prophylaxis group patient's age of first retinal detachment was selected for further matching (if there was a difference of more than three years, the selected unilateral prophylaxis group patient was considered unmatched and excluded from further matching analysis; analysis would then restart from step 4).
8. If the selected unilateral control group patient's age at last review was equal or older than the selected unilateral prophylaxis group patient's age at last review, they were considered for the final matching step (if the age at final review was less than the selected unilateral control group patient's age at last review, the matching process returned to step 7, selecting the unilateral control group patient with the next closest age of first retinal detachment).
9. The final matching step involved unmasking the retinal detachment status of the selected unilateral control group patient's second eye. If the selected unilateral control group patient did not have a second retinal detachment event or the age at which they had their second retinal detachment was older than the age at which the selected unilateral prophylaxis group patient had their prophylactic cryotherapy, they were considered an appropriate match. If the age of the selected unilateral control group patient at the time of their second retinal detachment was the same or younger than the age at which the selected

unilateral prophylaxis group patient had their cryotherapy, the match was considered inappropriate; the matching process then returned to step 7 (selecting the unilateral control group patient with the next closest age of first retinal detachment).

10. Once matched, these patients were removed from their respective unilateral prophylaxis and unilateral control groups and made unavailable for further matching.
11. Steps 4 through 10 were repeated using the unilateral prophylaxis group patient with the next longest follow-up after prophylactic cryotherapy as the next selected case for matching.
12. Matching continued until all unilateral prophylaxis group patients had been matched to an appropriate control or were excluded from matching.
13. The matched unilateral prophylaxis group patients were unmasked with regards to prophylactic cryotherapy failure.
14. Individual patient ages at last review in the matched unilateral control group (purposely selected to be equal or older) were compared to the individual patient ages at last review in the corresponding matched unilateral prophylaxis group and ‘cropped’ accordingly to equal the age at last review of their match. Any retinal detachment events that occurred in the matched unilateral control group patients during this ‘cropped’ period were excluded from further analysis.
15. Prevalence of retinal detachment was then compared between the matched unilateral prophylaxis and ‘cropped’ matched unilateral control groups.

2.3.9 Single eye dataset analysis

Single eye dataset analysis included all available study eyes; these datasets included eyes from patients that only had one eye that met study inclusion criteria (thereby being excluded from patient matching datasets). Single eyes were divided into the following groups for comparison:

1. **Prophylaxis eye group.** All eyes that underwent the Cambridge Prophylactic Cryotherapy protocol were included. This group was comprised of both eyes of all patients in the bilateral prophylaxis group, the eye that received prophylaxis in all patients in the unilateral prophylaxis group, and all eyes that received prophylaxis in those patients who had only one eye available to study (fellow eye did not meet study inclusion criteria).

2. **Control eye group.** All eyes that did not undergo the Cambridge Prophylactic Cryotherapy protocol were included. This group was comprised of both eyes of all patients in the bilateral control group, the eye that did not receive prophylaxis in all patients in the unilateral prophylaxis group, and all eyes that did not receive prophylaxis in those patients who had only one eye available to study (fellow eye did not meet study inclusion criteria).

3. **Excluded prophylaxis eye group.** All eyes that received prophylaxis in the unilateral prophylaxis group and all eyes that received prophylaxis in those patients who had only one eye available to study were excluded. This group was only comprised of both eyes of all patients in the bilateral prophylaxis group.

4. **Excluded control eye group.** All eyes that did not receive prophylaxis in the unilateral prophylaxis group and all eyes that did not receive prophylaxis in those patients who had only one eye available to study were excluded. This group was only comprised of both eyes of all patients in the bilateral control group.

Retinal detachment outcomes were compared between the prophylaxis eye group and the control eye group. In order to account for potential sampling bias weighting in favour of the effectiveness of prophylaxis, the excluded prophylaxis eye group and excluded control eye group comparison omitted all eyes that did not come from

patients in the bilateral prophylaxis and bilateral control groups; this included all eyes from patients with only single eyes available to study and every untreated eye with retinal detachment from the unilateral prophylaxis group (by definition this group required 100% first eye retinal detachment rates); this group was selected as it excluded patients deemed to be at highest risk of retinal detachment, and therefore reduced the prevalence of retinal detachment in the control group, effectively weighting selection bias against the effectiveness of treatment.

To eliminate the possibility that eyes belonging to the same patient were correlated, random single eye datasets were generated, in which one eye was randomly selected from each patient for further analysis (random prophylaxis eye group versus random control eye group and random excluded prophylaxis eye group versus random excluded control eye group). Random eye selection was made using a computerised random sampler and analysis was repeated three times in each comparison group to ensure no sampling bias was introduced through the randomised selection process; the outcomes deliberately report the smallest difference between groups to weigh against the effectiveness of prophylaxis and thereby providing the most rigorous test of any benefit in receiving prophylactic cryotherapy.

A risk ratio was estimated for having a retinal detachment event between the compared single eye groups receiving prophylaxis and their appropriate controls. Survival analysis was then made to compare time from birth to retinal detachment between the groups and their controls. Survival analysis was completed using Kaplan Meier plots, log rank tests and a Cox regression model to estimate hazard ratios and 95% confidence intervals. Covariate analysis using Cox proportional hazards models was performed to adjust for gender.

2.3.10 Side effects

The occurrence of the following prophylaxis side effects was assessed: lid and conjunctival inflammation, accommodation insufficiency, discomfort, photophobia, macular pucker and any reported perioperative surgical complication; anaesthetic recovery records were reviewed for episodes of nausea or vomiting.

Converted LogMar preoperative visual acuity (measured during admission on the day of surgery) was compared to converted LogMar postoperative visual acuity (measured at the four week postoperative outpatient review). Visual acuity documented at subsequent clinic reviews was noted in all cases with visual reduction until preoperative visual acuity levels were attained, or until the last clinic review.

Results

2.3.11 Demographic details

From the Vitreoretinal Research Unit electronic database, 976 patients with type 1 Stickler syndrome were identified; 551 patients from 256 family pedigrees met inclusion criteria, with 487 patients having both eyes and 64 patients with a single eye available to study.

COL2A1 mutations were formally tested in 87.7% of the participants (n=483); the mutation detection rate, using the Cambridge two-stage diagnostic screening strategy (Richards et al., 2006), was 96.9% at the time of study completion. The majority of patients who did not have molecular confirmation of a COL2A1 mutation, tended to be historical cases that no longer attended clinic review; the remainder were cases in which molecular testing was incomplete at the time of the study conclusion.

2.3.12 Patient dataset results

The prevalence of prophylaxis failure in patients who received bilateral or unilateral (following fellow eye retinal detachment) cryotherapy was compared to the prevalence of retinal detachment in appropriate control groups with both eyes available to study, before and after individual patient matching.

Patient demographic details are given in Table 2-2.

Table 2-2 Demographic details for patient datasets (both eyes available)

Group	Number of patients	Sex ratio (M:F)	Mean age at last review (years) (SD*)	Mean age at 1st retinal detachment (years) (SD*)	Mean age at 2nd retinal detachment (years) (SD*)	Mean age at prophylaxis (years) (SD*)	Mean follow-up post-prophylaxis (years) (SD*)
Bilateral prophylaxis	229	104:125	20.8 (16.9)	-	-	14.5 (15.9)	6.3 (6.4)
- no retinal detachment	210	92:118	19.6 (16.6)	-	-	13.7 (15.3)	5.9 (6.0)
- unilateral retinal detachment	18	11:7	34.6 (19.6)	29.3 (19.4)	-	24.1 (20.4)	10.6 (9.0)
- bilateral retinal detachment	1	1:0	10.9	4.2	4.2	4.0	6.8
Bilateral control	194	95:99	31.3 (21.6)	-	-	-	-
- no retinal detachment	90	38:52	18.6 (18.6)	-	-	-	-
- unilateral retinal detachment	20	9:11	37.0 (24.6)	24.8 (20.4)	-	-	-
- bilateral retinal detachment	84	48:36	43.4 (15.7)	15.2 (10.4)	22.0 (13.8)	-	-
Matched bilateral prophylaxis	165	78:87	19.8 (15.0)	-	-	11.6 (12.9)	7.7 (6.2)
- no retinal detachment	150	68:82	18.8 (14.3)	-	-	10.9 (12.3)	7.8 (6.0)
- unilateral retinal detachment	14	9:5	31.9 (17.5)	25.5 (16.8)	-	19.1 (17.0)	12.8 (9.0)
- bilateral retinal detachment	1	1:0	10.9	4.2	4.2	4.0	6.8
Matched bilateral control	165	83:82	19.8 (15.0)	-	-	-	-
- no retinal detachment	104	48:56	19.5 (15.8)	-	-	-	-
- unilateral retinal detachment	34	17:10	18.4 (13.2)	15.2 (13.1)	-	-	-
- bilateral retinal detachment	27	18:16	22.0 (14.1)	14.8 (12.1)	16.9 (12.0)	-	-
Unilateral prophylaxis	64	37:27	33.2 (18.0)	16.9 (13.5)	-	22.9 (15.7)	10.1 (10.4)
- unilateral retinal detachment	56	31:25	32.2 (18.3)	17.4 (13.9)	-	23.3 (15.6)	9.0 (9.7)
- bilateral retinal detachment	8	6:2	40.1 (14.2)	13.1 (10.2)	27.8 (15.8)	40.1 (14.2)	19.2 (11.8)
Unilateral control	104	57:47	42.2 (17.8)	17.0 (13.4)	-	-	-
- unilateral retinal detachment	20	9:11	37.0 (24.6)	24.8 (20.4)	-	-	-
- bilateral retinal detachment	84	48:36	43.4 (15.7)	15.2 (10.4)	22.0 (13.8)	-	-
Matched unilateral prophylaxis	39	23:16	31.4 (16.3)	14.2 (11.8)	-	17.8 (13.3)	13.7 (11.1)
- unilateral retinal detachment	33	19:14	30.7 (17.0)	14.9 (12.6)	-	19.0 (14.0)	11.7 (10.2)
- bilateral retinal detachment	6	4:2	35.5 (12.4)	10.6 (5.7)	21.0 (9.6)	11.1 (5.9)	24.6 (9.8)
Matched unilateral control	39	27:12	31.4 (16.3)	14.4 (11.6)	-	-	-
- unilateral retinal detachment	12	9:3	28.8 (16.7)	13.8 (13.2)	-	-	-
- bilateral retinal detachment	27	18:9	32.6 (16.3)	14.7 (11.1)	23.4 (14.1)	-	-

*SD denotes standard deviation

Bilateral prophylaxis group versus bilateral control group

Four hundred and twenty three patients were available for the bilateral prophylaxis and bilateral control group comparison; 229 patients received prophylactic cryotherapy in both eyes and 194 control patients received no prophylactic intervention in either eye.

The prevalence of retinal detachment in the bilateral prophylaxis group was 8.3% (19/229), of which 7.9% (18/229) were unilateral and 0.4% (1/229) bilateral. The prevalence of retinal detachment in the bilateral control group was 53.6% (104/194), of which 10.3% (20/194) were unilateral and 43.3% (84/194) bilateral (Figure 2-8). Of the 20 retinal detachment events occurring after prophylaxis, 12 required formal surgical repair and eight were managed with additional retinopexy alone; all 188 control group retinal detachments required formal surgical repair.

Although the mean age at final review was younger for the bilateral prophylaxis group (20.8 years) compared to the bilateral control group (31.3 years), the mean age at first retinal detachment occurred later in the bilateral prophylaxis group (28.4 years) compared to the bilateral control group (17.0 years).

The relative risk of retinal detachment in at least one eye was six and a half times greater for the bilateral control group compared to the bilateral prophylaxis group (relative risk, 6.46; 95% confidence interval: 4.12 to 10.13; $p<0.001$).

Kaplan-Meier survival plots were generated to compare time from birth until first eye retinal detachment or the end of follow up in both groups (Figure 2-9). Time from birth was selected, as type 1 Stickler syndrome is an inherited congenital disorder and patients are at risk of retinal detachment from birth; the plots do not distinguish time points at which each prophylaxis group patient underwent cryotherapy.

The log-rank test statistic ($\chi_1^2 = 87.23$; $p<0.001$) rejects the null hypothesis that the two groups have identical survival and hazard functions, suggesting the survival times between the bilateral prophylaxis and control groups are not the same.

The median survival time to first eye retinal detachment was 18.28 years (95% confidence interval, 14.92 to 21.63) in the bilateral control group, but a median survival time was not reached in the bilateral prophylaxis group (Figure 2-9). A Cox

proportional hazards model estimated a hazard ratio of 7.27 (95% confidence interval, 4.47 to 11.87; $p<0.001$), suggesting the bilateral control group was over seven times more likely to suffer from a retinal detachment in at least one eye compared to the bilateral prophylaxis group.

Covariate analysis using the Cox proportional hazards model to adjust for gender estimated a hazard ratio of 7.40 (95% confidence interval, 4.53 to 12.08; $p<0.001$), suggesting the bilateral control group was almost seven and a half times more likely to suffer from a retinal detachment in at least one eye compared to the bilateral prophylaxis group after accounting for gender. Males had more than double the risk of having at least one retinal detachment compared to females in the same treatment group (hazard ratio, 2.13; 95% confidence interval, 1.48 to 3.07; $p<0.001$).

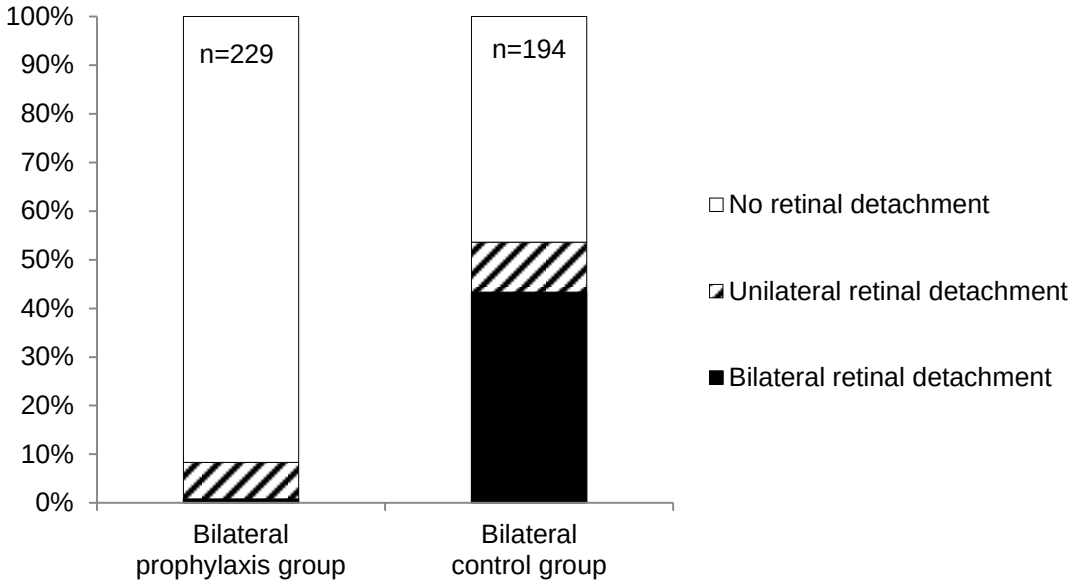

Figure 2-8 Prevalence of retinal detachment: bilateral prophylaxis group vs. bilateral control group

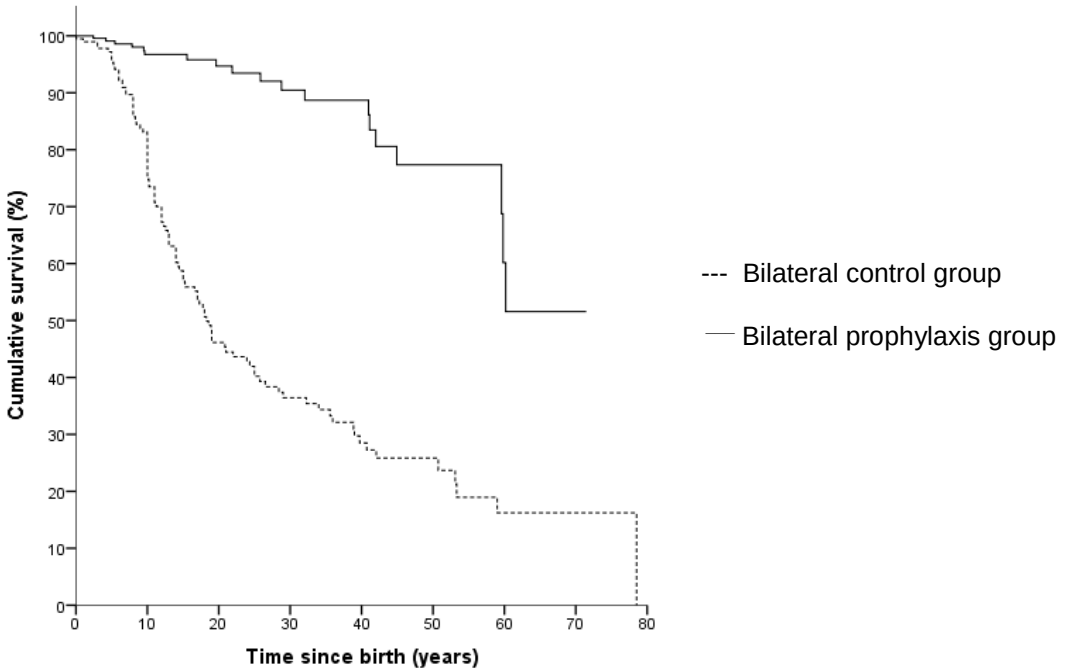

Figure 2-9 Kaplan-Meier survival plot: bilateral prophylaxis group vs. bilateral control group

Matched bilateral prophylaxis group versus matched bilateral control group

Three hundred and thirty patients were available for matched bilateral prophylaxis and matched bilateral control group comparison; 165 patients received prophylactic cryotherapy to both eyes and 165 control patients received no prophylactic intervention to either eye.

The prevalence of retinal detachment in the matched bilateral prophylaxis group was 9.1% (15/165), of which 8.5% (14/165) were unilateral and 0.6% (1/165) bilateral. The prevalence of retinal detachment in the matched bilateral control group was 37.0% (61/165), of which 16.4% (27/165) were unilateral and 20.6% (34/165) bilateral (Figure 2-10). Of the 16 retinal detachment events occurring after prophylaxis, 12 required formal surgical repair and four were managed with additional retinopexy alone; all 95 control group retinal detachments required formal surgical repair. Prior to the 'cropping' step in the matching protocol, the prevalence of retinal detachment in the matched bilateral control group was 61.8% (102/165); 89 retinal detachments were 'cropped' and omitted from final analysis.

After matching, the mean age at final review was 19.8 years in both the prophylaxis and control groups; the mean age at first retinal detachment occurred later in the matched bilateral prophylaxis group (23.5 years) compared to the matched bilateral control group (14.9 years).

The relative risk of retinal detachment in at least one eye was four times greater for the matched bilateral control group compared to the matched bilateral prophylaxis group (relative risk, 4.07; 95% confidence interval: 2.38 to 6.94; $p<0.001$).

McNemar's test (χ_1^2 = 31.12; $p<0.001$) rejected the null hypothesis that there is no association between having prophylaxis and having a retinal detachment.

The matching protocol ensured matched pairs were event-free until the time at which the prophylaxis case underwent cryotherapy. Therefore, Kaplan-Meier survival plots were generated to compare time from cryotherapy prophylaxis (or the corresponding time point in the matched control) until first eye retinal detachment or the end of follow up, in both groups (Figure 2-11).

The log-rank test statistic (χ_1^2 = 35.65; p<0.001) rejects the null hypothesis that the two groups have identical survival and hazard functions, suggesting the survival times between the matched bilateral prophylaxis and matched bilateral control groups are not the same.

The median survival time to first eye retinal detachment was 16.41 years (95% confidence interval, 5.31 to 27.51) in the matched bilateral control group, but a median survival time was not reached in the matched bilateral prophylaxis group (Figure 2-11). A Cox proportional hazards model estimated a hazard ratio of 4.77 (95% confidence interval, 2.71 to 8.40; p<0.001), suggesting the matched bilateral control group was almost five times more likely to suffer from a retinal detachment in at least one eye compared to the matched bilateral prophylaxis group.

Covariate analysis using the Cox proportional hazards model to adjust for gender estimated a hazard ratio of 4.97 (95% confidence interval, 2.82 to 8.78; p<0.001), suggesting the matched bilateral control group was five times more likely to suffer from a retinal detachment in at least one eye compared to the matched bilateral prophylaxis group after accounting for gender. Males had almost double the risk of having at least one retinal detachment compared to females in the same treatment group (hazard ratio, 1.93; 95% confidence interval, 1.21 to 3.07; p=0.006).

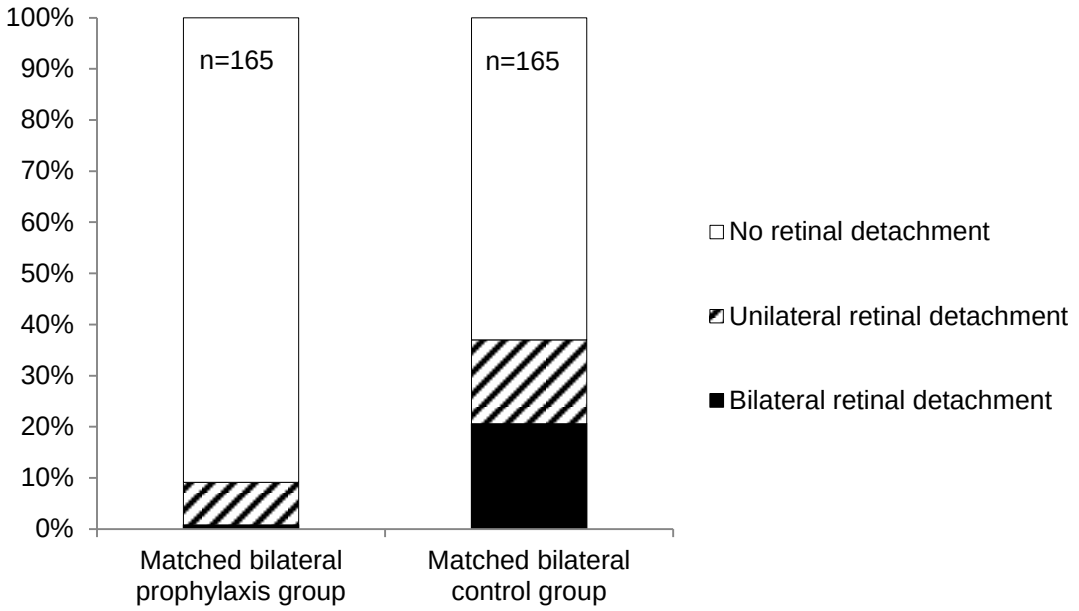

Figure 2-10 Prevalence of retinal detachment: matched bilateral prophylaxis group vs. matched bilateral control group

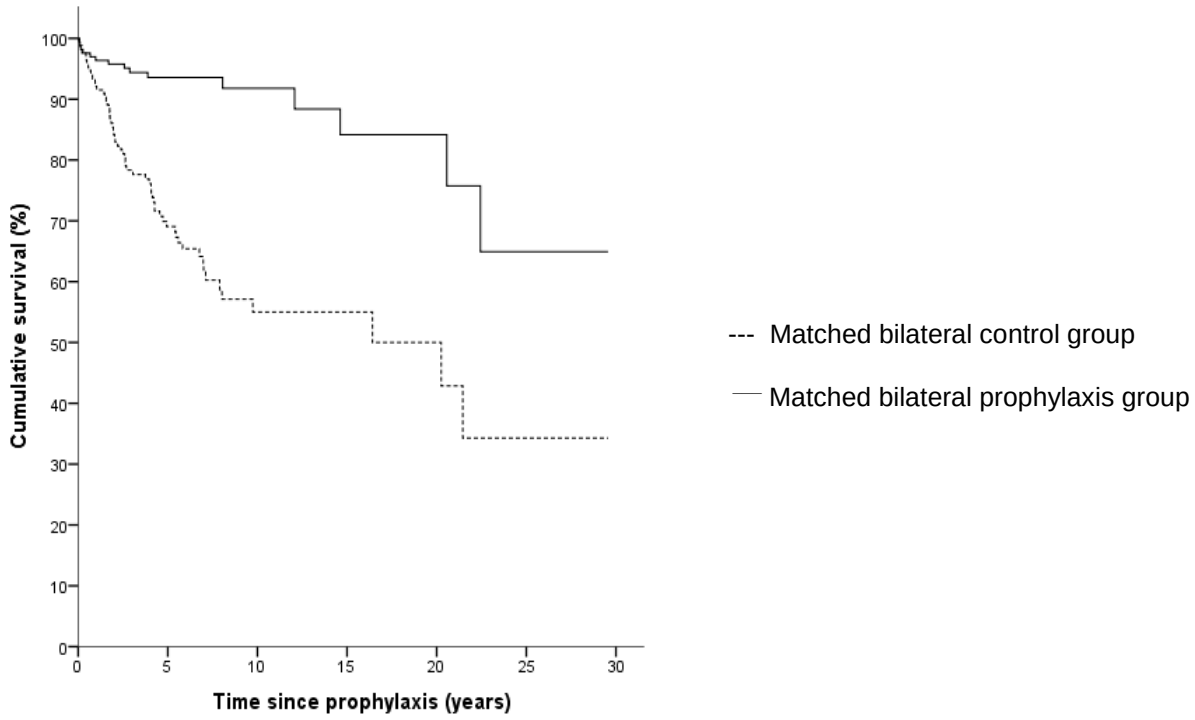

Figure 2-11 Kaplan-Meier survival plot: matched bilateral prophylaxis group vs. matched bilateral control group

Unilateral prophylaxis group versus unilateral control group

One hundred and sixty eight patients were available for the unilateral prophylaxis and unilateral control group comparison; 64 patients received unilateral prophylaxis to the contralateral eye following previous fellow eye retinal detachment, and 104 unilateral control patients received no prophylactic intervention following previous eye retinal detachment.

The prevalence of second eye retinal detachment in the unilateral prophylaxis group was 12.5% (8/64) compared to 80.8% (84/104) in the unilateral control group (Figure 2-12). Of the eight second eye retinal detachment events occurring after prophylaxis, six required formal surgical repair and two were managed with additional retinopexy alone; all 84 unilateral control group second eye retinal detachments required formal surgical repair.

Although the mean age at final review was younger for the unilateral prophylaxis group (33.2 years) compared to the unilateral control group (42.2 years), the mean age of second eye retinal detachment occurred later in the unilateral prophylaxis group (27.8 years) compared to the unilateral control group (22.0 years). The mean age at the time of first eye retinal detachment was similar between the groups (16.9 years in the unilateral prophylaxis group and 17.0 years in the unilateral control group).

The relative risk of second eye retinal detachment was six and a half times greater for the unilateral control group compared to the unilateral prophylaxis group (relative risk, 6.46; 95% confidence interval: 3.36 to 12.44; $p<0.001$).

Kaplan-Meier survival plots were generated to compare time from first eye retinal detachment until second eye retinal detachment or end of follow up, in both groups (Figure 2-13). However, these plots do not distinguish time points at which each unilateral prophylaxis group patient underwent cryotherapy.

The log-rank test statistic (χ_1^2 = 60.27, $p<0.001$) rejects the null hypothesis that the two groups have identical survival and hazard functions, suggesting the survival times between the unilateral prophylaxis and control groups are not the same.

The median survival time to second eye retinal detachment was 4.00 years (95% confidence interval, 2.17 to 5.83) in the unilateral control group compared to 51.60 years (95% confidence interval, 13.29 to 88.83) in the unilateral prophylaxis group. A Cox proportional hazards model estimated a hazard ratio of 10.06 (95% confidence interval, 4.86 to 20.84; $p<0.001$), suggesting the unilateral control group was ten times more likely to suffer from a second eye retinal detachment event compared to the unilateral prophylaxis group.

Covariate analysis using the Cox proportional hazards model to adjust for gender estimated a hazard ratio of 10.29 (95% confidence interval, 4.96 to 21.36; $p<0.001$), suggesting the unilateral control group was more than ten times more likely to suffer from a second eye retinal detachment compared to the unilateral prophylaxis group after accounting for gender. Males had a 17% reduced risk of having a second retinal detachment compared to females in the same treatment group (hazard ratio, 0.83; 95% confidence interval, 0.55 to 1.27; $p=0.396$); the effect of gender was not statistically significant in this analysis (possibly due to a reduced sample number).

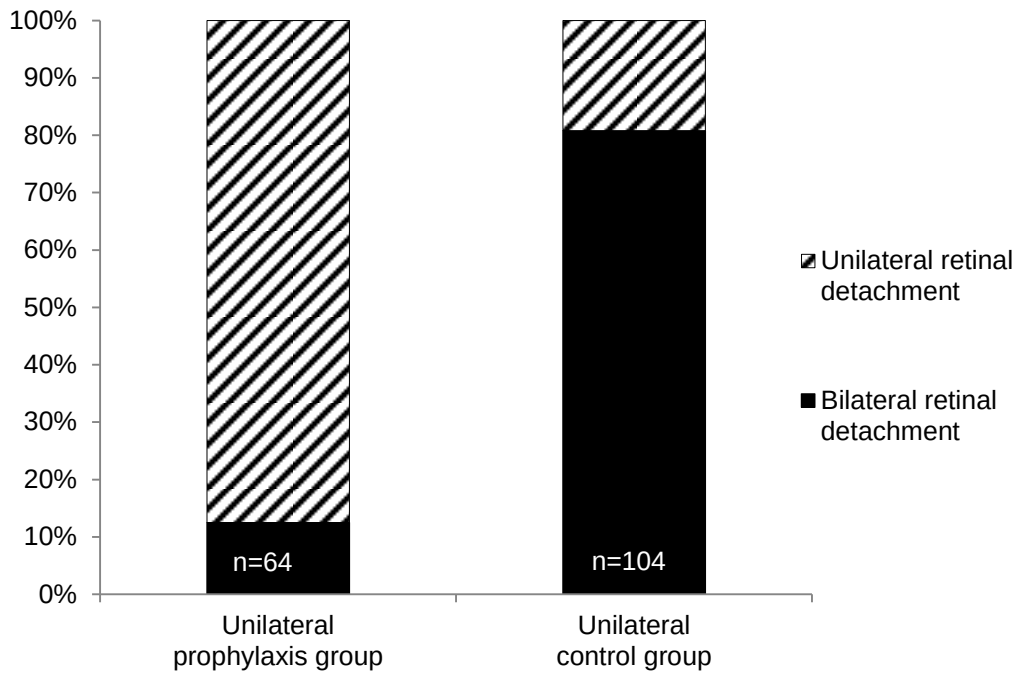

Figure 2-12 Prevalence of second eye retinal detachment: unilateral prophylaxis group vs. unilateral control group

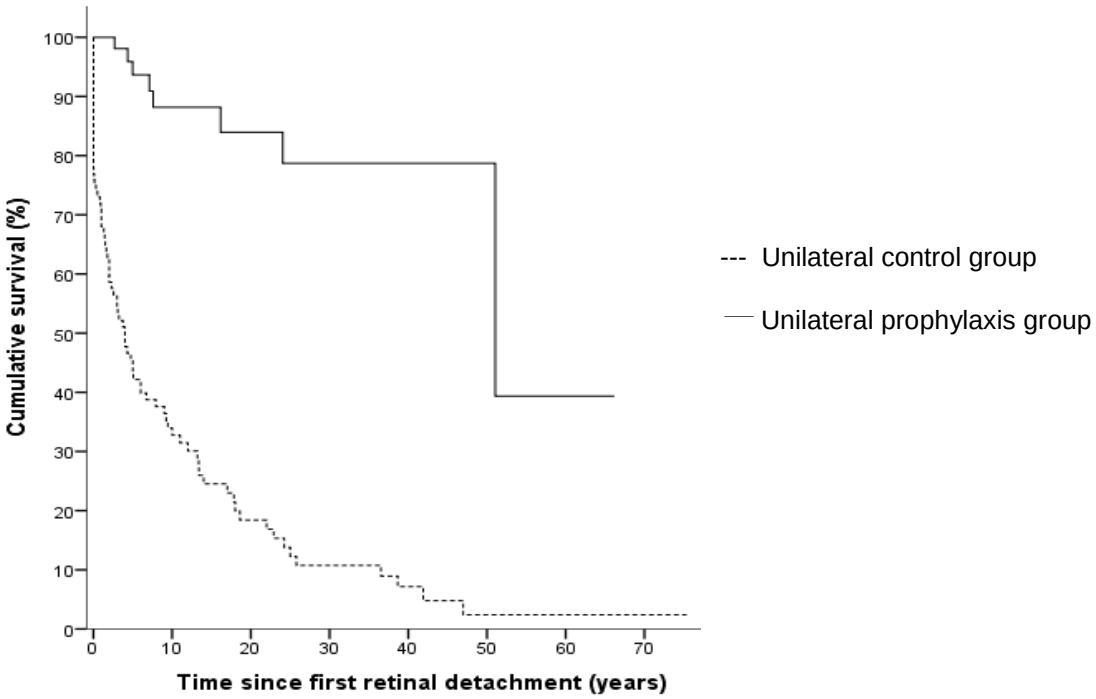

Figure 2-13 Kaplan-Meier survival plot: unilateral prophylaxis group vs. unilateral control group

Matched unilateral prophylaxis group versus matched unilateral control group

Seventy-eight patients were available for matched unilateral prophylaxis and matched unilateral control group comparison; 39 patients received unilateral prophylactic cryotherapy to their contralateral eye following previous fellow eye retinal detachment and 39 control patients received no prophylactic intervention following previous fellow eye retinal detachment.

The prevalence of second eye retinal detachment in the matched unilateral prophylaxis group was 15.4% (6/39) compared to 69.2% (27/39) in the matched unilateral control group (Figure 2-14). Of the six second eye retinal detachment events occurring after prophylaxis, five required formal surgical repair and one was managed with additional retinopexy alone; all 27 matched control group second eye retinal detachments required formal surgical repair. Prior to the 'cropping' step in the matching protocol, the prevalence of second eye retinal detachment in the matched unilateral control group was 87.2% (34/39); seven second eye retinal detachments were 'cropped' and omitted from final analysis.

After matching, the mean age at final review was 31.4 years in both the prophylaxis and control groups; the mean age of second eye retinal detachment was 21.0 years in the matched unilateral prophylaxis group compared to 23.4 years in the matched unilateral control group.

The relative risk of second eye retinal detachment was four and a half times greater for the matched unilateral control group compared to the matched unilateral prophylaxis group (relative risk, 4.50; 95% confidence interval: 2.02 to 10.02; $p<0.001$).

McNemar's test ($\chi_1^2 = 16.33$; $p<0.001$) rejected the null hypothesis that there is no association between having unilateral prophylaxis and having a second retinal detachment.

The matching protocol ensured matched pairs were event-free until the time at which the prophylaxis case underwent cryotherapy. Therefore, Kaplan-Meier survival plots were generated to compare time from cryotherapy prophylaxis (or the corresponding time point in the matched control) until second eye retinal detachment or the end of follow up, in both groups (Figure 2-15).

The log-rank test statistic (χ_1^2 = 23.59; p<0.001) rejects the null hypothesis that the two groups have identical survival and hazard functions, suggesting the survival times between the matched unilateral prophylaxis and matched unilateral control groups are not the same.

The median survival time to second eye retinal detachment was 5.93 years (95% confidence interval, 0.00 to 13.66) in the matched unilateral control group, but a median survival time was not reached in the matched unilateral prophylaxis group (Figure 2-15). A Cox proportional hazards model estimated a hazard ratio of 6.85 (95% confidence interval, 2.80 to 16.75; p<0.001), suggesting the matched unilateral control group was almost seven times more likely to suffer a second retinal detachment compared to the matched unilateral prophylaxis group.

Covariate analysis using the Cox proportional hazards model to adjust for gender estimated a hazard ratio of 8.36 (95% confidence interval, 3.24 to 21.57; p<0.001), suggesting the matched unilateral control group was over eight times more likely to suffer a second eye retinal detachment compared to the matched unilateral prophylaxis group after accounting for gender. Males had a 44% reduced risk of having a second retinal detachment compared to females in the same treatment group (hazard ratio, 0.56; 95% confidence interval, 0.26 to 1.22; p=0.561); the effect of gender was not statistically significant in this analysis and likely due to a reduced sample number.

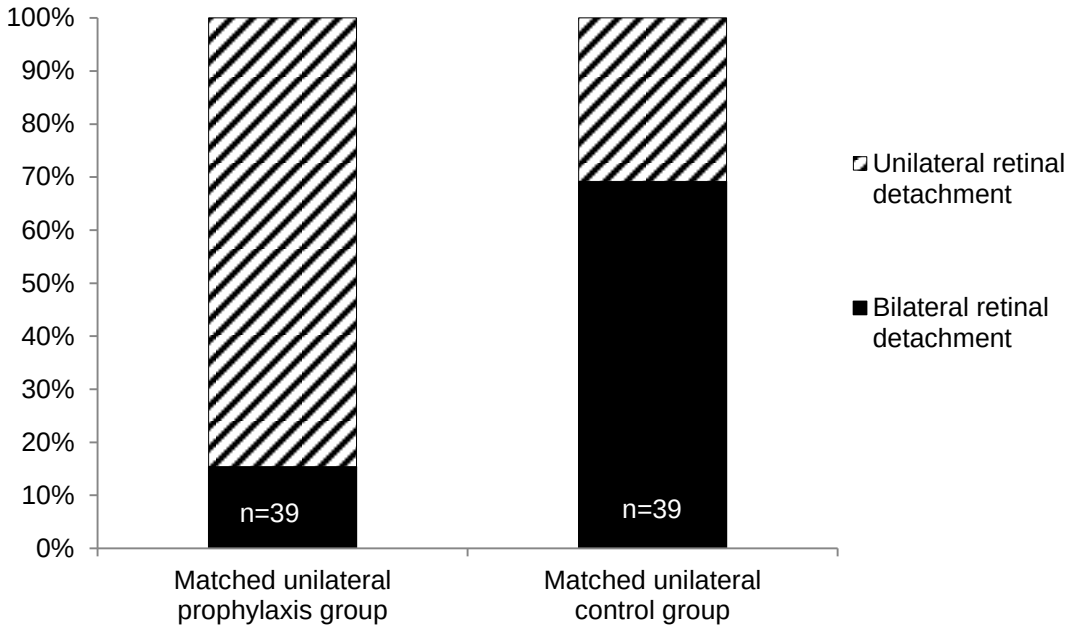

Figure 2-14 Prevalence of retinal detachment: matched unilateral prophylaxis group vs. matched unilateral control group

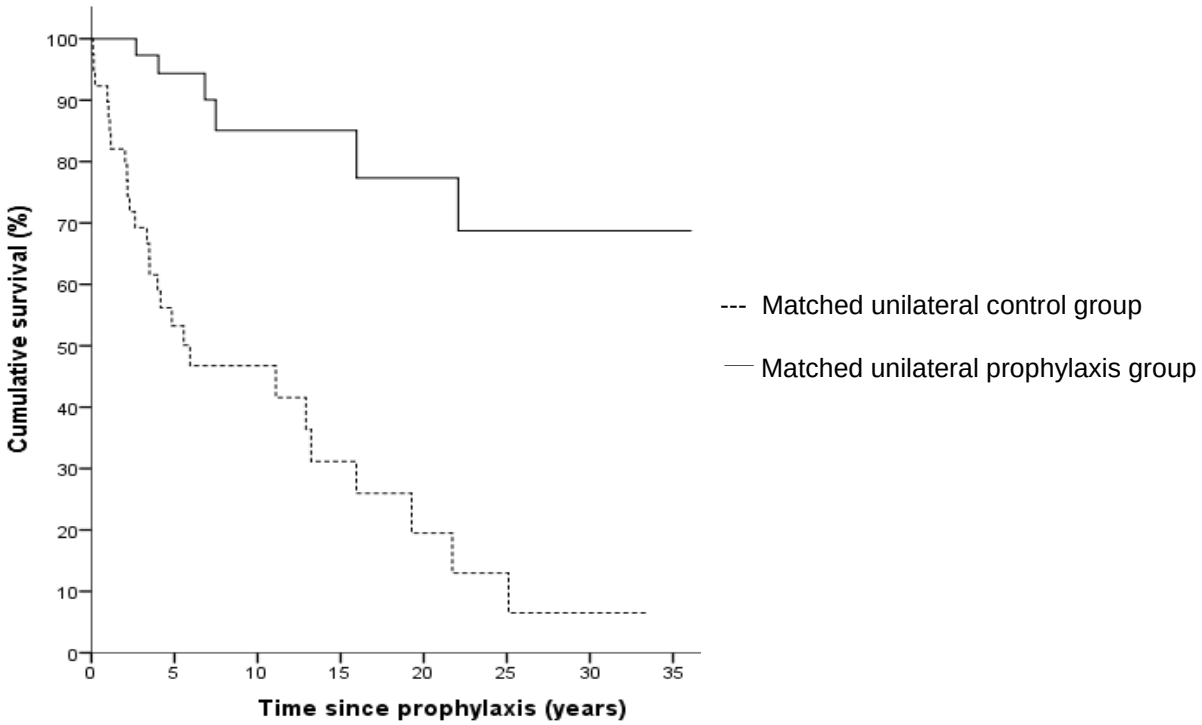

Figure 2-15 Kaplan-Meier survival plot: matched unilateral prophylaxis group vs. matched unilateral control group

2.3.13 Single eye dataset results

The prevalence of prophylaxis failure in eyes that received cryotherapy was compared to the prevalence of retinal detachment in appropriate control eyes that received no prophylaxis for all eyes available to study and in a data subset of excluded single eyes; analysis was repeated after randomly selecting one eye from each patient.

Demographic details are available in Table 2-3.

Table 2-3 Demographic details for single eye datasets

Group	Number of eyes	Sex ratio (M:F)	Mean age at last review (years) (SD*)	Mean age at retinal detachment (years) (SD*)	Mean age at prophylaxis (years) (SD*)	Mean follow-up post-prophylaxis (years) (SD*)
Prophylaxis eye	528	249:279	22.5 (17.6)	-	15.9 (16.4)	6.7 (7.1)
- no retinal detachment	500	230:270	21.9 (17.3)	-	15.6 (16.2)	6.4 (6.7)
- retinal detachment	28	19:9	34.5 (18.5)	27.1 (18.5)	21.5 (19.2)	13.1 (10.4)
Control eye	510	258:252	32.6 (20.9)	-	-	-
- no retinal detachment	205	85:120	20.8 (19.9)	-	-	-
- retinal detachment	305	173:132	40.5 (17.5)	19.2 (13.9)	-	-
Random prophylaxis eye	263	121:142	22.7 (17.5)	-	16.0 (16.5)	6.7 (7.2)
- no retinal detachment	253	113:240	22.5 (17.5)	-	16.1 (16.7)	6.5 (6.9)
- retinal detachment	10	8:2	26.8 (18.5)	17.9 (16.0)	13.7 (13.2)	13.1 (10.9)
Random control eye	288	150:138	33.4 (20.8)	-	-	-
- no retinal detachment	106	43:63	22.4 (21.2)	-	-	-
- retinal detachment	182	107:75	39.8 (17.6)	19.4 (13.9)	-	-
Excluded prophylaxis eye	458	208:250	20.8 (16.9)	-	14.5 (15.9)	6.3 (6.4)
- no retinal detachment	438	195:243	20.2 (16.5)	-	14.2 (15.6)	6.1 (6.2)
- retinal detachment	20	13:7	32.3 (19.9)	26.8 (19.9)	22.1 (20.3)	10.2 (8.6)
Excluded control eye	388	190:198	31.3 (21.6)	-	-	-
- no retinal detachment	200	85:115	20.5 (20.0)	-	-	-
- retinal detachment	188	105:83	42.8 (16.9)	19.2 (13.7)	-	-
Random excluded prophylaxis eye	229	104:125	20.8 (16.9)	-	14.5 (15.9)	6.3 (6.4)
- no retinal detachment	222	99:123	20.6 (16.7)	-	14.5 (16.0)	6.1 (6.2)
- retinal detachment	7	5:2	26.5 (21.5)	19.7 (18.8)	15.7 (15.2)	10.8 (10.8)
Random excluded control eye	194	95:99	31.3 (21.6)	-	-	-
- no retinal detachment	101	43:58	21.7 (21.4)	-	-	-
- retinal detachment	93	52:41	41.6 (16.6)	18.7 (13.2)	-	-

*SD denotes standard deviation

Prophylaxis eye group versus control eye group

One thousand and thirty eight eyes from 551 patients (487 patients with both eyes and 64 patients with one eye) were available for analysis; 528 eyes received prophylactic cryotherapy and 510 control eyes received no prophylactic intervention.

The prevalence of retinal detachment in the eyes receiving prophylaxis was 5.3% (28/528) compared to 59.8% (305/510) in the control eyes (Figure 2-16). Of the 28 retinal detachment events occurring after prophylaxis, 18 required formal surgical repair and ten were managed with additional retinopexy alone; all 305 control eye retinal detachments required formal surgical repair.

Although the mean age at final review was younger for the eyes receiving prophylaxis (22.5 years) compared to the control eyes (32.6 years), the mean age at retinal detachment occurred later in the prophylaxis eyes (27.1 years) compared to the control eyes (19.2 years), suggesting a delay in the age of retinal detachment in those patients who underwent prophylactic cryotherapy.

The relative risk of retinal detachment was over 11 times greater for the control eyes compared to those receiving prophylaxis (relative risk, 11.28; 95% confidence interval: 7.81 to 16.28; p<0.001).

Kaplan-Meier survival plots were generated to compare time from birth until retinal detachment or the end of follow up in both groups (Figure 2-17). As mentioned above, time from birth was selected, as type 1 Stickler syndrome is an inherited congenital disorder and patients are at risk of retinal detachment from birth; the plots do not distinguish time points at which each prophylaxis group patient underwent cryotherapy.

The log-rank test statistic (χ_1^2 = 275.69; p<0.001) rejects the null hypothesis that the two groups have identical survival and hazard functions, suggesting the survival times between the prophylaxis and control groups are not the same.

The median survival time to retinal detachment was 20.00 years (95% confidence interval, 17.02 to 22.98) in the control eye group, but a median survival time was not reached in the prophylaxis eye group (Figure 2-17). A Cox regression model estimated a hazard ratio of 12.70 (95% confidence interval, 8.62 to 18.71; p<0.001),

suggesting the control eyes were over twelve and a half times more likely to suffer from a retinal detachment compared to the eyes receiving prophylaxis.

Multivariate analysis using the Cox proportional hazards model to adjust for gender estimated a hazard ratio of 12.70 (95% confidence interval, 8.62 to 18.71; $p<0.001$) suggesting that the control eyes were over twelve and a half times more likely to suffer from a retinal detachment compared to the eyes receiving prophylaxis group after accounting for gender. Males had an almost double the risk of having a retinal detachment compared to females in the same group (hazard ratio, 1.93; 95% confidence interval, 1.55 to 2.40; $p<0.001$). The fact that adjusting for gender does not alter the hazard ratio to two decimal places, suggests the effect of prophylactic cryotherapy on reducing the risk of retinal detachment is independent of gender.

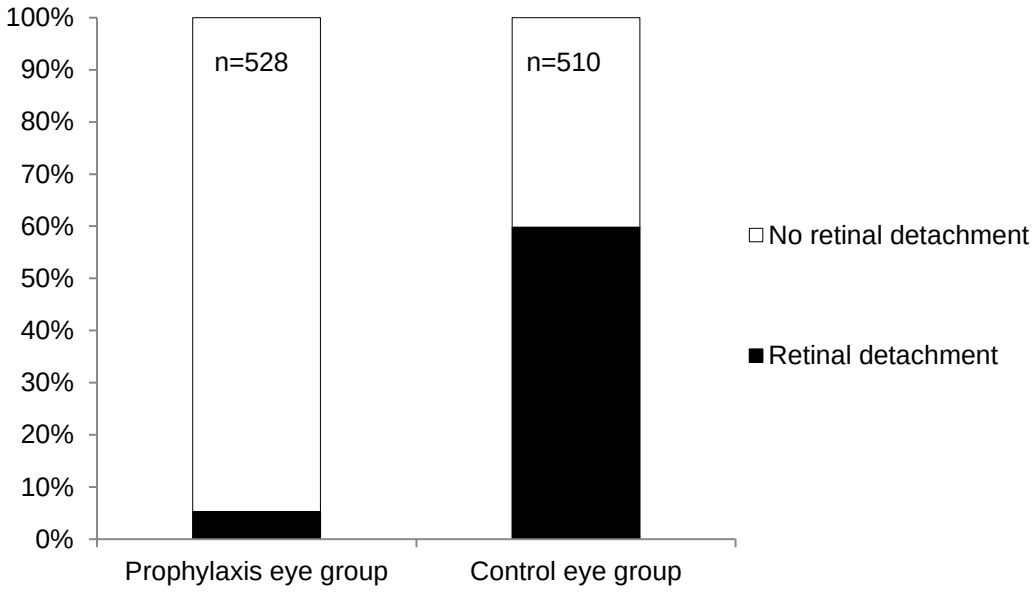

Figure 2-16 Prevalence of retinal detachment: prophylaxis eye group vs. control eye group

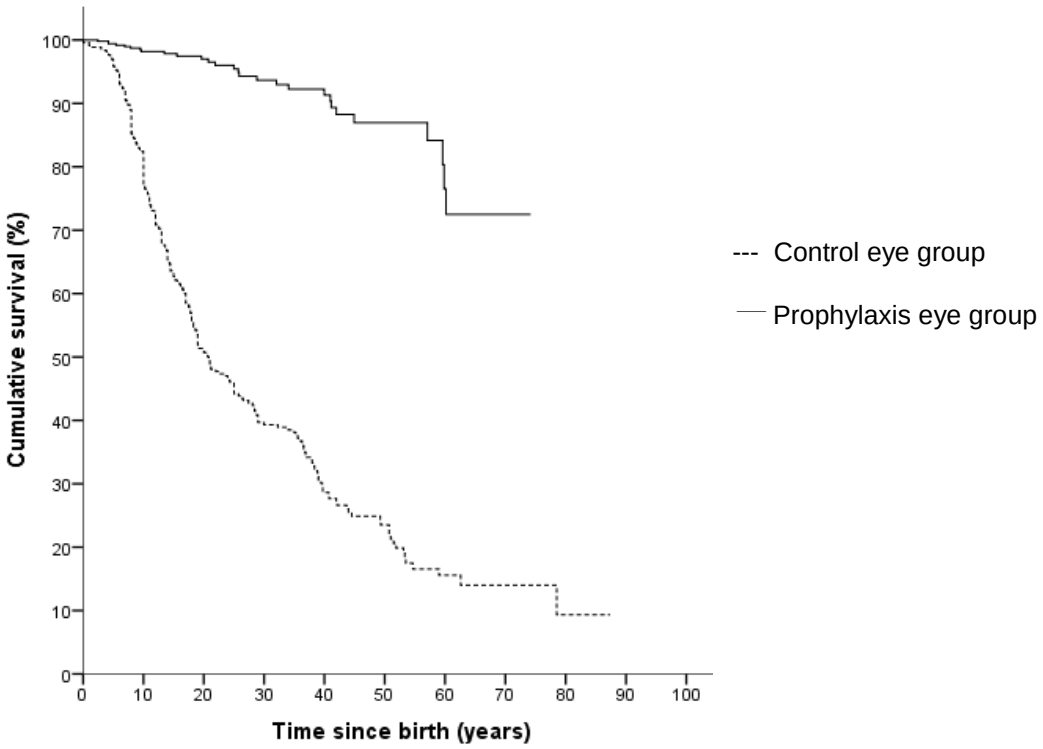

Figure 2-17 Kaplan-Meier survival plot: prophylaxis eye group vs. control eye group

Random prophylaxis eye group versus random control eye group

From the 487 patients with both eyes available for analysis, one eye was randomly selected and pooled with the 64 eyes from the patients with only one eye available to study. Of the resulting 551 single eyes, 263 received prophylactic cryotherapy and 288 received no prophylactic intervention. Randomly selected single eye analysis was used to exclude any correlation that may exist between eyes from the same patient.

The prevalence of retinal detachment in the randomly selected eyes receiving prophylaxis was 3.8% (10/263) compared to 63.2% (182/288) in the randomly selected control eyes (Figure 2-18). Of the ten retinal detachment events occurring after prophylaxis, eight required formal surgical repair and two were managed with additional retinopexy alone; all 182 control eye retinal detachments required formal surgical repair.

The mean age at final review was 22.7 years for the random prophylaxis eye group and 33.4 years for the random control eye group; the mean age at retinal detachment was 17.9 years in the eyes receiving prophylaxis and 19.4 years in the control eyes.

The relative risk of retinal detachment for the control eyes was over sixteen and a half times compared to those receiving prophylaxis (relative risk, 16.62; 95% confidence interval: 8.99 to 30.72; $p<0.001$).

Kaplan-Meier survival plots were generated to compare time from birth until retinal detachment or the end of follow up in both groups (Figure 2-19).

The log-rank test statistic ($\chi_1^2 = 155.64$; $p<0.001$) rejects the null hypothesis that the two groups have identical survival and hazard functions, suggesting the survival times between the randomly selected prophylaxis and control eye groups are not the same.

The median survival time to retinal detachment was 19.20 years (95% confidence interval, 14.58 to 23.81) in the randomly selected control eye group, but a median survival time was not reached in the randomly selected prophylaxis eye group (Figure 2-19). A Cox regression model estimated a hazard ratio of 18.27 (95%

confidence interval, 9.66 to 34.54; p<0.001), suggesting the control eyes were over eighteen times more likely to suffer from a retinal detachment compared to the eyes receiving prophylaxis.

Covariate analysis using the Cox proportional hazards model to adjust for gender estimated a hazard ratio of 17.91 (95% confidence interval, 9.47 to 33.86; p<0.001), suggesting the control eyes were nearly eighteen times more likely to suffer from a retinal detachment compared to the eyes receiving prophylaxis group after accounting for gender. Males had twice the risk of having a retinal detachment compared to females in the same group (hazard ratio, 2.02; 95% confidence interval, 1.51 to 2.70; p<0.001).

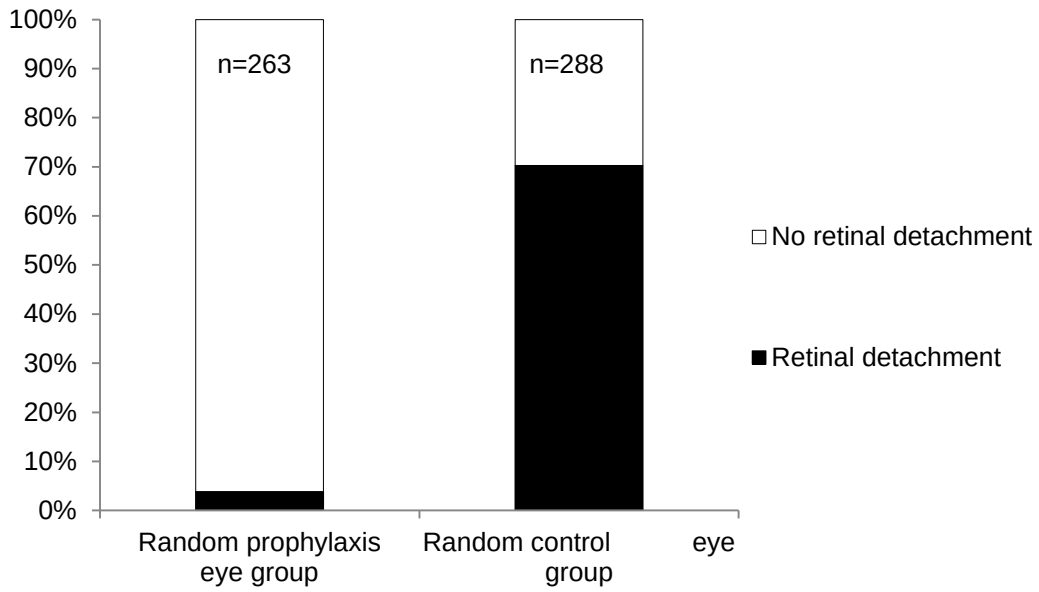

Figure 2-18 Retinal detachment prevalence: random prophylaxis eye group vs. random control eye group

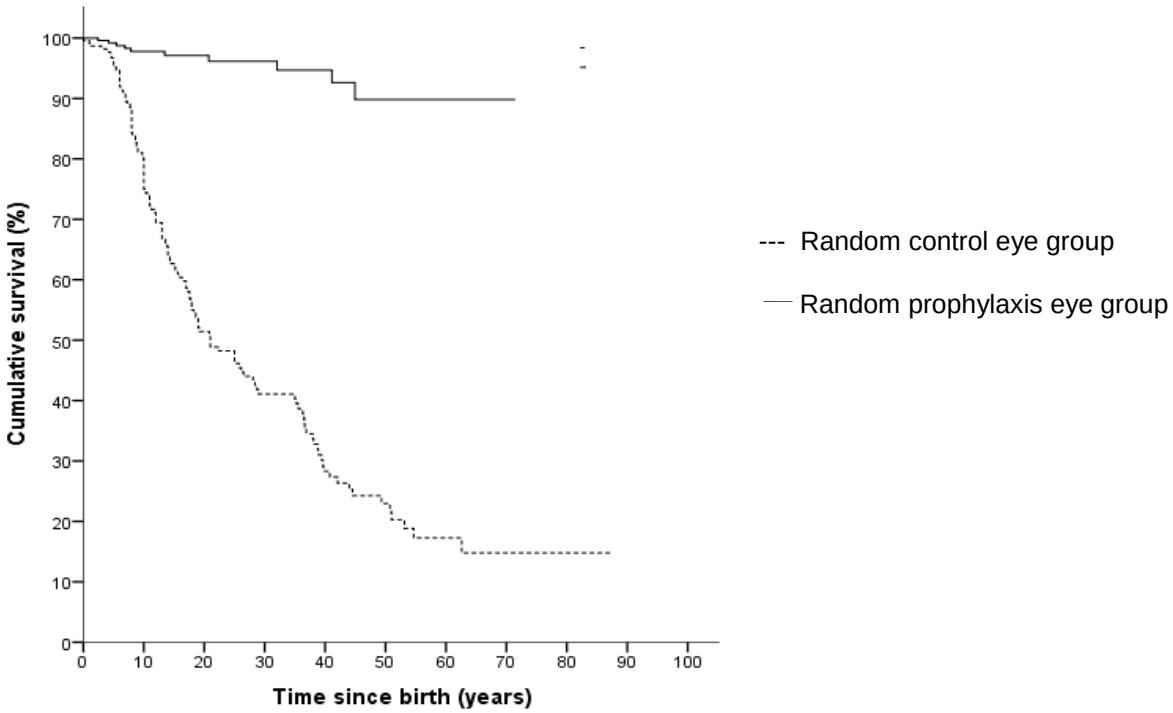

Figure 2-19 Kaplan-Meier survival plot: random prophylaxis eye group vs. random control eye group

Excluded prophylaxis eye group versus excluded control eye group

Eight hundred and forty six eyes from 423 patients were available for analysis; 458 eyes received prophylactic cryotherapy and 388 control eyes received no prophylactic intervention. This analysis excluded those sub-groups of patients deemed to be at greatest risk of retinal detachment (previous retinal detachment in their fellow eye) in order to investigate the potential effectiveness of prophylaxis in those patients who had not experienced a previous retinal detachment.

The prevalence of retinal detachment in the eyes receiving prophylaxis was 4.4% (20/458) compared to 48.5% (188/388) in the control eyes (Figure 2-20). Of the 20 retinal detachment events occurring after prophylaxis, 15 required formal surgical repair and five were managed with additional retinopexy alone; all 188 control eye retinal detachments required formal surgical repair.

Although the mean age at final review was younger for the eyes receiving prophylaxis (20.8 years) compared to the control eyes (31.3 years), the mean age at retinal detachment occurred later in the excluded prophylaxis eyes (26.8 years) than the excluded control eyes (19.2 years).

The relative risk of retinal detachment for the control eyes was over eleven times compared to those receiving prophylaxis (relative risk, 11.10; 95% confidence interval: 7.14 to 17.24; p<0.001).

Kaplan-Meier survival plots were generated to compare time from birth until retinal detachment or the end of follow up in both groups (Figure 2-21).

The log-rank test statistic (χ_1^2 = 168.91; p<0.001) rejects the null hypothesis that the two groups have identical survival and hazard functions, suggesting the survival times between the eyes receiving prophylaxis and control eyes are not the same.

The median survival time to retinal detachment was 25.00 years (95% confidence interval, 20.67 to 29.33) in the excluded control eye group, but a median survival time was not reached in the excluded prophylaxis eye group (Figure 2-21). A Cox regression model estimated a hazard ratio of 11.21 (95% confidence interval, 7.07 to 17.79; p<0.001), suggesting the control eyes were over eleven times more likely to suffer from a retinal detachment compared to the eyes receiving prophylaxis.

Covariate analysis using the Cox proportional hazards model to adjust for gender estimated a hazard ratio of 11.03 (95% confidence interval, 6.95 to 17.49; $p<0.001$), suggesting that control eyes were over eleven times more likely to suffer from a retinal detachment compared to the eyes receiving prophylaxis group after accounting for gender. Males had an increased risk of having a retinal detachment compared to females in the same group (hazard ratio, 1.86; 95% confidence interval, 1.41 to 2.45; $p<0.001$).

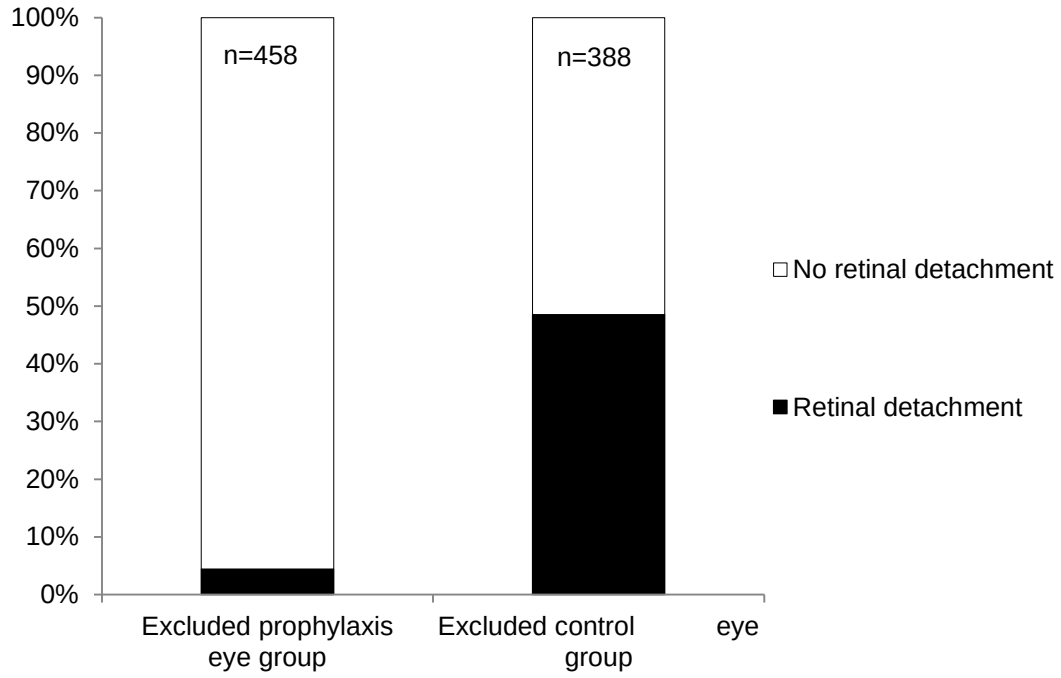

Figure 2-20 Prevalence of retinal detachment: excluded prophylaxis eye group vs. excluded control eye group

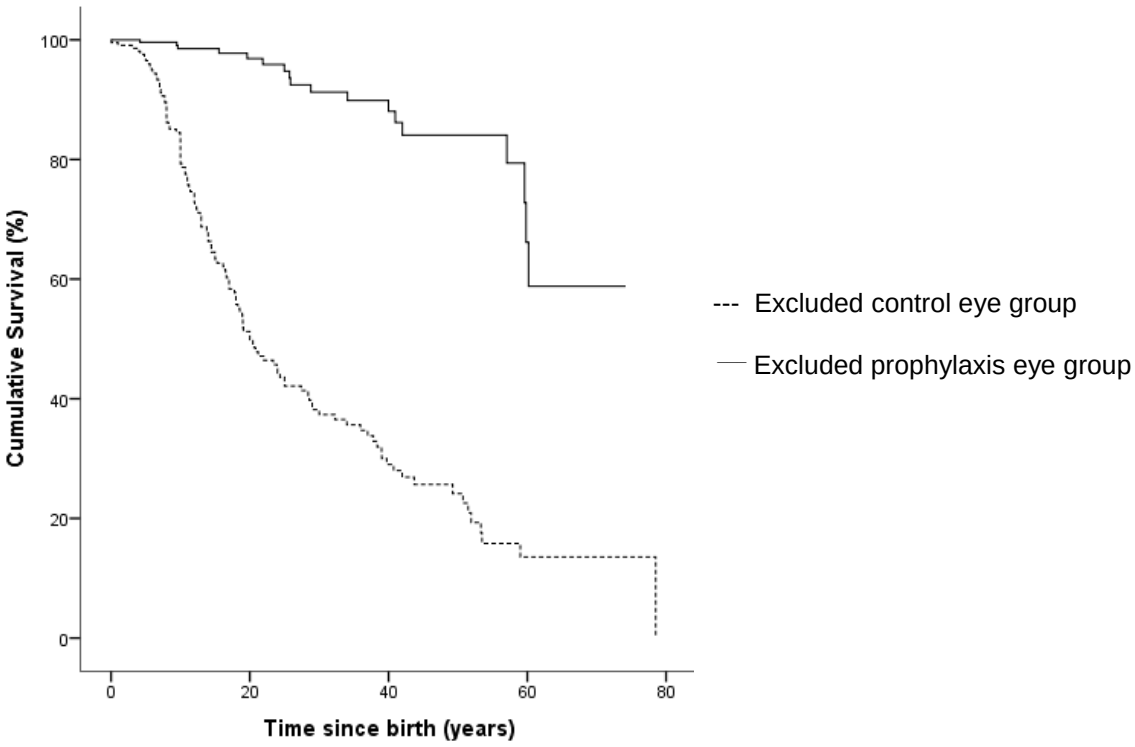

Figure 2-21 Kaplan-Meier survival plot: excluded prophylaxis eye group vs. excluded control eye group

Random excluded prophylaxis eye group versus random excluded control eye group

Of the 423 patients with both eyes available for analysis, one eye was randomly selected from each patient; 229 eyes received prophylactic cryotherapy and 194 received no prophylactic intervention. This analysis excluded those sub-groups of patients deemed to be at greatest risk of retinal detachment (previous retinal detachment in their fellow eye) in order to investigate the potential effectiveness of prophylaxis in those patients who had not experienced a previous retinal detachment. Furthermore, randomly selected single eye analysis was used to exclude any correlation that may exist between eyes from the same patient.

The prevalence of retinal detachment in the randomly selected eyes receiving prophylaxis was 3.1% (7/229) compared to 47.9% (93/194) in the randomly selected control eyes (Figure 2-22). Of the seven retinal detachment events occurring after prophylaxis, six required formal surgical repair and one was managed with additional retinopexy alone; all 182 control eye retinal detachments required formal surgical repair.

Although the mean age at final review was older for those eyes receiving prophylaxis (20.8 years) compared control eyes (31.3 years), the mean age at retinal detachment occurred later in the prophylaxis eyes (19.7 years) compared to the control eyes (18.7 years).

The relative risk of retinal detachment was over fifteen and a half times greater for the control eyes compared to those receiving prophylaxis (relative risk, 15.68; 95% confidence interval: 7.45 to 33.00; $p<0.001$).

Kaplan-Meier survival plots were generated to compare time from birth until retinal detachment or the end of follow up in both groups (Figure 2-23).

The log-rank test statistic ($\chi_1^2 = 91.96$; $p<0.001$) rejects the null hypothesis that the two groups have identical survival and hazard functions, suggesting the survival times between the randomly selected prophylaxis and control eye groups are not the same.

The median survival time to retinal detachment was 26.11 years (95% confidence interval, 20.21 to 32.01) in the randomly selected excluded control eye group, but a median survival time was not reached in the randomly selected excluded prophylaxis eye group (Figure 2-23). A Cox regression model estimated a hazard ratio of 15.82 (95% confidence interval, 7.34 to 34.11; $p<0.001$), suggesting the control eyes were over fifteen and half times more likely to suffer from a retinal detachment compared to the eyes receiving prophylaxis.

Covariate analysis using the Cox proportional hazards model to adjust for gender estimated a hazard ratio of 15.43 (95% confidence interval, 7.16 to 33.28; $p<0.001$), suggesting the control eyes were over fifteen times more likely to suffer from a retinal detachment compared to the eyes receiving prophylaxis after accounting for gender. Males had an increased risk of having a retinal detachment compared to females in the same group (hazard ratio, 1.75; 95% confidence interval, 1.18 to 2.60; $p<0.001$).

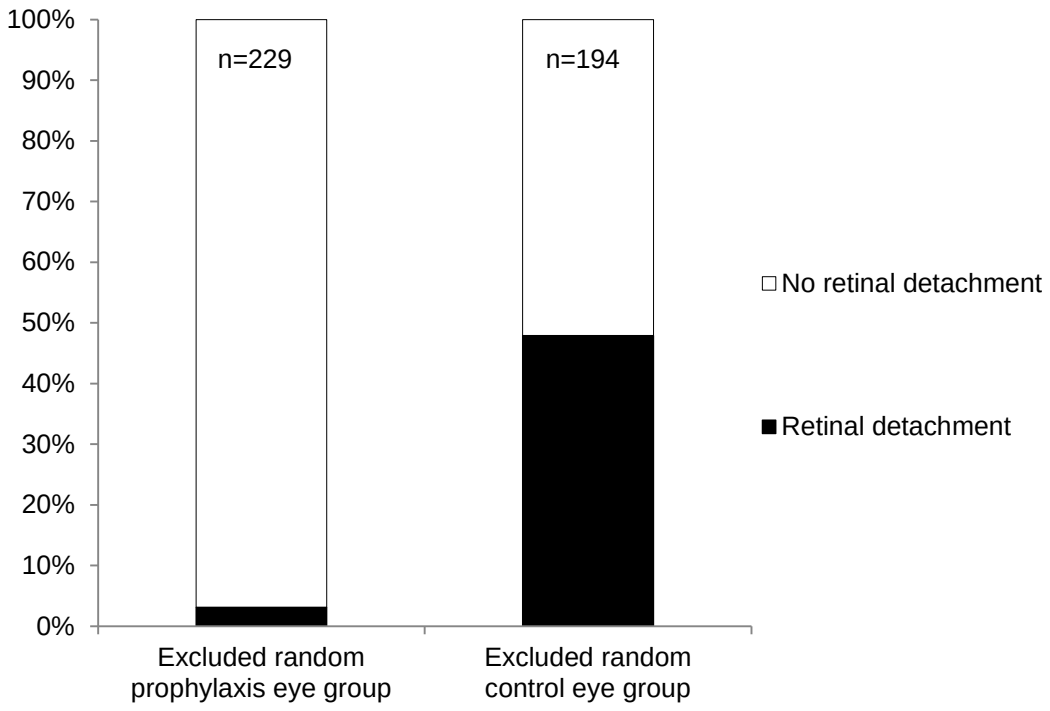

Figure 2-22 Retinal detachment prevalence: excluded random prophylaxis eye group vs. excluded random control eye group

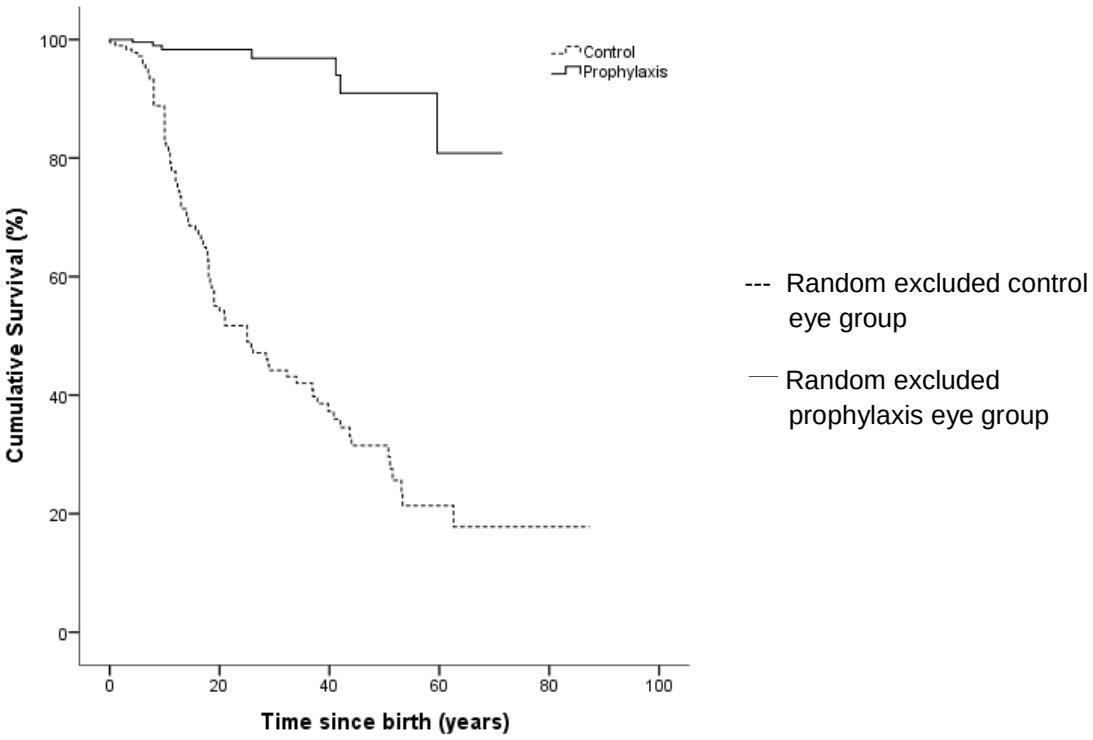

Figure 2-23 Kaplan-Meier survival plot: random excluded prophylaxis eye group vs. random excluded control eye group

2.3.14 Results summary

The results of all conducted analyses are summarised in Table 2-4 and Table 2-5.

Table 2-4 Results summary table: the prevalence of retinal detachment in prophylaxis vs. control groups

Group	Prevalence of retinal detachment	Unilateral retinal detachment	Bilateral retinal detachment
Bilateral prophylaxis	8.3% (19/229)	7.9% (18/229)	0.4% (1/229)
Bilateral control	53.6% (104/194)	10.3% (20/194)	43.3% (84/194)
Matched bilateral prophylaxis	9.1% (15/165)	8.5% (14/165)	0.6% (1/165)
Matched bilateral control	37.0% (61/165)	16.4% (27/165)	20.6% (34/165)
Unilateral prophylaxis	100% (64/64)	100% (64/64)	12.5% (8/64)
Unilateral control	100% (104/104)	100% (104/104)	80.8% (84/104)
Matched unilateral prophylaxis	100% (39/39)	100% (39/39)	15.4% (6/39)
Matched unilateral control	100% (39/39)	100% (39/39)	69.2% (27/39)
Prophylaxis eye	5.3% (28/528)	-	-
Control eye	59.8% (305/510)	-	-
Random prophylaxis eye	3.8% (10/263)	-	-
Random control eye	63.2% (182/288)	-	-
Excluded prophylaxis eye	4.4% (20/458)	-	-
Excluded control eye	48.5% (188/388)	-	-
Random excluded prophylaxis eye	3.1% (7/229)	-	-
Random excluded control eye	47.9% (93/194)	-	-

Table 2-5 Results summary table: risk ratios and hazard ratios for prophylaxis vs. control groups

Group	Analysis	Total number (prophylaxis: control)	Risk ratio (95% CI*)	Hazard ratio (95% CI*)	Gender adjusted hazard ratio (95% CI*)
Bilateral prophylaxis vs. Bilateral control	Unmatched patients	423 (229:194)	6.46 (4.12, 10.13)	7.27 (4.47, 11.87)	7.40 (4.53, 12.08)
	Matched patients	330 (165:165)	4.07 (2.38, 6.94)	4.77 (2.71, 8.40)	4.97 (2.82, 8.78)
Unilateral prophylaxis vs. Unilateral control	Unmatched patients	168 (64:104)	6.46 (3.36, 12.44)	10.06 (4.86, 20.84)	10.29 (4.96, 21.36)
	Matched patients	78 (39:39)	4.50 (2.02, 10.02)	6.85 (2.80, 16.75)	8.36 (3.24, 21.57)
Prophylaxis eye vs. Control eye	All available eyes	1038 (528:510)	11.28 (7.81, 16.28)	12.70 (8.62, 18.71)	12.70 (8.62, 18.71)
	Randomly selected eyes	551 (263:288)	16.62 (8.99, 30.72)	18.27 (9.66, 34.54)	17.91 (9.47, 33.86)
Excluded prophylaxis eye vs. Excluded control eye	All excluded eyes	846 (458:388)	11.10 (7.14, 17.24)	11.21 (7.07, 17.79)	11.03 (6.95, 17.49)
	Randomly selected eyes	423 (229:194)	15.68 (7.45, 33.00)	15.82 (7.34, 34.11)	15.43 (7.16, 33.28)

*CI denotes confidence interval

2.3.15 Prophylactic cryotherapy failure

Failure of retinal cryotherapy prophylaxis occurred in 9.0% (27/299) of patients (5.3% (28/528) of eyes receiving treatment). The mean age at the time of cryotherapy in the failed cases was 21.5 years (range, 2.4 to 59.6; standard deviation, 19.2) and the mean time from treatment to prophylaxis failure was 5.6 years (range, 0.1 to 22.4; standard deviation, 7.2).

Eighteen eyes (from 17 patients) required formal surgical retinal detachment repair. Six of these cases were due to retinal breaks identified posterior to the cryotherapy treatment barrier, five cases were attributed to treated breaks being lifted off or extending through the cryotherapy treatment barrier and one case was for a break that developed at the junction of the posterior edge of the cryotherapy treatment barrier and untreated retina. No aetiological break was reported in six cases requiring surgical retinal detachment repair, two of which presented with associated proliferative vitreoretinopathy due to delayed presentation following retinal detachment.

Of the ten cases classed as prophylaxis failure, but managed with additional retinopexy alone, seven cases were for retinal breaks occurring posterior to the cryotherapy treatment barrier (three of which had associated sub-retinal fluid), two cases were for localised retinal detachments within the prophylaxis barrier that were being held by the cryotherapy treatment (but a further retinopexy barrier was applied for additional security), and one case was for a suspected break at the junction of the posterior edge of the cryotherapy treatment barrier and untreated retina.

All failure cases were unilateral except one bilateral case, which developed in a four year old child with a co-existing diagnosis of Down syndrome; the operation record documented concerns regarding the appearance of the peripheral retina at the time of cryotherapy. Bilateral prophylactic cryotherapy failure was diagnosed 51 days following treatment; the right retinal detachment had associated proliferative vitreoretinopathy and the left retinal detachment was secondary to an inferior horseshoe tear posterior to the cryotherapy treatment barrier.

2.3.16 Side effects

The Cambridge Prophylactic Cryotherapy protocol caused no long-term side effects in any of the 528 eyes (299 patients) that underwent prophylactic intervention; in particular, no cases of unexplained visual loss, macular pucker or intraoperative choroidal haemorrhage occurred.

The mean pre and postoperative converted LogMar visual acuity recorded in 419 eyes (237 patients) was 0.29 (range, -0.18 to -1.80; standard deviation, 0.29) and 0.25 (range, -0.18 to -1.30; standard deviation, 0.24) respectively. Vision remained unaltered in 45.1% (189/419), improved in 32.2% (135/419) and deteriorated in 22.7% (95/419) of eyes at the four week postoperative review. Of those eyes that experienced a visual acuity reduction, only five eyes had a reduction of more than one line of Snellen acuity equivalent; four eyes were from patients who were less than four years of age. Subsequent clinical review revealed any visual acuity decline returned to, or was better than, preoperative visual acuity levels. The only eye that did not regain preoperative visual acuity levels was from a 38.4-year-old patient who was documented to have a Foster Fuch's spot and progressive macular atrophy accounting for the continued reduction in their central vision.

Reported side effects are listed in Table 2-6.

Table 2-6 Reported patient side effect

Side effect	Number of patients affected (percentage)	Mean patient age (years) (SD*)	Mean time to resolution (weeks) (SD*)
Lid/conjunctival inflammation (mild)	76/299 (25.4%)	10.7 (9.9)	<4
Lid/conjunctival inflammation (moderate)	42/299 (14.1%)	17.5 (18.4)	<4
Lid/conjunctival inflammation (marked)	20/299 (6.7%)	14.8 (16.0)	<4
Nausea and/or vomiting	37/299 (12.3%)	16.0 (12.6)	<1
Accommodation insufficiency	28/299 (9.4%)	25.8 (14.2)	5.3 (2.5)
Ocular discomfort	7/299 (2.3%)	21.2 (18.0)	<1
Anisocoria/mydriasis	6/299 (2.0%)	30.2 (23.1)	6.8 (2.9)
Photophobia	3/299 (1.0%)	25.1 (24.6)	2.7 (1.2)
Itchy eyes	2/299 (0.7%)	9.2 (2.5)	<1
New floaters	1/299 (0.3%)	18.3	6

*SD denotes standard deviation

2.4 Discussion

2.4.1 The natural history of retinal detachment in type 1 Stickler syndrome

Despite an increasing understanding of the molecular genetic aetiology of the Stickler syndromes (Table 2-1), the rate of retinal detachment and subsequent visual loss in the disorder remains high (Ang et al., 2008; Donoso et al., 2002; Parma et al., 2002; Stickler et al., 2001).

In the largest global cohort of type 1 Stickler patients (reported above), the bilateral control group median survival time to first retinal detachment was 18.3 years (Figure 2-9) and the unilateral control group median survival time from first to second eye retinal detachment was 4.0 years (Figure 2-13). These conservative survival time statistics characterise for the first time the natural history of the disorder, illustrating that half of all untreated type 1 Stickler syndrome patients will have their first retinal detachment within the first two decades of life, and half of all patients who suffer a retinal detachment are likely to suffer a second eye retinal detachment within four years of the first.

Although type 1 Stickler syndrome is an inherited congenital disorder and present from birth, the risk of retinal detachment appears to be life-long; the oldest patient in the current series to suffer their first eye retinal detachment was 78.5 years old. However, the most disturbing cases are the late presentations of preverbal children with inoperable, bilateral retinal detachments. Severe visual impairment, compounded by hearing, speech and mobility problems associated with this disorder, result in a significant lifelong impact on the future of these young people. Although rare before the age of one and a half years of age, the youngest child seen in the current series with retinal detachments was six weeks of age.

2.4.2 The Cambridge Prophylactic Cryotherapy protocol

Historically, the Cambridge Prophylactic Cryotherapy protocol was offered to children from approximately five years of age. This was the typical age when they were old enough to cooperate with accurate vitreous phenotyping on slit lamp biomicroscopic examination, required to clinically confirm the presence of the type 1 membranous anomaly and type 1 Stickler syndrome. Recent development and

provision of two-stage diagnostic screening (Richards et al., 2006) means that type 1 Stickler syndrome can now be accurately identified and confirmed in over 90% of cases (Richards et al., 2010). Further refinement with specialised minigene and multiplex ligation-dependent probe amplification analysis has resulted in a mutation detection rate of 96.9% at the time of completion of this study. Early and accurate molecular diagnosis now makes it possible to offer prophylaxis at any age before potential retinal detachments occur; the youngest patient to receive prophylaxis in our series was 10.8 months.

Since 1975, the Vitreoretinal Research Clinic at Addenbrooke's Hospital (nationally commissioned Stickler Syndrome Diagnostic Service since 2011) has been offering type 1 Stickler syndrome patients the Cambridge Prophylactic Cryopexy protocol; for 37 years this standardised prophylactic retinal intervention has been delivered according to a consistent rationale and protocol. The rationale of the prophylaxis strategy is to prevent retinal detachment secondary to giant retinal tears. Prevention of "conventional" posterior breaks would not be expected or intended and this limitation is clarified with patients consenting to treatment; the expectation is to substantially reduce (but not eliminate) the risk of retinal detachment.

Cryotherapy rather than prophylactic laser retinopexy was used for every treated patient in this series as past experience has shown it to be safe when deployed according to this specific protocol (Ang et al., 2008), and using a single standardised intervention avoids introducing a further confounding variable of a different treatment modality. The results provide the first benchmark against which future treatment modalities or strategies could be compared.

2.4.3 Validation of study design

It is accepted that any retrospective analysis should be interpreted with caution as they may be more prone to bias; previous studies of prophylaxis in Stickler syndrome are no exception (Ang et al., 2008; Leiba et al., 1996; Monin et al., 1994). Although all patients were reviewed on the first postoperative day and one month after prophylaxis to evaluate individual responses to treatment and side effects, it is accepted that the retrospective nature of the current study may have underreported short-term side effects. However, when thoughtfully designed, retrospective studies, such as Lane-Claypon's 1926 seminal investigations into breast cancer risk factors

(Lane-Claypon, 1926), can contribute vital information that is impossible, impractical or unethical to ascertain prospectively (Mann, 2003). Given the inevitable constraints when studying rare genetic disorders, and the results of the current study, it is unlikely that a prospective randomised trial could ever be commissioned to assess the efficacy of retinal prophylaxis in Stickler syndrome on practical or ethical grounds.

The significant treatment effects of prophylaxis in the current retrospective study are so large it is highly unlikely to be all due to bias and confounding factors. In fact, the study has been deliberately designed to weight against the benefit of treatment to ensure true treatment effect is underestimated.

For example, the primary outcome measure of retinal detachment in the prophylaxis groups was defined to include all cases of prophylaxis failure requiring formal retinal detachment surgery, in addition to any post-prophylactic retinopexy without surgical repair (even if the retinopexy was indicated for posteriorly located tears that were never intended to be prevented by the anterior cryotherapy barrier). In contrast only retinal detachment requiring formal surgical repair was included in the control groups (all control patients receiving previous retinopexy were excluded from analysis). When reviewing the causes of retinal prophylaxis failure in the 28 eyes (18 of which required formal surgical retinal detachment repair and ten cases which were managed with retinopexy alone), it is apparent that expanding the study end point of retinal detachment to include cases managed without formal surgical repair in the treatment group could be considered to overestimate the failure rate by more than one third. In addition, it could be argued that all cases of failure caused by retinal breaks posterior to the cryotherapy treatment barrier (six of which required formal retinal detachment repair and seven required retinopexy alone) are not a cause of primary prophylaxis failure as the treatment protocol is explicitly designed not to prevent retinal detachments from these breaks.

Furthermore, matching protocols between the bilateral and unilateral patient groups also permitted all retinal detachment events (including post-prophylaxis retinopexy) and follow-up time to be included for prophylaxis patients, but ‘cropped’ follow-up time resulted in lost retinal detachment events in the control groups. These measures intentionally weight bias against the efficacy of treatment, thereby reinforcing any demonstrated protective result.

A criticism of previous studies has been the inclusion of inappropriate controls with the suggestion that the majority of patients without retinal detachment receive prophylaxis, leaving the major source of control patients as those who have already suffered a retinal detachment and incurred the outcome event (Aylward et al., 2008).

The best available estimate of the prevalence of retinal detachment in Stickler syndrome comes from the Stickler syndrome support group surveys (59.8% [189/316], of which not all patients were type 1 and many had undergone previous cryotherapy) (Stickler et al., 2001), large family pedigree studies (57.6% [95/165] to 65.2% [43/66]) (Donoso et al., 2002; Parma et al., 2002) and hospital eye service studies (73.0% [81/111]) (Ang et al., 2008). Given the rate of retinal detachment in the bilateral control group (53.6% [104/194]) is lower than the published prevalence data, it is unconvincing that this criticism would be appropriate to the current study. Our conservative estimate is due to the Vitreoretinal Research Unit's algorithm of tracing undiagnosed family members through family pedigrees from presenting probands and the study exclusion criteria. In addition, this potential bias has been addressed in the current study by creating comparable intervention and control groups; individual patient matching protocols ensured that patients receiving prophylaxis did so prior to any potential retinal detachment event in their individually matched control.

Although there may be some uncertainty over the precise estimate of treatment effect, all outcomes show a clear benefit of the Cambridge Prophylactic Cryotherapy protocol in reducing the risk of retinal detachment in type 1 Stickler syndrome (Table 2-4 and Table 2-5) and current findings support the previous study conducted on a sample of the current cohort population (Ang et al., 2008).

2.4.4 Summary

This study compares 299 patients and 528 eyes receiving prophylaxis with up to 36.1 years of follow up, with 252 control patients and 510 control eyes respectively. It is the largest type 1 Stickler syndrome case controlled cohort, with the longest post interventional follow up published to date. All analyses, despite being deliberately weighted against treatment effect, consistently demonstrated that prophylaxis is safe and definitively reduces the risk of retinal detachment.

The results suggest that the Cambridge Prophylactic Cryotherapy protocol should be offered to all type 1 Stickler syndrome patients to reduce their risk of retinal detachment that is so high in this subgroup of the disorder.

3 Pathogenesis: The posterior hyaloid membrane and its associated laminocytes

"Few subjects in histology have been the occasion of so much difference of opinion as the structure of the vitreous humour of the eye. The tissue is so transparent, its structural elements so delicate and difficult to observe under the microscope, that so much variance in opinion is scarcely surprising." (Younan, 1884)

3.1 Background

Having established that retinal detachment can be prevented or reduced in a defined high-risk population, investigations now focus on the pathogenesis of retinal detachment in the wider population.

The nature of the vitreoretinal junction is a fundamental starting point in the process of posterior vitreous detachment, the most common precursor to rhegmatogenous retinal detachment. Understanding this relationship between the vitreous and the internal limiting membrane is essential to understanding the aetiology of retinal detachment, and potential future prophylactic and treatment strategies.

3.1.1 Basement membranes

The hallmark in the evolution of multicellular organisms, some six hundred million years ago, was the development of extracellular matrices. These supporting molecular configurations, which include basement membranes, have evolved into a variety of specialised structures that perform tissue specific functions. Basement membranes have intimate cellular associations that appear to be central in determining their biological purpose, the significance of which is reiterated by the observation that, except for a few sponges, basement membranes are found in all members of the animal kingdom (Rohrbach and Timpl, 1993). The evolutionary importance of basement membranes to the basic nature of multicellular organisms is perhaps best demonstrated by the fact that basement membrane components are already present at the two-cell stage of development (Timpl and Dziadek, 1986).

Since the seminal description of basal lamina as discrete morphological structures forming continuous sheet interfaces around tissues by Todd and Bowman in the 1850s (Todd and Bowman, 1850), improvements in histological staining practices, such as the use of periodic acid-Schiff reagent to detect complex carbohydrates (Hotchkiss, 1948), have facilitated visualisation of this ‘anhistous membrane’ that does not stain with conventional haematoxylin and eosin. Furthermore, the advancements in imaging technology, such as the introduction of electron microscopy, has enabled ultrastructural interrogation (Pease and Baker, 1950); the International Anatomical Nomenclature Committee recommend the terms ‘lamina lucida’ (the pale layer of the basement membrane adjacent to the cell membrane),

‘lamina densa’ (the darker layer below the lamina lucida) and ‘lamina fibroreticularis’ (the outer region which is in continuity with the adjacent extracellular matrix) (Laurie and Leblond, 1985).

With the expansion of biological analytical techniques, there has been an exponential increase in the molecular characterisation of connective tissue. Despite the discovery of the type I collagen triple helix (Ramachandran and Kartha, 1954), the outline of its molecular structure (Cowan et al., 1955; Ramachandran and Kartha, 1955; Rich and Crick, 1955) and the fundamentals of molecular packing (Hodge and Schmitt, 1960; Schmitt et al., 1955) between the 1950s and 1960s, it soon became apparent that, although type I collagen was the most abundant collagen, it was only one of many proteins in the collagen family, with the discovery of type II and type III fibrillar collagens (Miller and Matukas, 1969; Miller et al., 1971) in the early 1970s.

Following pepsin digestion of anterior lens capsules, Kefalides reported a solubilised collagenous protein formed by three identical α-like chains; he proposed that basement membranes contained this unique non-fibrillar collagen, which he called type IV collagen (Kefalides, 1971). Further evaluation of type IV collagen has revealed an ability for spontaneous self-assembly into sheets of spidery branching nets (Duncan et al., 1983), analogous to a ‘chicken wire’ meshwork. This stable but flexible three-dimensional network functions as a scaffold for non-collagenous glycoprotein rich components (such as laminin, fibronectin, nidogen and heparin sulphate proteoglycans) to be incorporated through specific collagenous binding sites (Fox et al., 1991; Leblond and Inoue, 1989; Timpl, 1989).

Our insights into basement membrane structure and function have expanded to appreciate that these structures have complex molecular components organised into three-dimensional functional matrices. These matrices perform important roles in cellular-extracellular matrix interactions and differentiation, influencing development and maintenance of phenotype (Merker, 1994). Basement membranes are not static matrices for tissue support, but rather dynamic in their interaction of specific peptide domains with cell surface receptors. In addition, basement membranes serve as selective semipermeable membranes to molecular traffic between tissue compartments (Farquhar et al., 1961), reservoirs that modulate local concentrations of growth factors and cytokines (Hynes, 2009; Schlötzer-Schrehardt et al., 2007) and have proposed roles in calcium homeostasis (Carafoli, 1987). Basement

membranes are also able to regulate cell polarity (Raftopoulou and Hall, 2004; Rizzolo, 1991; Russell et al., 2003), adhesion, spreading and migration via their cytoskeletal effects (Hamelers et al., 2005; Hamill et al., 2009; Sehgal et al., 2006) and influence wound healing (Torricelli et al., 2013).

Testament to the physiological importance of basement membranes are the functional changes observed in certain acquired inflammatory and metabolic disorders such as Goodpasture's syndrome (Butkowski et al., 1987; Weber et al., 1990) and diabetes (Engerman and Colquhoun, 1982; Farquhar et al., 1961; Johnson et al., 1981; Kanwar and Farquhar, 1979), and the dramatic pathology observed in basement membrane hereditary conditions such as Alport syndrome (Knebelmann et al., 1996; Spear, 1973; Yoshikawa et al., 1982) and epidermolysis bullosa (Anton-Lamprecht, 1978; Christiano et al., 1996; Davison, 1965).

3.1.2 The internal limiting membrane

There are several well characterised basement membranes in the human eye. These include the eponymously named Bowman's membrane (located between the corneal epithelium and corneal stroma) (Wilson and Hong, 2000), Descemet's membrane (located between the corneal stroma and corneal endothelium) (Johnson et al., 1982) and Bruch's membrane (located between the retinal pigment epithelium and choriocapillaris) (Booij et al., 2010), in addition to the lens capsule (located between crystalline lens epithelial cells and the aqueous humour/anterior hyaloid) (Danysh and Duncan, 2009). Excluding the basement membranes of the choriocapillaris and retinal vasculature, arguably, the largest ocular basement membrane is the internal limiting membrane at the vitreoretinal interface.

The earliest anatomical references to the vitreoretinal interface comes from Gottsche in 1836, who identified a lamellar tissue in close relationship to the inner nervous elements of the retina, and Michaelis in 1837, who described a serous inner layer of the retina; the term internal limiting membrane, however, is attributed to Pacini in 1845, who referred to the homologous structure on the vitreous surface of the retina as the 'membrana limitante' (Pedler, 1961). In 1871, using a silver impregnation technique for light microscopy, Retzius detailed the morphology of the 'membrana limitans retinae interna' of human and animal retinae and categorically concluded that the membranous structure was not a true plasma membrane but

rather formed by the flat vitrad ends of radial fibres (Retzius, 1871). The concept that the internal limiting membrane is made of the expanded vitreal foot processes of Müller glia became widely accepted (Menner, 1930; Polyak, 1941). Retzuis' original observations, however, have been debated and further refined, with modern consensus seeming to consider the internal limiting membrane to be a distinct extracellular basement membrane between the inner surface of the retina and the extracellular matrix of the vitreous; investigators have now concluded that the internal limiting membrane is a separate structure from the plasma membrane of Müller glia, which are likely to form, develop and insert into it, but do not comprise it (Wolff, 1937, 1961; Pedler, 1961; Cohen, 1961; Heegaard et al., 1986; Uga and Smelser, 1973; Seiler et al., 1995).

In addition to its anatomical location, further supporting evidence that the internal limiting membrane is a basement membrane comes from interrogation of its molecular composition. Studies have demonstrated that the internal limiting membrane to be composed of collagen IV (Jerdan et al., 1986; Kleppel and Michael, 1990), laminin and fibronectin (Kohno et al., 1987) and carbohydrate residues (Rhodes, 1982).

The ultrastructure of the internal limiting membrane has been well characterised by electron microscopy. The descriptions from the original studies conducted by Fine (Fine, 1961) and Fine and Tousimis (Fine and Tousimis, 1961), have been confirmed and reiterated in several subsequent studies (Daicker et al., 1977; Gärtner, 1965; Hogan et al., 1971; Malecaze et al., 1985; Masutani-Noda and Yamada, 1983) and further expanded by Foos (Foos, 1972a). Foos described variations of the internal limiting membrane in three distinct topographical zones within the eye; in the basal zone the internal limiting membrane was uniformly thin, but reported it to be progressively and irregularly thickened in the equatorial and posterior zones, in addition to loss of the anteriorly observed Müller vitreal surface attachment plaques in the posterior zone (Figure 3-1).

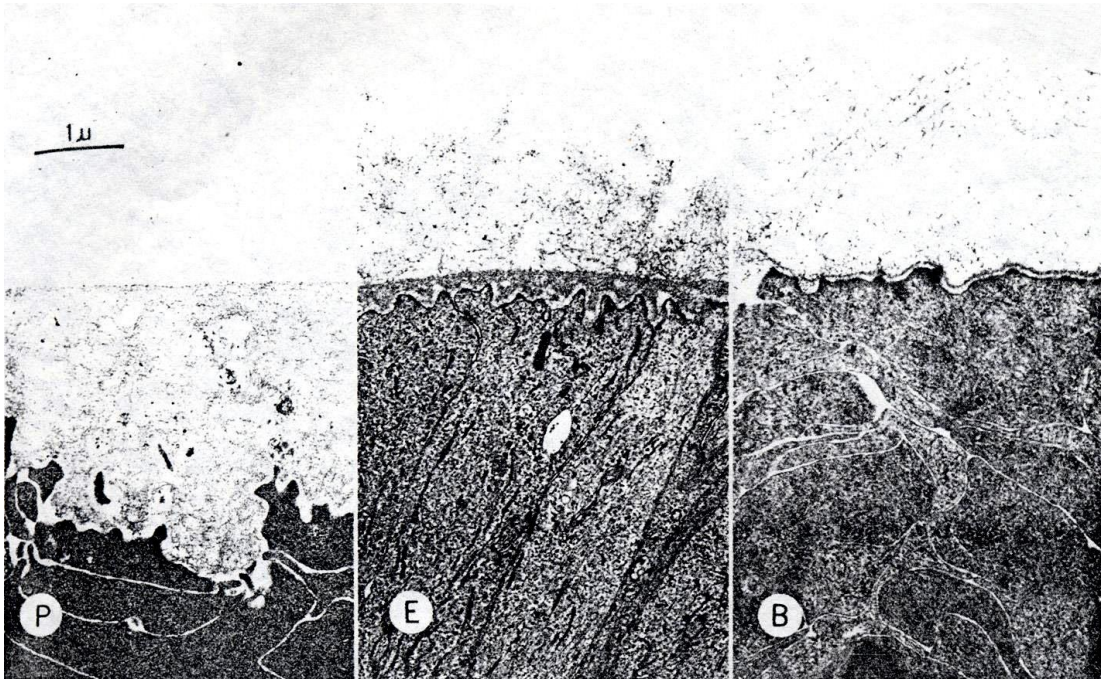

Figure 3-1 Topographical variations of the internal limiting membrane

Transmission electron micrograph of the vitreoretinal interface demonstrating: (P) posterior zone with markedly thickened internal limiting membrane (37-fold increase in thickness compared to the basal zone), note the characteristically smooth vitreal aspect and irregular retinal aspect following the contour of underlying Müller glia, in addition to the conspicuous loss of Müller vitreal surface attachment plaques, (E) equatorial zone with progressive loss of internal limiting membrane thickness and retinal aspect irregularity (six-fold increase in thickness compared to the basal zone), note the presence of Müller vitreal surface attachment plaques, (B) basal zone with uniformly thin internal limiting membrane following undulations of the retinal surface, note presence of Müller vitreal surface attachment plaques (x11850).

Reproduced with permission from Investigative Ophthalmology (Foos, 1972a).

Seeking to investigate if the internal limiting membrane thickened with age in a fashion consistent with other ocular basement membranes (Murphy et al., 1984; Danysh and Duncan, 2009), Heegaard reported on a series of adult eyes from the third to tenth decade of life and compared them with foetal eyes (Heegaard, 1994). The internal limiting membrane of foetal eyes was found to be uniformly thin in all regions and followed the surface contour of Müller glia compared to the internal limiting membrane of adult eyes that reiterated similar topographical variance findings of progressive thickening and irregularity posteriorly (with a characteristic smooth inner vitreal surface and undulating outer cellular surface), as described by Foos (Foos, 1972a). Although the internal limiting membrane was found to be markedly thicker in adult eyes compared to foetal eyes at 24 weeks gestation, there was no reported statistical correlation of increasing thickness with increasing age; the author attributed the lack of trend to small study numbers (a pair of eyes from two adults from each of the third through to the tenth decades, except for the sixth decade where only one pair of eyes was obtained), in addition to technical issues of averaging median thickness values of a structure with complex external folds, and using different examination techniques.

Reappraising Heegaard's original data, it is apparent that the maximum thickness of the internal limiting membrane at the posterior pole appeared to peak at between the ages of 30 to 50 years (median thickness: 3230nm) in specimens examined by transmission electron microscopy, and between the ages of 60 to 80 years (median thickness: 1336nm) for specimens examined by scanning electron microscopy. A conceivable explanation may be that the thickness of the internal limiting membrane peaked between the ages of 40 to 70 and declined thereafter (especially plausible as no reference was made to posterior vitreous detachment status in the examined eyes), and this would confound any attempts at correlating increasing thickness with increasing age.

The aetiological importance of the internal limiting membrane and its associated cell population in the context of the vitreoretinal interface disorders (such as retinal detachment, proliferative vitreoretinopathy, macular pucker, cellophane maculopathy, macular holes and the vitreomacular adhesion disorders) has been the subject of much research (Cherfan et al., 1988; Gandorfer et al., 2002; Green et al., 1979; Guérin et al., 1990; Hiscott et al., 1984; Kampik et al., 1980; Morino et al., 1990; Smiddy et al., 1990). However, despite belonging to a spectrum, the heterogeneity of these individual conditions has made comparisons difficult between

studies and correlation of the findings problematic. In an attempt to address these concerns, Snead and co-workers (Snead et al., 2004) immunohistochemically examined surgical specimens from four clinically distinct vitreomaculopathy subgroups; internal limiting membrane samples from patients in these subgroups (who had no previous intraocular surgery or retinopexy) were compared with post-mortem eyes (with and without uncomplicated posterior vitreous detachment). Basement membrane from the surgical internal limiting membrane specimens was the principle component identified in all four subgroups, with prominent hyperconvolution and reduplication of the internal limiting membrane apparent in the macular pucker and cellophane maculopathy subgroups (Figure 3-2). Although not discussed in this study, control light micrographs of post-mortem eyes with uncomplicated senile posterior vitreous detachment appeared to show similar but less extensive duplication, thickening, contracture and even schisis of the posterior hyaloid membrane (Figure 3-3).

This is perhaps unsurprising since systemic reduplication or lamellation of basement membranes is frequently found around capillaries in patients with diabetic micro-angiopathy (Fischer et al., 1982; Vracko, 1974) and increasing basement membrane production is a well characterised cellular response to sublethal injury (Martinez-Hernandez and Amenta, 1983).

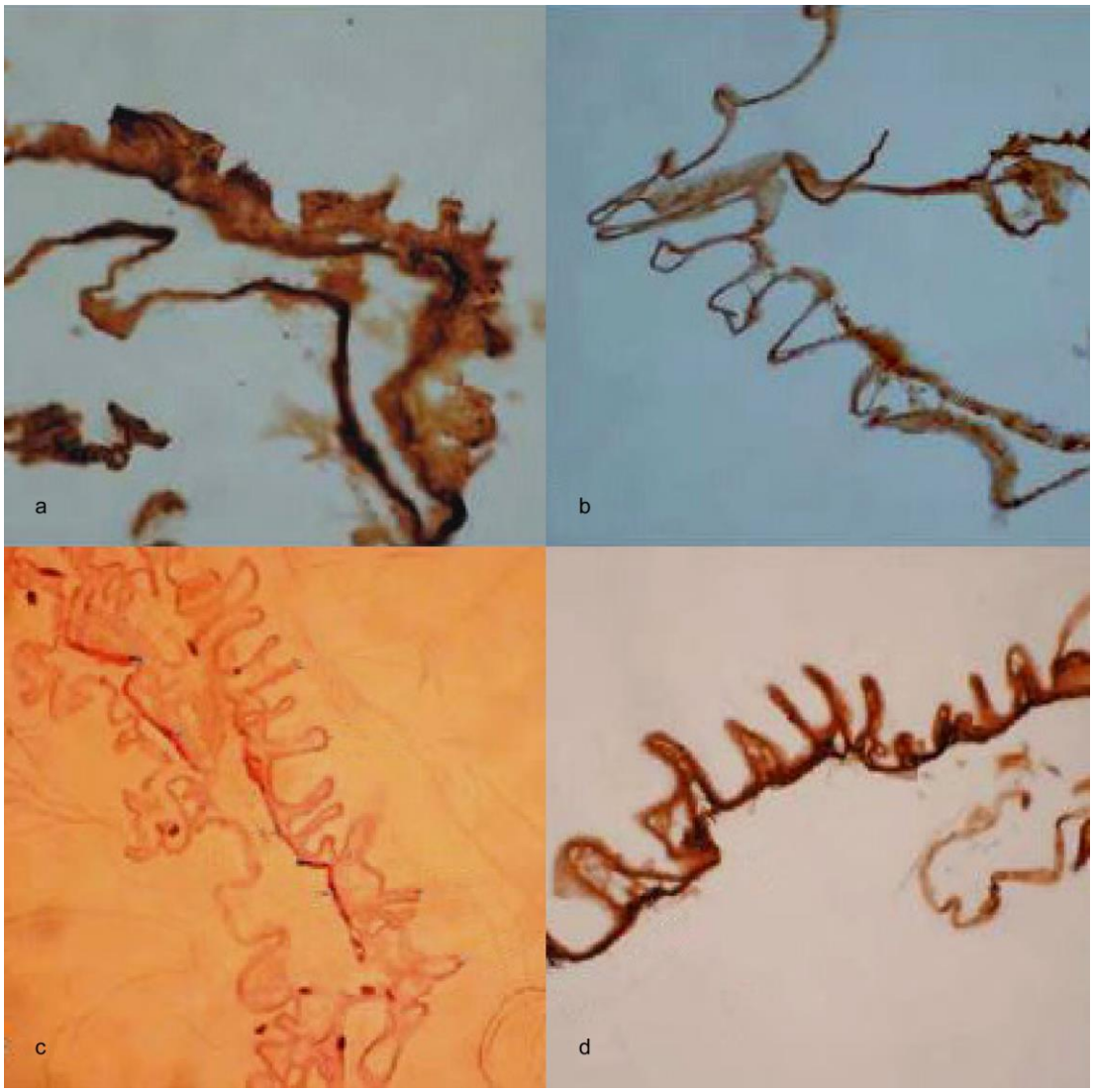

Figure 3-2 Hyperconvolution of the internal limiting membrane

Light micrographs demonstrating internal limiting membrane surgical specimens from: (a) and (b) macular pucker cases stained with anti-collagen IV antibody, note rounded nodules representing remodelling of duplicated basement membrane in (a) and hyperconvoluted segments with basement membrane duplications in (b) (x400), (c) and (d) cellophane maculopathy cases illustrating hyperconvolution and duplication of the internal limiting membrane, note haematoxylin and eosin staining in (c) and anti-collagen IV antibody staining in (d) (x400).

Images courtesy of Dr David Snead (Snead et al., 2004).

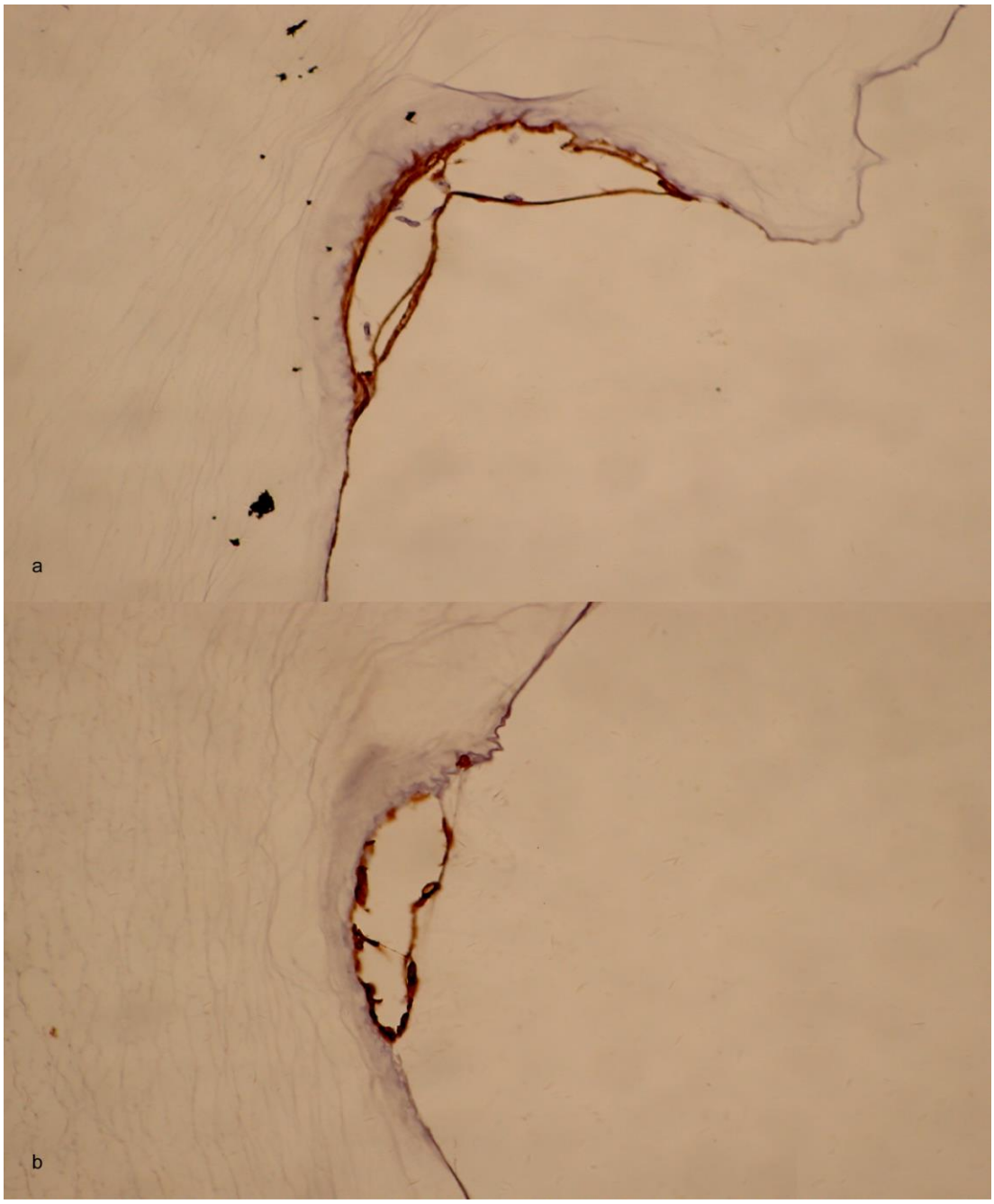

Figure 3-3 Duplications of the posterior hyaloid membrane

Light micrographs demonstrating focal duplication, thickening, contracture and schisis of the posterior hyaloid membrane in cadaveric globes which had ante-mortem clinical confirmation of uncomplicated senile posterior vitreous detachment, note laminocyte cells closely associated to membrane. Focal positive staining for (a) anti-collagen IV antibody and (b) anti-glial fibrillary acidic protein (GFAP) antibody (x400).

Images courtesy of Dr David Snead (Snead et al., 2004).

3.1.3 Posterior vitreous detachment and the posterior hyaloid membrane

The vitreous humour is the largest anatomical structure in the eye; it fills the posterior segment of the eye, occupying over three quarters of the total ocular volume. In common with connective tissues in the rest of the body, the vitreous is a collection of extracellular matrix components with a paucity of resident cells. Unlike other parts of the body, the vitreous has evolved to maintain an optically clear media given its critical position in the visual pathway (between the crystalline lens anteriorly and retina posteriorly).

Most mammals have a solid vitreous throughout life, however, there are a few primate species, such as the owl monkey (*Douroucoulis aotus trivirgatus*) and bush baby (*Galagidae*), that undergo physiological vitreous liquefaction as a developmental phenomenon before they reach adulthood (Balazs, 1973). Uniquely in humans, the vitreous undergoes a progressive morphological remodelling with an increase in fluid-filled lacunae (synchisis) (Foos and Wheeler, 1982) and an increase in collagenous condensations (syneresis) (Sebag, 1987) as part of the aging process. The vitreous, that is firmly adherent to the retina in youth, may undergo vitreoretinal dehiscence and detach from the surface of the retina during the process of posterior vitreous detachment.

Posterior vitreous detachment may be an asymptomatic finding in many patients, however, in those patients who are symptomatic, separation of the vitreous from the retina is associated with an acute onset of ‘flashes and floaters’; flashes refer to the pathognomonic features of temporal photopsia, described as a momentary arc of light in the lateral field of vision, whilst floaters refer to the subjective perception of the shadows cast onto the retina by vitreal opacities (Murakami et al., 1983; Snead et al., 2008).

Despite posterior vitreous detachment being a common ocular event that will affect the majority of individuals in an aging population (Akiba, 1993; Snead et al., 1994b; Weber-Krause and Eckardt, 1997), there is still little consensus regarding its precise definition. Review of the literature reveals two main theories:

1. Currently the predominantly accepted theory defines posterior vitreous detachment as the separation of the dense outer layer of type II collagen fibrils of the vitreous, known as the posterior vitreous cortex, from the internal

limiting membrane of the retina (American Academy of Ophthalmology Retina Panel, 2008; Kuhn and Aylward, 2014; Sebag, 1989; Stalmans et al., 2012; Steel and Lotery, 2013). Proponents of this concept advocate the term posterior hyaloid face to describe the outermost cortical layer of the vitreous. Clinical diagnosis of a suspected posterior vitreous detachment is based upon the classic patient history of reported new onset 'flashes and floaters', with or without the identification of epipapillary glial tissue torn form the optic nerve head (Weiss ring) noted in the posterior vitreous cortex on slit lamp biomicroscopy.

2. The less prevalent theory of posterior vitreous detachment defines the process as the separation of the vitreous and its enveloping posterior hyaloid membrane from the surface of the retina (Ang et al., 2005; Kakehashi et al., 2014; Snead et al., 2008). Proponents of this concept advocate the term posterior hyaloid membrane to describe the membranous structure encasing the detached vitreous (Figure 3-3, Figure 3-4 and Figure 3-5). Clinical diagnosis of a suspected posterior vitreous detachment is based upon the classic patient history of reported new onset 'flashes and floaters', in addition to the identification of a continuous, discrete, highly creased and refractile membranous sheet observed by slit lamp dynamic vitreous biomicroscopy with a wide illumination-observation angle (Figure 3-7 and Video Appendix 1.3). This theory considers the Weiss ring to be a defect in the posterior hyaloid membrane, surrounded by a cellular cuff of laminocyte cells that delineate the recent position of attachment to the optic nerve head (Figure 3-6). The posterior hyaloid membrane, which was not present prior to the posterior vitreous detachment (but apparent after) is considered by definition to arise from part of the internal limiting membrane on the surface of the retina in its attached state.

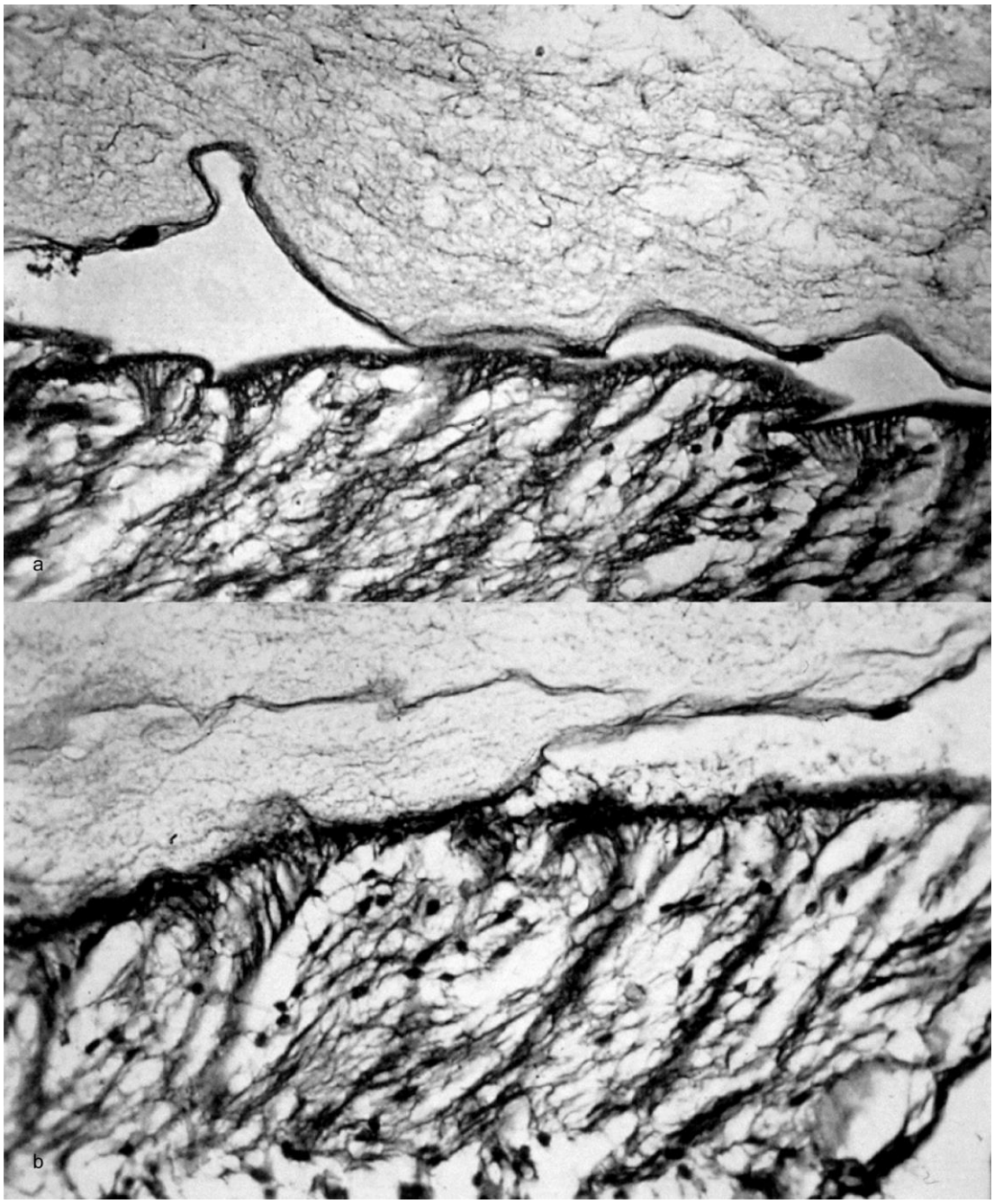

Figure 3-4 The posterior hyaloid membrane

Light micrographs presented by Zimmerman and Straatsma at the second conference of the Retina Foundation in 1958 to illustrate the concept of the posterior hyaloid membrane as a distinct and separate histological structure of the vitreoretinal interface; the presence of associated cells are noted, but no detailed account is given: (a) and (b) Rinehart-Abul-Haj stain (x305).

Reproduced with permission from Elsevier (Upminster Local History Group., 1960).

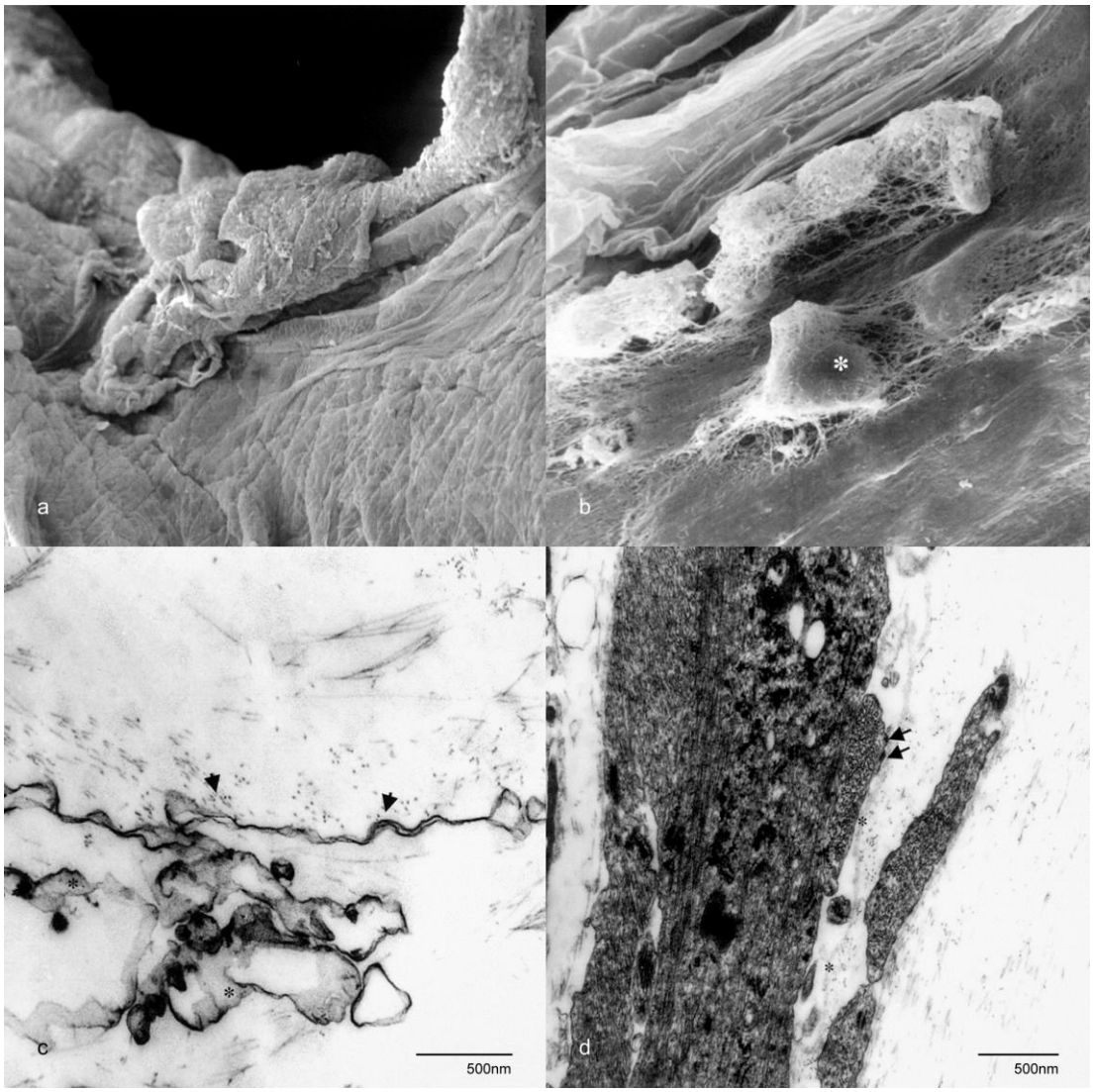

Figure 3-5 Electron microscopy of the posterior hyaloid membrane and associated laminocytes

Please turn over for figure legend

Figure 3-5 Electron microscopy of the posterior hyaloid membrane and associated laminocytes

Electron micrographs of posterior hyaloid membranes from donors with ante-mortem clinical confirmation of posterior vitreous detachment: (a) low magnification scanning electron micrograph of the posterior aspect of a detached Weiss ring, note the irregular coarse appearance of the retinal aspect of the posterior hyaloid membrane, in addition to cortical gel spilling over into the retrohyaloid space, (b) low magnification scanning electron micrograph demonstrating the smooth vitreal aspect of the posterior hyaloid membrane adjacent to areas of fibrillar cortical gel (* denotes a laminocyte cell), (c) high magnification transmission electron micrograph demonstrating a cross-section through extensively convoluted posterior hyaloid membrane (* denotes areas of membrane in tangential section and the arrows depict collagen fibrils on the vitreal aspect of the posterior hyaloid membrane), (d) high magnification transmission electron micrograph demonstrating laminocyte cellular component association with the posterior hyaloid membrane (* denotes the relationship of collagen fibrils to the posterior hyaloid membrane and the arrows denote hemi-desmosome attachment plaques).

Images courtesy of Mr Martin Snead (Snead et al., 2002).

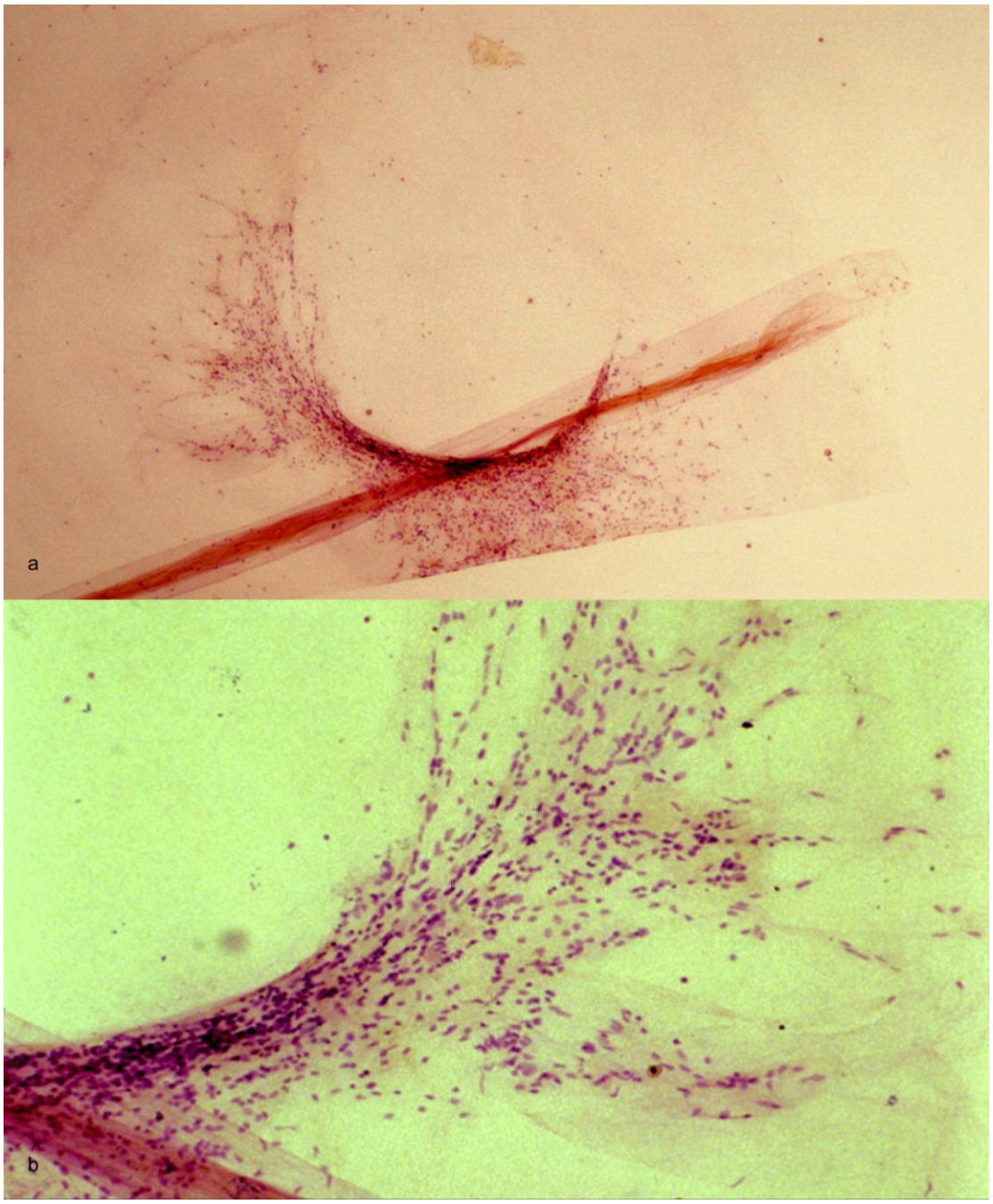

Figure 3-6 Histology of the Weiss ring

Light micrographs demonstrating a Weiss ring defect in flat mounted posterior hyaloid membranes: (a) and (b) stained with haematoxylin and eosin (x100, x200 respectively).

Images courtesy of Mr Martin Snead (Snead et al., 2002).

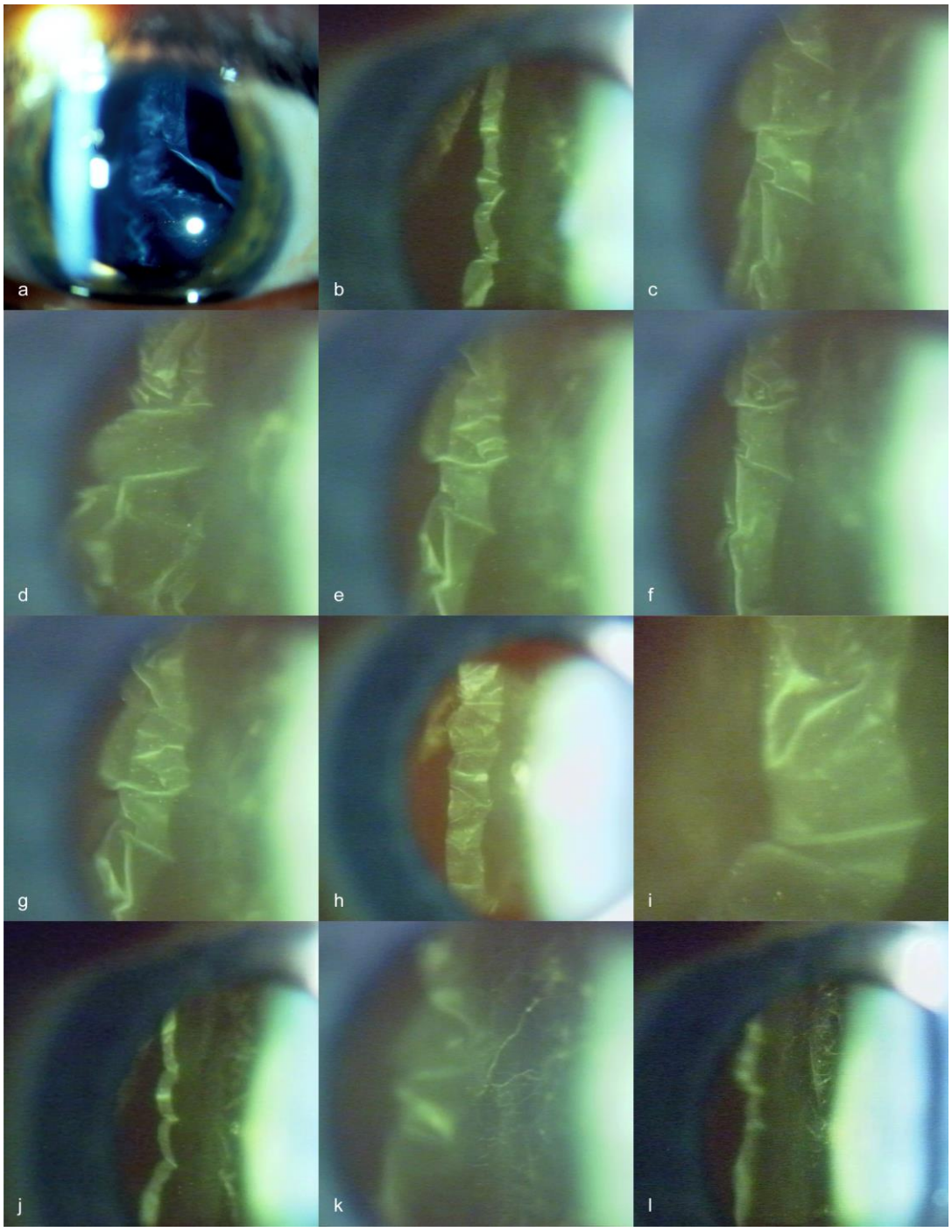

Figure 3-7 The clinical appearance of the posterior hyaloid membrane

Slit lamp biomicroscopy images demonstrating the clinical appearance of the posterior hyaloid membrane following posterior vitreous detachment, note the classic creased and crinkled topographical appearance, in addition to the vitreous fibrils anterior to the membrane in (j), (k) and (l) and the associated cells studded onto the surface of the membrane in (i).

Photographs courtesy of Dr Paul Meyer.

3.1.4 Laminocytes

Although the presence of cells intimately associated with the posterior hyaloid membrane has been apparent in published histological reports of the vitreoretinal interface for decades, little attention has been paid to their presence; this is surprising given their potentially important location with respect to the process of posterior vitreous detachment (Figure 3-4).

In 2002, Snead and colleagues proposed the term ‘laminocyte’ to be designated to the cell population integral to the posterior hyaloid membrane (Snead et al., 2002). The term was suggested to classify this distinct cellular population, emphasising their association with the basal lamina of the posterior hyaloid membrane, in addition to the laminar array pattern of distribution.

Light microscopy has demonstrated laminocytes to be spindle shaped cells with indistinct cytoplasm and oval or round nuclei. They are only seen abutting the posterior hyaloid membrane (Figure 3-3 and Figure 3-4) and have a classic distribution pattern, being most densely populated around the Weiss ring, becoming less densely populated peripherally (Figure 3-6). Electron microscopic investigations have confirmed the intimate relationship of laminocytes to the vitreal aspect of the posterior hyaloid membrane (Figure 3-5b and Figure 3-5d) (Snead et al., 2004, 2002, 2008).

Close inspection of the clinically detached posterior hyaloid membrane in vivo using slit lamp dynamic vitreous biomicroscopy with a wide illumination-observation angle, reveals the membrane to be studded with laminocyte cells that correlate to light microscopy findings in vitro (Figure 3-7i) (Snead et al., 2008).

Limited immunohistochemical interrogations of laminocytes in cadaveric globes (from donors with ante-mortem clinical confirmation of posterior vitreous detachment) have demonstrated focal and patchy staining of laminocytes with anti-glial fibrillary acidic protein (GFAP) antibodies that was reported to be variable in nature (Figure 3-3b); similarly, anti-collagen IV antibodies demonstrated focal and patchy staining to the associated posterior hyaloid membrane (Figure 3-3a). Evaluation of cadaveric globes without posterior vitreous detachment demonstrated weak positivity of the retinal internal limiting membrane for type IV collagen and a

monolayer of GFAP positive cells lining the vitreal aspect of the internal limiting membrane (Snead et al., 2004, 2002, 2008).

3.2 Hypothesis

The posterior hyaloid membrane may not be a condensation of posterior vitreous cortex commonly referred to as the posterior hyaloid face, but rather a true basement membrane or separately distinct structure that encases the extracellular matrix of the vitreous body. This basal lamina may separate from the surface of the retina during the process of posterior vitreous detachment and form as a result of dehiscence of the retinal internal limiting membrane.

Accounting for those elderly patients who never undergo posterior vitreous detachment and those young patients with intraocular inflammation who do (in addition to potentially explaining the reported acute onset of 'flashes and floaters' symptomatology), it is conceivable that posterior vitreous detachment may not be an entirely age related syneretic and synchitic process, but possibly a violent, biological event occurring in predisposed individuals. The laminocyte cell population integral to the posterior hyaloid membrane may contribute actively to posterior vitreous detachment and knowledge of their phenotypic lineage may add insight into the process.

In order to investigate the pathogenesis of retinal detachment, it is necessary to investigate the pathogenesis of posterior vitreous detachment; the primary objectives of this study are to investigate the histological correlate of the posterior hyaloid membrane observed clinically in patients presenting with a posterior vitreous detachment, in addition to interrogating the associated resident laminocyte cell population.

3.3 Material and methods

3.3.1 Ethical approval

This project was conducted following National Research Ethics Service approval (NRES 05/Q2802/77) and all investigations were conducted in accordance with the principles of the Declaration of Helsinki with regards to research on human tissue.

3.3.2 Globe tissue

Human eye globe tissue was supplied by the Corneal Transplant Service Eye Bank, University of Bristol, under a Material Transfer Agreement.

Following enucleation from consented organ donors, an 18mm corneoscleral button was trephined and the anterior chamber of the anterior segment removed for subsequent corneal transplantation surgery. The remaining globe tissue, comprised of all structures internal to and including the scleral coat posteriorly and iris anteriorly (Figure 3-8a), was fixed in 4% paraformaldehyde at 4°C for up to the five days during collection periods.

Globe tissues were transported by cold chain courier and upon receipt, repeatedly rinsed in cold phosphate buffered saline, cryoprotected in a 30% sucrose/phosphate buffered saline solution and frozen in acetone chilled in liquid nitrogen; frozen globes were stored at -80°C prior to being thawed on ice for dissection at room temperature.

3.3.3 Dissection protocol

Knowing previous studies have demonstrated that the cadaveric posterior vitreous detachment is consistent with, and a true representation of antemortem posterior vitreous detachment (Snead et al., 1994b, 2002), a dissection technique was developed in order to isolate posterior hyaloid membranes from donated eye globe tissue for immunological investigations.

Dissection technique

Dissection commenced with a circumferential, full thickness scleral coat incision into the suprachoroidal space; the incision was placed posteriorly around the optic nerve stalk (Figure 3-8b). Anteriorly, the iris was removed circumferentially at its root (Figure 3-8c) and the prolapsing anterior vitreous trimmed to remove retrolenticular membranes. The suprachoroidal spaced was entered anteriorly and blunt-dissected posteriorly towards the initial peripapillary scleral incision. Radial full thickness scleral incisions (connecting the anterior scleral edge to the posterior peripapillary incision) facilitated removal of the scleral coat from the remaining eviscerated vitreous body, covered by retina and choroid, and attached posteriorly to the optic nerve stalk and surrounding rim of scleral tissue (Figure 3-8d).

Posterior vitreous detachment status evaluation

To evaluate posterior vitreous detachment status, a modification to the 'suspended-in-air examination', originally described by Foos (Foos, 1972b) was employed. Instead of sectioning a globe by longitudinal section into two halves that were suspended in air, the modified air suspension technique assessed the shape of the eviscerated contents whilst suspended in air from the optic nerve stalk remnant; this was done before and after removal of the choroid (Figure 3-9a, Figure 3-9b and Figure 3-9c, Figure 3-9d respectively).

Air-suspended eviscerated globe tissue with a posterior vitreous detachment formed a 'long-necked conical flask' configuration (Figure 3-9a and Figure 3-9c) compared to a rounded 'bell jar' configuration (Figure 3-9b and Figure 3-9d) observed in those without posterior vitreous detachment.

Posterior hyaloid membrane isolation

Eviscerated globe tissue deemed to have a posterior vitreous detachment was selected for further dissection.

In these cases the posterior circumferential attachment of the retina to the detached vitreous was frequently observed to be unable to support the weight of the vitreous

body when re-suspended and would spontaneously tear along this region of attachment (the junction of the ‘neck’ and ‘body’ in the ‘long-necked flask’ analogy, Figure 3-10a). Cases where the retina was able to support the weight of the vitreous body were incised at this junction.

The final configuration of the dissected globe tissue before isolation of the posterior hyaloid membrane comprised the vitreous body, surrounded by an annulus of adherent retina anteriorly and with the transparent posterior pole of the vitreous body exposed posteriorly (Figure 3-10b). Posterior to anterior 18mm trephination through the vitreous body allowed removal of the anterior annulus of retinal tissue and peripheral anterior vitreous gel (Figure 3-10c), resulting in a core of clear vitreous gel with its associated posterior hyaloid membrane lining the posterior vitreous face (Figure 3-10d).

The trephined gel core was examined using a Zeiss Primo Vert phase contrast light microscope to identify the posterior hyaloid membrane; posterior hyaloid membranes were readily identified as distinct creased and crinkled refractile sheets on the posterior surface of the trephined gel core.

Under direct phase visualisation, the vitreous body was debulked and the posterior hyaloid membrane divided to facilitate later slide mounting. Isolated posterior hyaloid membranes fragments were stored in phosphate buffered saline at 4°C prior to immunohistochemical staining.

3.3.4 Retinal internal limiting membrane isolation

In order to interrogate the surface of the retina following posterior vitreous detachment, posterior pole retinal tissue collected from globe tissue evaluated to have undergone posterior vitreous detachment (Figure 3-9c and Figure 3-10a) was collected and stored in phosphate buffered saline (PBS) at 4°C prior to immunohistochemical staining and flat mount preparation for examination.

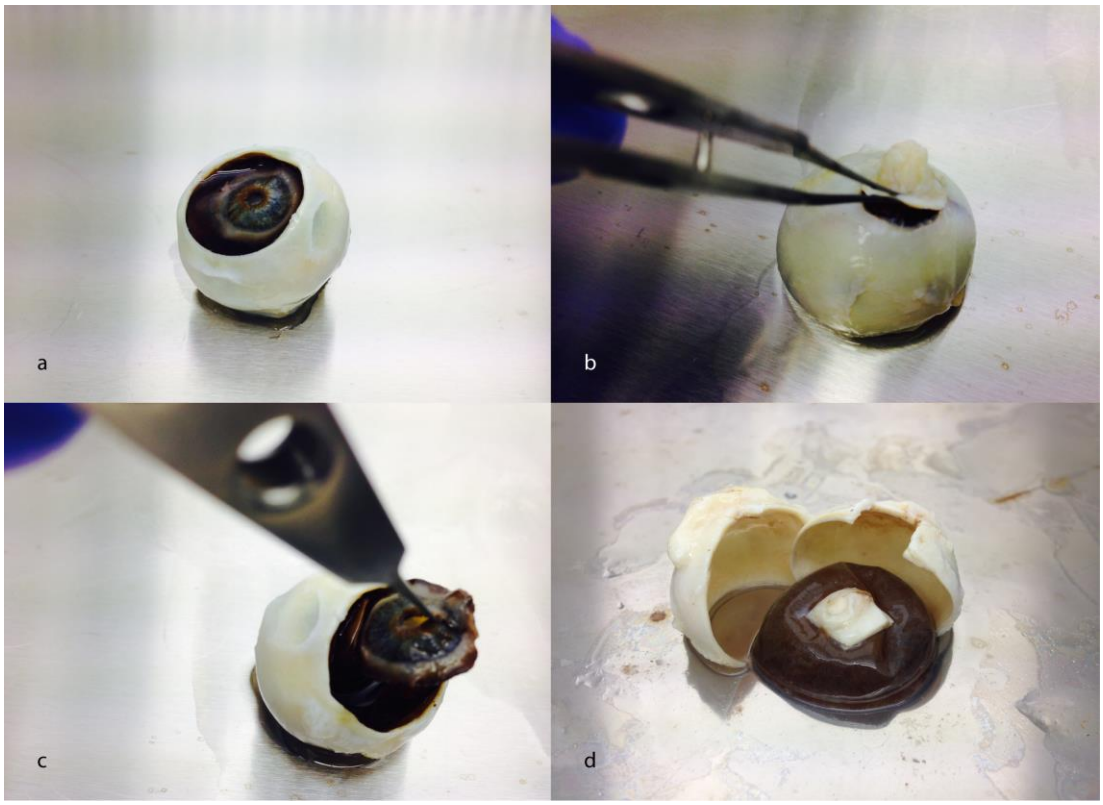

Figure 3-8 Dissection technique

Colour photographs demonstrating: (a) globe tissue as received from the Corneal Transplant Service Eye Bank prior to dissection, (b) peripapillary full thickness scleral incision entering suprachoroidal space, (c) circumferential iris root incision, (d) radial scleral incisions facilitating removal of scleral coat from the eviscerated vitreous body (enveloped by retina and choroid but remaining attached to the optic nerve stalk posteriorly).

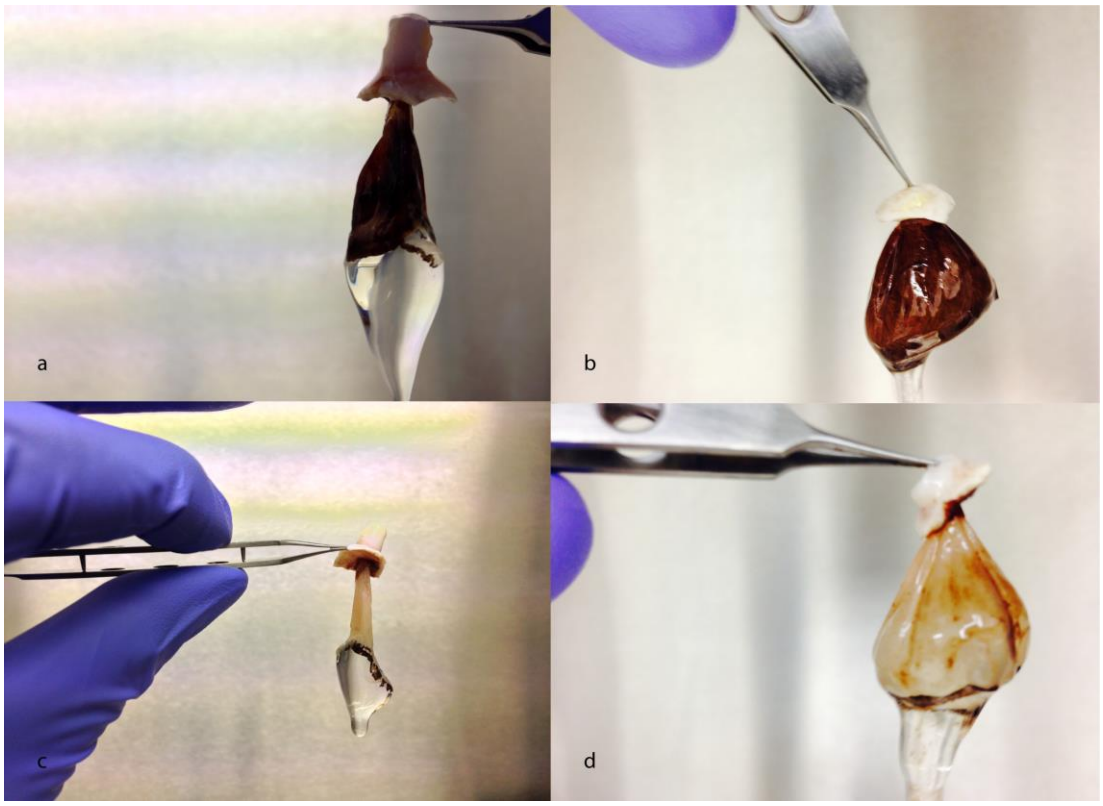

Figure 3-9 Posterior vitreous detachment evaluation

Colour photographs demonstrating the modified air suspension technique: (a) eviscerated globe tissue with surrounding choroidal coat demonstrating the ‘long-necked conical flask’ configuration (detached posterior hyaloid membrane), (b) eviscerated globe tissue with surrounding choroidal coat demonstrating the ‘bell jar’ configuration (attached posterior hyaloid membrane), (c) eviscerated globe tissue following choroidal coat removal confirming the ‘long-necked conical flask’ configuration (detached posterior hyaloid membrane), (d) eviscerated globe tissue following choroidal coat removal confirming the ‘bell jar’ configuration (attached posterior hyaloid membrane).

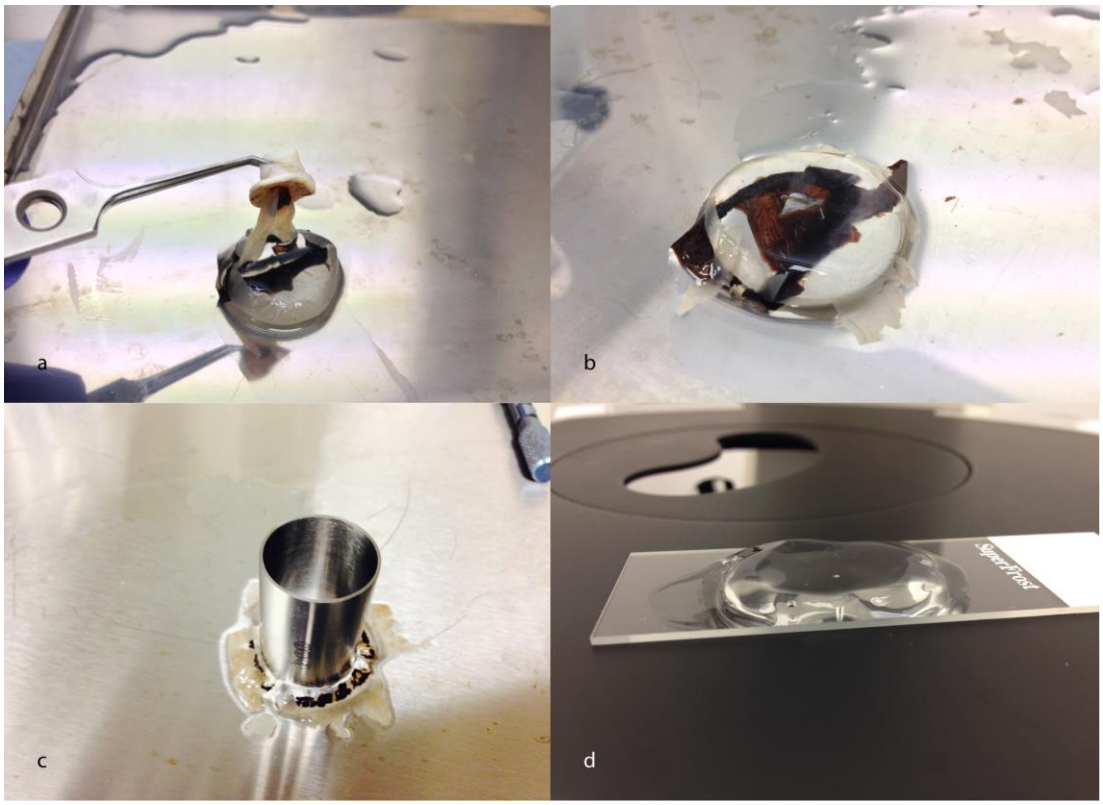

Figure 3-10 Posterior hyaloid membrane isolation

Colour photographs demonstrating: (a) the inability of the enveloping retina to support the weight of the vitreous body when re-suspended in air; (b) the vitreous body surrounded by an annulus of adherent retina anteriorly and the transparent posterior pole of the vitreous body exposed posteriorly; (c) 18mm trephination through the central vitreous body; (d) clear vitreous gel core with associated posterior hyaloid membrane lining the posterior vitreous face.

3.3.5 Control tissue

Control tissues were obtained from human kidney, tonsil, brain, skin, and hyaline cartilage, and supplied by the Arden Tissue Bank, University Hospital Coventry, under a Material Transfer Agreement. Optic nerve and retinal control tissues were obtained from randomly selected human globe tissue prior to dissection (Section 3.3.1).

Mirroring globe tissue fixation and processing, control tissues were fixed in 4% paraformaldehyde at 4°C, repeatedly washed in PBS and cryoprotected in a 30% sucrose/PBS prior to freezing in acetone chilled in liquid nitrogen.

Cryosections were cut using a Leica CM-1850 Cryostat at -20°C after embedding in OCT™ (Tissue-Tek®) and then mounted on positively charged Leica X-tra™ Adhesive slides. Frozen tissue sections were cut at 10µm, except for retina, which was cut from a central calotte of frozen globe tissue as 40µm sagittal sections through the optic nerve head to preserve architecture. Cut sections were stored at -80°C prior to being thawed at 4°C for immunohistochemical staining.

3.3.6 Immunohistochemistry

Isolated posterior hyaloid membranes were stained free floating in 24 well plates; positive control tissues were stained on slides using conventional immunofluorescent techniques.

Staining protocol

Prior to staining, all tissues were blocked and permeablised overnight at 4°C in PBS with 1:20 donkey serum, 0.5% bovine serum albumin and 0.1% Triton™ X-100, which was also used for all washes and to dilute antibodies. Primary and secondary antibodies were sequentially incubated over consecutive nights at 4°C; three blocking solution washes were performed before and after secondary antibody incubation. 6.25mg/ml 4',6-diamidino-2-phenylindole (DAPI) was used to stain nuclei before tissues were mounted in a prepared water-based mounting medium (6g glycerol, 2.4g Moviol 4-88, 6ml nuclease-free water and 12ml

tris(hydroxymethyl)aminomethane buffer) and covered with Leica Surgipath® coverslips.

Antibodies for immunophenotyping

Primary antibodies raised against collagen IV, laminin and fibronectin were selected to immunophenotype basement membranes. Primary antibodies raised against opticin were selected to immunophenotype vitreous gel.

To investigate laminocyte immunophenotype, primary antibodies raised against cluster of differentiation (CD) 11 (leucocyte marker), CD68 (monocyte/macrophage marker), cellular retinaldehyde-binding protein (CRALBP) (Müller glia marker), pan-cytokeratin (epithelial marker), ezrin (retinal pigment epithelium marker), ionized calcium-binding adapter molecule 1 (Iba1) (macrophage/microglial marker), GFAP (astrocyte/Müller glia marker), major histocompatibility complex (MHC) class II (macrophage/antigen presenting cell marker), S100 calcium binding protein B (S100B) (astrocyte/Müller glia marker) and vimentin (mesenchymal/fibroblast/astrocyte/Müller glia marker) were selected.

Antibody concentrations were based on the recommended dilutions reported in similar immunofluorescent applications; concentrations were optimised using serial dilutions.

Details of primary and secondary antibody sources and dilutions are shown in Table 3-1 and Table 3-2.

Table 3-1 Primary antibodies

Primary antibody	Manufacturer	Catalog #	Species	Dilution
Basement membrane markers				
Anti-collagen IV	Abcam	ab6586	Rabbit polyclonal	1:100
Anti-fibronectin	Abcam	ab26245	Mouse monoclonal [A17]	1:100
Anti-laminin	Abcam	ab11575	Rabbit polyclonal	1:200
Vitreous gel markers				
Anti-opticin	Abcam	ab170886	Rabbit monoclonal [EPR11980(B)]	1:250
Cell phenotype markers				
Anti-CD11b	Abcam	ab63317	Mouse monoclonal [2Q902]	1:200
Anti-CD68	DAKO	M0718	Mouse monoclonal [EBM11]	1:200
Anti-CRALBP	Abcam	ab15051	Mouse monoclonal [B2]	1:200
Anti-cytokeratin	DAKO	M3515	Mouse monoclonal [AE1/AE3]	1:50
Anti-ezrin	Sigma-Aldrich	E8897	Mouse monoclonal [3C12]	1:10000
Anti-GFAP	DAKO	Z0334	Rabbit polyclonal	1:500
Anti-Iba1	Abcam	ab5076	Goat polyclonal	1:100
Anti-MHC class II	Abcam	ab55152	Mouse monoclonal [6C6]	10ug/ml
Anti-S100B	Abcam	ab11178	Mouse monoclonal [SH-B1]	1:1000
Anti-vimentin	DAKO	M7020	Mouse monoclonal [Vim3B4]	1:500

CD denotes cluster of differentiation
CRALBP denotes cellular retinaldehyde-binding protein
GFAP denotes glial fibrillary acidic protein
Iba1 denotes ionized calcium-binding adapter molecule 1
MHC denotes major histocompatibility complex
S100B denotes S100 calcium binding protein B

Table 3-2 Secondary antibodies

Secondary antibody	Manufacturer	Catalog #	Species	Dilution
Alexa Fluor® 488	Life Technologies	A21202	Donkey anti-Mouse	1:500
Alexa Fluor® 568	Life Technologies	A10042	Donkey anti-Rabbit	1:500
Alexa Fluor® 647	Life Technologies	A21447	Donkey anti-Goat	1:250

3.3.7 Confocal microscopy

Digital confocal micrograph images were acquired on a Zeiss Observer Z1 inverted LSM 700 Confocal Laser Scanning Microscope. Separation of fluorescence signals by sequential laser frequency excitation at 400nm, 440nm, 470nm and 535nm prevented multi-channel crosstalk. Generated .lsm data files were processed with Carl Zeiss ZEN 2012 SP1 (black edition) software.

Scanning protocols included phase and confocal low magnification (EC Plan-Neofluar® 10x0.30 Ph1 M27 Objective) composite tile scans to ascertain global topography of posterior hyaloid membrane specimens, in addition to phase and confocal high magnification (EC Plan-Apochromat® 63x1.40 Oil Ph3 M27 Objective) z-stack imaging to identify laminocyte cell candidates.

In order to categorise an eligible subpopulation of cells as laminocytes, efforts were made to identify cells that occupied an expected and intrinsically associated relation to the posterior hyaloid membrane.

Posterior hyaloid membranes, vitreous gel and identified laminocyte cells were immunologically phenotyped using the selected panel of primary antibodies detailed in Table 3-1.

3.4 Results

In all reported confocal micrograph images primary antibodies raised in mice, rabbit and goat species are pseudocoloured green, red and magenta respectively; DAPI nuclear staining is pseudocoloured blue.

Positive and negative antibody control figures are cross-referenced to Appendix 6.1 and Appendix 6.2 respectively.

3.4.1 Phase contrast microscopy of the posterior hyaloid membrane

Isolated posterior hyaloid membranes were consistently identified as distinct, creased and crinkled glassy sheets on phase contrast microscopy (Figure 3-11a). Residual attached vitreous gel had a rucked and undulating appearance (Figure 3-11b and Figure 3-11c) but was readily distinguishable from the adjacent posterior hyaloid membrane which was phase dense with definitive sharp cut edges (Figure 3-11d).

Physically manipulating samplings under direct phase contrast microscopy visualisation further demonstrated differences between the posterior hyaloid membrane and the vitreous gel; the membrane component was relatively inflexible and reluctant to unfold, preferring to remain in a crumpled orientation, whilst the gel component had a pliable and elastic nature, returning to its original orientation after being handled.

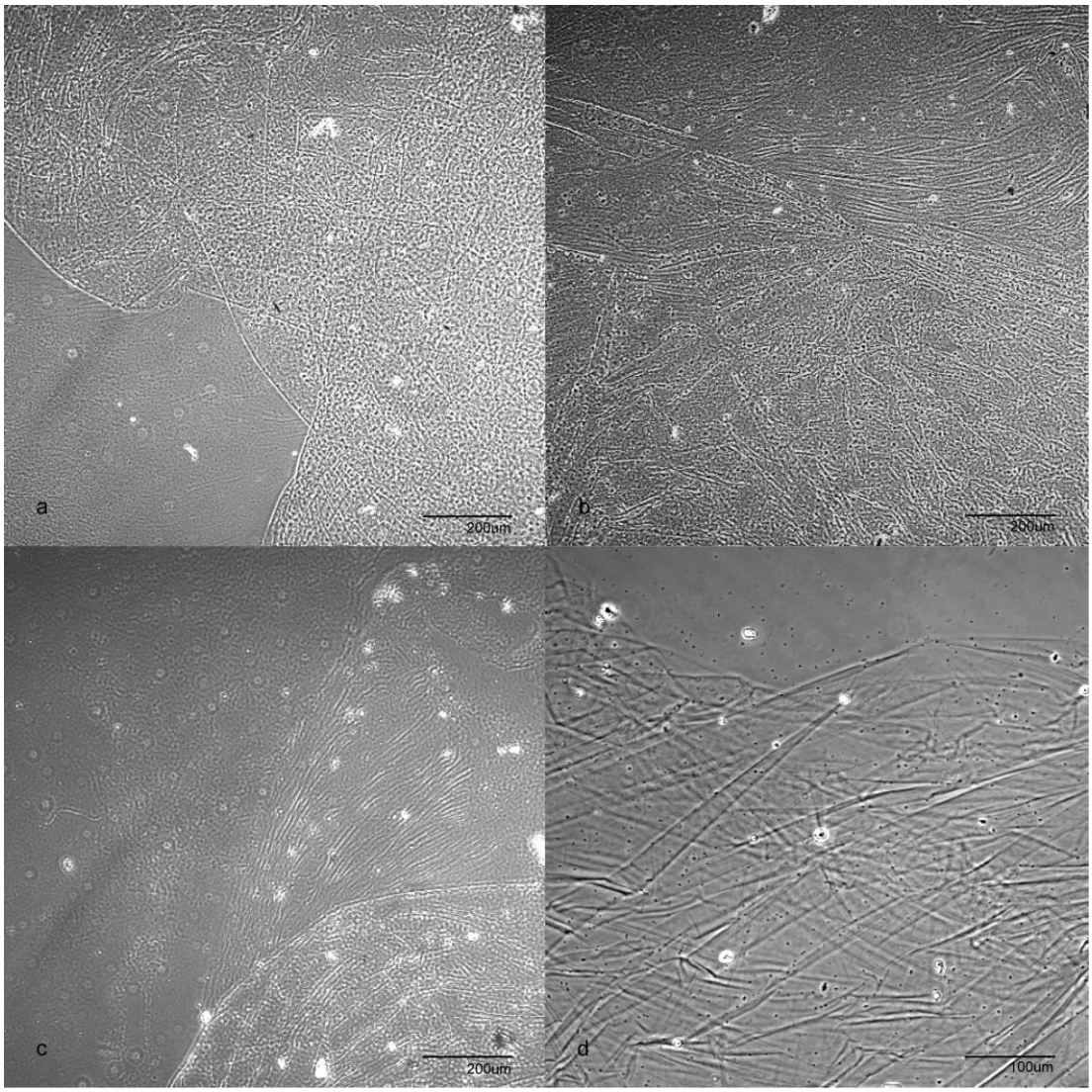

Figure 3-11 Posterior hyaloid membrane phase contrast microscopy

Phase contrast micrograph series demonstrating: (a) glassy, phase-dense appearance of the posterior hyaloid membrane (x5), (b) rippled vitreous gel appearance (upper right corner) adjacent to the posterior hyaloid membrane (lower half of image) (x5), (c) distinct boundary between vitreous gel (upper right corner) and posterior hyaloid membrane (lower right corner) (x5), (d) high power view illustrating a definitive cut edge of the posterior hyaloid membrane (x10).

3.4.2 Basement membrane immunohistochemistry

Posterior hyaloid membrane immunostaining for collagen IV

Isolated posterior hyaloid membrane specimens consistently demonstrated positive immunofluorescence with rabbit polyclonal anti-collagen IV antibodies. Immunofluorescent images characterised membranous sheets with definitive sharp cut edges (Figure 3-12a and Figure 3-12b). Surface topography micrographs revealed the membrane to have a highly creased and crinkled appearance (Figure 3-12c).

Z-stack cross-section confocal analysis (Figure 3-12d) and three-dimensional image reconstructions demonstrated a smooth configuration to the vitreal aspect (Figure 3-12e) and an irregular coarse configuration to the retinal aspect (Figure 3-12f) of the posterior hyaloid membrane.

See Appendix Figure 6-1 for anti-collagen IV antibody positive controls and Appendix Figure 6-15c and Figure 6-15d for posterior hyaloid membrane negative controls.

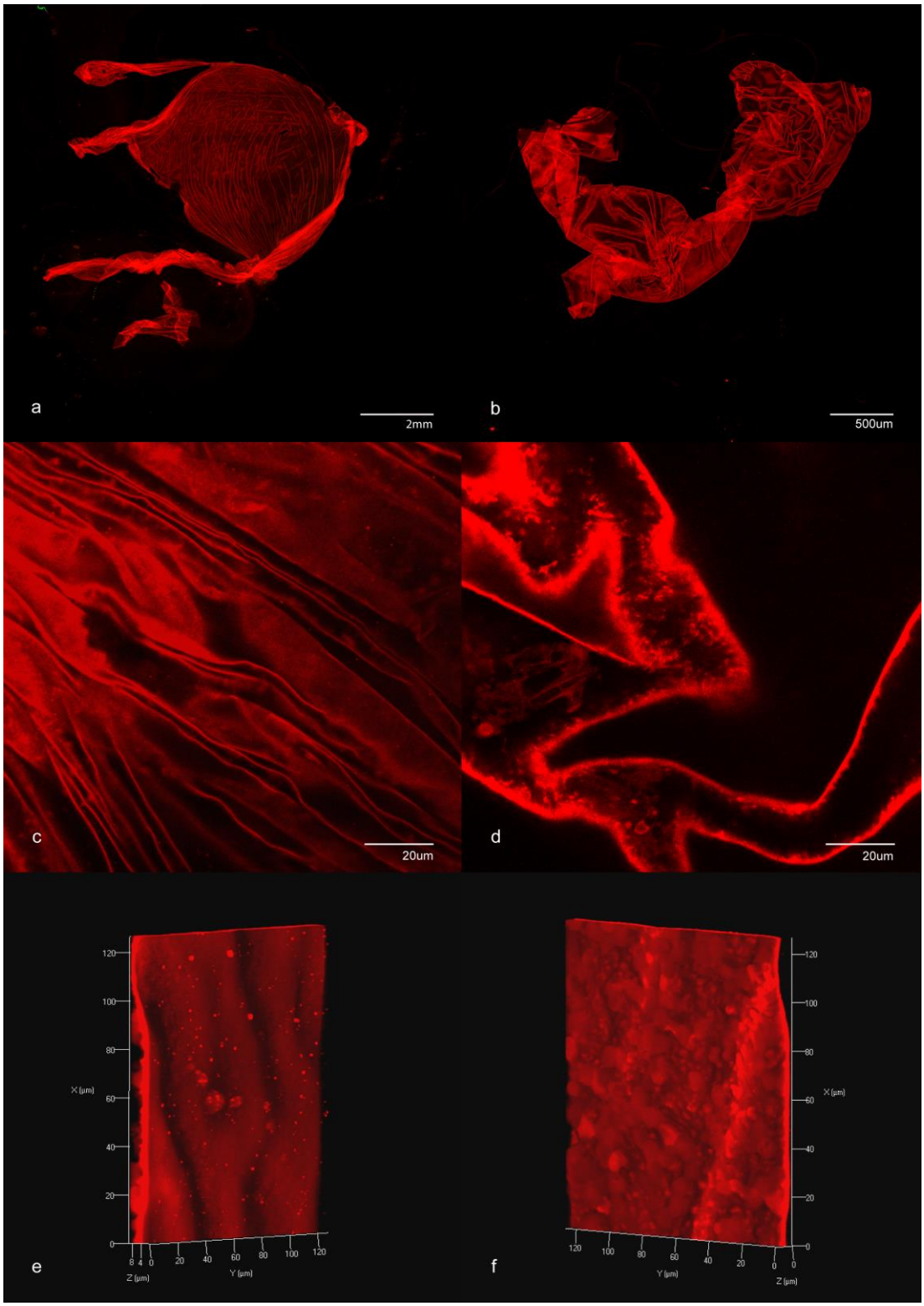

Figure 3-12 Posterior hyaloid membrane immunohistochemistry: collagen IV

Please turn over for figure legend

Figure 3-12 Posterior hyaloid membrane immunohistochemistry: collagen IV

Posterior hyaloid membrane confocal micrograph series stained with antibodies to collagen IV (red fluorescence, Alexa Fluor® 568) demonstrating: (a) 10x10 tile scan (x5), (b) 3x3 tile scan (x5), (c) surface topography (x63), (d) z-stack cross-section through membrane fold (x63), (e) and (f) z-stack three-dimensional image reconstructions illustrating smooth vitreal aspect and coarse retinal aspect of the posterior hyaloid membrane respectively.

Posterior hyaloid membrane immunostaining for laminin

Isolated posterior hyaloid membrane specimens consistently demonstrated positive immunofluorescence with rabbit polyclonal anti-laminin antibodies. Immunofluorescent images characterised membranous sheets with definitive sharp cut edges (Figure 3-13a and Figure 3-13b). Surface topography micrographs revealed the membrane to have a highly creased and crinkled appearance (Figure 3-13c).

Z-stack cross-section confocal analysis (Figure 3-13d) and three-dimensional image reconstructions demonstrated a smooth configuration to the vitreal aspect (Figure 3-13e) and an irregular coarse configuration to the retinal aspect (Figure 3-13f) of the posterior hyaloid membrane.

See Appendix Figure 6-2 for anti-laminin antibody positive controls and Appendix Figure 6-15c and Figure 6-15d for posterior hyaloid membrane negative controls.

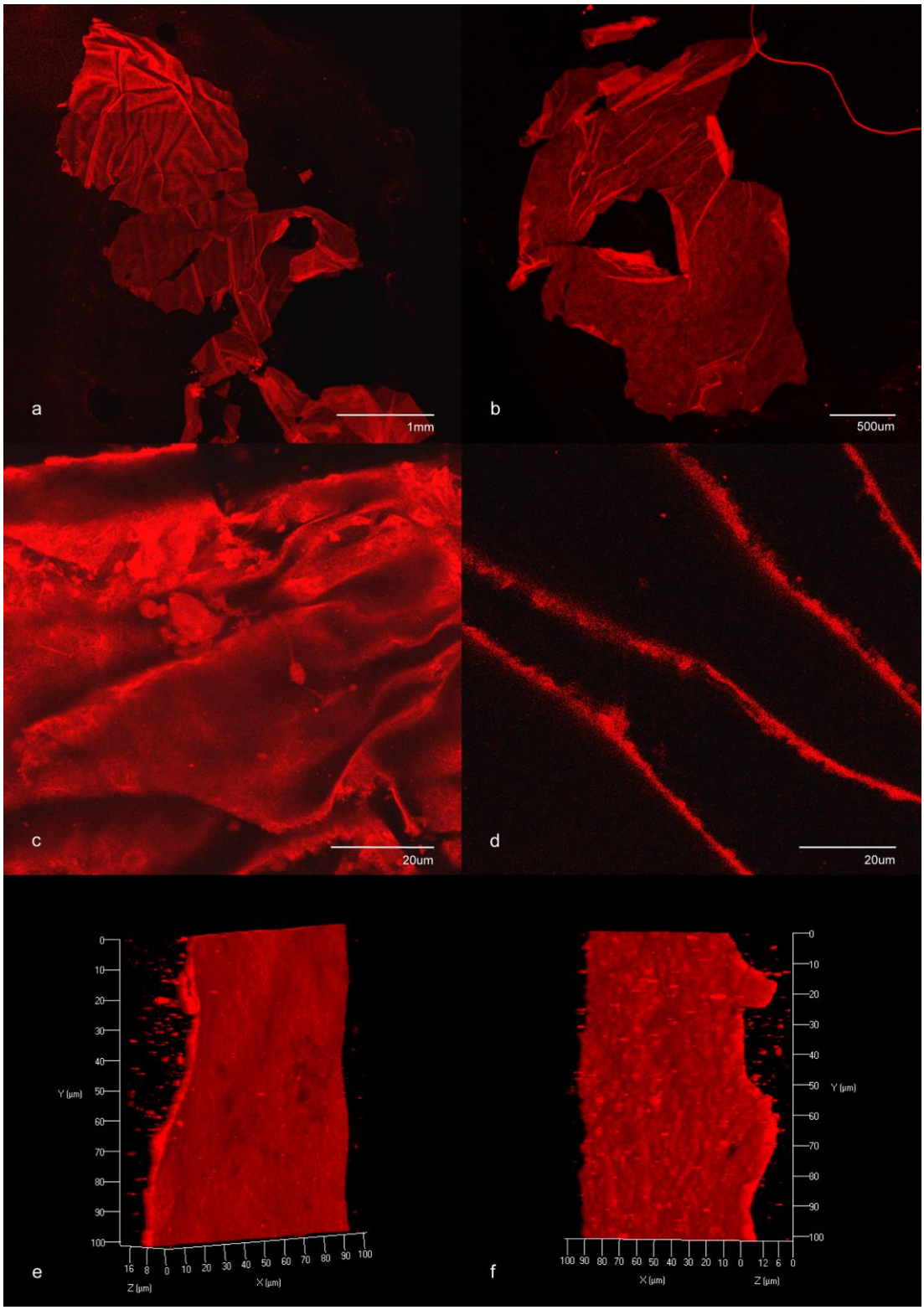

Figure 3-13 Posterior hyaloid membrane immunohistochemistry: laminin

Please turn over for figure legend

Figure 3-13 Posterior hyaloid membrane immunohistochemistry: laminin

Posterior hyaloid membrane confocal micrograph series stained with antibodies to laminin (red fluorescence, Alexa Fluor® 568) demonstrating: (a) 5x5 tile scan (x5), (b) 3x3 tile scan (x5), (c) surface topography (x63), (d) z-stack cross-section through membrane fold (x63), (e) and (f) z-stack three-dimensional image reconstructions illustrating smooth vitreal aspect and coarse retinal aspect of the posterior hyaloid membrane respectively.

Posterior hyaloid membrane immunostaining for fibronectin

Isolated posterior hyaloid membrane specimens consistently demonstrated positive immunofluorescence with mouse monoclonal anti-fibronectin antibodies. Staining was not restricted to membranes with immunofluorescent images characterising membranous sheets with definitive sharp cut edges, in addition to non-specific delineation of residually attached vitreous gel (Figure 3-14a and Figure 3-14b).

Z-stack cross-section confocal analysis reiterated the anti-fibronectin antibody binding pattern to the posterior hyaloid membrane and vitreous gel (Figure 3-14c and Figure 3-14d), however, both aspects of the membrane appeared smooth with no observed irregular coarse configuration to the retinal aspect as delineated with anti-collagen IV and anti-laminin antibodies (Figure 3-12d and Figure 3-13d respectively). Three-dimensional image reconstructions confirmed a smooth configuration to the retinal aspect (Figure 3-14e) and a granular non-specific gel staining to the vitreal aspect (Figure 3-14f) of the posterior hyaloid membrane.

See Appendix Figure 6-3 for anti-fibronectin antibody positive controls and Appendix Figure 6-15a and Figure 6-15b for posterior hyaloid membrane negative controls.

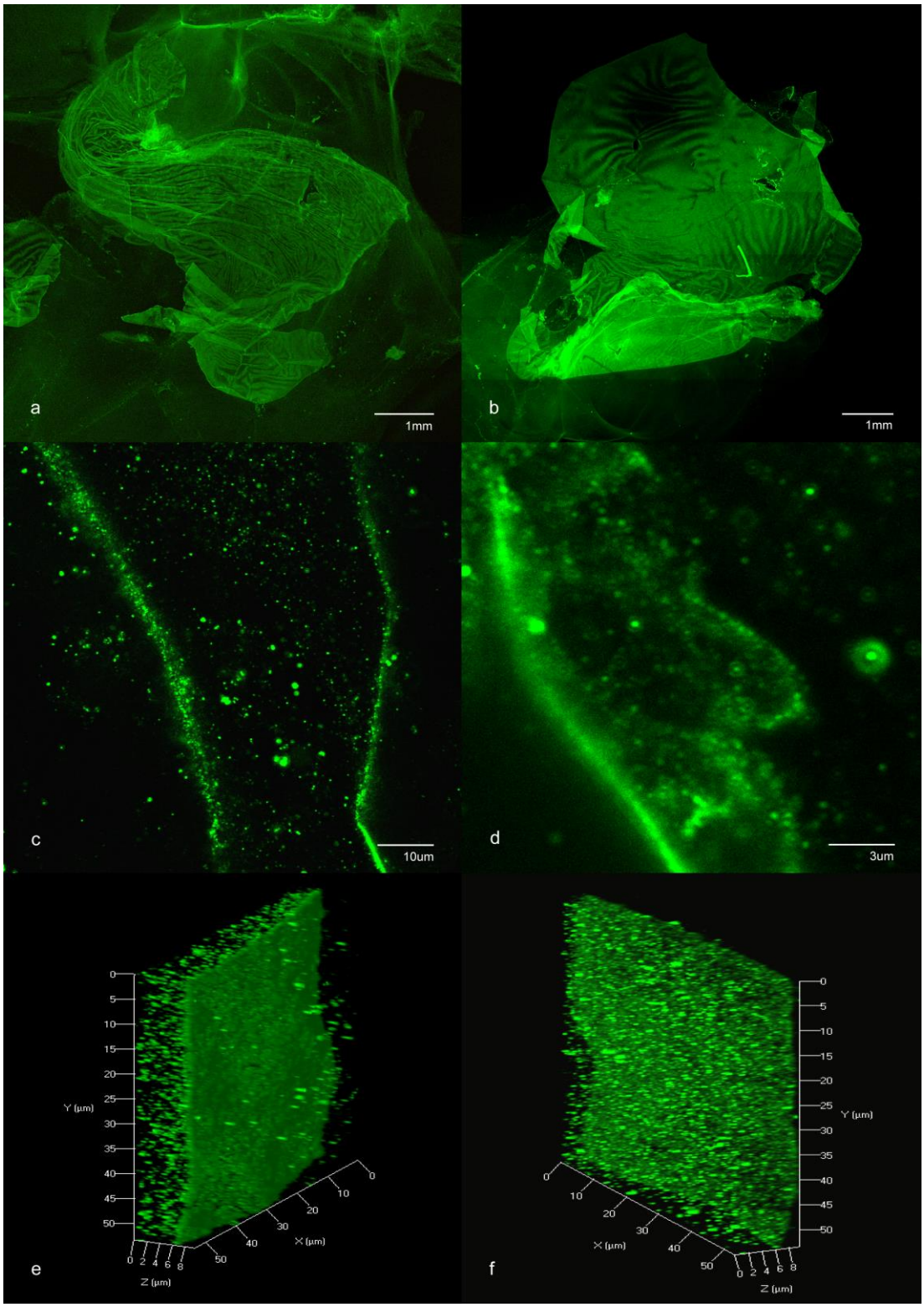

Figure 3-14 Posterior hyaloid membrane immunohistochemistry: fibronectin

Please turn over for figure legend

Figure 3-14 Posterior hyaloid membrane immunohistochemistry: fibronectin

Posterior hyaloid membrane confocal micrograph series stained with antibodies to fibronectin (green fluorescence, Alexa Fluor® 488) demonstrating: (a) 6x6 tile scan (x5), (b) 7x7 tile scan (x5), (c) z-stack cross-section through membrane fold and vitreous gel (x81.9), (d) z-stack cross-section through membrane fold and vitreous gel (x308.7), (e) and (f) z-stack three-dimensional image reconstructions illustrating smooth retinal aspect of the posterior hyaloid membrane and a non-specific gel staining on the vitreal aspect respectively.

3.4.3 Vitreous gel immunohistochemistry

Vitreous gel immunostaining for opticin

Vitreous gel consistently demonstrated positive immunofluorescence with rabbit monoclonal anti-opticin antibodies. Staining delineated individual vitreous gel fibrils (Figure 3-15a and Figure 3-15b).

Z-stack cross-section confocal analysis reiterated the anti-opticin antibody binding pattern to the posterior hyaloid membrane and vitreous gel with a distinct condensation of vitreal fibres observed at the gel-membrane interface (Figure 3-15c and Figure 3-15d). Three-dimensional image reconstructions demonstrated a smooth configuration to the vitreal and retinal aspect of the gel-membrane interface that mirrored the folds and convolutions of the underlying posterior hyaloid membrane (Figure 3-15e and Figure 3-15f respectively). There was no irregular coarse configuration to the retinal aspect of this interface as observed with anti-collagen IV and anti-laminin antibodies (Figure 3-12d and Figure 3-13d respectively).

See Appendix Figure 6-4 for anti-opticin antibody positive controls and Appendix Figure 6-15c and Figure 6-15d for posterior hyaloid membrane negative controls.

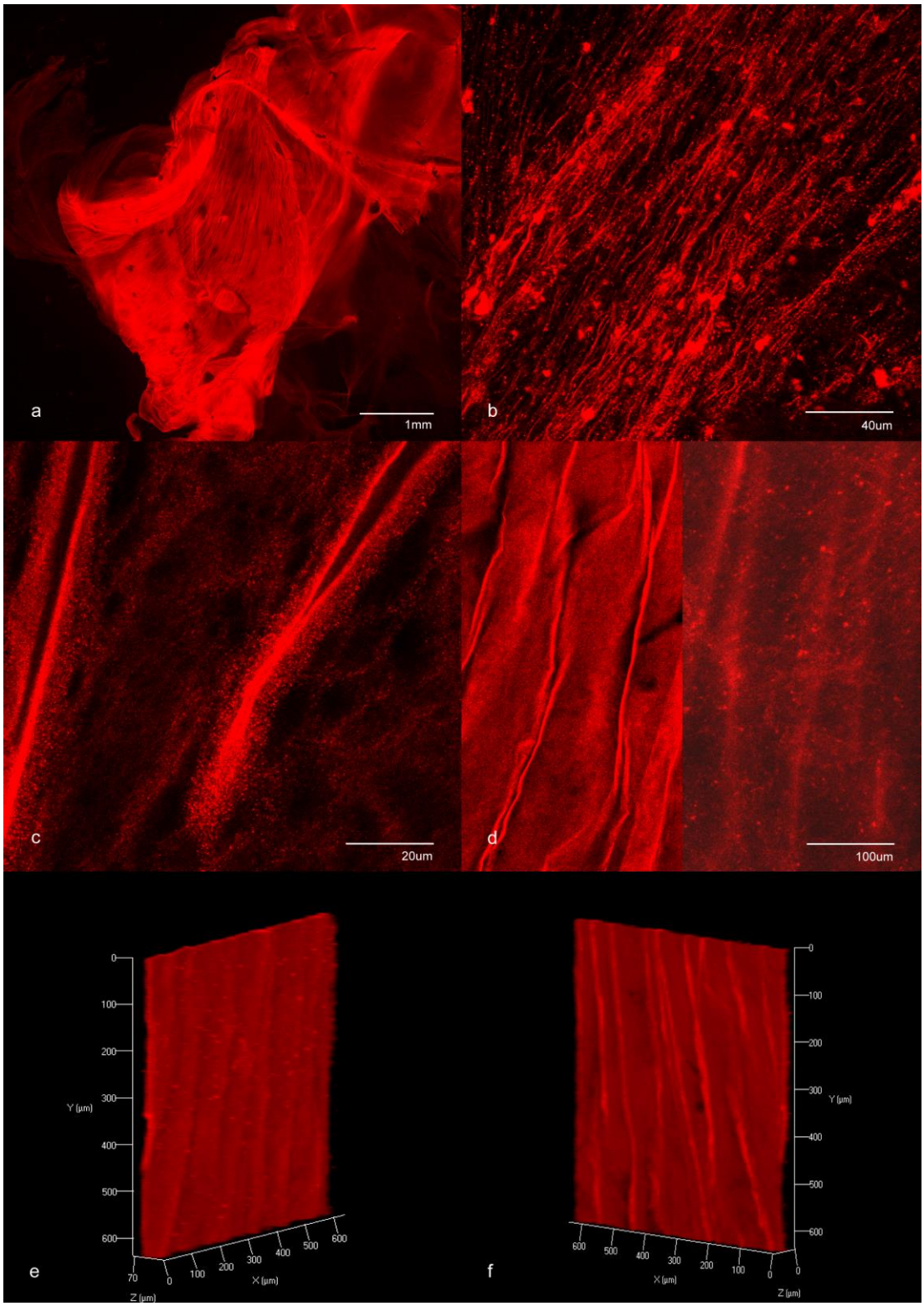

Figure 3-15 Posterior hyaloid membrane and vitreous gel immunohistochemistry: opticin

Please turn over for figure legend

Figure 3-15 Posterior hyaloid membrane and vitreous gel immunohistochemistry: opticin

Posterior hyaloid membrane and vitreous gel confocal micrograph series micrographs stained with antibodies to opticin (red fluorescence, Alexa Fluor® 568) demonstrating: (a) 5x5 tile scan (x5), (b) vitreous fibres (x31.5), (c) z-stack cross-section through membrane fold and vitreous gel (x63), (d) z-stack surface topography of retinal aspect of membrane (left panel) with corresponding gel-membrane interface cross-section (right panel) (x10), (e) and (f) z-stack three-dimensional image reconstructions illustrating smooth vitreal and retinal aspects of the gel interface and posterior hyaloid membrane respectively.

3.4.4 Posterior hyaloid membrane and associated retinal macroglia marker immunohistochemistry

Posterior hyaloid membrane immunostaining for CRALBP

Isolated posterior hyaloid membrane specimens demonstrated discrete areas of positive immunofluorescence with mouse monoclonal anti-CRALBP antibodies. Although staining varied in intensity, z-stack cross-sectional analysis (Figure 3-16a, Figure 3-16b) and three-dimensional reconstruction images (Figure 3-16c, Figure 3-16d) consistently demonstrated the immunofluorescence to be associated with the retinal aspect of the posterior hyaloid membrane.

See Appendix Figure 6-5 for anti-CRALBP antibody positive controls and Appendix Figure 6-15a and Figure 6-15b for posterior hyaloid membrane negative controls.

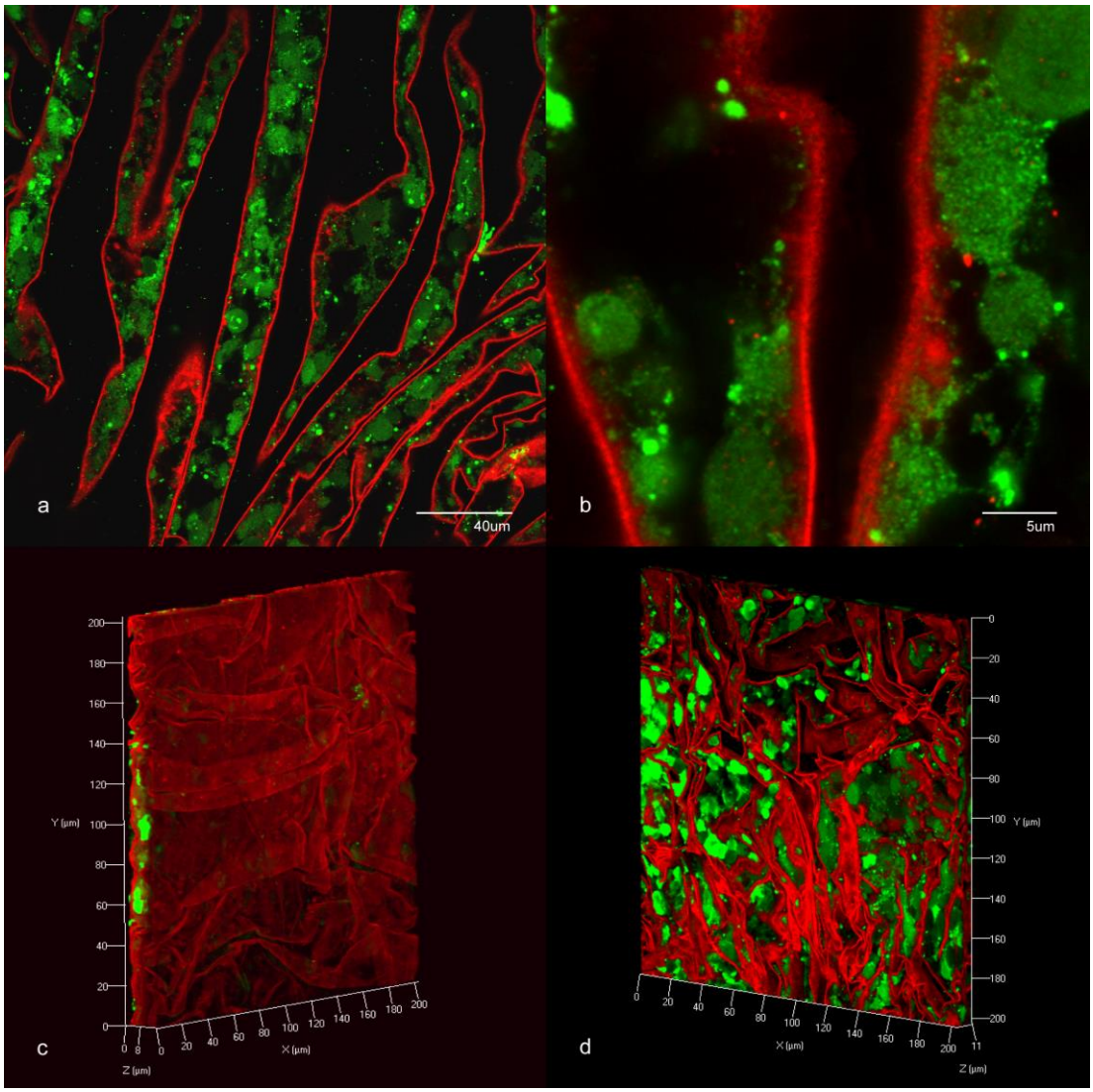

Figure 3-16 Posterior hyaloid membrane and associated retinal macroglia immunohistochemistry: CRALBP

Posterior hyaloid membrane confocal micrograph series stained with antibodies to CRALBP (green fluorescence, Alexa Fluor® 488) and collagen IV (red fluorescence, Alexa Fluor® 488) demonstrating: (a) and (b) z-stack cross-sections demonstrating discrete areas of variable CRALBP staining consistently localised to the retinal aspect of the membrane (x31.5, x182.7 respectively), (c) and (d) z-stack three-dimensional image reconstructions reiterating distribution of CRALBP staining to the retinal aspect of the membrane.

Posterior hyaloid membrane immunostaining for S100B

Isolated posterior hyaloid membrane specimens demonstrated scanty discrete areas of positive immunofluorescence with mouse monoclonal anti-S100B antibodies. Although staining was minimal compared to that seen with anti-CRALBP antibodies (Figure 3-16), z-stack cross-sectional analysis (Figure 3-17, Figure 3-16a) and three-dimensional reconstruction images (Figure 3-17b, Figure 3-17c, Figure 3-17d) consistently demonstrated this borderline immunofluorescence to be associated with the retinal aspect of the posterior hyaloid membrane.

See Appendix Figure 6-6 for anti-S100B antibody positive controls and Appendix Figure 6-15a and Figure 6-15b for posterior hyaloid membrane negative controls.

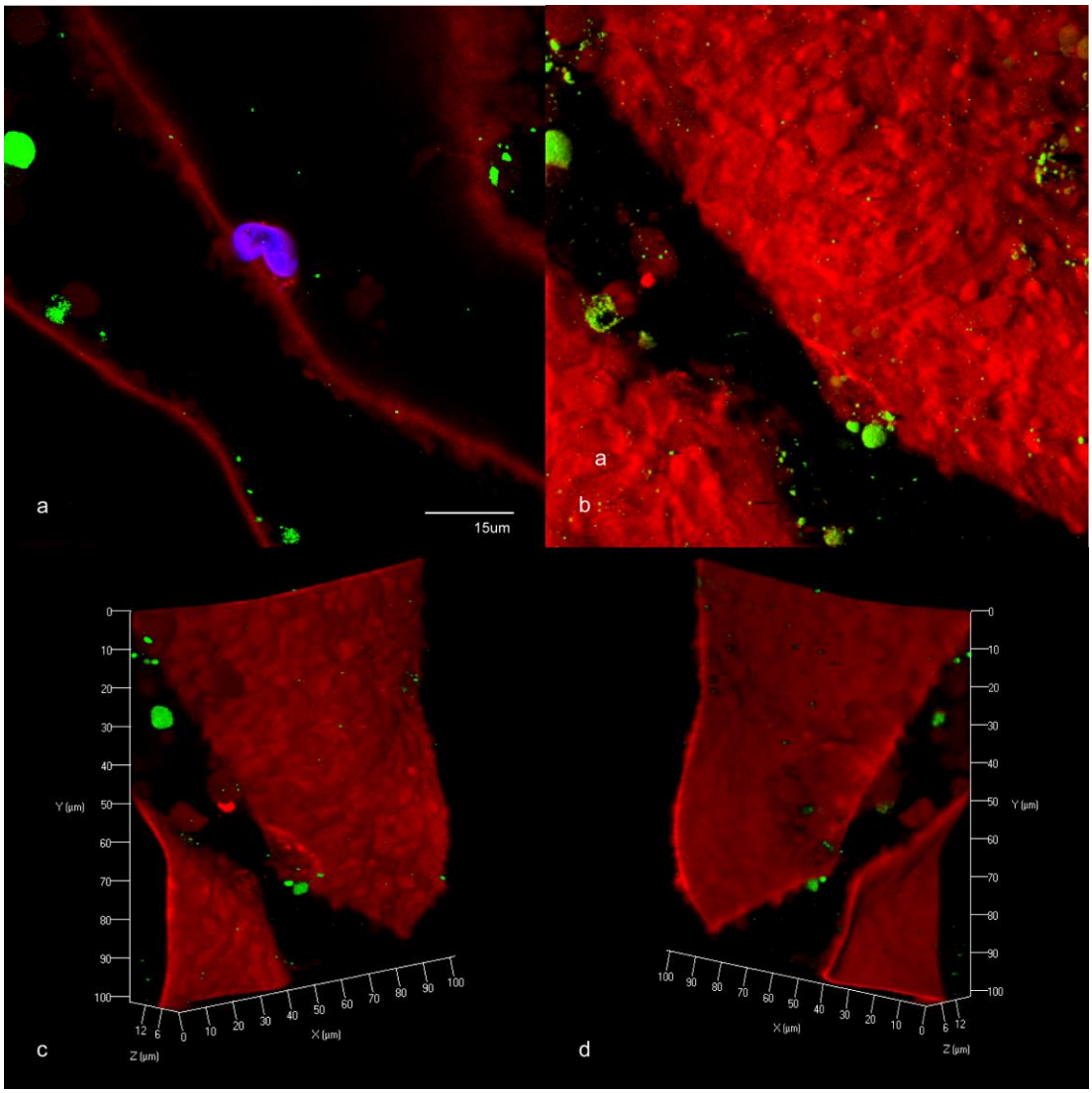

Figure 3-17 Posterior hyaloid membrane and associated retinal macroglia immunohistochemistry: S100B

Posterior hyaloid membrane confocal micrograph series stained with antibodies to S100B (green fluorescence, Alexa Fluor® 488) and collagen IV (red fluorescence, Alexa Fluor® 568) demonstrating: (a) z-stack cross-section demonstrating discrete areas of S100B staining consistently localised to the retinal aspect of the membrane (note laminocyte cell nucleus stained with DAPI (blue fluorescence) on vitreal aspect of the membrane) (x63), (b) z-stack three-dimensional surface shadow reconstruction demonstrating association of S100B to retinal aspect of the membrane (x63), (c) and (d) z-stack three-dimensional image reconstructions reiterating distribution of S100b staining to retinal aspect of the membrane.

Posterior hyaloid membrane immunostaining for vimentin

Isolated posterior hyaloid membrane specimens demonstrated scanty discrete areas of positive immunofluorescence with mouse monoclonal anti-vimentin antibodies. Although the extent of staining was less than that seen with anti-CRALBP antibodies (Figure 3-16), z-stack cross-sectional analysis (Figure 3-18, Figure 3-16a, Figure 3-18b) and three-dimensional reconstruction images (Figure 3-18c, Figure 3-18d) consistently demonstrated the immunofluorescence to be associated with the retinal aspect of the posterior hyaloid membrane.

See Appendix Figure 6-7 for anti-vimentin antibody positive controls and Appendix Figure 6-15a and Figure 6-15b for posterior hyaloid membrane negative controls.

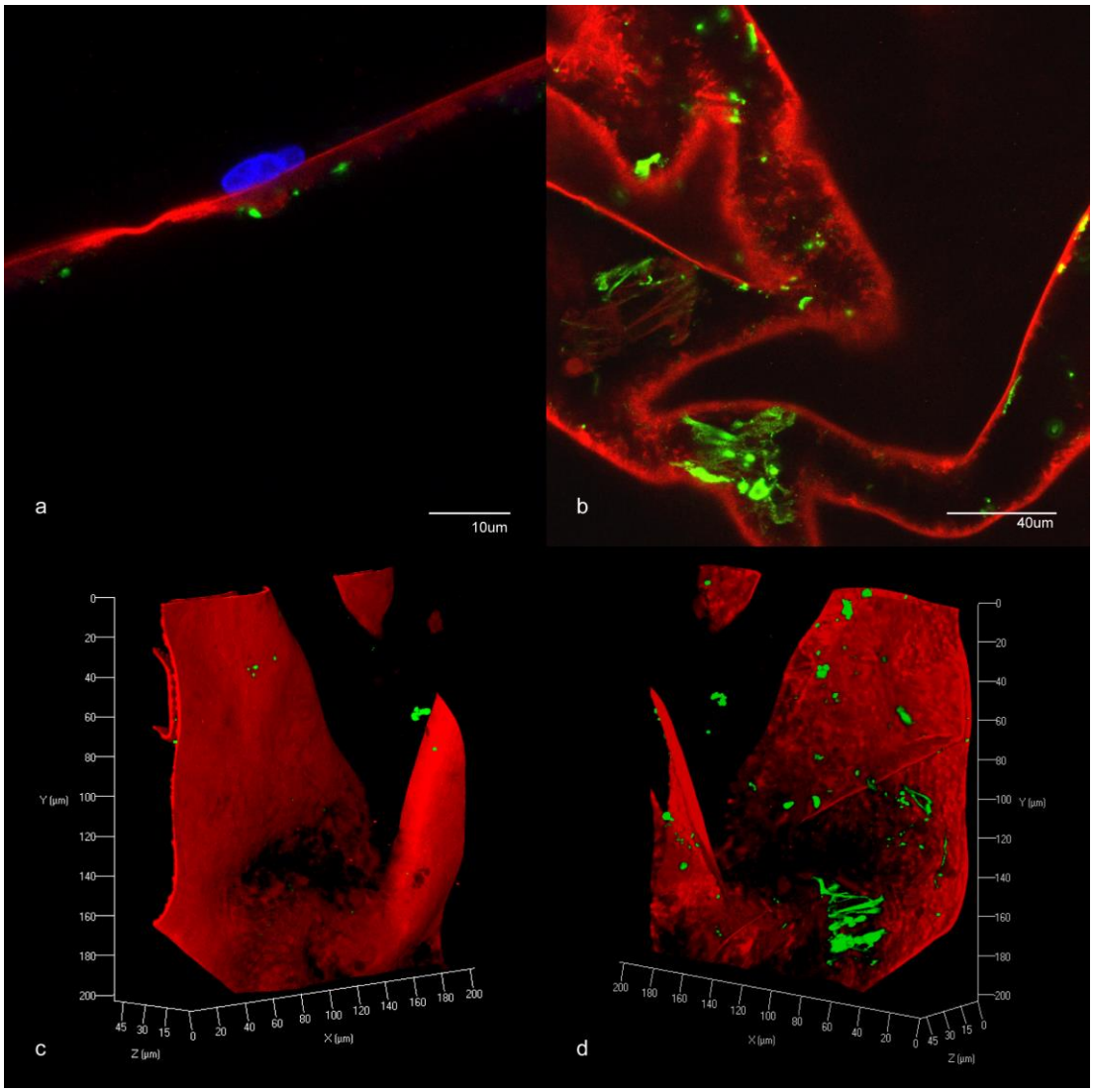

Figure 3-18 Posterior hyaloid membrane and associated retinal macroglia immunohistochemistry: vimentin

Posterior hyaloid membrane confocal micrograph series stained with antibodies to vimentin (green fluorescence, Alexa Fluor® 488) and collagen IV (red fluorescence, Alexa Fluor® 568) demonstrating: (a) and (b) z-stack cross-sections demonstrating discrete areas of vimentin staining consistently localised to the retinal aspect of the membrane (note laminocyte cell nucleus stained with DAPI (blue fluorescence) on vitreal aspect of the membrane in (a)) (x31.5), (c) and (d) z-stack three-dimensional image reconstructions reiterating distribution of vimentin staining to retinal aspect of the membrane.

3.4.5 Retinal internal limiting membrane immunohistochemistry following posterior vitreous detachment

Internal limiting membrane specimens from retinal fragments attached to the periphery of detached posterior hyaloid membranes (Figure 3-19) and posterior pole retinal flat mounts from of eyes with posterior vitreous detachment (Figure 3-20) were evaluated with anti-collagen IV antibodies.

Immunofluorescent images demonstrated the anticipated vascular branching pattern of superficial retinal blood vessels, delineated by their endothelial basement membranes; the vascular net appeared to be associated with the surrounding internal limiting membrane.

The internal limiting membrane formed a continuous, less intensely fluorescent sheet, best demonstrated at its edges (Figure 3-19b, Figure 3-19c, Figure 3-20a, Figure 3-20b).

See Appendix Figure 6-1 for anti-collagen IV antibody positive controls; note Appendix Figure 6-1c demonstrates positive anti-collagen IV staining for the internal limiting membrane and associated retinal blood vessel. See Appendix Figure 6-16 for the retinal flat mount negative controls.

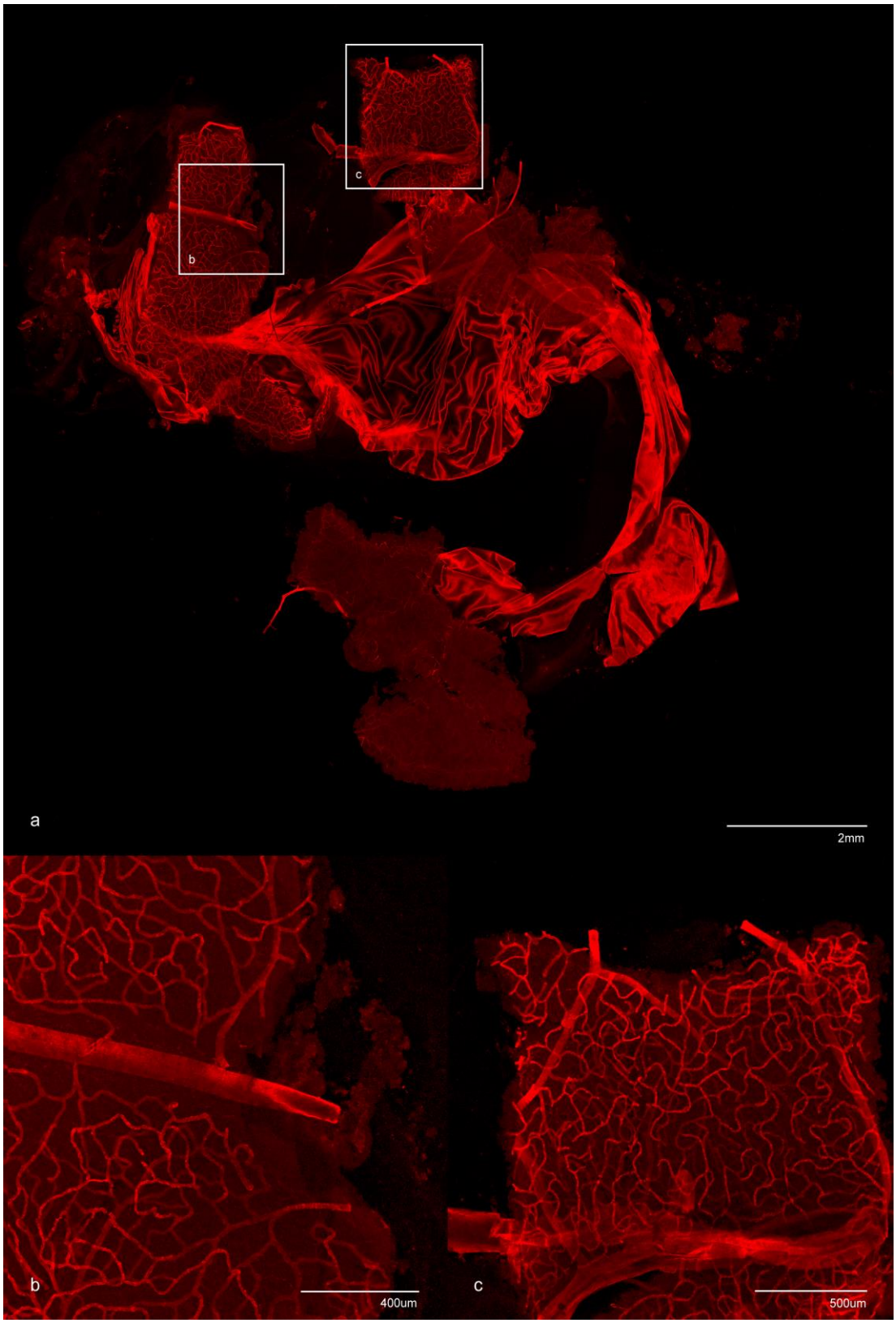

Figure 3-19 Internal limiting membrane immunohistochemistry: collagen IV

Please turn over for figure legend

Figure 3-19 Internal limiting membrane immunohistochemistry: collagen IV

Confocal micrograph stained with antibodies to collagen IV (red fluorescence, Alexa Fluor® 568) demonstrating: (a) 10x10 tile scan of the posterior hyaloid membrane centrally with peripherally attached retinal fragments, identified by their surface vascular markings (x5), (b) and (c) magnified windows of retinal fragments in (a) demonstrating the internal limiting membrane (most apparent at its edges) with the associated microvascular network delineated by its endothelial basement membrane (x21.6, x16 respectively).

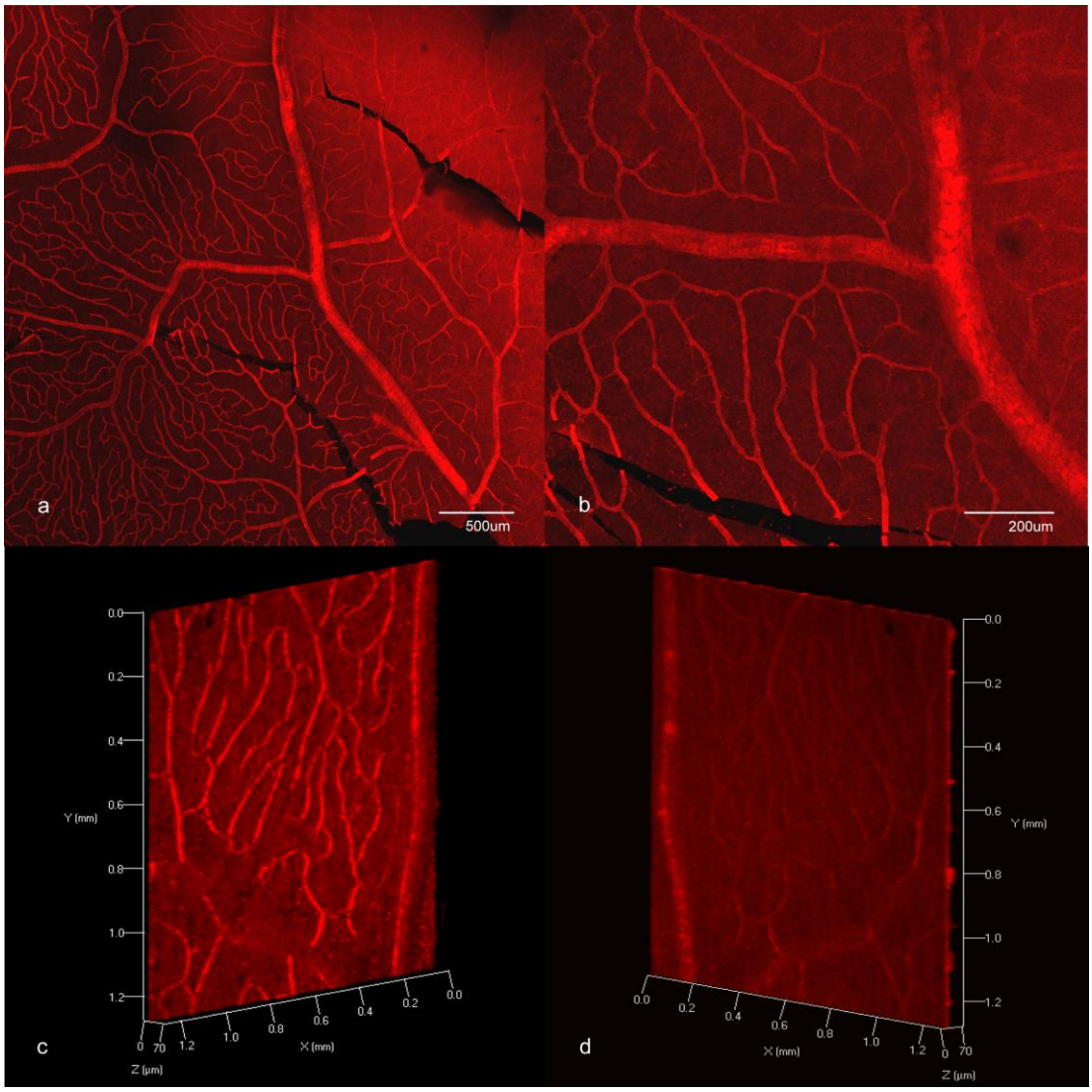

Figure 3-20 Internal limiting membrane immunohistochemistry: collagen IV

Confocal micrograph series stained with antibodies to collagen IV (red fluorescence, Alexa Fluor® 568) demonstrating: (a) 3x3 tile scan of retinal posterior pole flat mount following posterior vitreous detachment (note greater internal limiting membrane immunofluorescence in the upper right corner compared to bottom left due to retinal undulation altering focal plane) (x5), (b) magnified view of artifactual retinal break in (a) demonstrating internal limiting membrane edge (x5), (c) and (d) z-stack three-dimensional reconstructions of the illustrating the relationship of the internal limiting membrane to the retinal microvascular network (retinal and vitreal aspect respectively).

3.4.6 Laminocyte phenotype

A phenotypically distinct cell population, recognised by their large ‘cashew’ shaped nuclei (frequently appearing binucleated in cross-section) and branched, extensive dendritic morphology, were the only subpopulation of vitreal cells identified to be adherent to the posterior hyaloid membrane (Figure 3-21, Figure 3-22). These readily identifiable cells were always apparent on the vitreal aspect of the posterior hyaloid membrane and were found in all specimens examined.

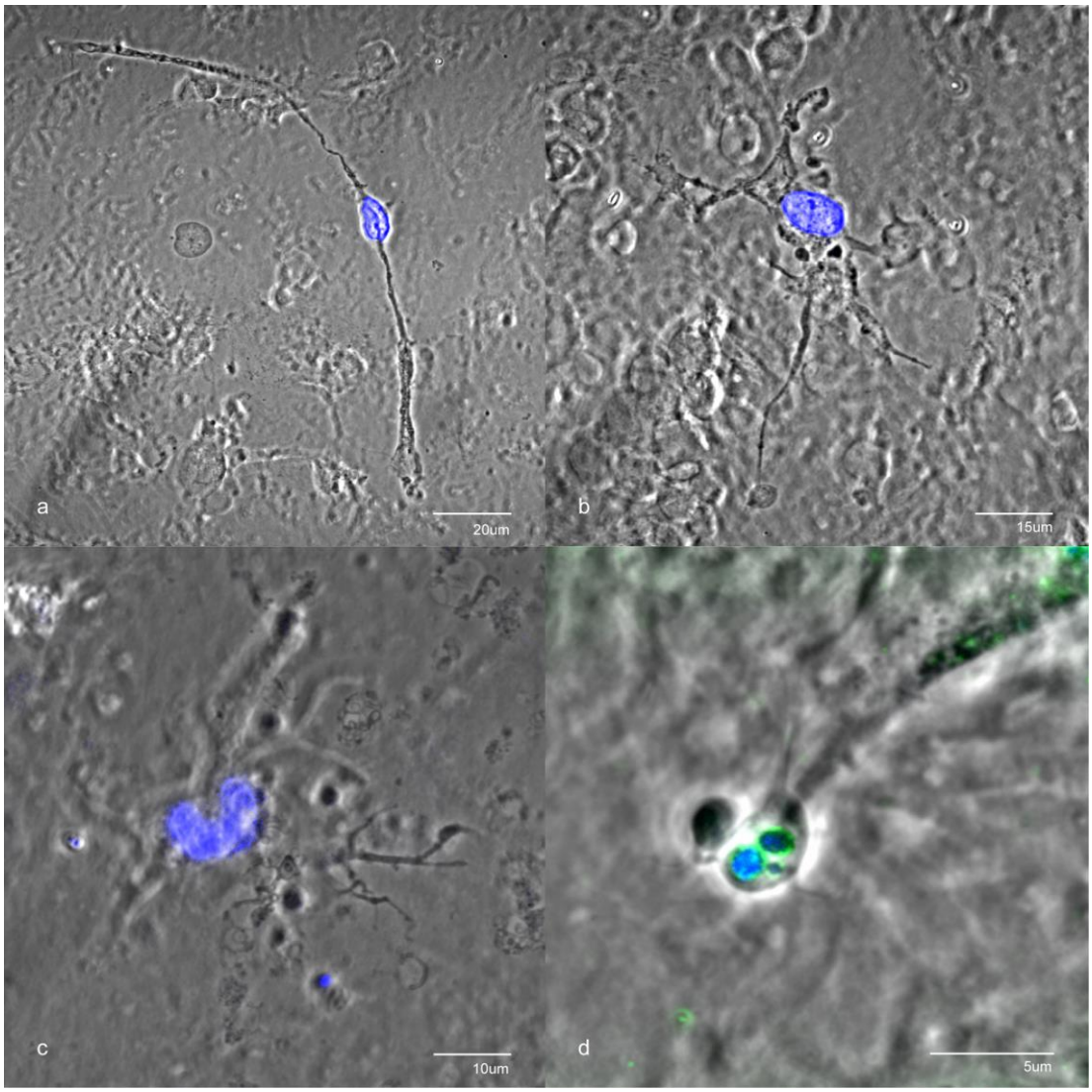

Figure 3-21 Laminocyte phenotype

Confocal micrograph series with phase contrast overlay demonstrating cells adherent to the posterior hyaloid membrane with: (a) elongated pseudopodia, scanty somatic cytoplasm and large nucleus (appearing binucleate in cross-section) (x44.1), (b) extensive dendritic morphology (x63), (c) large ‘cashew’ shaped nucleus (x100.8), (d) phagocytic terminal bulb with associated nuclear material and positive CD68 cytoplasmic granule staining (220.5x). Tissue stained with DAPI (blue fluorescence) to identify nuclei and nuclear material.

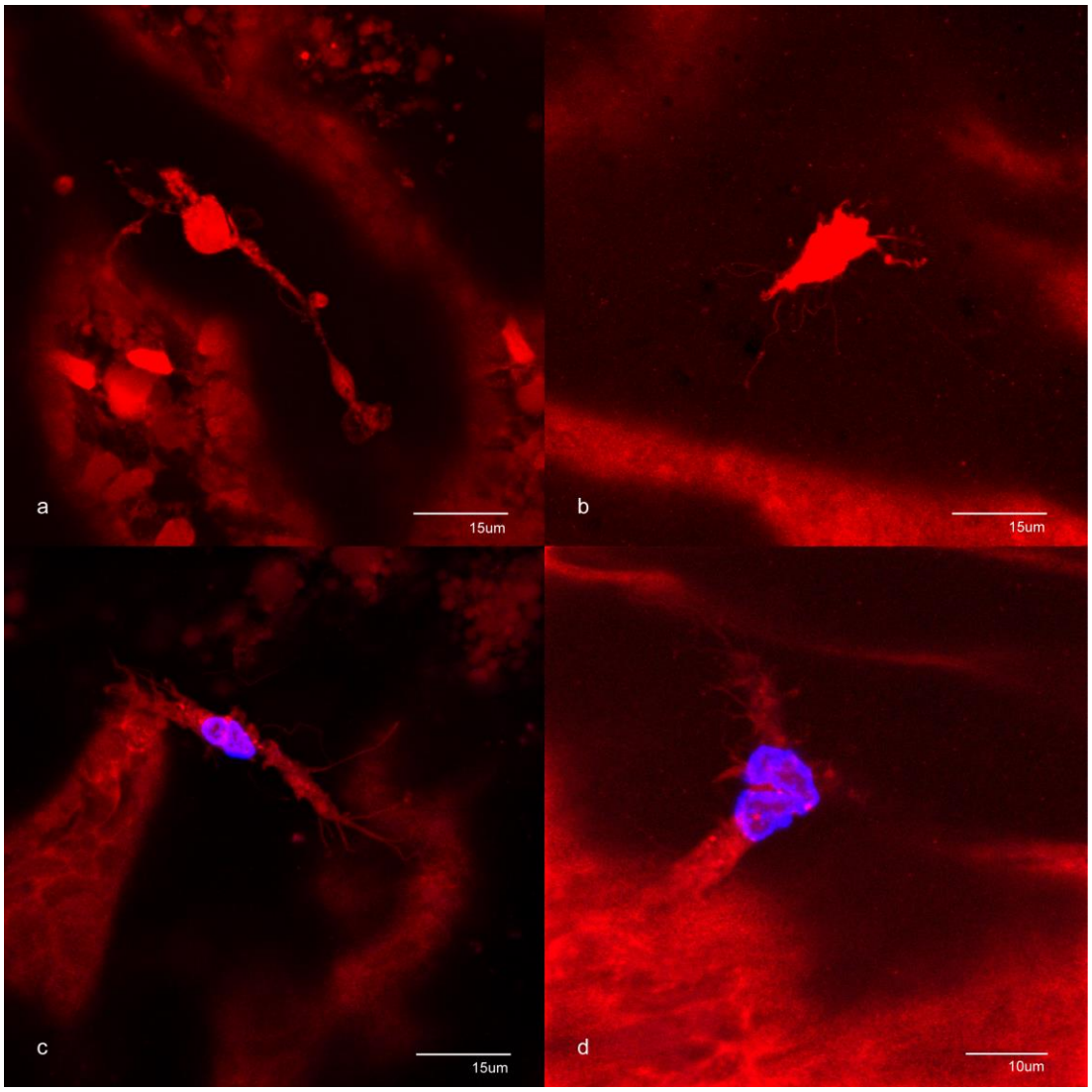

Figure 3-22 Laminocyte phenotype

Confocal micrograph series of a posterior hyaloid membrane specimen stained with antibodies to collagen IV (red fluorescence, Alexa Fluor® 568) and DAPI (blue fluorescence); scanning microscope detector gain setting maximised to produce a non-specific fluorescent signal in order to delineate cellular morphology: (a) and (b) demonstrate elongated pseudopodia and extensive dendritic morphology, note non-specificity indicated by loss of nuclear void (x63), (c) large nucleus (appearing binucleate in cross-section) (x63), (d) integrally adherent to the underlying posterior hyaloid membrane (x110.8).

3.4.7 Laminocyte immunohistochemical phenotyping

Laminocyte immunostaining for GFAP

All examined laminocyte cells, identified to be adherent to the posterior hyaloid membrane on phase contrast microscopy, demonstrated positive staining with rabbit polyclonal anti-GFAP antibodies. Immunofluorescence appeared localised to the cell body and cytoplasmic extensions along branching pseudopodia. In addition, the vast majority of laminocyte cells demonstrated nuclear staining (Figure 3-23), whilst a minority (all from a single posterior hyaloid membrane specimen) did not (Figure 3-24).

See Appendix Figure 6-12 for rabbit polyclonal anti-GFAP antibody positive controls and Appendix Figure 6-17c and Figure 6-17d for laminocyte negative controls.

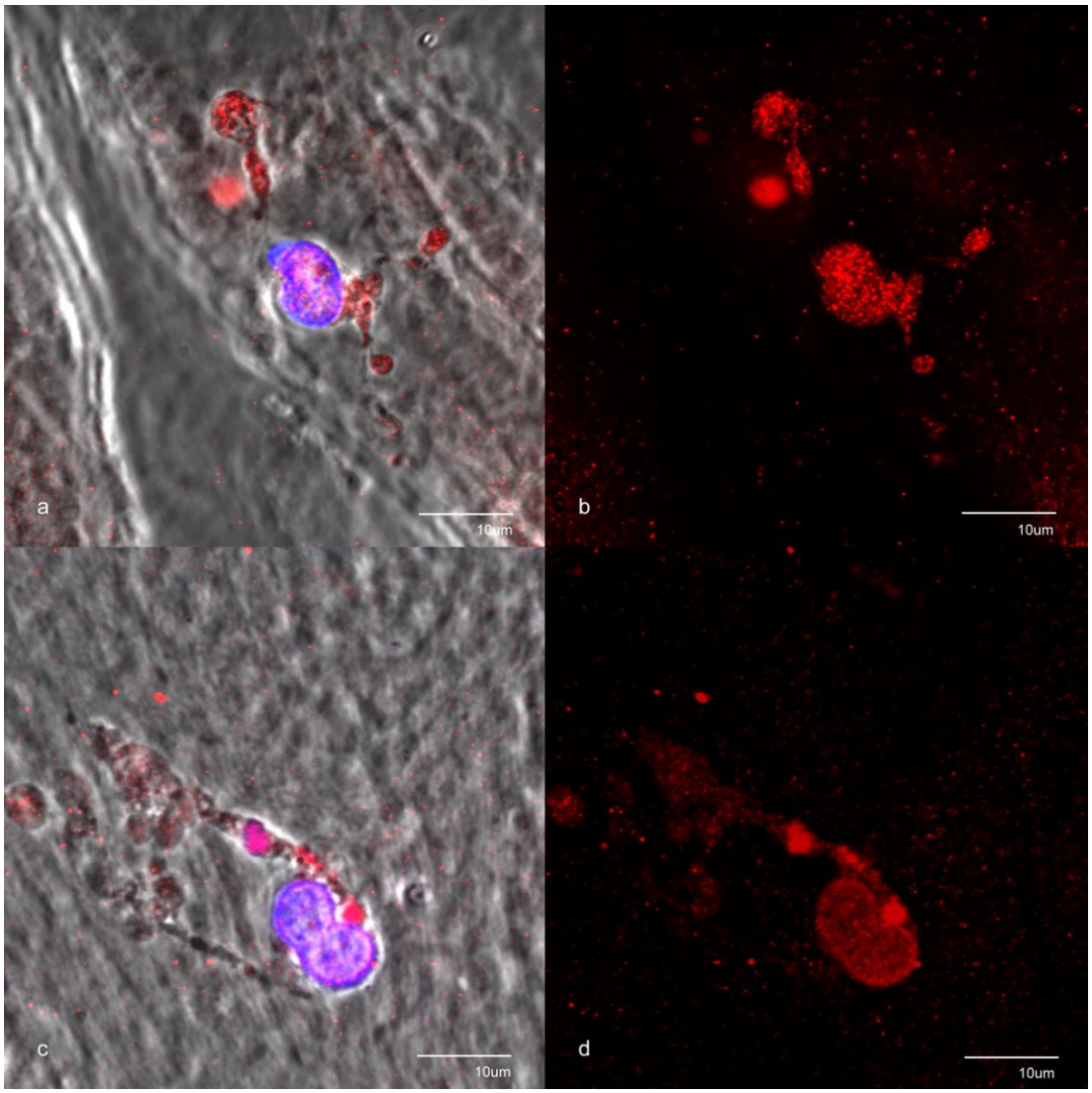

Figure 3-23 Laminocyte immunohistochemistry: GFAP

Confocal micrograph series stained with GFAP (red fluorescence, Alexa Fluor® 568) and DAPI (blue fluorescence) demonstrating: (a) and (b) with and without phase contrast overlay respectively (x107.1), (c) and (d) with and without phase contrast overlay respectively (x126). Note cytosolic and nuclear staining.

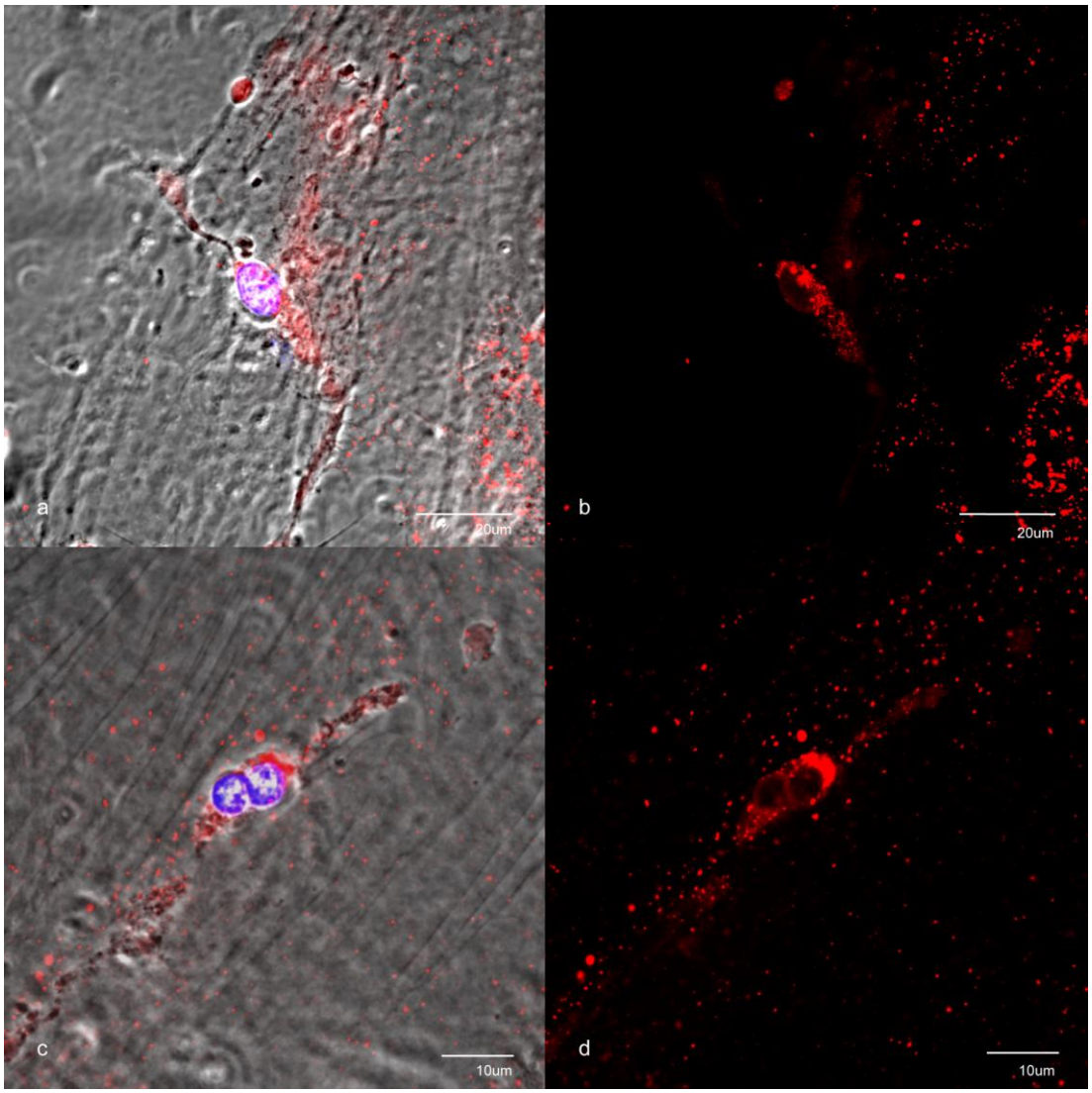

Figure 3-24 Laminocyte immunohistochemistry: GFAP

Confocal micrograph series stained with GFAP (red fluorescence, Alexa Fluor® 568) and DAPI (blue fluorescence) demonstrating: (a) and (b) with and without phase contrast overlay respectively (x63), (c) and (d) with and without phase contrast overlay respectively (x94.5). Note cytosolic but no nuclear staining.

Laminocyte immunostaining for MHC Class II

Laminocyte cells, identified to be adherent to the posterior hyaloid membrane on phase contrast microscopy, consistently demonstrated positive immunofluorescence with mouse monoclonal anti-MHC Class II antibodies. Staining was specific and localised along the extent of their branching pseudopodia (Figure 3-25and Figure 3-26).

Staining intensity was strong, with immunofluorescence strength sufficient to readily and reliably detect the cells by xenon arc lamp (Leistungselektronik Jena Gmbh HXP-120C) epifluorescent microscopy.

See Figure 3-27 for co-staining of anti-MHC Class II and anti-GFAP antibody.

See Appendix Figure 6-8 for anti-MHC Class II antibody positive controls and Appendix Figure 6-17a and Figure 6-17b for laminocyte negative controls.

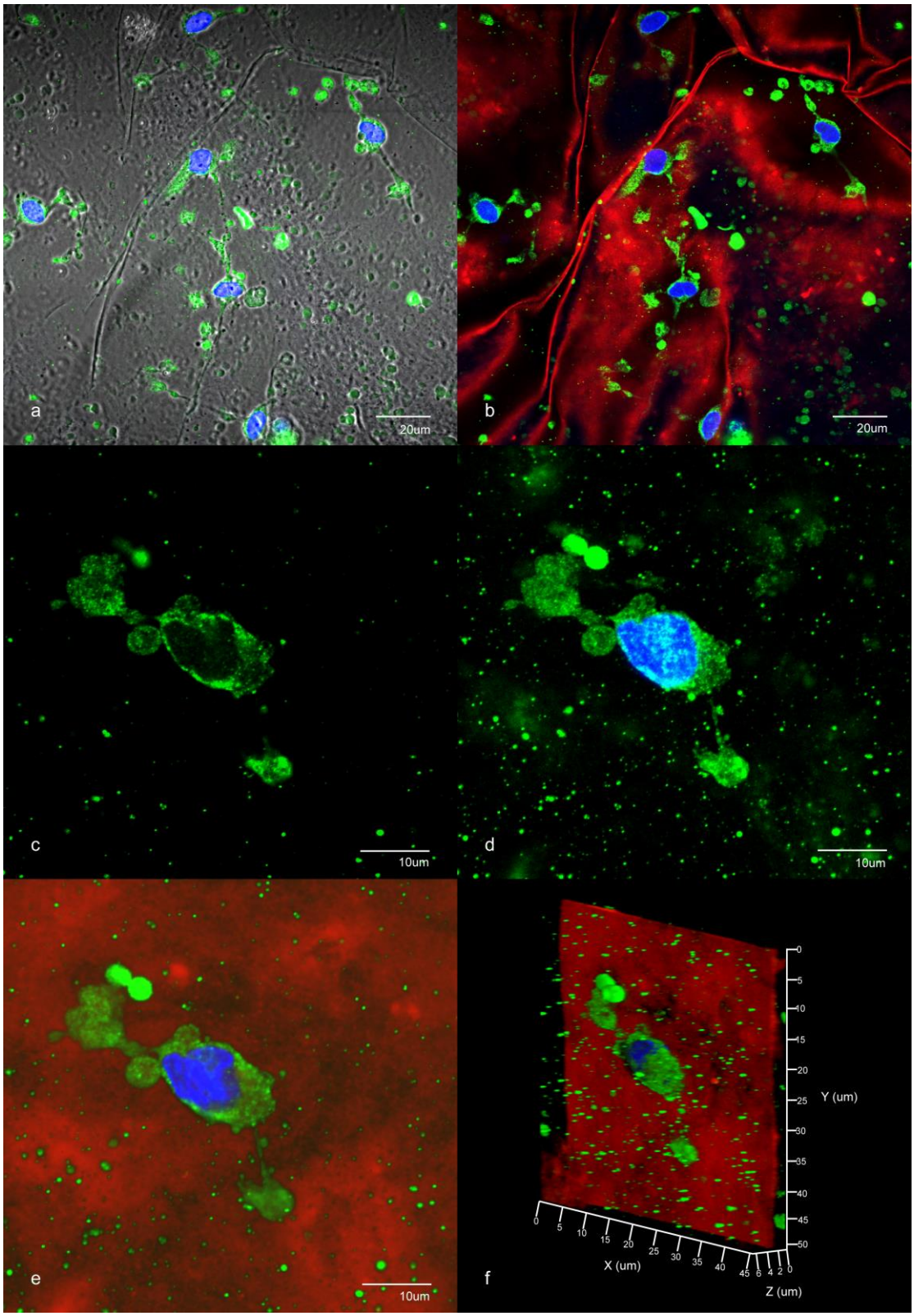

Figure 3-25 Laminocyte immunohistochemistry: MHC Class II

Please turn over for figure legend

Figure 3-25 Laminocyte immunohistochemistry: MHC Class II

Confocal micrograph series stained with antibodies to MHC Class II (green fluorescence, Alexa Fluor® 488), collagen IV (red fluorescence, Alexa Fluor® 568) and DAPI (blue fluorescence) demonstrating: (a) and (b) multiple laminocytes positive for MHC Class II antigens (x31.5), (c) to (f) MHC Class II immunofluorescence delineating cell morphology, note (c) perinuclear staining, (d) z-stack maximum image projection, (e) z-stack three-dimensional surface shadow reconstruction image, (f) z-stack three-dimensional image reconstruction illustrating intrinsic relationship of MHC Class II positive laminocyte to posterior hyaloid membrane. (x113.4)

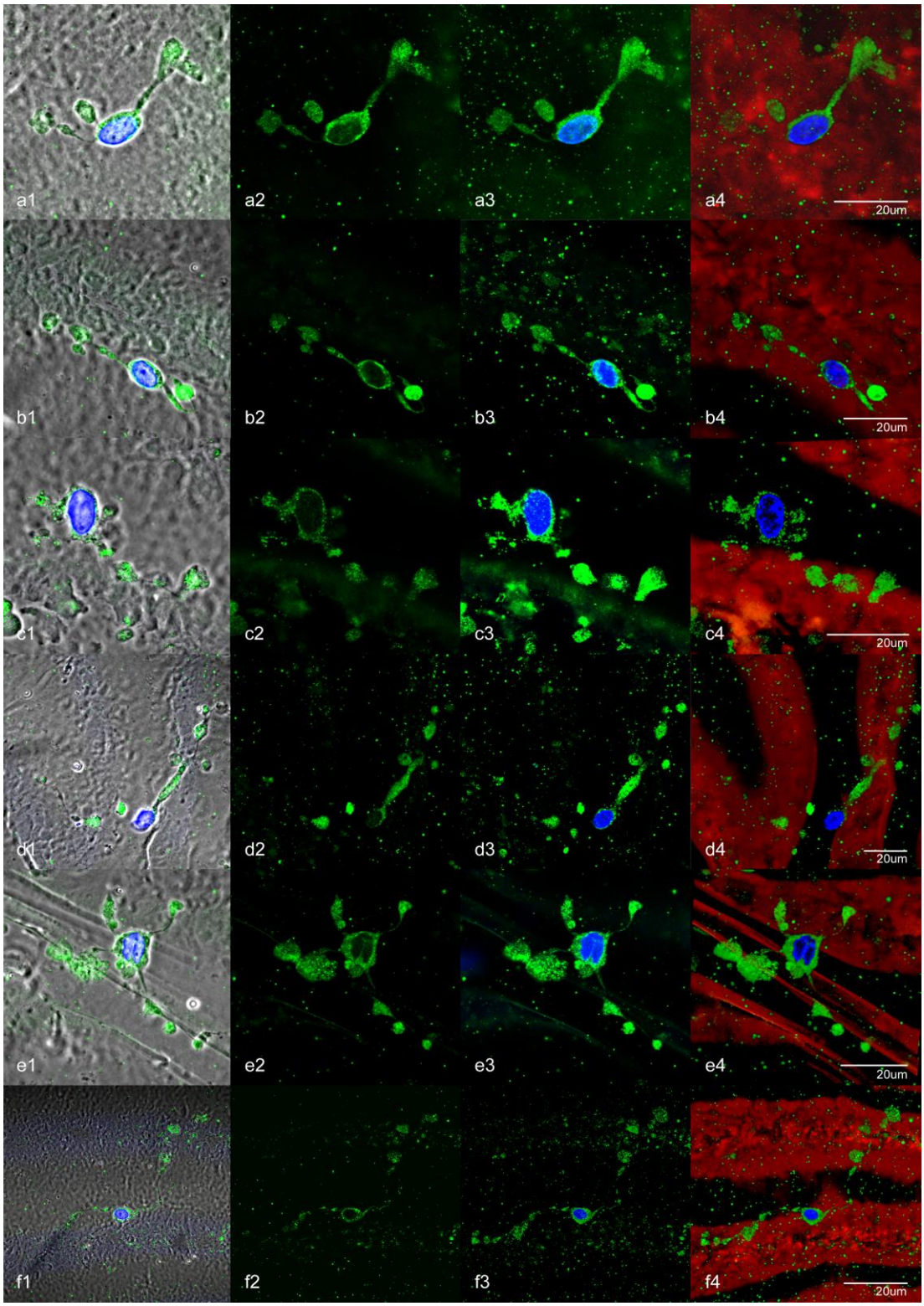

Figure 3-26 Laminocyte immunohistochemistry: MHC Class II

Please turn over for figure legend

Figure 3-26 Laminocyte immunohistochemistry: MHC Class II

Confocal micrograph series stained with antibodies to MHC Class II (green fluorescence, Alexa Fluor® 488), collagen IV (red fluorescence, Alexa Fluor® 568) and DAPI (blue fluorescence) demonstrating consistent MHC Class II immunofluorescence for six consecutively imaged laminocytes tabulated in rows (a) to (f): column (1) and (2) represent immunofluorescent images with and without phase contrast overlay respectively, note perinuclear staining in column (2), column (3) represents z-stack maximum image projection reconstructions to summate the distribution of MHC Class II along pseudopodia, column (4) represents z-stack three-dimensional image reconstructions illustrating the intimate relationship of cells to the posterior hyaloid membrane.

Magnification: (a) x100.8, (b) x88.2, (c) x113.4, (d) x63, (e) x88.2, (f) x37.8.

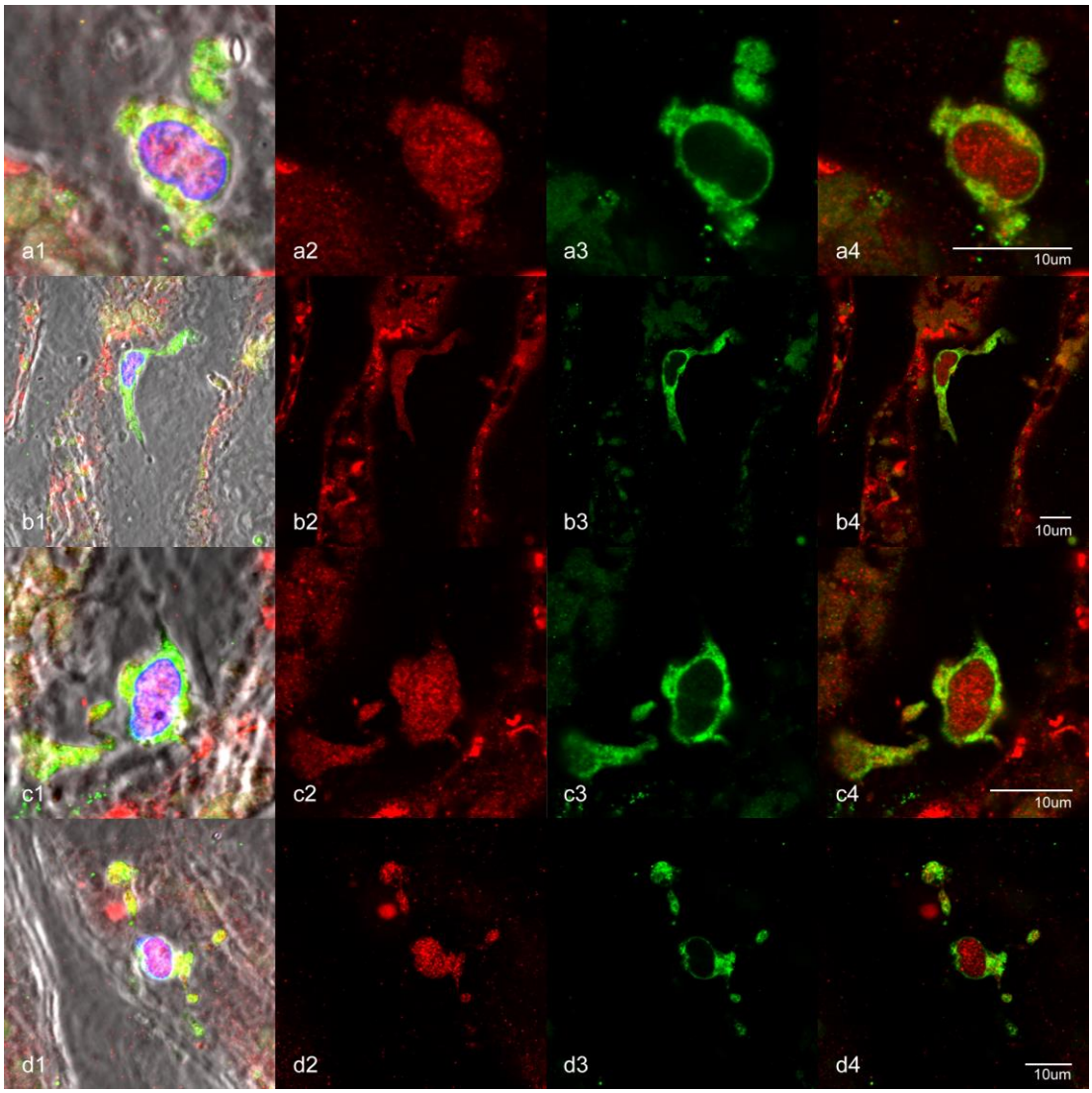

Figure 3-27 Laminocyte immunohistochemistry: GFAP and MHC class II co-staining

Confocal micrograph series stained with antibodies to MHC Class II (green fluorescence, Alexa Fluor® 488), GFAP (red fluorescence, Alexa Fluor® 568) and DAPI (blue fluorescence) demonstrating co-staining of four consecutively imaged laminocytes tabulated in rows (a) to (d): column (1) represents immunofluorescent images with phase contrast overlay, column (2) and (3) represent single channel GFAP and MHC class II immunofluorescence respectively (note GFAP nuclear staining and MHC Class II perinuclear staining patterns), column (4) represents co-staining of GFAP and MHC class II immunofluorescence depicted in yellow.

Magnification: (a) x233, (b) x63, (c) x170.1, (d) x107.1

Laminocyte immunostaining for CD68

Laminocyte cells, identified to be adherent to the posterior hyaloid membrane on phase contrast microscopy, consistently demonstrated positive immunofluorescence with mouse monoclonal anti-CD68 antibodies. Staining was specific and localised to cytoplasmic granules along the extent of their branching pseudopodia (Figure 3-28 and Figure 3-29).

Although staining intensity was granular and mild to moderate in intensity, it was apparent in every laminocyte identified by phase contrast microscopy and immunofluorescence was of sufficient strength to readily and reliably detect the cells by xenon arc lamp (Leistungselektronik Jena Gmbh HXP-120C) epifluorescent microscopy.

Furthermore, CD68 immunofluorescence was association with DAPI immunofluorescence in the phagocytic terminal bulbs of the branching dendritic pseudopodia (Figure 3-21b).

See Figure 3-30 for co-staining of anti-CD68 and anti-GFAP antibody.

See Appendix Figure 6-9 for anti-CD68 antibody positive controls and Appendix Figure 6-17a and Figure 6-17b for laminocyte negative controls.

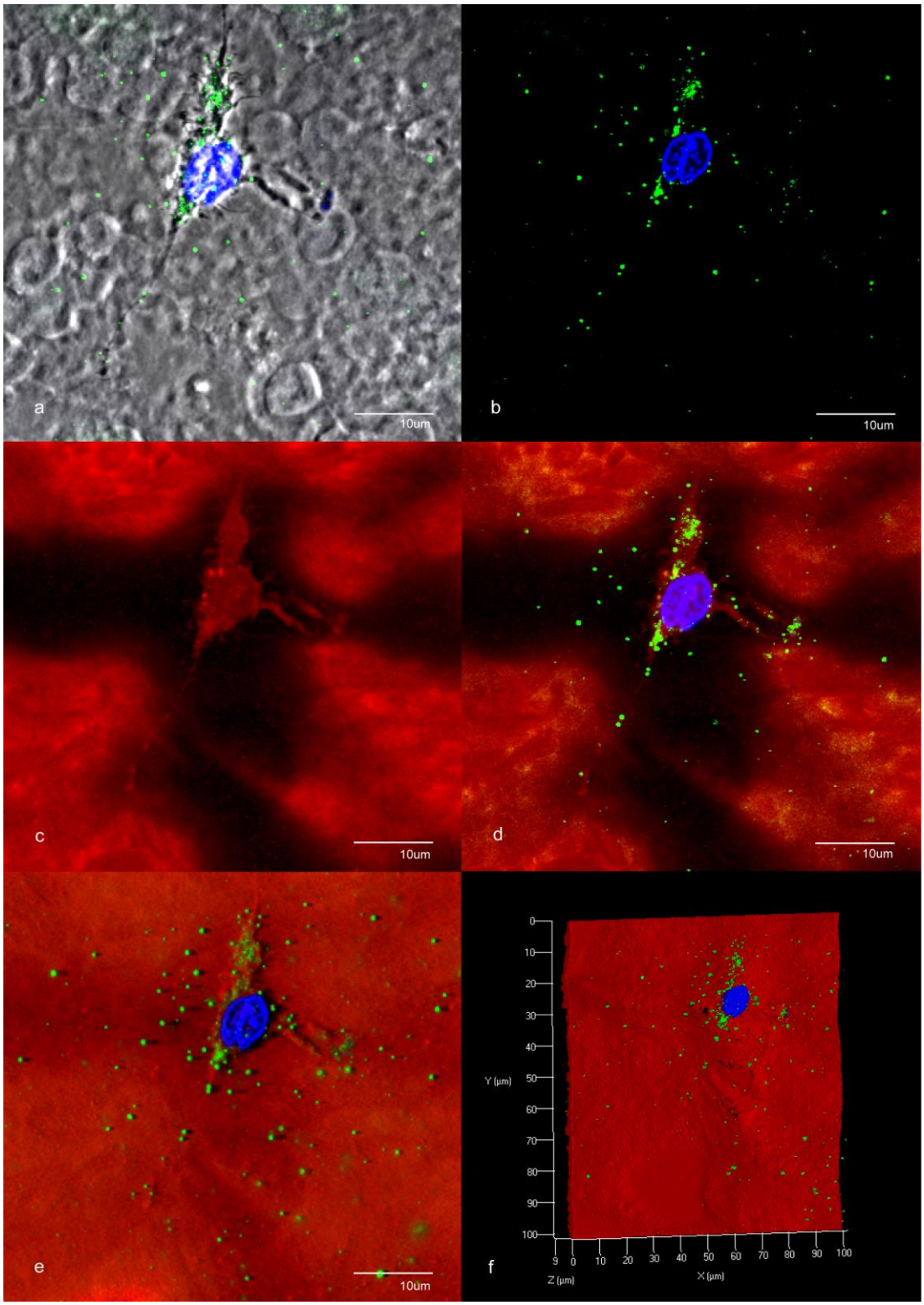

Figure 3-28 Laminocyte immunohistochemistry: CD68

Please turn over for figure reference

Figure 3-28 Laminocyte immunohistochemistry: CD68

Confocal micrograph series stained with antibodies to CD68 (green fluorescence, Alexa Fluor® 488), collagen IV (red fluorescence, Alexa Fluor® 568) and DAPI (blue fluorescence) demonstrating: (a) and (b) laminocyte with positive CD68 immunofluorescence localised to granules along branching pseudopodia, with and without phase contrast overlay respectively (x63), (c) and (d) scanning microscope detector gain setting maximised to produce non-specific autofluorescent signal in order to delineate cellular morphology (demonstrated by loss of nuclear void in (c)), without and with CD68 and DAPI immunofluorescence respectively (x63), (e) z-stack three-dimensional surface shadow reconstruction (x63), (f) z-stack three-dimensional image reconstruction illustrating intrinsic relationship of CD68 positive laminocyte to posterior hyaloid membrane.

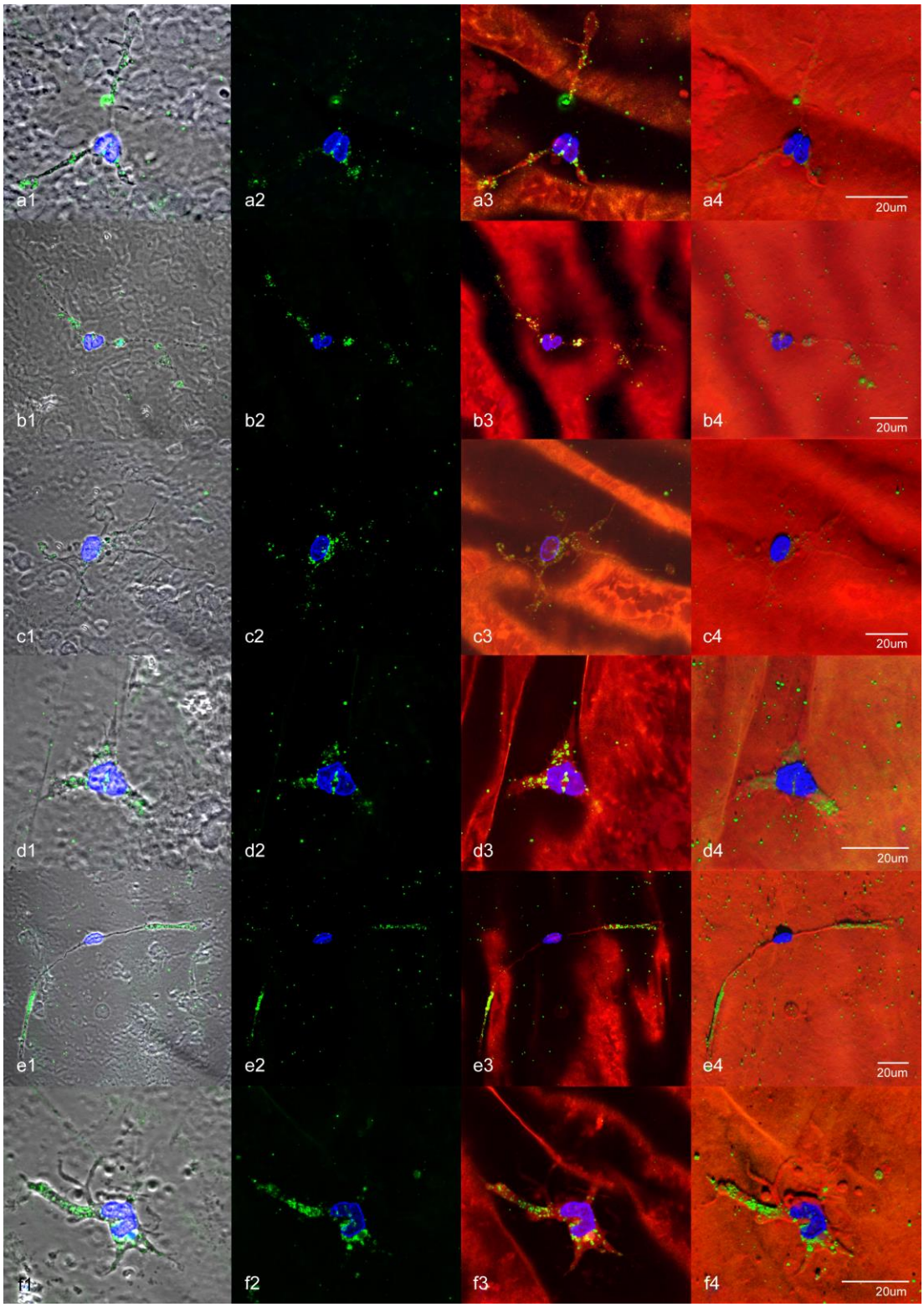

Figure 3-29 Laminocyte immunohistochemistry: CD68

Please turn over for figure reference

Figure 3-29 Laminocyte immunohistochemistry: CD68

Confocal micrograph series stained with antibodies to CD68 (green fluorescence, Alexa Fluor® 488), collagen IV (red fluorescence, Alexa Fluor® 568) and DAPI (blue fluorescence) demonstrating immunofluorescence for six consecutively imaged laminocytes tabulated in rows (a) to (f): column (1) and (2) represent immunofluorescent images with and without phase contrast overlay respectively, column (3) represents maximum image projection reconstructions to summate the distribution of CD68 along pseudopodia, in addition to scanning microscope detector gain setting maximised to produce non-specific autofluorescent signal in order to delineate cellular morphology (posterior hyaloid membrane stained with rabbit polyclonal anti-collagen IV antibody), column (4) represents a three-dimensional surface shadow reconstruction.

Magnification: (a) x81.9, (b) x50.4, (c) x63, (d) x100.8, (e) x44.1, (f) x100.8.

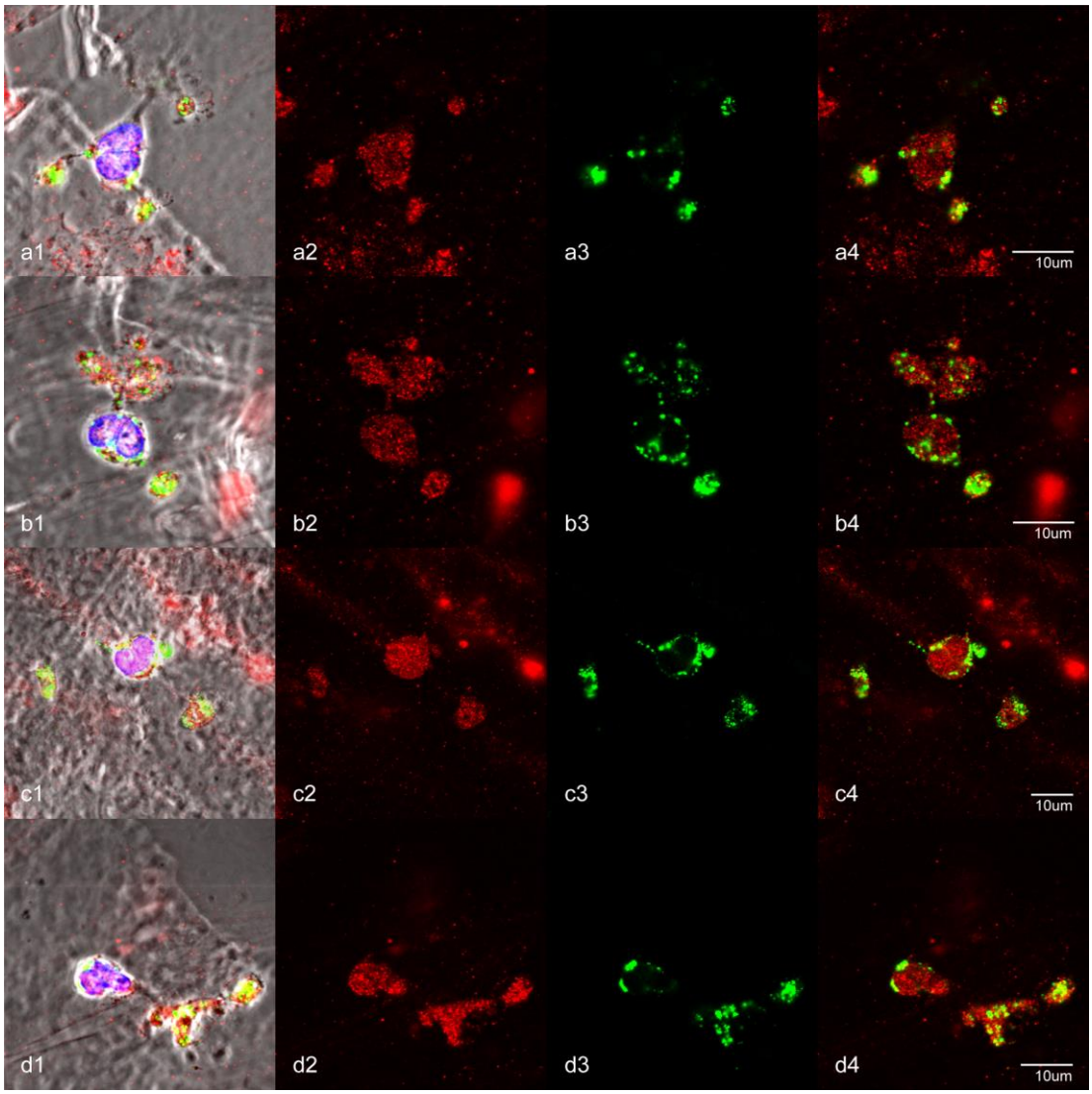

Figure 3-30 Laminocyte immunohistochemistry: GFAP and CD68 co-staining

Confocal micrograph series stained with antibodies to CD68 (green fluorescence, Alexa Fluor® 488), GFAP (red fluorescence, Alexa Fluor® 568) and DAPI (blue fluorescence) demonstrating co-staining of four consecutively imaged laminocytes tabulated in rows (a) to (d): column (1) represents immunofluorescent images with phase contrast overlay, column (2) and (3) represent single channel GFAP and CD68 immunofluorescence respectively (note GFAP nuclear staining and CD68 perinuclear staining patterns), column (4) represents co-staining of GFAP and MHC class II immunofluorescence depicted in yellow.

Magnification: (a) x132, (b) x132, (c) x94.5, (d) x119.7

Laminocyte immunostaining for CD11

Laminocyte cells, identified to be adherent to the posterior hyaloid membrane on phase contrast microscopy, consistently demonstrated no detectable immunofluorescence with mouse monoclonal anti-CD11 antibodies (Figure 3-31).

See Appendix Figure 6-10 for anti-CD11 antibody positive controls and Appendix Figure 6-17a and Figure 6-17b for laminocyte negative controls.

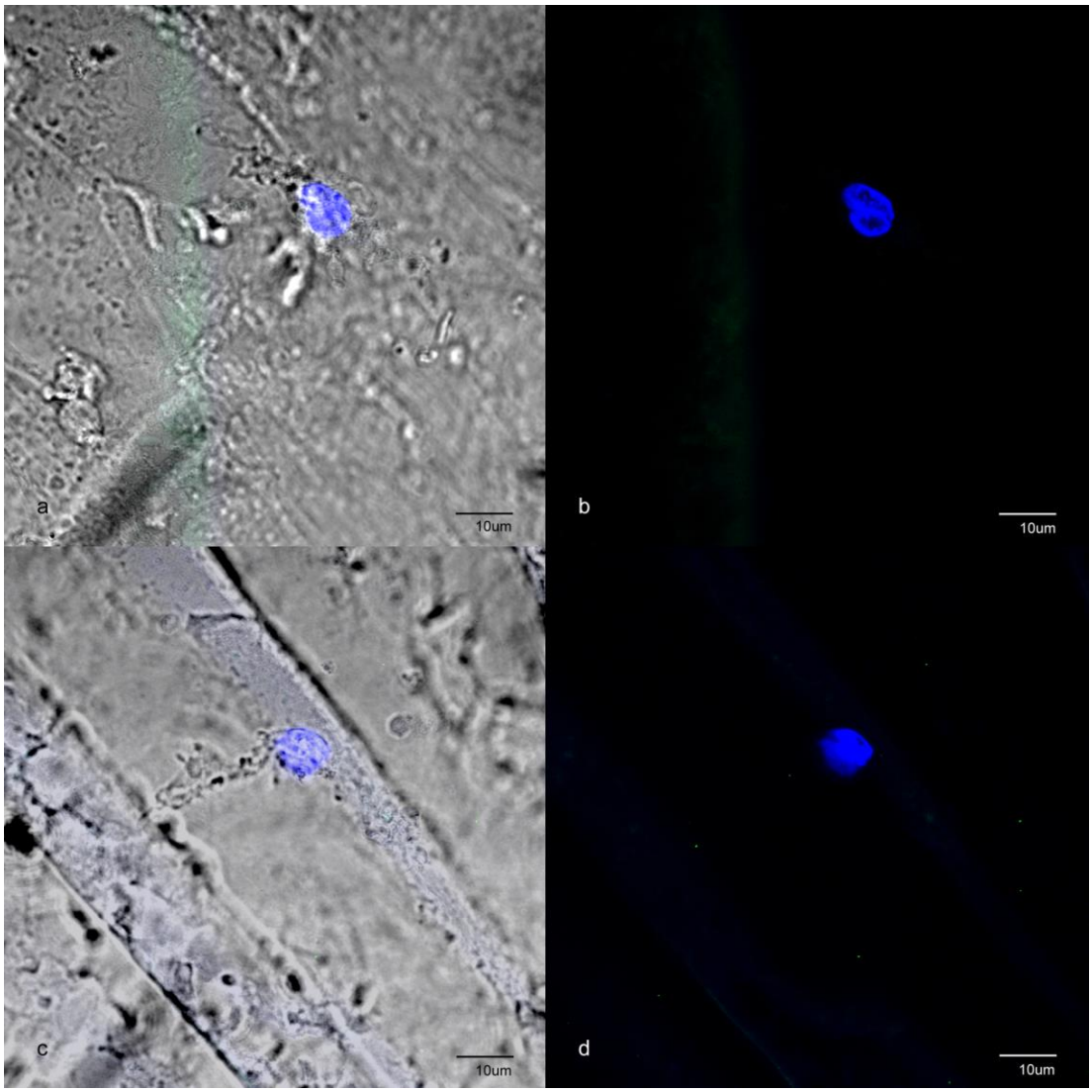

Figure 3-31 Laminocyte immunohistochemistry: CD11

Confocal micrograph series stained with antibodies to CD11 (green fluorescence, Alexa Fluor® 488) and DAPI (blue fluorescence) demonstrating negative CD11 immunofluorescence: (a) and (b) with and without phase contrast overlay respectively (x63), (c) and (d) with and without phase contrast overlay respectively (x63).

Laminocyte immunostaining for Iba1

Laminocyte cells, identified to be adherent to the posterior hyaloid membrane on phase contrast microscopy, consistently demonstrated no detectable immunofluorescence with goat polyclonal anti-Iba1 antibodies (Figure 3-32).

See Appendix Figure 6-11 for anti-Iba1 antibody positive controls and Appendix Figure 6-17e and Figure 6-17f for laminocyte negative controls.

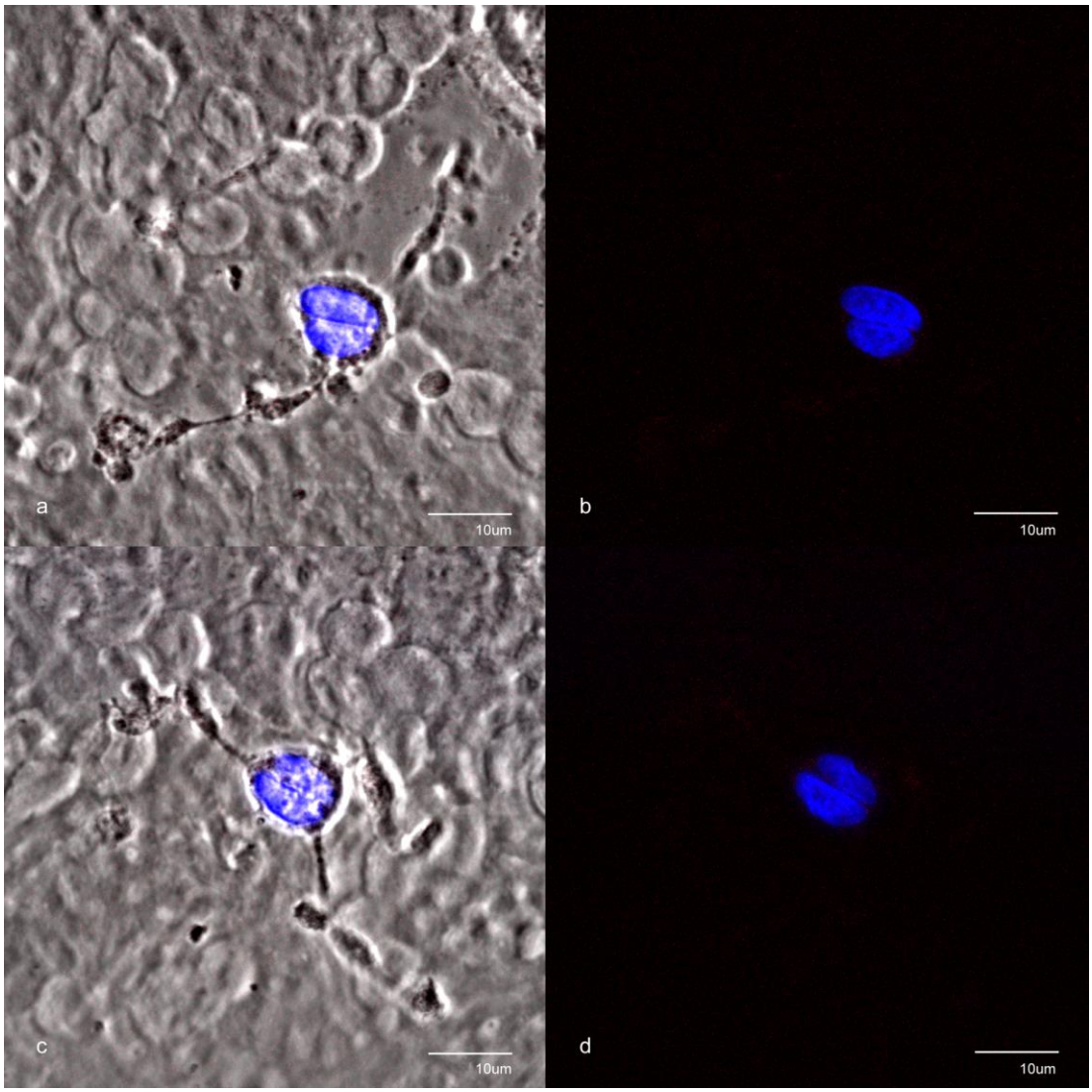

Figure 3-32 Laminocyte immunohistochemistry: Iba1

Confocal micrograph series stained with antibodies to Iba1 (magenta fluorescence, Alexa Fluor® 647) and DAPI (blue fluorescence) demonstrating laminocytes with negative Iba1 immunofluorescence: (a) and (b) with and without phase contrast overlay respectively (x63), (c) and (d) with and without phase contrast overlay respectively (x63).

CRALBP

Laminocyte cells, identified to be adherent to the posterior hyaloid membrane on phase contrast microscopy, consistently demonstrated no detectable immunofluorescence with mouse monoclonal anti-CRALBP antibodies (Figure 3-33).

See Appendix Figure 6-5 for anti-CRALBP antibody positive controls and Appendix Figure 6-17a and Figure 6-17b for laminocyte negative controls.

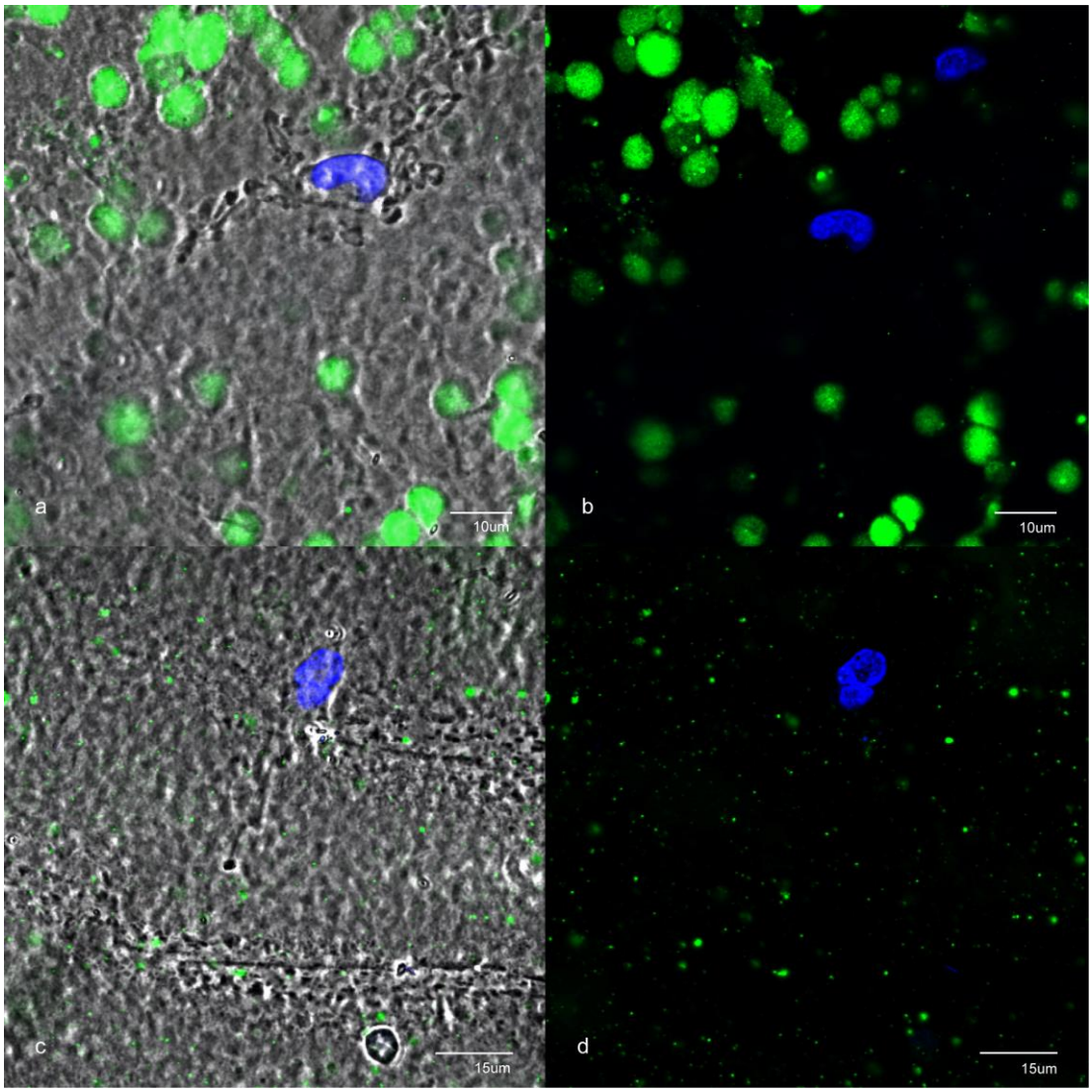

Figure 3-33 Laminocyte immunohistochemistry: CRALBP

Confocal micrograph series stained with antibodies to CRALBP (green fluorescence, Alexa Fluor® 488) and DAPI (blue fluorescence) demonstrating laminocytes with negative CRALBP immunofluorescence: (a) and (b) with and without phase contrast overlay respectively (x75.6), (c) and (d) with and without phase contrast overlay respectively (x63).

Note: CRALBP immunofluorescence apparent on the retinal side of the posterior hyaloid membrane in (a) and (b) but not present in (c) and (d) due to confocal optical sectioning through a membrane trough in (a) and (b) and through a membrane peak in (c) and (d) (Section 3.4.4 and Figure 3-16 for further details of CRALBP staining in relation to the posterior hyaloid membrane).

Laminocyte immunostaining for S100B

Laminocyte cells, identified to be adherent to the posterior hyaloid membrane on phase contrast microscopy, consistently demonstrated no detectable immunofluorescence with mouse monoclonal anti-S100B antibodies (Figure 3-34).

See Appendix Figure 6-6 for anti-S100B antibody positive controls and Appendix Figure 6-17a and Figure 6-17b for laminocyte negative controls.

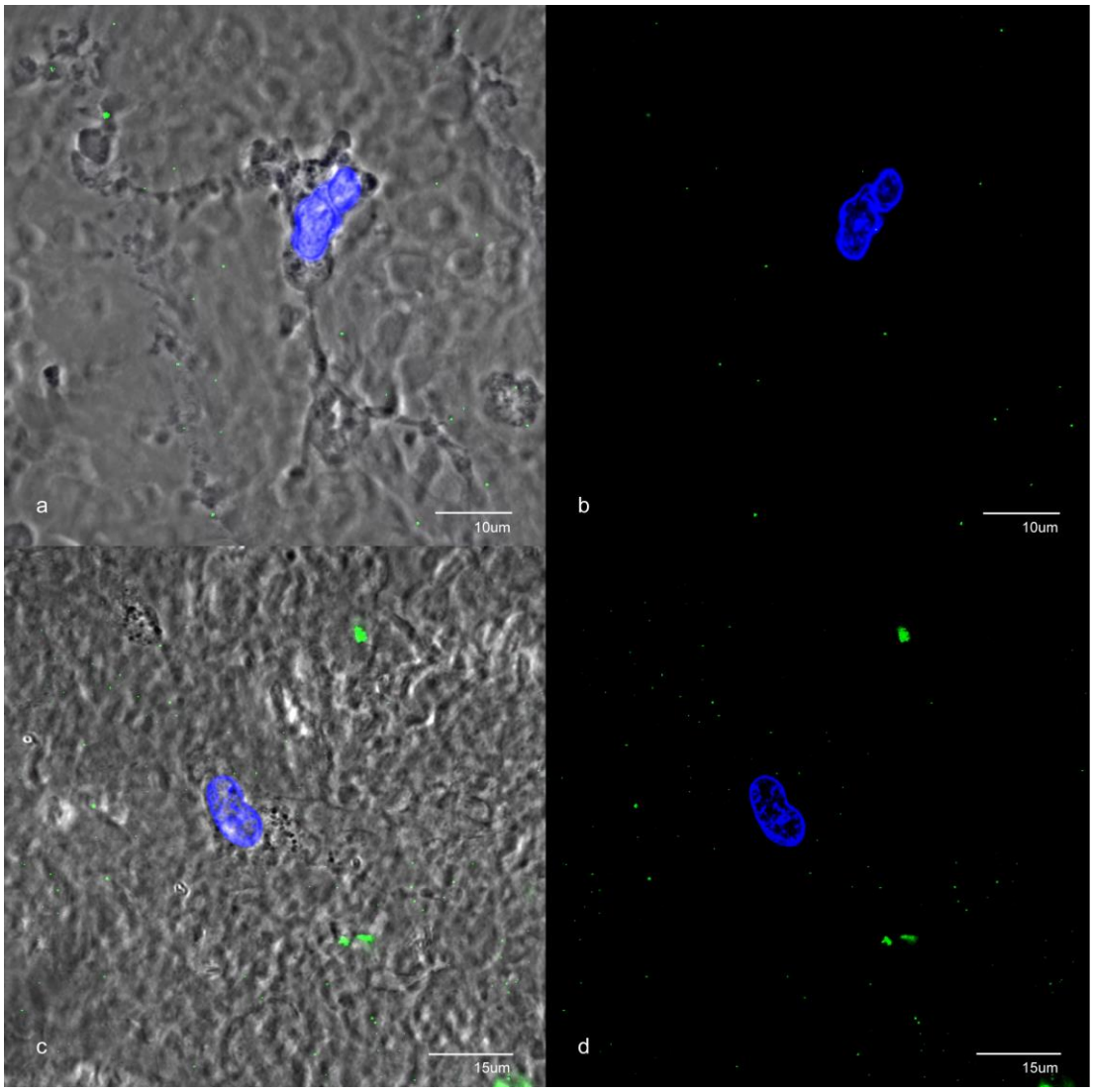

Figure 3-34 Laminocyte immunohistochemistry: S100B

Confocal micrograph series stained with antibodies to S100B (green fluorescence, Alexa Fluor® 488) and DAPI (blue fluorescence) demonstrating laminocytes with negative S100B immunofluorescence: (a) and (b) with and without phase contrast overlay respectively (x81.9), (c) and (d) with and without phase contrast overlay respectively (x63).

Laminocyte immunostaining for vimentin

Laminocyte cells, identified to be adherent to the posterior hyaloid membrane on phase contrast microscopy, consistently demonstrated no detectable immunofluorescence with mouse monoclonal anti-vimentin antibodies (Figure 3-35).

See Appendix Figure 6-7 for anti-vimentin antibody positive controls and Appendix Figure 6-17a and Figure 6-17b for laminocyte negative controls.

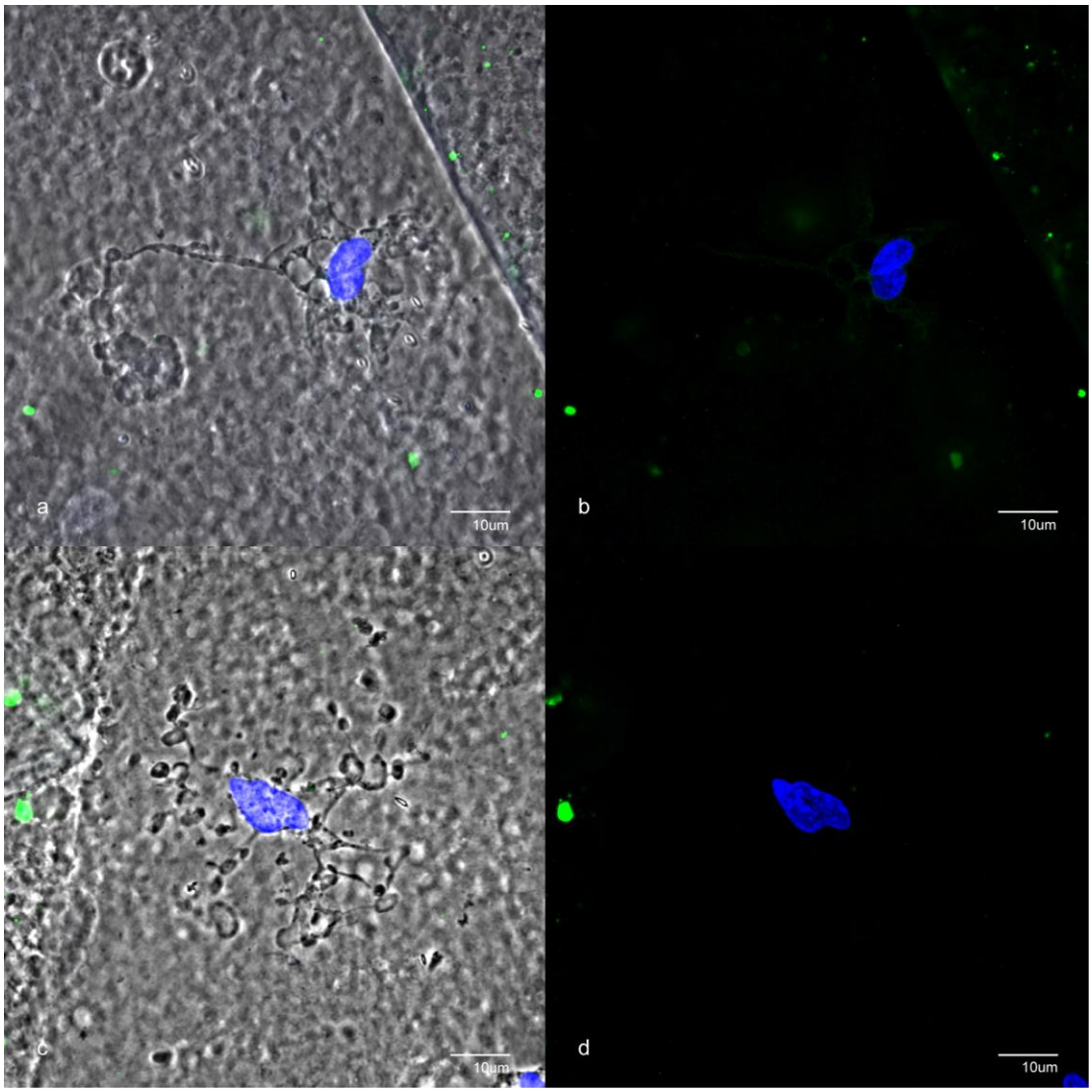

Figure 3-35 Laminocyte immunohistochemistry: vimentin

Confocal micrograph series stained with antibodies to vimentin (green fluorescence, Alexa Fluor® 488) and DAPI (blue fluorescence) demonstrating laminocytes with negative vimentin immunofluorescence: (a) and (b) with and without phase contrast overlay respectively (x63), (c) and (d) with and without phase contrast overlay respectively (x63).

Laminocyte immunostaining for ezrin

Laminocyte cells, identified to be adherent to the posterior hyaloid membrane on phase contrast microscopy, consistently demonstrated no detectable immunofluorescence with mouse monoclonal anti-ezrin antibodies (Figure 3-36).

See Appendix Figure 6-13 for anti-ezrin antibody positive controls and Appendix Figure 6-17a and Figure 6-17b for laminocyte negative controls.

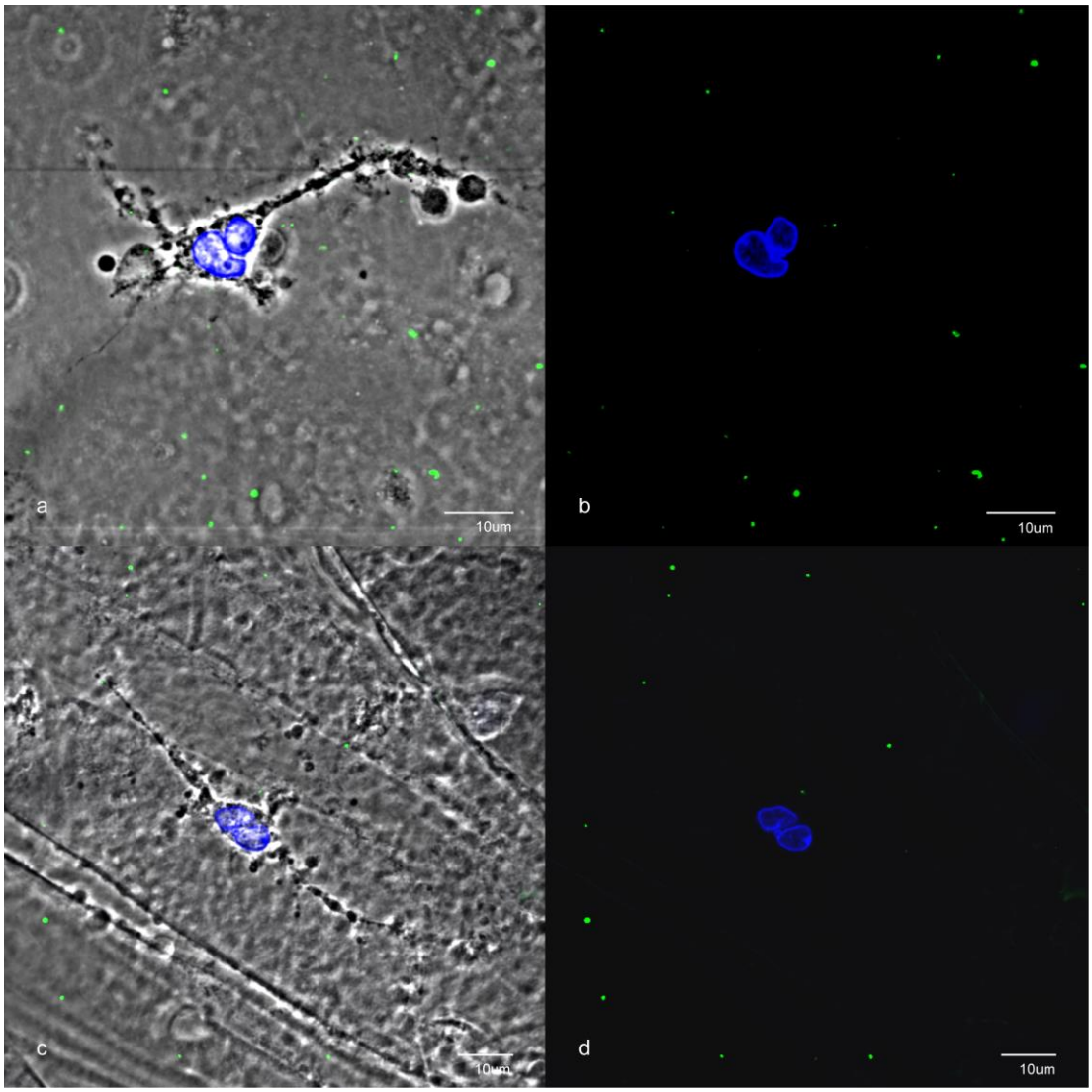

Figure 3-36 Laminocyte immunohistochemistry: ezrin

Confocal micrograph series stained with antibodies to ezrin (green fluorescence, Alexa Fluor® 488) and DAPI (blue fluorescence) demonstrating laminocytes with negative ezrin immunofluorescence: (a) and (b) with and without phase contrast overlay respectively (x81.9), (c) and (d) with and without phase contrast overlay respectively (x63).

Laminocyte immunostaining to cytokeratin

Laminocyte cells, identified to be adherent to the posterior hyaloid membrane on phase contrast microscopy, consistently demonstrated no detectable immunofluorescence with mouse monoclonal anti-cytokeratin antibodies (Figure 3-37).

See Appendix Figure 6-14 for anti-ezrin antibody positive controls and Appendix Figure 6-17a and Figure 6-17b for laminocyte negative controls.

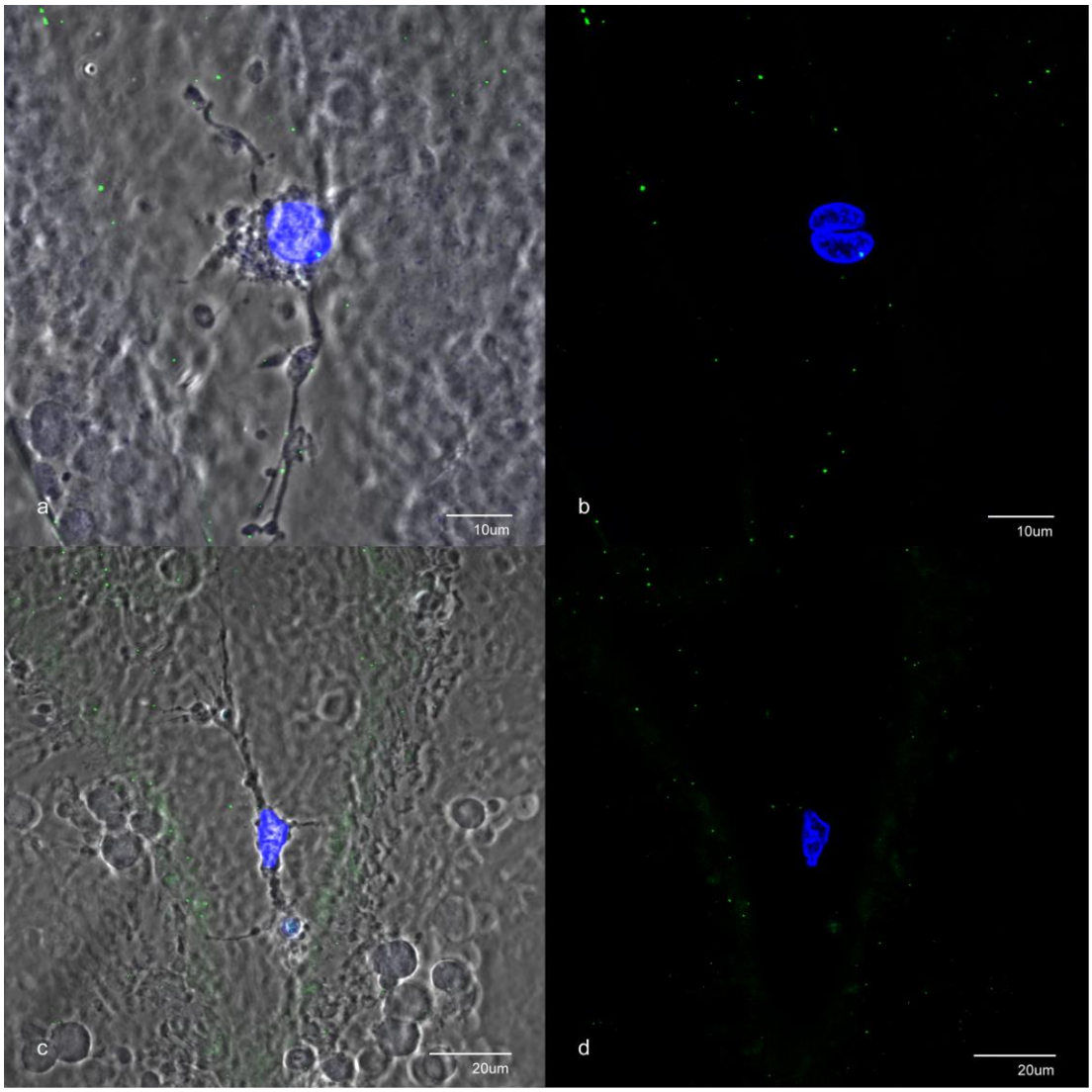

Figure 3-37 Laminocyte immunohistochemistry: cytokeratin

Confocal micrograph series stained with antibodies to cytokeratin (green fluorescence, Alexa Fluor® 488) and DAPI (blue fluorescence) demonstrating laminocytes with negative cytokeratin immunofluorescence: (a) and (b) with and without phase contrast overlay respectively (x75.6), (c) and (d) with and without phase contrast overlay respectively (x50.4).

3.4.8 Immunohistochemistry results summary

The results for all immunohistochemical investigations are summarised in Table 3.3.

Table 3-3 Immunohistochemistry results summary

Primary anitbody	Laminocytes	Vitreous	Posterior hyaloid membrane
Anti-collagen IV			Positive stain with vitreal/retinal aspect distinction
Anti-laminin			Positive stain with vitreal/retinal aspect distinction
Anti-fibronectin		Non-specific stain	Stained without vitreal/retinal aspect distinction
Anti-opticin		Positive fibrillar stain	Stained without vitreal/retinal aspect distinction
Anti-GFAP	Positive stain *		
Anti-MHC class II	Positive stain		
Anti-CD68	Positive stain		
Anti-CD11b	Negative stain		
Anti-Iba1	Negative stain		
Anti-CRALBP	Negative stain		Diffuse fragmented stain on retinal aspect
Anti-S100B	Negative stain		Minimal stain on retinal aspect
Anti-vimentin	Negative stain		Minimal stain on retinal aspect
Anti-ezrin	Negative stain		
Anti-cytokeratin	Negative stain		

* Denotes positive staining not as expected for glial cells

3.5 Discussion

3.5.1 Validation of study design

Globe tissue

For repeatable results that can be dependably extrapolated, histological investigations are entirely dependent on the quality of the supplied tissue to be examined.

In some respects, the eye is a fortunate organ to investigate histologically, as donor globe retrieval can be delayed up to 24 hours post-mortem (Gaum et al., 2012), without excessive accumulation of ocular surface microbial load (due to loss of tears and blink reflex) and without excessive accumulation of metabolic waste products in the aqueous humour (Armitage and Easty, 1997). Furthermore, unlike the heart, lung, liver and pancreas, which are perfusion sensitive organs and require transplantation within four to twelve hours (Egan, 1992; Reich and Guy, 2012; Wheeldon, 1991), organ culture medium allows donor corneas to be stored for up to five weeks before transplantation (Pels and Rijneveld, 2009). In the current study, globe tissue specimens received from the Corneal Transplant Service Eye Bank were fixed in 4% paraformaldehyde at the time viable corneal tissue was harvested for storage; given the similar avascular nature of the vitreous and the cornea, in addition to continual cold chain storage, it is possible that there was little anoxic cellular response in the examined tissue and the presented histological results are likely to be a true reflection of the ante-mortem state.

Despite removal of an 18mm corneoscleral button for subsequent corneal transplantation, the majority of globe tissue specimens received were found to be anatomically intact on gross examination; conservation of the iris architecture and apposition of the intraocular crystalline lens to the pupillary aperture anteriorly, in arrangement with an intact scleral coat laterally and posteriorly, appeared to provide sufficient support to preserve the posterior segment contents. A minority of the globe tissue specimens received were not anatomically preserved on gross examination and were excluded from further investigation.

Dissection protocol

In some respects, the vitreous is an unfortunate structure to examine histologically; it is an amorphous, transparent structure that is comprised of 98 to 99% water (Graymore, 1970). In the current study, a novel dissection technique was developed to address these challenges, in addition to:

1. Reliably determining the posterior vitreous detachment status of globe tissue prior to isolation of the posterior hyaloid membrane.

2. Isolating posterior hyaloid membranes in a manner that would facilitate en face microscopic examination.

Pivotal to the primary objective of interrogating the histological correlate of the posterior hyaloid membrane observed clinically in patients with acute posterior vitreous detachment (using off-axis slit lamp biomicroscopy) (Figure 3-7 and Video Appendix 1.3), was to ensure that only globe tissue that had sustained a posterior vitreous detachment was selected. Posterior vitreous detachment status was evaluated using a modification to the 'suspended-in-air examination' (Foos, 1972b). The modified air suspension technique assessed the shape of the eviscerated contents (before and after removal of the choroid whilst suspended in air from the optic nerve stalk remnant) as an alternative to examining sectioned globe calottes vertically supported by wire hooks, as originally described by Foos. Although Foos' technique was attempted in initial dissections in the current study, it was found to be technically challenging to cut globe tissue calottes without distorting the ocular anatomy and unreliable in determining posterior vitreous detachment status; this may be a result of using posterior segment globe tissue in comparison to whole globes used by Foos.

Prospective studies have demonstrated that cadaveric posterior vitreous detachment is consistent with, and a true representation of antemortem posterior vitreous detachment (Snead et al., 1994b, 2002). These studies validate Foos' 'suspended-in-air examination' and the current dissection technique, suggesting the observed posterior vitreous detachments are not postmortem artifacts.

Retrieval of intact sheets of posterior hyaloid membrane, that could be flat mounted for en face microscopic examination, was sought to enable a topographical 'bird's eye view' of the tissue that would allow direct comparison with the clinical appearance of the posterior hyaloid membrane observed on slit lamp biomicroscopy. Furthermore, en face examination was sought to facilitate a global morphological examination of laminocytes (compared to existing cross-sectional views), in addition to their relationship with the posterior hyaloid membrane using confocal microscopy z-stack imaging.

3.5.2 Phenotypic characteristics of the posterior hyaloid membrane and its likely clinical correlate

Topographical appearance

Expectedly, the topographical appearance of isolated posterior hyaloid membranes seen on phase (Figure 3-11d) and confocal microscopy (Figure 3-12a, Figure 3-12b, Figure 3-12c, Figure 3-13a, Figure 3-13b, Figure 3-13c, Figure 3-14a, Figure 3-14b and Figure 3-19a) correlate well. Both imaging modalities demonstrate delineated sheets with a consistently creased and crinkled surface appearance. Comparison to the biomicroscopic topographical appearance of the posterior hyaloid membrane observed clinically in patients presenting with posterior vitreous detachment (Figure 3-7 and Video Appendix 1.3), highlights and confirms the similarities between these structures.

The impression gained when manipulating in vitro posterior hyaloid membrane specimens (under phase contrast microscopy) is of a firm but flexible film, reminiscent of the impression one gains from observing the movement of the posterior hyaloid membrane on dynamic vitreous microscopy in vivo (slit lamp biomicroscopic examination of the vitreous between voluntary vertical saccadic eye movements utilising a wide illumination-observation angle) (Video Appendix 1.3).

Furthermore, high power slit lamp biomicroscopic in vivo examination demonstrates occasional cells studded onto the surface of the posterior hyaloid membrane (Figure 3-7i and Video Appendix 1.3), an appearance in keeping with the resident laminocyte cell population described in the literature (Snead et al., 2004, 2002) and identified in the current study.

This study demonstrates that the posterior hyaloid membrane specimens isolated from human globe tissue in the current study are the in vitro correlates of the posterior hyaloid membrane seen in vivo when examining patients with a posterior vitreous detachment.

Basement membrane immunohistochemistry

The posterior hyaloid membrane specimens in the current study reliably and repeatedly stained with anti-collagen IV antibodies and anti-laminin antibodies (Figure 3-12 and Figure 3-13). Staining appeared specific, distinctly delineating morphology and demonstrating the characteristic creased and crinkled surface topography. As type IV collagen and laminin are recognised as basement membrane defining components (Fox et al., 1991; Kefalides, 1971; Kohno et al., 1987; Leblond and Inoue, 1989; Timpl and Dziadek, 1986; Timpl et al., 1981), it is apparent that the isolated posterior hyaloid membranes reported in the current study are sheets of true basement membrane.

Fibronectin is a ubiquitous extracellular matrix molecule and a known component of basement membranes and the vitreoretinal interface (Chen et al., 2009; Kohno et al., 1987; Stalmans et al., 2012; 1993). Anti-fibronectin antibody staining of posterior hyaloid membranes confirmed these assertions by demonstrating immunofluorescent staining patterns that was specific for, but not restricted to membranes (less specific delineation of residually attached vitreous gel) (Figure 3-14).

3.5.3 Origins of the posterior hyaloid membrane

The detached posterior hyaloid membrane specimens isolated in the current study have been demonstrated to be true basement membranes that correlate closely to the appearance of posterior hyaloid membranes observed on slit lamp biomicroscopy (Figure 3-7 and Video Appendix 1.3).

The results of this study suggest that prior to posterior vitreous detachment, the posterior hyaloid membrane must form part of the internal limiting membrane of the retina. It is conceivable that the vitreous, with its firm attachment to the internal limiting membrane, becomes detached from the surface of the retina along a plane

of weakness or split in an age thickened (Section 3.1.2) and/or hyperconvoluted (Snead et al., 2004) internal limiting membrane during the process of posterior vitreous detachment.

The configuration of isolated posterior hyaloid membranes in cross-section and three-dimensional reconstructions, when stained with anti-collagen IV and anti-laminin antibodies in this study, consistently demonstrate a smooth vitreal aspect and an irregularly coarse retinal aspect (Figure 3-12d, Figure 3-12e, Figure 3-12f and Figure 3-13d, Figure 3-13e, Figure 3-13f respectively). This configuration is highly reminiscent of the electron micrograph cross-sections of the internal limiting membrane (Figure 3-1P and Figure 3-1E), again supporting the hypothesis that prior to separation the posterior hyaloid membrane isolates originate from the internal limiting membrane on the surface of the retina.

Furthermore, immunofluorescent investigations in the current study depicting the association of retinal macroglia markers to the retinal aspect of isolated posterior hyaloid membranes (most notably anti-CRALBP antibodies used to identify Müller glia) (Figure 3-16, Figure 3-17 and Figure 3-18), appear to confirm a retinal origin and further evidence these membranes are derived from the internal limiting membrane.

To discount an important argument that agrees with the aforementioned findings, but attributes them to an artifactual split of the internal limiting membrane off the surface of the retina during vitreous processing, anti-collagen IV immunofluorescence was undertaken on retinal specimens from dissected globe tissues that were evaluated to have a posterior vitreous detachment (using the modified air suspension test, in addition to having the corresponding posterior hyaloid membranes isolated). Immunofluorescent images demonstrated the anticipated vascular branching pattern of the superficial retinal blood vessels, delineated by their endothelial basement membranes, in association with a continuous sheet of internal limiting membrane on the retinal surface (Figure 3-19 and Figure 3-20).

In addition to validating the dissection protocol employed in the current study, the present findings suggest that isolated posterior hyaloid membrane specimens are not an artifactual split of the internal limiting membrane off the surface of the retina. Interpretations of the findings are more likely to indicate that the process of posterior

vitreous detachment represents an intramembranous split of the retinal internal limiting membrane that results in an anterior lamellar (recognised as the posterior hyaloid membrane) that encases and remains attached to the detached vitreous gel at the original vitreoretinal interface, and a residual posterior lamella (recognised as internal limiting membrane) on the surface of the retina. Alternatively, the results may indicate the process of posterior vitreous detachment involves complete detachment of the internal limiting membrane into the vitreous cavity, with reformation of the internal limiting membrane on the surface of the retina.

3.5.4 Vitreous gel immunohistochemistry

Opticin is highly expressed in the adult eye and present throughout the vitreous where it is thought to stabilise the vitreous gel structure by associating with collagen fibrils (through binding to chondroitin sulphate proteoglycans) (Reardon et al., 2000). Furthermore, opticin has been demonstrated to be particularly concentrated at the internal limiting membrane, where it binds heparin sulphate proteoglycans, a major component of basement membranes (including the internal limiting membrane) (Hindson et al., 2005). It has been suggested that opticin, through its binding affinity for glycosaminoglycans (including heparin and chondroitin sulphates) could link vitreous collagen fibrils to the inner limiting membrane, acting as a “molecular glue” at the vitreoretinal interface (Le Goff and Bishop, 2007).

As proof of concept, vitreous gel residually attached to isolated posterior hyaloid membrane specimens was immunohistochemically phenotyped using anti-opticin antibodies; immunofluorescent images confirm the expected opticin vitreous distribution in a fibrillar pattern, in addition to a concentrated “molecular glue” layer at the vitreoretinal interface (Figure 3-15).

3.5.5 Phenotypical characteristics of laminocytes

Laminocytes, defined as the cell population intimately associated to the posterior hyaloid membrane, were identified in all examined specimens in the current study. Identified laminocyte cells appeared to be phenotypically distinctive, demonstrating constantly recognisable morphological and structural features. These typically included characteristically large ‘cashew’ shaped nuclei that occasionally appeared

binucleated in cross-section, in addition to somatic cytoplasm that commonly extended into two or three main pseudopodia, that in turn often branched heavily, resulting in an extensively variable dendritic morphology (Figure 3-21 and Figure 3-22). The nuclear and somatic appearance was so characteristic that laminocyte cells in the current study were readily identifiable on epifluorescent or phase contrast microscopy respectively.

Although previous histological studies have reported laminocytes to be spindle shaped cells with round or oval nuclei and scanty cytoplasm (Figure 3-3), these investigations have been limited by relatively low magnification light microscopy with no delineation of cellular morphology on phase contrast microscopy or immunofluorescence, in addition to only cross-sectional interpretations of morphology. In keeping with previous electron microscopic findings (Figure 3-5), laminocytes in the current study were only identified on the vitreal aspect of the posterior hyaloid membrane (Snead et al., 2002, 2008). Furthermore, although electron microscopy is recognised to be prone to processing artefact, the three-dimensional laminocyte morphology demonstrated on scanning electron microscopy (Figure 3-5b) is more in keeping with a dendritic branching cell with a large central nucleus, than the reported spindle shaped cells observed under light microscopy. The reported characteristic distribution pattern of laminocytes (densely populated around the Weiss ring, becoming less densely populated peripherally) was beyond the scope of the current study as isolated posterior hyaloid membranes were debulked and dissected into fragments to facilitate processing.

Previous immunohistochemical phenotyping of laminocytes has been limited to anti-GFAP and anti-collagen IV antibodies. Studies on cadaveric globes, with (Figure 3-3) and without posterior vitreous detachment, demonstrated focal and patchy staining of laminocytes with GFAP, and weak positive staining of the associated posterior hyaloid membrane and internal limiting membrane for type IV collagen (Snead et al., 2004, 2002, 2008). GFAP positivity was interpreted as to indicate that laminocytes were of glial origin, which prompted the comparison to glial cells associated with asymptomatic, simple epiretinal membranes originally reported by Foos (Foos, 1974).

Foos observed cells of the vitreoretinal interface in eight autopsy eyes, which he reported to have long flattened processes he described as exceedingly delicate and spreading remarkable distances along the retinal surface; he noted extending cell

processes typically branched in two or three chief directions. Abundant cytoskeletal filaments and the appearance of an active perikaryon with an abundant granular cytoplasmic reticulum and a conspicuous Gogli apparatus were identified by electron microscopy. He also noted the cells had no basement membrane apparent on their vitreal aspect. These reported characteristics appear to align well with the morphological appearance of laminocytes described in the current study. Although no staining was employed by Foos, the cells were identified as glial and he hypothesised that these cells migrated through self-sealing breaks in the internal limiting membrane to form simple epiretinal membranes (Foos, 1974). An alternative explanation may be that the cells identified by Foos were in fact laminocytes, and the observed breaks in the internal limiting membrane were artifactual.

In the current study, anti-GFAP antibody labelling was detected in all identified laminocytes (Figure 3-23). Immunofluorescence was demonstrated within the cytoplasmic dendritic extensions, in addition to the cell nucleus (except for a minority of cells in one examined posterior hyaloid specimen, where only cytoplasmic immunofluorescence was detected (Figure 3-24)). Although loss of the nuclear void may indicate non-specific fluorescence and imply non-specific staining of cytosolic labelling antibodies (Figure 3-22), the detection of GFAP in the nucleus has been demonstrated in previous studies (Danielyan et al., 2007) and is consistent with in vitro studies demonstrating the interaction of this type III intermediate filament protein with DNA (Tolstonog et al., 2000; Traub, 1995). However, with the exception of nuclear laminins, intermediate filaments are not generally found in the nucleus; the classically anticipated staining pattern for GFAP would be in a cytoplasmic filamentous pattern, with a non-staining nuclear void. The current equivocal GFAP findings are therefore not entirely explainable and should be interpreted with caution. Further investigations would be required to ascertain if laminocyte definitively express GFAP, this could be achived by RNA extraction followed by reverse transcription quantitative PCR and/or protein extraction followed by Western blotting from isolated laminocytes.

Previous extrapolations that suggest laminocytes are of glial origin due to their expression of GFAP (Snead et al., 2004, 2002, 2008) may not necessarily be supported by observations in the current study. The antibody panel used, which recognised retinal astrocyte and Müller glia epitopes demonstrated no positive immunofluorescence in laminocytes utilising anti-CRALB, anti-S100B and anti-vimentin antibodies (Figure 3-33, Figure 3-34 and Figure 3-35 respectively). In

addition, although GFAP was originally considered to be a specific marker protein for astrocytes and reactive Müller glia (Brenner, 1994; Brenner et al., 1994), there is increasing evidence demonstrating the presence of this intermediate filament protein in chondrocytes, fibroblasts, hepatic stellate cells, keratinocytes, kidney glomeruli mesangial cells and podocytes, lens epithelial cells, Leydig cells of the testis and pancreatic stellate cells (Apte et al., 1998; Buniatian et al., 2002; Danielyan et al., 2007; Hainfellner et al., 2001; Lu et al., 2001; Riccalton-Banks et al., 2003).

Furthermore, laminocytes demonstrated reliable and repeatable positive immunofluorescence with anti-CD68 (monocyte/macrophage marker) and anti-MHC class II (antigen presenting cell marker) antibodies (Figure 3-28, Figure 3-29 and Figure 3-25, Figure 3-26 respectively, in addition to co-staining with GFAP in Figure 3-30 and Figure 3-27 respectively), but were negative with anti-Iba1 antibody used to identify microglia (Figure 3-32).

These observations would suggest that laminocytes may constitute a macrophage subpopulation resident in the vitreous. In addition to a compatible dendritic morphology delineated by phase contrast microscopy and autofluorescence (Figure 3-21 and Figure 3-22 respectively), further evidence of a potential macrophage lineage is the presence of phagocytic terminal bulbs at the end of laminocyte dendritic processes that showed CD68 positive granules in association with endocytosed nuclear material (Figure 3-21d).

Hyalocytes are a well characterised vitreal cell population, with reported macrophage features. The term hyalocytes refers to the resident cells of the cortical or peripheral vitreous (Balazs et al., 1964; Hamburg, 1959; Szirmai and Balazs, 1958). These cells have been characterised as having lobulated nuclei, multiple cytoplasmic projections and moderate numbers of mitochondria and secretory granules, in addition to a well-developed Golgi apparatus (Balazs et al., 1964; Hogan, 1971). They are located at an average of 500µm from the inner retinal surface and are concentrated in the anterior vitreous and adjacent to the optic disc (the posterior distribution pattern around the optic disc being reminiscent of that originally used to describe laminocyte distribution (Snead et al., 2002)).

Recent studies (Matsumoto et al., 2007; Noda et al., 2004; Qiao et al., 2005; Zhu et al., 1999) have dispelled the notion that hyalocytes are quiescent resting cells; they have been demonstrated to actively maintain the transparent and avascular nature

of the vitreous. The effects of hyalocytes on the vitreal environment can be broadly classified into three main categories (Sakamoto and Ishibashi, 2011):

1. Extracellular matrix synthesis. Hyalocytes have been reported to produce vitreal extracellular matrix components, including collagen, hyaluronic acid and glycosaminoglycans (Newsome et al., 1976; Nishitsuka et al., 2007; Osterlin and Jacobson, 1968; Rittig et al., 1993; Sommer et al., 2008)

2. Modulation of intraocular immunity. In order to retain transparency of the visual pathway whilst maintaining microbial defences, the eye has evolved to become an immune-privileged site (Stein-Streilein and Streilein, 2002; Streilein, 2003). In a similar fashion to which F4/80 (a macrophage marker) positive bone marrow-derived antigen presenting cells (present in the ciliary body and iris) are able to induce peripheral immunological tolerance (anterior chamber-associated immune deviation) (Stein-Streilein, 2008; Streilein et al., 1997), vitreous cavity-associated immune deviation has been demonstrated to significantly delay antigen-specific delayed-type hypersensitivity responses following injection of an intravitreal antigen; the only antigen presenting cell candidates were reported to be hyalocytes, which were documented to be F4/80 positive (Sonoda et al., 2005).

3. Modulation of intraocular inflammation. The assertion that hyalocytes have characteristics shared with macrophages, including phagocytic activity with surface receptors for IgG and complement components (Grabner et al., 1980), has propagated numerous in vitro investigations on cultured hyalocytes in an attempt to understand the complex array of cytokines produced by these cells and hypothesised to drive common ocular disorders like diabetes and age-related macular degeneration (Hata et al., 2008; Noda et al., 2004; Tkachuk et al., 2009).

In addition, hyalocytes have also been demonstrated to have a high binding affinity to, and a remarkable contractile ability of extracellular collagenous gel matrices (Hirayama et al., 2004; Kita et al., 2008; Schaefer et al., 1996). Matrix contraction is a pathophysiological feature implicated in various vitreoretinal disorders, such as proliferative vitreoretinopathy, diabetic macular oedema and the formation of epiretinal membranes and macular holes (Gandorfer et al., 2009; Matsumoto et al.,

2007; Ueno et al., 2007), and this could be extrapolated to include posterior vitreous detachment.

Morphological studies suggest hyalocytes are derived from a monocyte/macrophage lineage (Balazs et al., 1964, 1980; Ogawa, 2002; Salu et al., 1985), although a paucity of lysosomes has highlighted differences with typical macrophages (Hogan, 1971). However, under physiological conditions, it has been demonstrated that hyalocytes originate from bone marrow (Qiao et al., 2005; Sakamoto, 2003; Sakamoto and Ishibashi, 2011). Immunohistochemical studies have demonstrated that hyalocytes express the leucocyte associated antigens CD11a, CD 45, CD64 and MHC class II antigens. However, they have been shown to conspicuously lack CD68, an antigen expressed by virtually all tissue macrophages; in addition, hyalocytes express S100, but not GFAP, CRALBP or cytokeratin (Grabner et al., 1980; Jacobson, 1984; Lazarus and Hageman, 1994; Schönfeld, 1996; Zhu et al., 1999).

Because there are striking morphological similarities with hyalocytes (Figure 3-38), in addition to the close proximity in the shared extracellular matrix environment, it is tempting to extrapolate that laminocytes are hyalocytes that have been sequestered onto the posterior hyaloid membrane or hyalocytes are laminocytes that that lost their attachment to the vitreoretinal interface. However, despite similarities, the current study has demonstrated fundamental differences between these distinctly different cell types, namely the expression of CD68 and GFAP in laminocytes (Figure 3-28, Figure 3-29 and Figure 3-23, Figure 3-24 respectively, in addition to Figure 3-30 for co-staining), and the lack of expression of CD11 or S100B as reported in hyalocytes (Figure 3-31 and Figure 3-34 respectively).

Additional immunophenotyping with antibodies directed against recognised mesenchymal (vimentin, Figure 3-35) and epithelial (ezrin and cytokeratin, Figure 3-36 and Figure 3-37 respectively) tissue epitopes did not demonstrate positive immunofluorescence, suggesting laminocytes are unlikely to be of retinal pigment epithelium or fibroblast lineage.

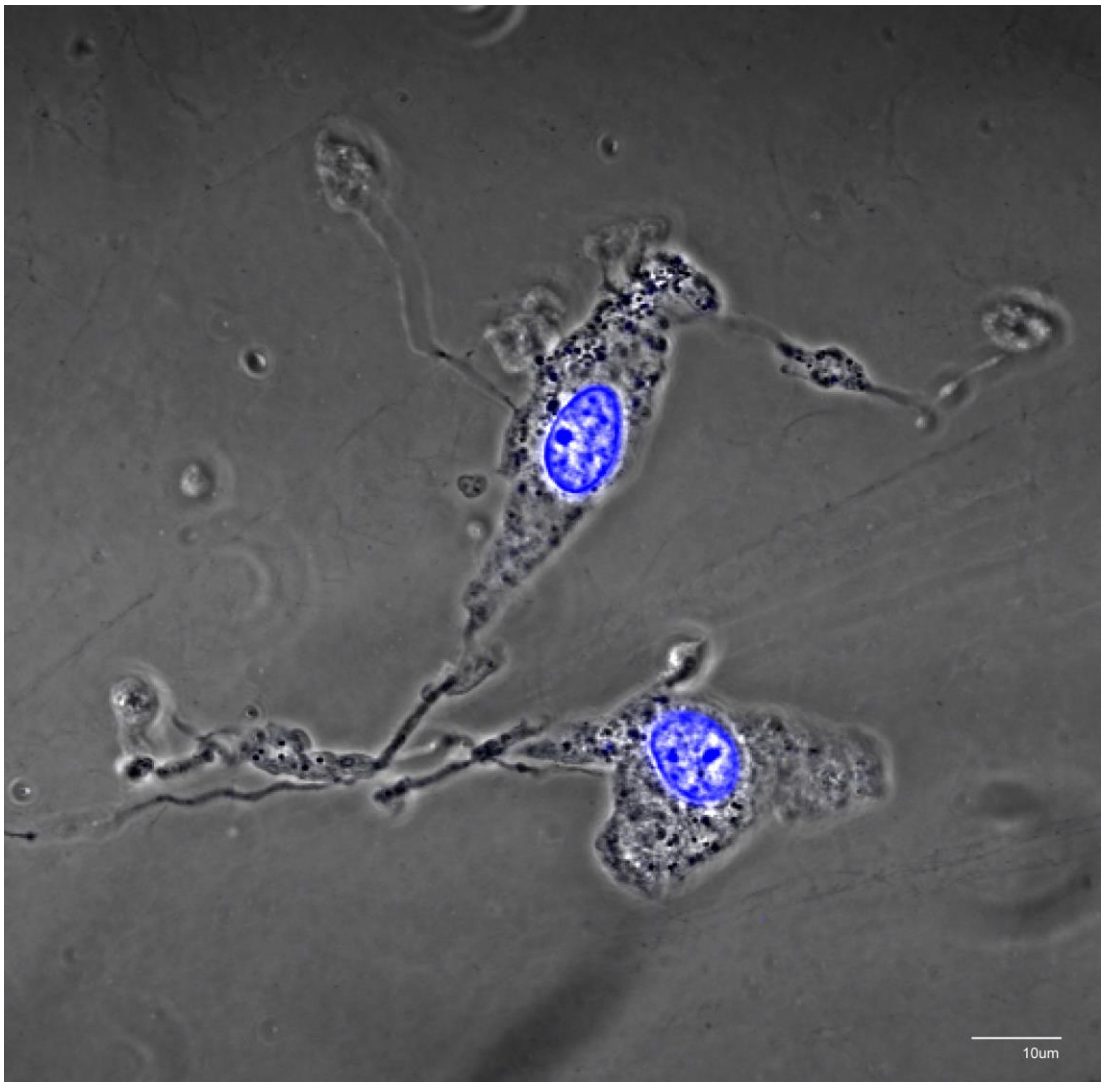

Figure 3-38 Hyalocytes

Phase contrast microscopy of two hyalocytes in peripheral vitreous gel demonstrating multiple cytoplasmic projections, in addition to conspicuous cytoplasmic granules (x50.4).

3.5.6 Potential role of laminocytes

The function of GFAP, a highly conserved intermediate filament protein, in cells outside the central nervous system not yet been identified. GFAP has been demonstrated to be expressed by perivascular cells of many mammalian organ systems, in addition to fibroblasts (including lung alveoli fibroblasts) and cutaneous keratinocytes. These specific anatomical sites have demonstrated recurrent co-staining of metallothionein and MHC class II antigens in association with GFAP (Buniatian et al., 2002; Danielyan et al., 2007). The intriguing distribution of a common set of antigens at the blood-tissue interfaces of internal organs and the air-tissue interfaces of the integumentary and respiratory systems has developed the concept that these proteins are involved in a universal mechanism controlling tissue homeostasis and protection. Furthermore, a simultaneous up-regulation of GFAP and MHC class II in nude mice, that was barely detectable in immunodeficient mice, suggested a possible role in antigen presenting functions (Danielyan et al., 2007).

The findings presented in the current study would suggest that laminocytes are extracellular matrix tissue macrophages, found adherent to the vitreal aspect of the posterior hyaloid membrane. The observation that laminocytes may express GFAP co-staining with MHC class II, in addition to their anatomical location at a tissue interface, is intriguing with regards to a universal theory of tissue homeostasis and protection at tissue interfaces.

The suggestion that laminocytes may potentially play a role in antigen presentation in the vitreous is a novel and important finding with regards to vitreous cavity immunity, a concept classically associated with hyalocyte function and their suspected role in vitreous cavity-associated immune deviation (Sonoda et al., 2005). The observation that laminocytes express MHC II antigens suggests they are unlikely to express F4/80. This assertion would suggest an improbable role in ocular immune privilege (Stein-Streilein, 2008; Streilein et al., 1997), but rather an important role in pathophysiological vitreal inflammation.

The intimate association of laminocytes to the posterior hyaloid membrane potentially make them well placed to be involved in the process of posterior vitreous detachment. In view of the structural similarities that exist between laminocytes and hyalocytes, it is conceivable that evidence demonstrating the ability of hyalocytes to contract three-dimensional extracellular collagenous gel matrices (Hirayama et al.,

2004; Kita et al., 2008; Schaefer et al., 1996) could potentially be extrapolated to include laminocytes; if laminocytes did possess such an ability, they would be prime contenders in a cellular hypothesis of posterior vitreous detachment.

3.5.7 Summary

The current study developed a novel dissection technique to reliably isolate posterior hyaloid membranes and reports a modified air-suspension test developed to aid in ascertaining the status of posterior vitreous detachment in donor globe tissue.

Isolated posterior hyaloid membranes were immunologically interrogated to reveal that they are distinct basement membranes, composed of type IV collagen and laminin. In addition, investigations suggest the posterior hyaloid membrane originates from the internal limiting membrane of the retina. The membranes identified and interrogated in this study correlate with posterior hyaloid membranes observed clinically in patients presenting with posterior vitreous detachment.

Furthermore, the laminocyte cell population, adherent to the vitreal aspect of the posterior hyaloid membrane, was identified and immunologically phenotyped. The results suggest that this population of cells is a distinctly unique subset of macrophages that possibly express GFAP. Given their integral anatomical association with the posterior hyaloid membrane, laminocytes may play a critical role in the process of posterior vitreous detachment.

4 Conclusion

Designing a research study requires judgments regarding methodology, and when there are several different options, any chosen decision results in loss of objectivity. Furthermore, clinical and laboratory studies, although imperative to advancing scientific understanding and knowledge, are limited to current investigative technologies and techniques, in addition to subjective interpretation of the outcomes and results.

The current studies have been conducted with an acute awareness of these limitations and have been carefully designed to address these potential concerns. The methodology employed in the retrospective clinical investigations into the efficacy and safety of prophylactic cryotherapy has been especially considered, addressing previously highlighted issues with regards to control group comparisons (Aylward et al., 2008), in addition to being deliberately weighted against the effectiveness of treatment. The results confirm that the Cambridge Prophylactic Cryotherapy protocol reduces the risk of retinal detachment in type 1 Stickler syndrome and should be offered as a prophylactic treatment option to all patients with the disorder as the gold standard of practice.

Understanding the fundamental principles of posterior vitreous detachment in order to considerately manage and potentially prevent the complications associated with the process is a fundamental strategy for the future success in treating the spectrum vitreoretinal interface disorders and retinal detachment. Furthermore, the advancement of biotechnological techniques and development of new polymers has led to the emergence of innovative intravitreal treatments, including intravitreal pharmaceutics and implant devices (Herrero-Vanrell et al., 2014; Lambiase et al., 2014), in addition to novel gene-mediated interventions delivered by viral vectors (Boye, 2014; Lipinski et al., 2013; Rowe-Rendleman et al., 2014) and potential stem cell therapies (Uy et al., 2013; Johnson and Martin, 2013; Li et al., 2012; Huang et al., 2011). These treatments utilise the immune-privileged character of the vitreous cavity as a therapeutic platform; however, a more detailed knowledge of the vitreous environment is required in order to understand and predict potential outcomes of these and future therapies.

5 References

Ahmad, N.N., Ala-Kokko, L., Knowlton, R.G., Jimenez, S.A., Weaver, E.J., Maguire, J.I., Tasman, W., and Prockop, D.J. (1991). Stop codon in the procollagen II gene (COL2A1) in a family with the Stickler syndrome (arthro-ophthalmopathy). Proc. Natl. Acad. Sci. U. S. A. *88*, 6624–6627.

Akiba, J. (1993). Prevalence of posterior vitreous detachment in high myopia. Ophthalmology *100*, 1384–1388.

3. American Academy of Ophthalmology Retina Panel. Preferred Practice Pattern® Guidelines. Posterior Vitreous Detachment, Retinal Breaks and Lattice Degeneration. San Francisco, CA: American Academy of Ophthalmology, 2008. (Accessed June, 2014) [Internet]. Available from: http://one.aao.org/ppp

Ang, A., Poulson, A.V., Snead, D.R., and Snead, M.P. (2005). Posterior vitreous detachment: current concepts and management. Compr. Ophthalmol. Update *6*, 167–175.

Ang, A., Poulson, A.V., Goodburn, S.F., Richards, A.J., Scott, J.D., and Snead, M.P. (2008). Retinal detachment and prophylaxis in type 1 Stickler syndrome. Ophthalmology *115*, 164–168.

Ang, G.S., Townend, J., and Lois, N. (2012). Interventions for prevention of giant retinal tear in the fellow eye. Cochrane Database Syst. Rev. Online *2*, CD006909.

Annunen, S., Körkkö, J., Czarny, M., Warman, M.L., Brunner, H.G., Kääriäinen, H., Mulliken, J.B., Tranebjaerg, L., Brooks, D.G., Cox, G.F., et al. (1999). Splicing mutations of 54-bp exons in the COL11A1 gene cause Marshall syndrome, but other mutations cause overlapping Marshall/Stickler phenotypes. Am. J. Hum. Genet. *65*, 974–983.

Anton-Lamprecht, I. (1978). Electron microscopy in the early diagnosis of genetic disorders of the skin. Dermatologica *157*, 65–85.

Apte, M.V., Haber, P.S., Applegate, T.L., Norton, I.D., McCaughan, G.W., Korsten, M.A., Pirola, R.C., and Wilson, J.S. (1998). Periacinar stellate shaped cells in rat pancreas: identification, isolation, and culture. Gut *43*, 128–133.

Armitage, W.J., and Easty, D.L. (1997). Factors influencing the suitability of organ-cultured corneas for transplantation. Invest. Ophthalmol. Vis. Sci. *38*, 16–24.

Aylward, B., daCruz, L., Ezra, E., Sullivan, P., MacLaren, R.E., Charteris, D., Gregor, Z., Bainbridge, J., and Minihan, M. (2008). Stickler syndrome. Ophthalmology *115*, 1636–1637; author reply 1637–1638.

Baker, S., Booth, C., Fillman, C., Shapiro, M., Blair, M.P., Hyland, J.C., and Ala-Kokko, L. (2011). A loss of function mutation in the COL9A2 gene causes autosomal recessive Stickler syndrome. Am. J. Med. Genet. A. *155A*, 1668–1672.

Balazs, E.A. (1973). Fine structure and function of ocular tissues. The vitreous. Int. Ophthalmol. Clin. *13*, 169–187.

Balazs, E.A., Toth, L.Z., Eckl, E.A., and Mitchell, A.P. (1964). Studies on the vitreous body. XII. Cytological and histochemical studies on the cortical tissue layer. Exp. Eye Res. *3*, 57–71.

Balazs, E.A., Toth, L.Z., and Ozanics, V. (1980). Cytological studies on the developing vitreous as related to the hyaloid vessel system. Albrecht Von Graefes Arch. Für Klin. Exp. Ophthalmol. Albrecht Von Graefes Arch. Clin. Exp. Ophthalmol. *213*, 71–85.

Booij, J.C., Baas, D.C., Beisekeeva, J., Gorgels, T.G.M.F., and Bergen, A. a. B. (2010). The dynamic nature of Bruch's membrane. Prog. Retin. Eye Res. *29*, 1–18.

Boye, S.E. (2014). Insights gained from gene therapy in animal models of retGC1 deficiency. Front. Mol. Neurosci. *7*, 43.

Brenner, M. (1994). Structure and transcriptional regulation of the GFAP gene. Brain Pathol. Zurich Switz. *4*, 245–257.

Brenner, M., Kisseberth, W.C., Su, Y., Besnard, F., and Messing, A. (1994). GFAP promoter directs astrocyte-specific expression in transgenic mice. J. Neurosci. Off. J. Soc. Neurosci. *14*, 1030–1037.

Brunner, H.G., van Beersum, S.E., Warman, M.L., Olsen, B.R., Ropers, H.H., and Mariman, E.C. (1994). A Stickler syndrome gene is linked to chromosome 6 near the COL11A2 gene. Hum. Mol. Genet. *3*, 1561–1564.

Buniatian, G.H., Hartmann, H.-J., Traub, P., Wiesinger, H., Albinus, M., Nagel, W., Shoeman, R., Mecke, D., and Weser, U. (2002). Glial fibrillary acidic protein-positive cells of the kidney are capable of raising a protective biochemical barrier similar to astrocytes: expression of metallothionein in podocytes. Anat. Rec. *267*, 296–306.

Burton, T.C. (1982). Recovery of visual acuity after retinal detachment involving the macula. Trans. Am. Ophthalmol. Soc. *80*, 475–497.

Butkowski, R.J., Langeveld, J.P., Wieslander, J., Hamilton, J., and Hudson, B.G. (1987). Localization of the Goodpasture epitope to a novel chain of basement membrane collagen. J. Biol. Chem. *262*, 7874–7877.

Byer, N.E. (1989). Long-term natural history of lattice degeneration of the retina. Ophthalmology *96*, 1396–1401; discussion 1401–1402.

Byer, N.E. (1998). What happens to untreated asymptomatic retinal breaks, and are they affected by posterior vitreous detachment? Ophthalmology *105*, 1045–1049; discussion 1049–1050.

Van Camp, G., Snoeckx, R.L., Hilgert, N., van den Ende, J., Fukuoka, H., Wagatsuma, M., Suzuki, H., Smets, R.M.E., Vanhoenacker, F., Declau, F., et al. (2006). A new autosomal recessive form of Stickler syndrome is caused by a mutation in the COL9A1 gene. Am. J. Hum. Genet. *79*, 449–457.

Carafoli, E. (1987). Intracellular calcium homeostasis. Annu. Rev. Biochem. *56*, 395–433.

Carroll, C., Papaioannou, D., Rees, A., and Kaltenthaler, E. (2011). The clinical effectiveness and safety of prophylactic retinal interventions to reduce the risk of retinal detachment and subsequent vision loss in adults and children with Stickler

syndrome: a systematic review. Health Technol. Assess. Winch. Engl. *15*, iii – xiv, 1–62.

Chauhan, D.S., Downie, J.A., Eckstein, M., and Aylward, G.W. (2006). Failure of prophylactic retinopexy in fellow eyes without a posterior vitreous detachment. Arch. Ophthalmol. *124*, 968–971.

Chen, W., Mo, W., Sun, K., Huang, X., Zhang, Y., and Song, H. (2009). Microplasmin degrades fibronectin and laminin at vitreoretinal interface and outer retina during enzymatic vitrectomy. Curr. Eye Res. *34*, 1057–1064.

Cherfan, G.M., Smiddy, W.E., Michels, R.G., de la Cruz, Z., Wilkinson, C.P., and Green, W.R. (1988). Clinicopathologic correlation of pigmented epiretinal membranes. Am. J. Ophthalmol. *106*, 536–545.

Chignell, A.H., Fison, L.G., Davies, E.W., Hartley, R.E., and Gundry, M.F. (1973). Failure in retinal detachment surgery. Br. J. Ophthalmol. *57*, 525–530.

Cho, H., Yamada, Y., and Yoo, T.J. (1991). Ultrastructural changes of cochlea in mice with hereditary chondrodysplasia (cho/cho). Ann. N. Y. Acad. Sci. *630*, 259–261.

Christiano, A.M., McGrath, J.A., Tan, K.C., and Uitto, J. (1996). Glycine substitutions in the triple-helical region of type VII collagen result in a spectrum of dystrophic epidermolysis bullosa phenotypes and patterns of inheritance. Am. J. Hum. Genet. *58*, 671–681.

Cohen, A.I. (1961). Electron microscopic observations of the internal limiting membrane and optic fiber layer of the retina of the Rhesus monkey (M. mulatta). Am. J. Anat. *108*, 179–197.

Colyear, B.H., Jr, and Pishel, D.K. (1960). Preventive treatment of retinal detachment by means of light coagulation. Trans. Pac. Coast Otoophthalmol. Soc. Annu. Meet. *41*, 193–217.

Cowan, P.M., McGavin, S., and North, A.C. (1955). The polypeptide chain configuration of collagen. Nature *176*, 1062–1064.

Cuppage, F.E., Huseman, R.A., Chapman, A., and Grantham, J.J. (1980). Ultrastructure and function of cysts from human adult polycystic kidneys. Kidney Int. *17*, 372–381.

Custodis, E. (1952). Beobachtungen bei der diathermischen Behandlung der Netzhautablösung und ein Hinweis zur Therapie der Amotio Retinae. Ber Dtsch. Ophth Gesellsch *57*, 227–230.

Custodis, E. (1953). Bedeutet die plombenaufniihung auf die sklera einen fortschritt in der operativen behandlung der netzhautablosung? Ber Dtsch. Ophth Gesellsch *58*, 102–105.

Custodis, E. (1956). Die behandlung der netzhautablosung durch umschriebene diathermie-ko- agulation und einer mittels plombenaufniihung erzeugten eindellung der sklera im bereich des risses. Klin Monatsbl Augenheilkd *129*, 476–495.

Daicker, B., Guggenheim, R., and Gywat, L. (1977). [Findings on retinal surface by scanning electron microscopy. II. Vitreous detachment (author's transl)]. Albrecht

Von Graefes Arch. Für Klin. Exp. Ophthalmol. Albrecht Von Graefes Arch. Clin. Exp. Ophthalmol. *204*, 19–29.

Danielyan, L., Tolstonog, G., Traub, P., Salvetter, J., Gleiter, C.H., Reisig, D., Gebhardt, R., and Buniatian, G.H. (2007). Colocalization of glial fibrillary acidic protein, metallothionein, and MHC II in human, rat, NOD/SCID, and nude mouse skin keratinocytes and fibroblasts. J. Invest. Dermatol. *127*, 555–563.

Danysh, B.P., and Duncan, M.K. (2009). The lens capsule. Exp. Eye Res. *88*, 151–164.

Davis, M.D. (1974). Natural history of retinal breaks without detachment. Arch. Ophthalmol. *92*, 183–194.

Davison, B.C. (1965). Epidermolysis bullosa. J. Med. Genet. *2*, 233–242.

Diederen, R.M.H., La Heij, E.C., Kessels, A.G.H., Goezinne, F., Liem, A.T.A., and Hendrikse, F. (2007). Scleral buckling surgery after macula-off retinal detachment: worse visual outcome after more than 6 days. Ophthalmology *114*, 705–709.

Donoso, L.A., Edwards, A.O., Frost, A.T., Ritter, R., Ahmad, N.N., Vrabec, T., Rogers, J., and Meyer, D. (2002). Identification of a stop codon mutation in exon 2 of the collagen 2A1 gene in a large stickler syndrome family. Am. J. Ophthalmol. *134*, 720–727.

Duncan, K.G., Fessler, L.I., Bächinger, H.P., and Fessler, J.H. (1983). Procollagen IV. Association to tetramers. J. Biol. Chem. *258*, 5869–5877.

Egan, T.M. (1992). Lung preservation. Semin. Thorac. Cardiovasc. Surg. *4*, 83–89.

Engerman, R.L., and Colquhoun, P.J. (1982). Epithelial and mesothelial basement membranes in diabetic patients and dogs. Diabetologia *23*, 521–524.

Farquhar, M.G., Wissig, S.L., and PALADE, G.E. (1961). Glomerular permeability. I. Ferritin transfer across the normal glomerular capillary wall. J. Exp. Med. *113*, 47–66.

Fine, B.S. (1961). Limiting membranes of the sensory retina and pigment epithelium. An electron microscopic study. Arch. Ophthalmol. *66*, 847–860.

Fine, B.S., and Tousimis, A.J. (1961). The structure of the vitreous body and the suspensory ligaments of the lens. Arch. Ophthalmol. *65*, 95–110.

Fischer, V.W., Barner, H.B., and LaRose, L.S. (1982). Quadriceps and myocardial capillary basal laminae. Their comparison in diabetic patients. Arch. Pathol. Lab. Med. *106*, 336–341.

Folk, J.C., Arrindell, E.L., and Klugman, M.R. (1989). The fellow eye of patients with phakic lattice retinal detachment. Ophthalmology *96*, 72–79.

Foos, R.Y. (1972a). Vitreoretinal juncture; topographical variations. Invest. Ophthalmol. *11*, 801–808.

Foos, R.Y. (1972b). Posterior vitreous detachment. Trans. - Am. Acad. Ophthalmol. Otolaryngol. Am. Acad. Ophthalmol. Otolaryngol. *76*, 480–497.

Foos, R.Y. (1974). Vitreoretinal juncture--simple epiretinal membranes. Albrecht Von Graefes Arch. Für Klin. Exp. Ophthalmol. Albrecht Von Graefes Arch. Clin. Exp. Ophthalmol. *189*, 231–250.

Foos, R.Y., and Wheeler, N.C. (1982). Vitreoretinal juncture. Synchysis senilis and posterior vitreous detachment. Ophthalmology *89*, 1502–1512.

Fox, J.W., Mayer, U., Nischt, R., Aumailley, M., Reinhardt, D., Wiedemann, H., Mann, K., Timpl, R., Krieg, T., and Engel, J. (1991). Recombinant nidogen consists of three globular domains and mediates binding of laminin to collagen type IV. EMBO J. *10*, 3137–3146.

Gandorfer, A., Rohleder, M., and Kampik, A. (2002). Epiretinal pathology of vitreomacular traction syndrome. Br. J. Ophthalmol. *86*, 902–909.

Gandorfer, A., Scheler, R., Haritoglou, C., Schumann, R., Nentwich, M., and Kampik, A. (2009). Pathology of the macular hole rim in flat-mounted internal limiting membrane specimens. Retina Phila. Pa *29*, 1097–1105.

Gärtner, J. (1965). [The fine structure of the vitreous body cortex of the human eye at the ora serrata retinae in old age]. Albrecht Von Graefes Arch. Für Klin. Exp. Ophthalmol. Albrecht Von Graefes Arch. Clin. Exp. Ophthalmol. *168*, 529–562.

Gaum, L., Reynolds, I., Jones, M.N.A., Clarkson, A.J., Gillan, H.L., and Kaye, S.B. (2012). Tissue and corneal donation and transplantation in the UK. Br. J. Anaesth. *108 Suppl 1*, i43–i47.

Go, S.L., Maugeri, A., Mulder, J.J.S., van Driel, M.A., Cremers, F.P.M., and Hoyng, C.B. (2003). Autosomal dominant rhegmatogenous retinal detachment associated with an Arg453Ter mutation in the COL2A1 gene. Invest. Ophthalmol. Vis. Sci. *44*, 4035–4043.

Le Goff, M.M., and Bishop, P.N. (2007). Focus on molecules: opticin. Exp. Eye Res. *85*, 303–304.

Gonin, J. (1904). La pathogınie du dıcollement spontanı de la rıtine. Ann Ocul. *132*, 30–55.

Gonin, J. (1906). Dıcollement rıtinien. Encycl Franη Ophtalmol *6*, 947–1025.

Gonin, J. (1923). Guırison opıratoires de dıcollements rıtiniens. Rev Gın Ophtal *3*, 337–340.

Gonin, J. (1931). La thermoponction oblitırante des dıchirures rıtiniennes dans le dıcollement de la rıtine. Ann Ocul. *168*, 1–29.

Gonin, J. (1934). Divergences of principles and differences of technics in the treatment of retinal detachment. Am J Ophthalmol *17*, 74–79.

Grabner, G., Boltz, G., and Förster, O. (1980). Macrophage-like properaties of human hyalocytes. Invest. Ophthalmol. Vis. Sci. *19*, 333–340.

Grantham, J.J. (1983). Polycystic kidney disease: a predominance of giant nephrons. Am. J. Physiol. *244*, F3–F10.

Graymore, C.N. (1970). Biochemistry of the eye (Academic Press).

Green, W.R., Kenyon, K.R., Michels, R.G., Gilbert, H.D., and De La Cruz, Z. (1979). Ultrastructure of epiretinal membranes causing macular pucker after retinal re-attachment surgery. Trans. Ophthalmol. Soc. U. K. *99*, 65–77.

Guérin, C.J., Wolfshagen, R.W., Eifrig, D.E., and Anderson, D.H. (1990). Immunocytochemical identification of Müller's glia as a component of human epiretinal membranes. Invest. Ophthalmol. Vis. Sci. *31*, 1483–1491.

Hainfellner, J.A., Voigtländer, T., Ströbel, T., Mazal, P.R., Maddalena, A.S., Aguzzi, A., and Budka, H. (2001). Fibroblasts can express glial fibrillary acidic protein (GFAP) in vivo. J. Neuropathol. Exp. Neurol. *60*, 449–461.

Hamburg, A. (1959). Some investigations on the cells of the vitreous body. Ophthalmol. J. Int. Ophtalmol. Int. J. Ophthalmol. Z. Für Augenheilkd. *138*, 81–107.

Hamelers, I.H.L., Olivo, C., Mertens, A.E.E., Pegtel, D.M., van der Kammen, R.A., Sonnenberg, A., and Collard, J.G. (2005). The Rac activator Tiam1 is required for (alpha)3(beta)1-mediated laminin-5 deposition, cell spreading, and cell migration. J. Cell Biol. *171*, 871–881.

Hamill, K.J., Kligys, K., Hopkinson, S.B., and Jones, J.C.R. (2009). Laminin deposition in the extracellular matrix: a complex picture emerges. J. Cell Sci. *122*, 4409–4417.

Hassan, T.S., Sarrafizadeh, R., Ruby, A.J., Garretson, B.R., Kuczynski, B., and Williams, G.A. (2002). The effect of duration of macular detachment on results after the scleral buckle repair of primary, macula-off retinal detachments. Ophthalmology *109*, 146–152.

Hata, Y., Sassa, Y., Kita, T., Miura, M., Kano, K., Kawahara, S., Arita, R., Nakao, S., Shih, J.L., and Ishibashi, T. (2008). Vascular endothelial growth factor expression by hyalocytes and its regulation by glucocorticoid. Br. J. Ophthalmol. *92*, 1540–1544.

Haut, J., Monin, C., Diner-Nedey, S., and Van Effenterre, G. (1987). [Prevention of bilateralization of idiopathic retinal detachment by treatment with argon laser]. J. Fr. Ophtalmol. *10*, 717–722.

Heegaard, S. (1994). Structure of the human vitreoretinal border region. Ophthalmol. J. Int. Ophtalmol. Int. J. Ophthalmol. Z. Für Augenheilkd. *208*, 82–91.

Heegaard, S., Jensen, O.A., and Prause, J.U. (1986). Structure and composition of the inner limiting membrane of the retina. SEM on frozen resin-cracked and enzyme-digested retinas of Macaca mulatta. Graefes Arch. Clin. Exp. Ophthalmol. Albrecht Von Graefes Arch. Für Klin. Exp. Ophthalmol. *224*, 355–360.

Herrero-Vanrell, R., Bravo-Osuna, I., Andrés-Guerrero, V., Vicario-de-la-Torre, M., and Molina-Martínez, I.T. (2014). The potential of using biodegradable microspheres in retinal diseases and other intraocular pathologies. Prog. Retin. Eye Res.

Herrmann, J., France, T.D., Spranger, J.W., Opitz, J.M., and Wiffler, C. (1975). The Stickler syndrome (hereditary arthroophthalmopathy). Birth Defects Orig. Artic. Ser. *11*, 76–103.

Hindson, V.J., Gallagher, J.T., Halfter, W., and Bishop, P.N. (2005). Opticin binds to heparan and chondroitin sulfate proteoglycans. Invest. Ophthalmol. Vis. Sci. *46*, 4417–4423.

Hirayama, K., Hata, Y., Noda, Y., Miura, M., Yamanaka, I., Shimokawa, H., and Ishibashi, T. (2004). The involvement of the rho-kinase pathway and its regulation in cytokine-induced collagen gel contraction by hyalocytes. Invest. Ophthalmol. Vis. Sci. *45*, 3896–3903.

Hiscott, P.S., Grierson, I., and McLeod, D. (1984). Retinal pigment epithelial cells in epiretinal membranes: an immunohistochemical study. Br. J. Ophthalmol. *68*, 708–715.

Hodge, A.J., and Schmitt, F.O. (1960). The charge profile of the tropocollagen macromolecule and the packing arrangement in native-type collagen fibrils. Proc. Natl. Acad. Sci. U. S. A. *46*, 186–197.

Hogan, M.J. (1971). Histology of the human eye; an atlas and textbook (Philadelphia: Saunders).

Hogan, M.J., Alvarado, J.A., and Weddell, J.E. (1971). Histology of the Human Eye (Philadelphia: Saunders).

Hoornaert, K.P., Vereecke, I., Dewinter, C., Rosenberg, T., Beemer, F.A., Leroy, J.G., Bendix, L., Björck, E., Bonduelle, M., Boute, O., et al. (2010). Stickler syndrome caused by COL2A1 mutations: genotype-phenotype correlation in a series of 100 patients. Eur. J. Hum. Genet. EJHG *18*, 872–880.

Hotchkiss, R.D. (1948). A microchemical reaction resulting in the staining of polysaccharide structures in fixed tissue preparations. Arch. Biochem. *16*, 131–141.

Hovland, K.R. (1978). Vitreous findings in fellow eyes of aphakic retinal detachment. Am. J. Ophthalmol. *86*, 350–353.

Huang, Y., Enzmann, V., and Ildstad, S.T. (2011). Stem cell-based therapeutic applications in retinal degenerative diseases. Stem Cell Rev. *7*, 434–445.

Hynes, R.O. (2009). The extracellular matrix: not just pretty fibrils. Science *326*, 1216–1219.

Jacobson, B. (1984). Degradation of glycosaminoglycans by extracts of calf vitreous hyalocytes. Exp. Eye Res. *39*, 373–385.

Jerdan, J.A., Koa, L., and Glaser, B.M. (1986). The inner limiting membrane - a modified basement membrane? ARVO Abstr. Invest Ophthalmol Vis Sci 230.

Johnson, T.V., and Martin, K.R. (2013). Cell transplantation approaches to retinal ganglion cell neuroprotection in glaucoma. Curr. Opin. Pharmacol. *13*, 78–82.

Johnson, D.H., Bourne, W.M., and Campbell, R.J. (1982). The ultrastructure of Descemet's membrane. I. Changes with age in normal corneas. Arch. Ophthalmol. *100*, 1942–1947.

Johnson, P.C., Brendel, K., and Meezan, E. (1981). Human diabetic perineurial cell basement membrane thickening. Lab. Investig. J. Tech. Methods Pathol. *44*, 265–270.

Kakehashi, A., Takezawa, M., and Akiba, J. (2014). Classification of posterior vitreous detachment. Clin. Ophthalmol. Auckl. NZ *8*, 1–10.

Kampik, A., Green, W.R., Michels, R.G., and Nase, P.K. (1980). Ultrastructural features of progressive idiopathic epiretinal membrane removed by vitreous surgery. Am. J. Ophthalmol. *90*, 797–809.

Kanwar, Y.S., and Farquhar, M.G. (1979). Anionic sites in the glomerular basement membrane. In vivo and in vitro localization to the laminae rarae by cationic probes. J. Cell Biol. *81*, 137–153.

Kefalides, N.A. (1971). Isolation of a collagen from basement membranes containing three identical - chains. Biochem. Biophys. Res. Commun. *45*, 226–234.

Kita, T., Hata, Y., Arita, R., Kawahara, S., Miura, M., Nakao, S., Mochizuki, Y., Enaida, H., Goto, Y., Shimokawa, H., et al. (2008). Role of TGF-beta in proliferative vitreoretinal diseases and ROCK as a therapeutic target. Proc. Natl. Acad. Sci. U. S. A. *105*, 17504–17509.

Kleppel, M.M., and Michael, A.F. (1990). Expression of novel basement membrane components in the developing human kidney and eye. Am. J. Anat. *187*, 165–174.

Knebelmann, B., Breillat, C., Forestier, L., Arrondel, C., Jacassier, D., Giatras, I., Drouot, L., Deschênes, G., Grünfeld, J.P., Broyer, M., et al. (1996). Spectrum of mutations in the COL4A5 collagen gene in X-linked Alport syndrome. Am. J. Hum. Genet. *59*, 1221–1232.

Kohno, T., Sorgente, N., Ishibashi, T., Goodnight, R., and Ryan, S.J. (1987). Immunofluorescent studies of fibronectin and laminin in the human eye. Invest. Ophthalmol. Vis. Sci. *28*, 506–514.

Körkkö, J., Ritvaniemi, P., Haataja, L., Kääriäinen, H., Kivirikko, K.I., Prockop, D.J., and Ala-Kokko, L. (1993). Mutation in type II procollagen (COL2A1) that substitutes aspartate for glycine alpha 1-67 and that causes cataracts and retinal detachment: evidence for molecular heterogeneity in the Wagner syndrome and the Stickler syndrome (arthro-ophthalmopathy). Am. J. Hum. Genet. *53*, 55–61.

Kuhn, F., and Aylward, B. (2014). Rhegmatogenous retinal detachment: a reappraisal of its pathophysiology and treatment. Ophthalmic Res. *51*, 15–31.

Lambiase, A., Abdolrahimzadeh, S., and Recupero, S.M. (2014). An update on intravitreal implants in use for eye disorders. Drugs Today Barc. Spain 1998 *50*, 239–249.

Lane-Claypon, J. A further report on cancer of the breast with special reference to its antecedent conditions. Rep. Public Health Med. Subj. No 32 Minist. Health 1926.

Laurie, G.W., and Leblond, C.P. (1985). Basement membrane nomenclature. Nature *313*, 272.

Lazarus, H.S., and Hageman, G.S. (1994). In situ characterization of the human hyalocyte. Arch. Ophthalmol. *112*, 1356–1362.

Leblond, C.P., and Inoue, S. (1989). Structure, composition, and assembly of basement membrane. Am. J. Anat. *185*, 367–390.

Leiba, H., Oliver, M., and Pollack, A. (1996). Prophylactic laser photocoagulation in Stickler syndrome. Eye Lond. Engl. *10 (Pt 6)*, 701–708.

Lewis, G.P., Talaga, K.C., Linberg, K.A., Avery, R.L., and Fisher, S.K. (2004). The efficacy of delayed oxygen therapy in the treatment of experimental retinal detachment. Am. J. Ophthalmol. *137*, 1085–1095.

Li, Y., Tsai, Y.-T., Hsu, C.-W., Erol, D., Yang, J., Wu, W.-H., Davis, R.J., Egli, D., and Tsang, S.H. (2012). Long-term safety and efficacy of human-induced pluripotent stem cell (iPS) grafts in a preclinical model of retinitis pigmentosa. Mol. Med. Camb. Mass *18*, 1312–1319.

Liberfarb, R.M., and Hirose, T. (1982). The Wagner-Stickler syndrome. Birth Defects Orig. Artic. Ser. *18*, 525–538.

Lincoff, H., and Kreissig, I. (2000). Changing patterns in the surgery for retinal detachment: 1929 to 2000. Klin. Monatsblätter Für Augenheilkd. *216*, 352–359.

Lipinski, D.M., Thake, M., and MacLaren, R.E. (2013). Clinical applications of retinal gene therapy. Prog. Retin. Eye Res. *32*, 22–47.

Lu, S.C., Alvarez, L., Huang, Z.Z., Chen, L., An, W., Corrales, F.J., Avila, M.A., Kanel, G., and Mato, J.M. (2001). Methionine adenosyltransferase 1A knockout mice are predisposed to liver injury and exhibit increased expression of genes involved in proliferation. Proc. Natl. Acad. Sci. U. S. A. *98*, 5560–5565.

Machemer, R. (1968). Experimental retinal detachment in the owl monkey. II. Histology of retina and pigment epithelium. Am. J. Ophthalmol. *66*, 396–410.

Machemer, R., Buettner, H., Norton, E.W., and Parel, J.M. (1971). Vitrectomy: a pars plana approach. Trans. - Am. Acad. Ophthalmol. Otolaryngol. Am. Acad. Ophthalmol. Otolaryngol. *75*, 813–820.

Majava, M., Hoornaert, K.P., Bartholdi, D., Bouma, M.C., Bouman, K., Carrera, M., Devriendt, K., Hurst, J., Kitsos, G., Niedrist, D., et al. (2007). A report on 10 new patients with heterozygous mutations in the COL11A1 gene and a review of genotype-phenotype correlations in type XI collagenopathies. Am. J. Med. Genet. A. *143*, 258–264.

Malecaze, F., Caratero, C., Caratero, A., Arne, J.L., Mathis, A., Bec, P., and Planel, H. (1985). Some ultrastructural aspects of the vitreoretinal juncture. Ophthalmol. J. Int. Ophtalmol. Int. J. Ophthalmol. Z. Für Augenheilkd. *191*, 22–28.

Mann, C.J. (2003). Observational research methods. Research design II: cohort, cross sectional, and case-control studies. Emerg. Med. J. EMJ *20*, 54–60.

Martin, S., Richards, A.J., Yates, J.R., Scott, J.D., Pope, M., and Snead, M.P. (1999). Stickler syndrome: further mutations in COL11A1 and evidence for additional locus heterogeneity. Eur. J. Hum. Genet. EJHG *7*, 807–814.

Martinez-Hernandez, A., and Amenta, P.S. (1983). The basement membrane in pathology. Lab. Investig. J. Tech. Methods Pathol. *48*, 656–677.

Masutani-Noda, T., and Yamada, E. (1983). The mosaic pattern of the inner surface of vertebrate retina. Arch. Histol. Jpn. Nihon Soshikigaku Kiroku *46*, 393–400.

Matsumoto, H., Yamanaka, I., Hisatomi, T., Enaida, H., Ueno, A., Hata, Y., Sakamoto, T., Ogino, N., and Ishibashi, T. (2007). Triamcinolone acetonide-assisted pars plana vitrectomy improves residual posterior vitreous hyaloid removal:

ultrastructural analysis of the inner limiting membrane. Retina Phila. Pa *27*, 174–179.

McAlinden, A., Majava, M., Bishop, P.N., Perveen, R., Black, G.C.M., Pierpont, M.E., Ala-Kokko, L., and Männikkö, M. (2008). Missense and nonsense mutations in the alternatively-spliced exon 2 of COL2A1 cause the ocular variant of Stickler syndrome. Hum. Mutat. *29*, 83–90.

Menner, E. (1930). Über die Stützelemente in der Retina der Wirbeltiere. Z Zellforsch Mikrosk Anat *11*, 414–428.

Merker, H.J. (1994). Morphology of the basement membrane. Microsc. Res. Tech. *28*, 95–124.

Mervin, K., Valter, K., Maslim, J., Lewis, G., Fisher, S., and Stone, J. (1999). Limiting photoreceptor death and deconstruction during experimental retinal detachment: the value of oxygen supplementation. Am. J. Ophthalmol. *128*, 155–164.

Miller, E.J., and Matukas, V.J. (1969). Chick cartilage collagen: a new type of alpha 1 chain not present in bone or skin of the species. Proc. Natl. Acad. Sci. U. S. A. *64*, 1264–1268.

Miller, E.J., Epstein, E.H., Jr, and Piez, K.A. (1971). Identification of three genetically distinct collagens by cyanogen bromide cleavage of insoluble human skin and cartilage collagen. Biochem. Biophys. Res. Commun. *42*, 1024–1029.

Milutinovic, J., Agodoa, L.C., Cutler, R.E., and Striker, G.E. (1980). Autosomal dominant polycystic kidney disease. Early diagnosis and consideration of pathogenesis. Am. J. Clin. Pathol. *73*, 740–747.

Mitry, D., Awan, M.A., Borooah, S., Syrogiannis, A., Lim-Fat, C., Campbell, H., Wright, A.F., Fleck, B.W., Charteris, D.G., Yorston, D., et al. (2013). Long-term visual acuity and the duration of macular detachment: findings from a prospective population-based study. Br. J. Ophthalmol. *97*, 149–152.

Monin, C., Van Effenterre, G., Andre-Sereys, P., and Haut, J. (1994). Prevention of retinal detachment in Wagner-Stickler disease. Comparative study of different methods. Apropos of 22 cases. J. Fr. Ophtalmol. *17*, 167–174.

Morino, I., Hiscott, P., McKechnie, N., and Grierson, I. (1990). Variation in epiretinal membrane components with clinical duration of the proliferative tissue. Br. J. Ophthalmol. *74*, 393–399.

Murakami, K., Jalkh, A.E., Avila, M.P., Trempe, C.L., and Schepens, C.L. (1983). Vitreous floaters. Ophthalmology *90*, 1271–1276.

Murphy, C., Alvarado, J., and Juster, R. (1984). Prenatal and postnatal growth of the human Descemet's membrane. Invest. Ophthalmol. Vis. Sci. *25*, 1402–1415.

Newsome, D.A., Linsenmayer, T.F., and Trelstad, R.L. (1976). Vitreous body collagen. Evidence for a dual origin from the neural retina and hyalocytes. J. Cell Biol. *71*, 59–67.

Nielsen, C.E. (1981). Stickler's syndrome. Acta Ophthalmol. (Copenh.) *59*, 286–295.

Nishitsuka, K., Kashiwagi, Y., Tojo, N., Kanno, C., Takahashi, Y., Yamamoto, T., Heldin, P., and Yamashita, H. (2007). Hyaluronan production regulation from porcine hyalocyte cell line by cytokines. Exp. Eye Res. *85*, 539–545.

Noda, Y., Hata, Y., Hisatomi, T., Nakamura, Y., Hirayama, K., Miura, M., Nakao, S., Fujisawa, K., Sakamoto, T., and Ishibashi, T. (2004). Functional properties of hyalocytes under PDGF-rich conditions. Invest. Ophthalmol. Vis. Sci. *45*, 2107–2114.

Ogawa, K. (2002). Scanning electron microscopic study of hyalocytes in the guinea pig eye. Arch. Histol. Cytol. *65*, 263–268.

Osterlin, S.E., and Jacobson, B. (1968). The synthesis of hyaluronic acid in vitreous. I. Soluble and particulate transferases in hyalocytes. Exp. Eye Res. *7*, 497–510.

Ozgür, S., and Esgin, H. (2007). Macular function of successfully repaired macula-off retinal detachments. Retina Phila. Pa *27*, 358–364.

Parma, E.S., Körkkö, J., Hagler, W.S., and Ala-Kokko, L. (2002). Radial perivascular retinal degeneration: a key to the clinical diagnosis of an ocular variant of Stickler syndrome with minimal or no systemic manifestations. Am. J. Ophthalmol. *134*, 728–734.

Pastor, J.C., Fernández, I., Rodríguez de la Rúa, E., Coco, R., Sanabria-Ruiz Colmenares, M.R., Sánchez-Chicharro, D., Martinho, R., Ruiz Moreno, J.M., García Arumi, J., Suárez de Figueroa, M., et al. (2008). Surgical outcomes for primary rhegmatogenous retinal detachments in phakic and pseudophakic patients: the Retina 1 Project-report 2. Br. J. Ophthalmol. *92*, 378–382.

Pease, D.C., and Baker, R.F. (1950). Electron microscopy of the kidney. Am. J. Anat. *87*, 349–389.

Pedler, C. (1961). The inner limiting membrane of the retina. Br. J. Ophthalmol. *45*, 423–438.

Pels, E., and Rijneveld, W.J. (2009). Organ culture preservation for corneal tissue. Technical and quality aspects. Dev. Ophthalmol. *43*, 31–46.

Pollak, A., and Oliver, M. (1981). Argon laser photocoagulation of symptomatic flap tears and retinal breaks of fellow eyes. Br. J. Ophthalmol. *65*, 469–472.

Polyak, S.L. (1941). The Retina (Illinois: The University of Chicargo Press).

Poulson, A.V., Hooymans, J.M.M., Richards, A.J., Bearcroft, P., Murthy, R., Baguley, D.M., Scott, J.D., and Snead, M.P. (2004). Clinical features of type 2 Stickler syndrome. J. Med. Genet. *41*, e107.

Printzlau, A., and Andersen, M. (2004). Pierre Robin sequence in Denmark: a retrospective population-based epidemiological study. Cleft Palate-Craniofacial J. Off. Publ. Am. Cleft Palate-Craniofacial Assoc. *41*, 47–52.

Van de Put, M.A.J., Croonen, D., Nolte, I.M., Japing, W.J., Hooymans, J.M.M., and Los, L.I. (2014). Postoperative recovery of visual function after macula-off rhegmatogenous retinal detachment. PloS One *9*, e99787.

Qiao, H., Hisatomi, T., Sonoda, K.-H., Kura, S., Sassa, Y., Kinoshita, S., Nakamura, T., Sakamoto, T., and Ishibashi, T. (2005). The characterisation of hyalocytes: the origin, phenotype, and turnover. Br. J. Ophthalmol. *89*, 513–517.

Rachal, W.F., and Burton, T.C. (1979). Changing concepts of failures after retinal detachment surgery. Arch. Ophthalmol. *97*, 480–483.

Raftopoulou, M., and Hall, A. (2004). Cell migration: Rho GTPases lead the way. Dev. Biol. *265*, 23–32.

Rai, A., Wordsworth, P., Coppock, J.S., Zaphiropoulos, G.C., and Struthers, G.R. (1994). Hereditary arthro-ophthalmopathy (Stickler syndrome): a diagnosis to consider in familial premature osteoarthritis. Br. J. Rheumatol. *33*, 1175–1180.

Ramachandran, G.N., and Kartha, G. (1954). Structure of collagen. Nature *174*, 269–270.

Ramachandran, G.N., and Kartha, G. (1955). Structure of collagen. Nature *176*, 593–595.

Reardon, A.J., Le Goff, M., Briggs, M.D., McLeod, D., Sheehan, J.K., Thornton, D.J., and Bishop, P.N. (2000). Identification in vitreous and molecular cloning of opticin, a novel member of the family of leucine-rich repeat proteins of the extracellular matrix. J. Biol. Chem. *275*, 2123–2129.

Reich, D.J., and Guy, S.R. (2012). Donation after cardiac death in abdominal organ transplantation. Mt. Sinai J. Med. N. Y. *79*, 365–375.

Retzius, G. (1871). Om membrana limitans retinae interna. Nord Med Ark. *3*, 1–35.

Rhodes, R.H. (1982). An ultrastructural study of the complex carbohydrates of the mouse posterior vitreoretinal juncture. Invest. Ophthalmol. Vis. Sci. *22*, 460–477.

Riccalton-Banks, L., Bhandari, R., Fry, J., and Shakesheff, K.M. (2003). A simple method for the simultaneous isolation of stellate cells and hepatocytes from rat liver tissue. Mol. Cell. Biochem. *248*, 97–102.

Rich, A., and Crick, F.H. (1955). The structure of collagen. Nature *176*, 915–916.

Richards, A.J., Yates, J.R., Williams, R., Payne, S.J., Pope, F.M., Scott, J.D., and Snead, M.P. (1996). A family with Stickler syndrome type 2 has a mutation in the COL11A1 gene resulting in the substitution of glycine 97 by valine in alpha 1 (XI) collagen. Hum. Mol. Genet. *5*, 1339–1343.

Richards, A.J., Meredith, S., Poulson, A., Bearcroft, P., Crossland, G., Baguley, D.M., Scott, J.D., and Snead, M.P. (2005). A novel mutation of COL2A1 resulting in dominantly inherited rhegmatogenous retinal detachment. Invest. Ophthalmol. Vis. Sci. *46*, 663–668.

Richards, A.J., Laidlaw, M., Whittaker, J., Treacy, B., Rai, H., Bearcroft, P., Baguley, D.M., Poulson, A., Ang, A., Scott, J.D., et al. (2006). High efficiency of mutation detection in type 1 stickler syndrome using a two-stage approach: vitreoretinal assessment coupled with exon sequencing for screening COL2A1. Hum. Mutat. *27*, 696–704.

Richards, A.J., McNinch, A., Martin, H., Oakhill, K., Rai, H., Waller, S., Treacy, B., Whittaker, J., Meredith, S., Poulson, A., et al. (2010). Stickler syndrome and the vitreous phenotype: mutations in COL2A1 and COL11A1. Hum. Mutat. *31*, E1461–E1471.

Richards, A.J., Fincham, G.S., McNinch, A., Hill, D., Poulson, A.V., Castle, B., Lees, M.M., Moore, A.T., Scott, J.D., and Snead, M.P. (2013). Alternative splicing modifies the effect of mutations in COL11A1 and results in recessive type 2 Stickler syndrome with profound hearing loss. J. Med. Genet. *50*, 765–771.

Rittig, M., Flügel, C., Prehm, P., and Lütjen-Drecoll, E. (1993). Hyaluronan synthase immunoreactivity in the anterior segment of the primate eye. Graefes Arch. Clin. Exp. Ophthalmol. Albrecht Von Graefes Arch. Für Klin. Exp. Ophthalmol. *231*, 313–317.

Rizzolo, L.J. (1991). Basement membrane stimulates the polarized distribution of integrins but not the Na,K-ATPase in the retinal pigment epithelium. Cell Regul. *2*, 939–949.

Robertson, D.M., and Norton, E.W. (1973). Long-term follow-up of treated retinal breaks. Am. J. Ophthalmol. *75*, 395–404.

Rose, P.S., Ahn, N.U., Levy, H.P., Ahn, U.M., Davis, J., Liberfarb, R.M., Nallamshetty, L., Sponseller, P.D., and Francomano, C.A. (2001). Thoracolumbar spinal abnormalities in Stickler syndrome. Spine *26*, 403–409.

Rosengren, B. (1938). Über die Behandlung der Netzhautablösung mittelst Diathermie und Luftinjektion in den Glaskörper. Acta Ophthalmol. (Copenh.) *16*, 3–42.

Ross, W.H., and Kozy, D.W. (1998). Visual recovery in macula-off rhegmatogenous retinal detachments. Ophthalmology *105*, 2149–2153.

Rowe-Rendleman, C.L., Durazo, S.A., Kompella, U.B., Rittenhouse, K.D., Di Polo, A., Weiner, A.L., Grossniklaus, H.E., Naash, M.I., Lewin, A.S., Horsager, A., et al. (2014). Drug and gene delivery to the back of the eye: from bench to bedside. Invest. Ophthalmol. Vis. Sci. *55*, 2714–2730.

Russell, A.J., Fincher, E.F., Millman, L., Smith, R., Vela, V., Waterman, E.A., Dey, C.N., Guide, S., Weaver, V.M., and Marinkovich, M.P. (2003). Alpha 6 beta 4 integrin regulates keratinocyte chemotaxis through differential GTPase activation and antagonism of alpha 3 beta 1 integrin. J. Cell Sci. *116*, 3543–3556.

Sakamoto, T. (2003). [Cell biology of hyalocytes]. Nippon Ganka Gakkai Zasshi *107*, 866–882; discussion 883.

Sakamoto, T., and Ishibashi, T. (2011). Hyalocytes: essential cells of the vitreous cavity in vitreoretinal pathophysiology? Retina Phila. Pa *31*, 222–228.

Salu, P., Claeskens, W., De Wilde, A., Hijmans, W., and Wisse, E. (1985). Light and electron microscopic studies of the rat hyalocyte after perfusion fixation. Ophthalmic Res. *17*, 125–130.

Schaefer, T., Roux, M., Stuhlsatz, H.W., Herken, R., Coulomb, B., Krieg, T., and Smola, H. (1996). Glycosaminoglycans modulate cell-matrix interactions of human fibroblasts and endothelial cells in vitro. J. Cell Sci. *109 (Pt 2)*, 479–488.

Schlötzer-Schrehardt, U., Dietrich, T., Saito, K., Sorokin, L., Sasaki, T., Paulsson, M., and Kruse, F.E. (2007). Characterization of extracellular matrix components in the limbal epithelial stem cell compartment. Exp. Eye Res. *85*, 845–860.

Schmitt, F.O., Gross, J., and Highberger, J.H. (1955). Tropocollagen and the properties of fibrous collagen. Exp. Cell Res. 326–334.

Schönfeld, C.L. (1996). Hyalocytes inhibit retinal pigment epithelium cell proliferation in vitro. Ger. J. Ophthalmol. *5*, 224–228.

Scott, J.D. (1989). Duke-Elder lecture. Prevention and perspective in retinal detachment. Eye Lond. Engl. *3 (Pt 5)*, 491–515.

Sebag, J. (1987). Age-related changes in human vitreous structure. Graefes Arch. Clin. Exp. Ophthalmol. Albrecht Von Graefes Arch. Für Klin. Exp. Ophthalmol. *225*, 89–93.

Sebag, J. (1989). The vitreous: structure, function, and pathobiology (New York: Springer-Verlag).

Seery, C.M., Pruett, R.C., Liberfarb, R.M., and Cohen, B.Z. (1990). Distinctive cataract in the Stickler syndrome. Am. J. Ophthalmol. *110*, 143–148.

Sehgal, B.U., DeBiase, P.J., Matzno, S., Chew, T.-L., Claiborne, J.N., Hopkinson, S.B., Russell, A., Marinkovich, M.P., and Jones, J.C.R. (2006). Integrin beta4 regulates migratory behavior of keratinocytes by determining laminin-332 organization. J. Biol. Chem. *281*, 35487–35498.

Seiler, M.J., Aramant, R.B., and Bergström, A. (1995). Co-transplantation of embryonic retina and retinal pigment epithelial cells to rabbit retina. Curr. Eye Res. *14*, 199–207.

Sharma, T., Challa, J.K., Ravishankar, K.V., and Murugesan, R. (1994). Scleral buckling for retinal detachment. Predictors for anatomic failure. Retina Phila. Pa *14*, 338–343.

Shea, M., Davis, M.D., and Kamel, I. (1974). Retinal breaks without detachment, treated and untreated. Mod. Probl. Ophthalmol. *12*, 97–102.

Sirko-Osadsa, D.A., Murray, M.A., Scott, J.A., Lavery, M.A., Warman, M.L., and Robin, N.H. (1998). Stickler syndrome without eye involvement is caused by mutations in COL11A2, the gene encoding the alpha2(XI) chain of type XI collagen. J. Pediatr. *132*, 368–371.

Slepecky, N.B., Cefaratti, L.K., and Yoo, T.J. (1992). Type II and type IX collagen form heterotypic fibers in the tectorial membrane of the inner ear. Matrix Stuttg. Ger. *12*, 80–86.

Smiddy, W.E., Michels, R.G., and Green, W.R. (1990). Morphology, pathology, and surgery of idiopathic vitreoretinal macular disorders. A review. Retina Phila. Pa *10*, 288–296.

Smiddy, W.E., Flynn, H.W., Jr, Nicholson, D.H., Clarkson, J.G., Gass, J.D., Olsen, K.R., and Feuer, W. (1991). Results and complications in treated retinal breaks. Am. J. Ophthalmol. *112*, 623–631.

Snead, M.P. (1996). Hereditary vitreopathy. Eye Lond. Engl. *10 (Pt 6)*, 653–663.

Snead, M.P., and Yates, J.R. (1999). Clinical and Molecular genetics of Stickler syndrome. J. Med. Genet. *36*, 353–359.

Snead, D.R.J., Cullen, N., James, S., Poulson, A.V., Morris, A.H.C., Lukaris, A., Scott, J.D., Richards, A.J., and Snead, M.P. (2004). Hyperconvolution of the inner limiting membrane in vitreomaculopathies. Graefes Arch. Clin. Exp. Ophthalmol. Albrecht Von Graefes Arch. Für Klin. Exp. Ophthalmol. *242*, 853–862.

Snead, M.P., Payne, S.J., Barton, D.E., Yates, J.R., al-Imara, L., Pope, F.M., and Scott, J.D. (1994a). Stickler syndrome: correlation between vitreoretinal phenotypes and linkage to COL 2A1. Eye Lond. Engl. *8 (Pt 6)*, 609–614.

Snead, M.P., Snead, D.R., Mahmood, A.S., and Scott, J.D. (1994b). Vitreous detachment and the posterior hyaloid membrane: a clinicopathological study. Eye Lond. Engl. *8 (Pt 2)*, 204–209.

Snead, M.P., Yates, J.R., Pope, F.M., Temple, I.K., and Scott, J.D. (1996). Masked confirmation of linkage between type 1 congenital vitreous anomaly and COL 2A1 in Stickler syndrome. Graefes Arch. Clin. Exp. Ophthalmol. Albrecht Von Graefes Arch. Für Klin. Exp. Ophthalmol. *234*, 720–721.

Snead, M.P., Snead, D.R.J., Richards, A.J., Harrison, J.B., Poulson, A.V., Morris, A.H.C., Sheard, R.M., and Scott, J.D. (2002). Clinical, histological and ultrastructural studies of the posterior hyaloid membrane. Eye Lond. Engl. *16*, 447–453.

Snead, M.P., Snead, D.R.J., James, S., and Richards, A.J. (2008). Clinicopathological changes at the vitreoretinal junction: posterior vitreous detachment. Eye Lond. Engl. *22*, 1257–1262.

Snead, M.P., McNinch, A.M., Poulson, A.V., Bearcroft, P., Silverman, B., Gomersall, P., Parfect, V., and Richards, A.J. (2011). Stickler syndrome, ocular-only variants and a key diagnostic role for the ophthalmologist. Eye Lond. Engl. *25*, 1389–1400.

Sommer, F., Pollinger, K., Brandl, F., Weiser, B., Tessmar, J., Blunk, T., and Göpferich, A. (2008). Hyalocyte proliferation and ECM accumulation modulated by bFGF and TGF-beta1. Graefes Arch. Clin. Exp. Ophthalmol. Albrecht Von Graefes Arch. Für Klin. Exp. Ophthalmol. *246*, 1275–1284.

Sonoda, K.-H., Sakamoto, T., Qiao, H., Hisatomi, T., Oshima, T., Tsutsumi-Miyahara, C., Exley, M., Balk, S.P., Taniguchi, M., and Ishibashi, T. (2005). The analysis of systemic tolerance elicited by antigen inoculation into the vitreous cavity: vitreous cavity-associated immune deviation. Immunology *116*, 390–399.

Spear, G.S. (1973). Editorial: Alport's syndrome: a consideration of pathogenesis. Clin. Nephrol. *1*, 336–337.

Stalmans, P., Benz, M.S., Gandorfer, A., Kampik, A., Girach, A., Pakola, S., and Haller, J.A. (2012). Enzymatic vitreolysis with ocriplasmin for vitreomacular traction and macular holes. N. Engl. J. Med. *367*, 606–615.

Steel, D.H.W., and Lotery, A.J. (2013). Idiopathic vitreomacular traction and macular hole: a comprehensive review of pathophysiology, diagnosis, and treatment. Eye Lond. Engl. *27 Suppl 1*, S1–S21.

Stein-Streilein, J. (2008). Immune regulation and the eye. Trends Immunol. *29*, 548–554.

Stein-Streilein, J., and Streilein, J.W. (2002). Anterior chamber associated immune deviation (ACAID): regulation, biological relevance, and implications for therapy. Int. Rev. Immunol. *21*, 123–152.

Stickler, G.B., and Pugh, D.G. (1967). Hereditary progressive arthro-ophthalmopathy. II. Additional observations on vertebral abnormalities, a hearing defect, and a report of a similar case. Mayo Clin. Proc. *42*, 495–500.

Stickler, G.B., Belau, P.G., Farrell, F.J., Jones, J.D., Pugh, D.G., Steinberg, A.G., and Ward, L.E. (1965). Hereditary progressive arthro-ophthalmopathy. Mayo Clin. Proc. Mayo Clin. *40*, 433–455.

Stickler, G.B., Hughes, W., and Houchin, P. (2001). Clinical features of hereditary progressive arthro-ophthalmopathy (Stickler syndrome): a survey. Genet. Med. Off. J. Am. Coll. Med. Genet. *3*, 192–196.

Streilein, J.W. (2003). Ocular immune privilege: therapeutic opportunities from an experiment of nature. Nat. Rev. Immunol. *3*, 879–889.

Streilein, J.W., Okamoto, S., Hara, Y., Kosiewicz, M., and Ksander, B. (1997). Blood-borne signals that induce anterior chamber-associated immune deviation after intracameral injection of antigen. Invest. Ophthalmol. Vis. Sci. *38*, 2245–2254.

Szirmai, J.A., and Balazs, E.A. (1958). Studies on the structure of the vitreous body. III. Cells in the cortical layer. AMA Arch. Ophthalmol. *59*, 34–48.

Tani, P., Robertson, D.M., and Langworthy, A. (1981). Prognosis for central vision and anatomic reattachment in rhegmatogenous retinal detachment with macula detached. Am. J. Ophthalmol. *92*, 611–620.

Temple, I.K. (1989). Stickler's syndrome. J. Med. Genet. *26*, 119–126.

Thalmann, I. (1993). Collagen of accessory structures of organ of Corti. Connect. Tissue Res. *29*, 191–201.

Thilges, V., and Gonin, J. (1970). L'homme et son oeuvre. Ann Ocul. *203*, 631–637.

Timpl, R. (1989). Structure and biological activity of basement membrane proteins. Eur. J. Biochem. FEBS *180*, 487–502.

Timpl, R., and Dziadek, M. (1986). Structure, development, and molecular pathology of basement membranes. Int. Rev. Exp. Pathol. *29*, 1–112.

Timpl, R., Wiedemann, H., van Delden, V., Furthmayr, H., and Kühn, K. (1981). A network model for the organization of type IV collagen molecules in basement membranes. Eur. J. Biochem. FEBS *120*, 203–211.

Tkachuk, V.A., Plekhanova, O.S., and Parfyonova, Y.V. (2009). Regulation of arterial remodeling and angiogenesis by urokinase-type plasminogen activator. Can. J. Physiol. Pharmacol. *87*, 231–251.

Todd, R.B., and Bowman, W. (1850). The physiological anatomy and physiology of man (Philadelphia: Lea and Blanchard).

Tolstonog, G.V., Wang, X., Shoeman, R., and Traub, P. (2000). Intermediate filaments reconstituted from vimentin, desmin, and glial fibrillary acidic protein selectively bind repetitive and mobile DNA sequences from a mixture of mouse genomic DNA fragments. DNA Cell Biol. *19*, 647–677.

Torricelli, A.A.M., Singh, V., Santhiago, M.R., and Wilson, S.E. (2013). The corneal epithelial basement membrane: structure, function, and disease. Invest. Ophthalmol. Vis. Sci. *54*, 6390–6400.

Traub, P. (1995). Intermediate filaments and gene regulation. Physiol. Chem. Phys. Med. NMR *27*, 377–400.

Ueno, A., Enaida, H., Hata, Y., Hisatomi, T., Nakamura, T., Mochizuki, Y., Sakamoto, T., and Ishibashi, T. (2007). Long-term clinical outcomes and therapeutic benefits of triamcinolone-assisted pars plana vitrectomy for proliferative vitreoretinopathy: a case study. Eur. J. Ophthalmol. *17*, 392–398.

Uga, S., and Smelser, G.K. (1973). Electron microscopic study of the development of retinal Müllerian cells. Invest. Ophthalmol. *12*, 295–307.

Upminster Local History Group. (1960). Importance of the vitreous body in retina surgery with special emphasis on reoperations: second conference of the Retina Foundation,May 30 and 31, 1958. Book 12, (Upminster Local History Group).

Uy, H.S., Chan, P.S., and Cruz, F.M. (2013). Stem cell therapy: a novel approach for vision restoration in retinitis pigmentosa. Med. Hypothesis Discov. Innov. Ophthalmol. *2*, 52–55.

Vikkula, M., Mariman, E.C., Lui, V.C., Zhidkova, N.I., Tiller, G.E., Goldring, M.B., van Beersum, S.E., de Waal Malefijt, M.C., van den Hoogen, F.H., and Ropers, H.H. (1995). Autosomal dominant and recessive osteochondrodysplasias associated with the COL11A2 locus. Cell *80*, 431–437.

Vracko, R. (1974). Basal lamina layering in diabetes mellitus. Evidence for accelerated rate of cell death and cell regeneration. Diabetes *23*, 94–104.

Vu, C.D., Brown, J., Jr, Körkkö, J., Ritter, R., 3rd, and Edwards, A.O. (2003). Posterior chorioretinal atrophy and vitreous phenotype in a family with Stickler syndrome from a mutation in the COL2A1 gene. Ophthalmology *110*, 70–77.

Vuoristo, M.M., Pappas, J.G., Jansen, V., and Ala-Kokko, L. (2004). A stop codon mutation in COL11A2 induces exon skipping and leads to non-ocular Stickler syndrome. Am. J. Med. Genet. A. *130A*, 160–164.

Weber, M., Pullig, O., and Köhler, H. (1990). Distribution of Goodpasture antigens within various human basement membranes. Nephrol. Dial. Transplant. Off. Publ. Eur. Dial. Transpl. Assoc. - Eur. Ren. Assoc. *5*, 87–93.

Weber-Krause, B., and Eckardt, C. (1997). [Incidence of posterior vitreous detachment in the elderly]. Ophthalmol. Z. Dtsch. Ophthalmol. Ges. *94*, 619–623.

Wheeldon, D. (1991). Thoracic organ preservation. Perfusion *6*, 191–202.

Wilkin, D.J., Mortier, G.R., Johnson, C.L., Jones, M.C., de Paepe, A., Shohat, M., Wildin, R.S., Falk, R.E., and Cohn, D.H. (1998). Correlation of linkage data with

phenotype in eight families with Stickler syndrome. Am. J. Med. Genet. *80*, 121–127.

Wilkinson, C.P. (2012). Interventions for asymptomatic retinal breaks and lattice degeneration for preventing retinal detachment. Cochrane Database Syst. Rev. Online *3*, CD003170.

Williams, C.J., Ganguly, A., Considine, E., McCarron, S., Prockop, D.J., Walsh-Vockley, C., and Michels, V.V. (1996). A-2-->G transition at the 3' acceptor splice site of IVS17 characterizes the COL2A1 gene mutation in the original Stickler syndrome kindred. Am. J. Med. Genet. *63*, 461–467.

Wilson, S.E., and Hong, J.W. (2000). Bowman's layer structure and function: critical or dispensable to corneal function? A hypothesis. Cornea *19*, 417–420.

Wolfensberger, T.J. (2003). Jules Gonin. Pioneer of retinal detachment surgery. Indian J. Ophthalmol. *51*, 303–308.

Wolff, E. (1937). Internal limiting membrane of the retina. Trans Ophthalmol Soc UK 186–195.

Wolff, E. (1961). Anatomy of the eye and orbit. (Philadelphia: W.B. Saunders Co.).

Yoshikawa, N., White, R.H., and Cameron, A.H. (1982). Familial hematuria; clinico-pathological correlations. Clin. Nephrol. *17*, 172–182.

Younan, A.C. (1884). On the histology of the vitreous humour. J. Anat. Physiol. *19*, i1–i15.

Zhu, M., Provis, J.M., and Penfold, P.L. (1999). The human hyaloid system: cellular phenotypes and inter-relationships. Exp. Eye Res. *68*, 553–563.

(1993). Molecular and cellular aspects of basement membranes (San Diego: Academic Press).

6 Appendix

6.1 Positive controls

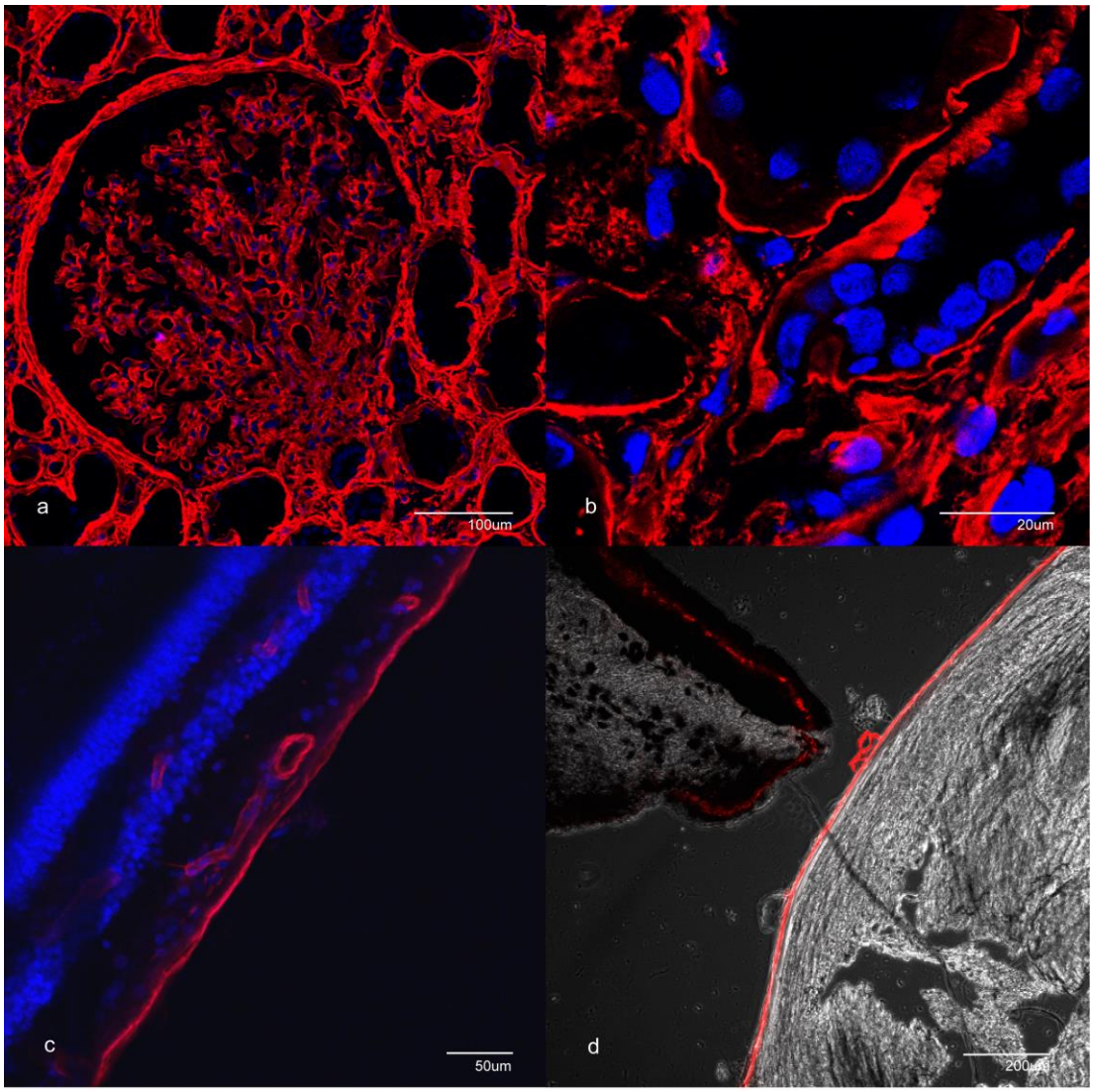

Figure 6-1 Positive control: rabbit polyclonal anti-collagen IV antibody

Confocal micrographs demonstrating: (a) renal glomerular and collecting tubule basement membrane (x12), (b) renal collecting tubule basement membrane (x63), (c) internal limiting membrane and intraretinal blood vessel basement membrane (x5), (d) intraocular crystalline lens capsule with phase contrast overlay (note ciliary body epithelial autofluorescence) (x5).

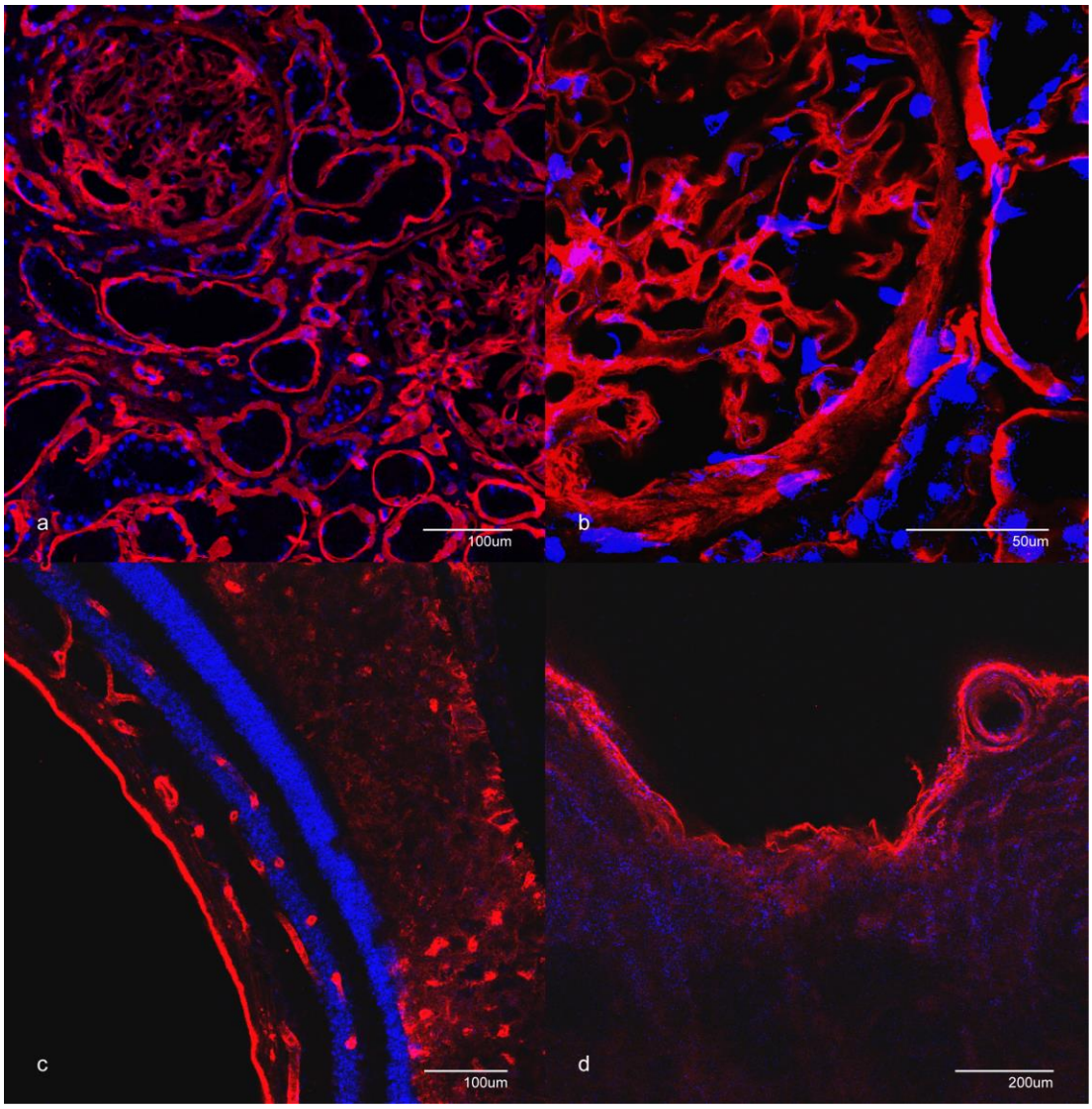

Figure 6-2 Positive control: rabbit polyclonal anti-laminin antibody

Confocal micrographs demonstrating: (a) renal glomerular and collecting tubule basement membrane (x10), (b) renal collecting tubule basement membrane (x31.5), (c) internal limiting membrane and intraretinal blood vessel basement membrane (x10), (d) internal limiting membrane extending over optic nerve head with retinal arcade blood vessel basement membrane (x5).

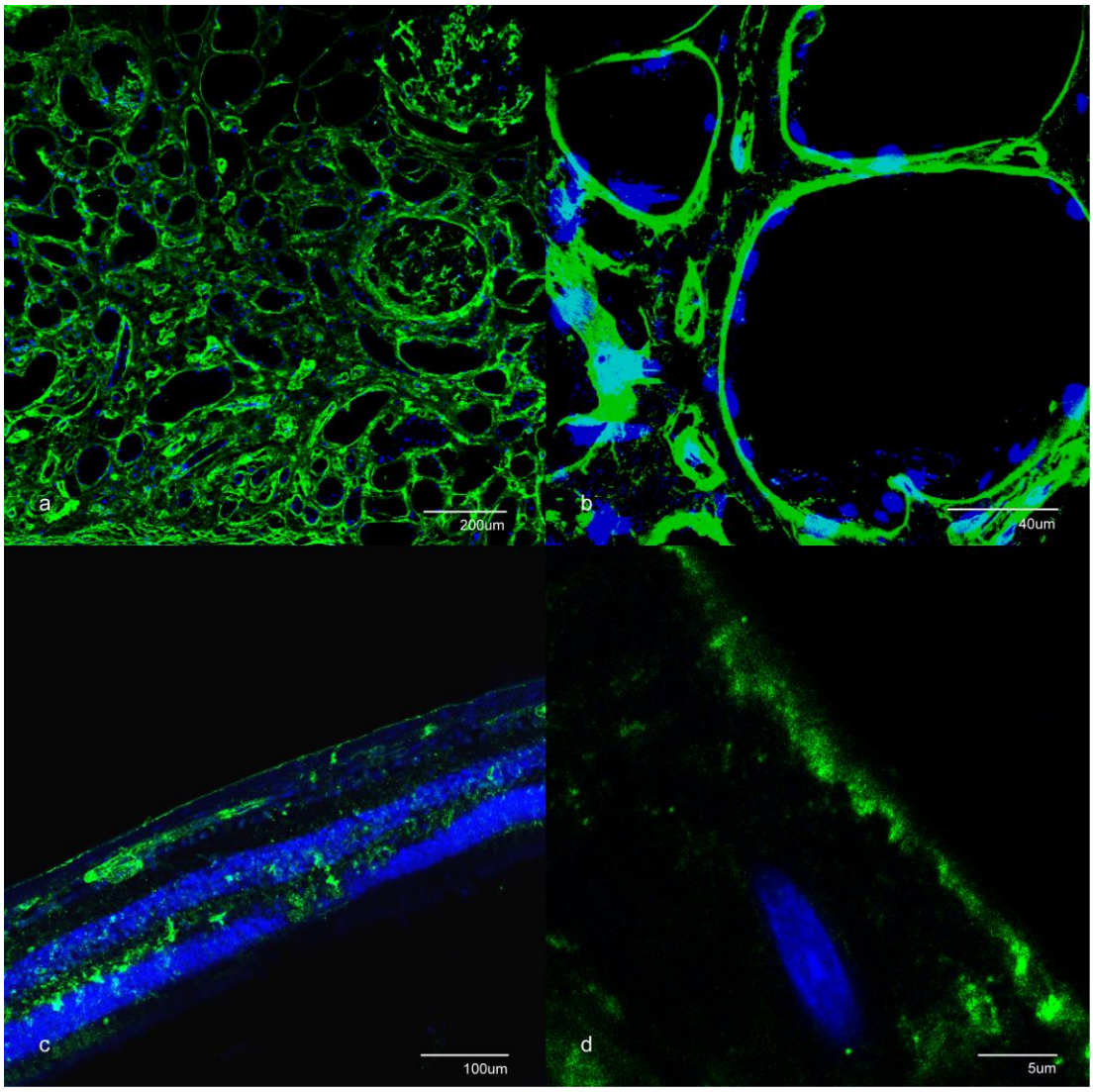

Figure 6-3 Positive control: mouse monoclonal anti-fibronectin antibody

Confocal micrographs demonstrating: (a) renal glomerular and collecting tubule basement membrane (x5), (b) renal collecting tubule basement membrane (x31.5), (c) internal limiting membrane and intraretinal blood vessel basement membrane (x10), (d) internal limiting membrane (x126).

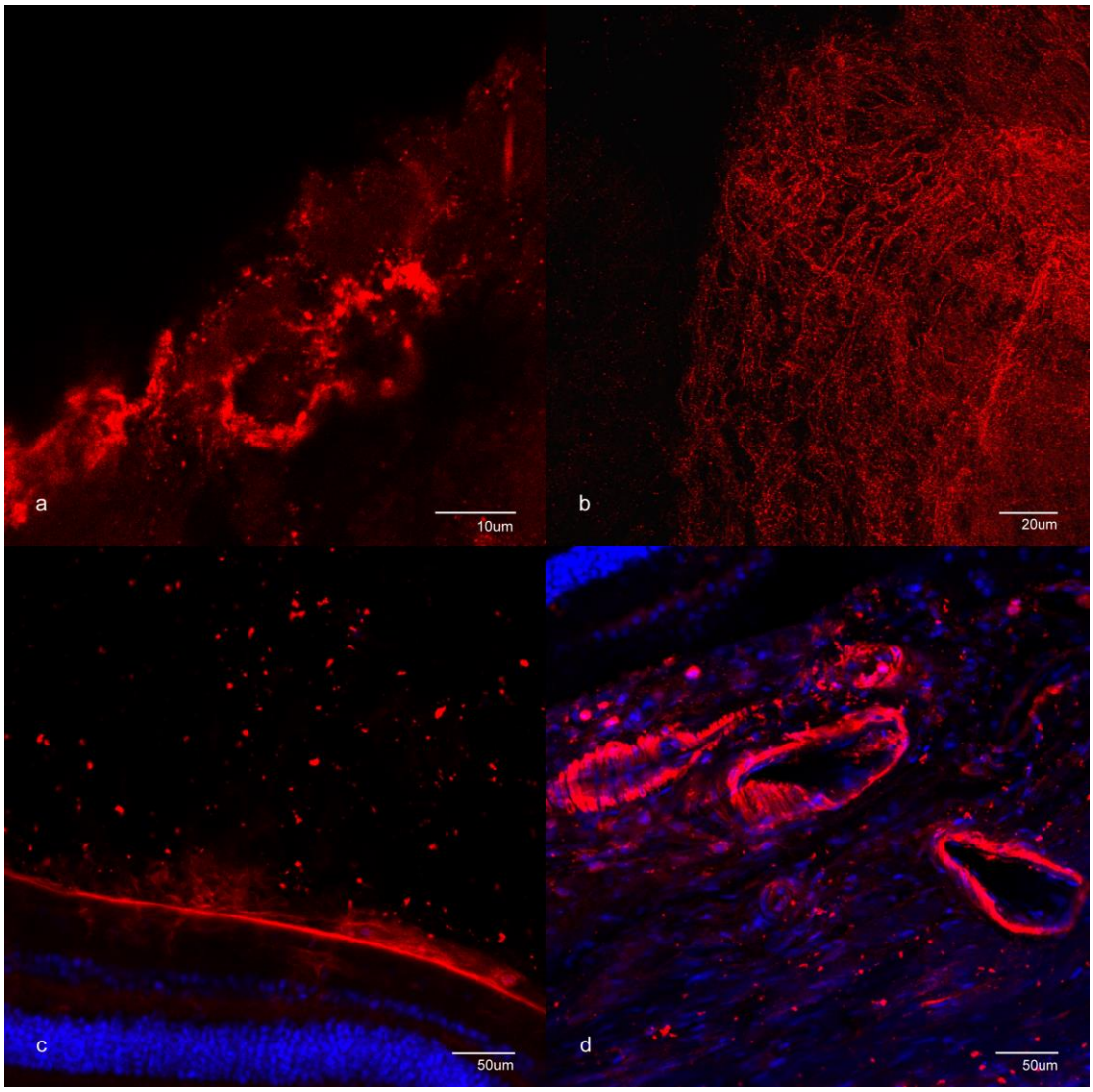

Figure 6-4 Positive control: rabbit monoclonal anti-opticin antibody

Confocal micrographs demonstrating: (a) hyaline cartilage (x94.5), (b) vitreous gel (x31.5), (c) interface between vitreous gel and internal limiting membrane (x15), (d) choroidal vasculature (x15).

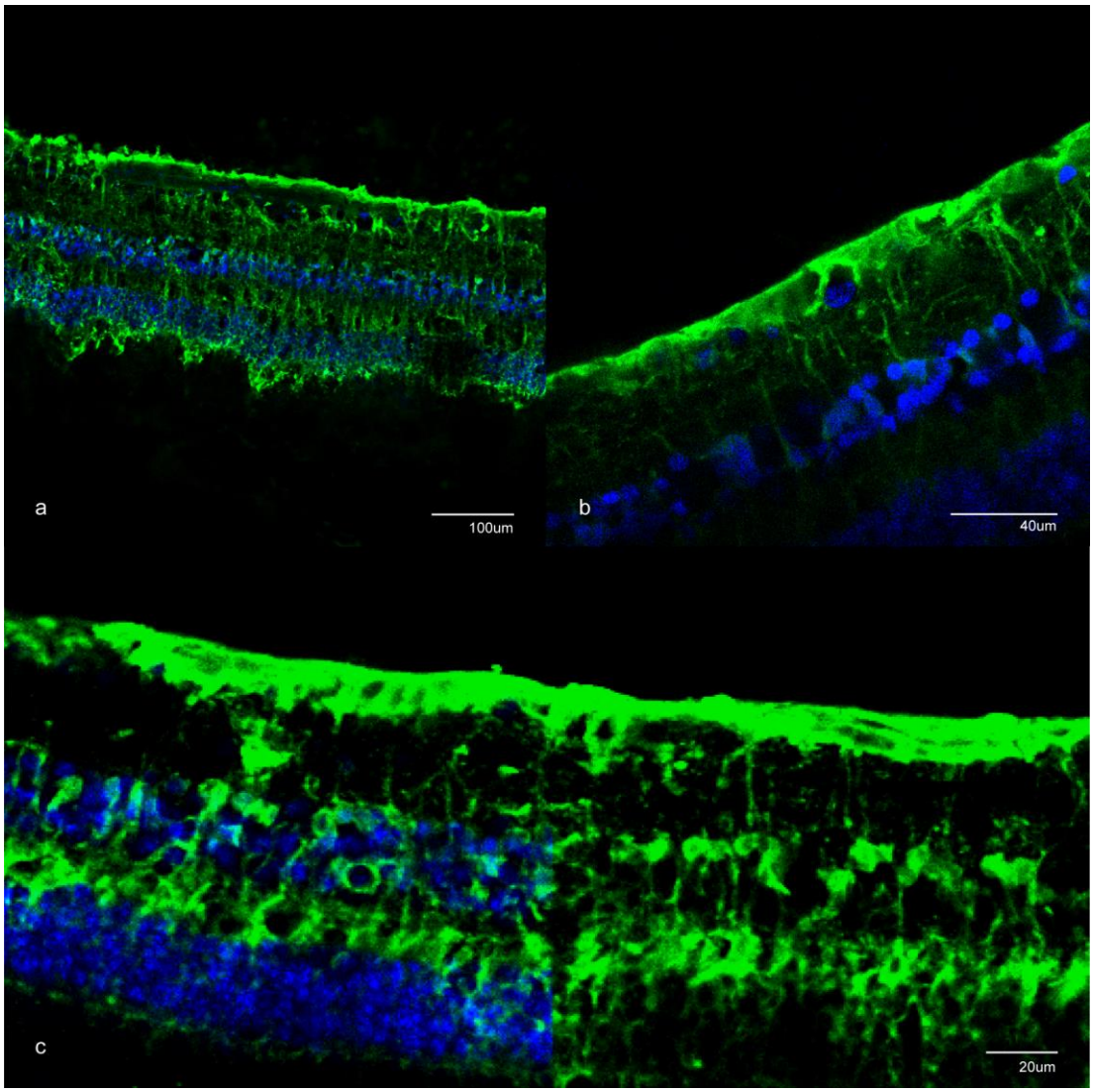

Figure 6-5 Positive control: CRALBP

Confocal micrographs demonstrating: (a) retinal Müller glia (x10), (b) Müller glia foot plates fusing to form internal limiting membrane (x31.5), (c) composite image with inner and outer nuclear layer present (left half) and removed (right half) to illustrate relationship to Müller glial (x18).

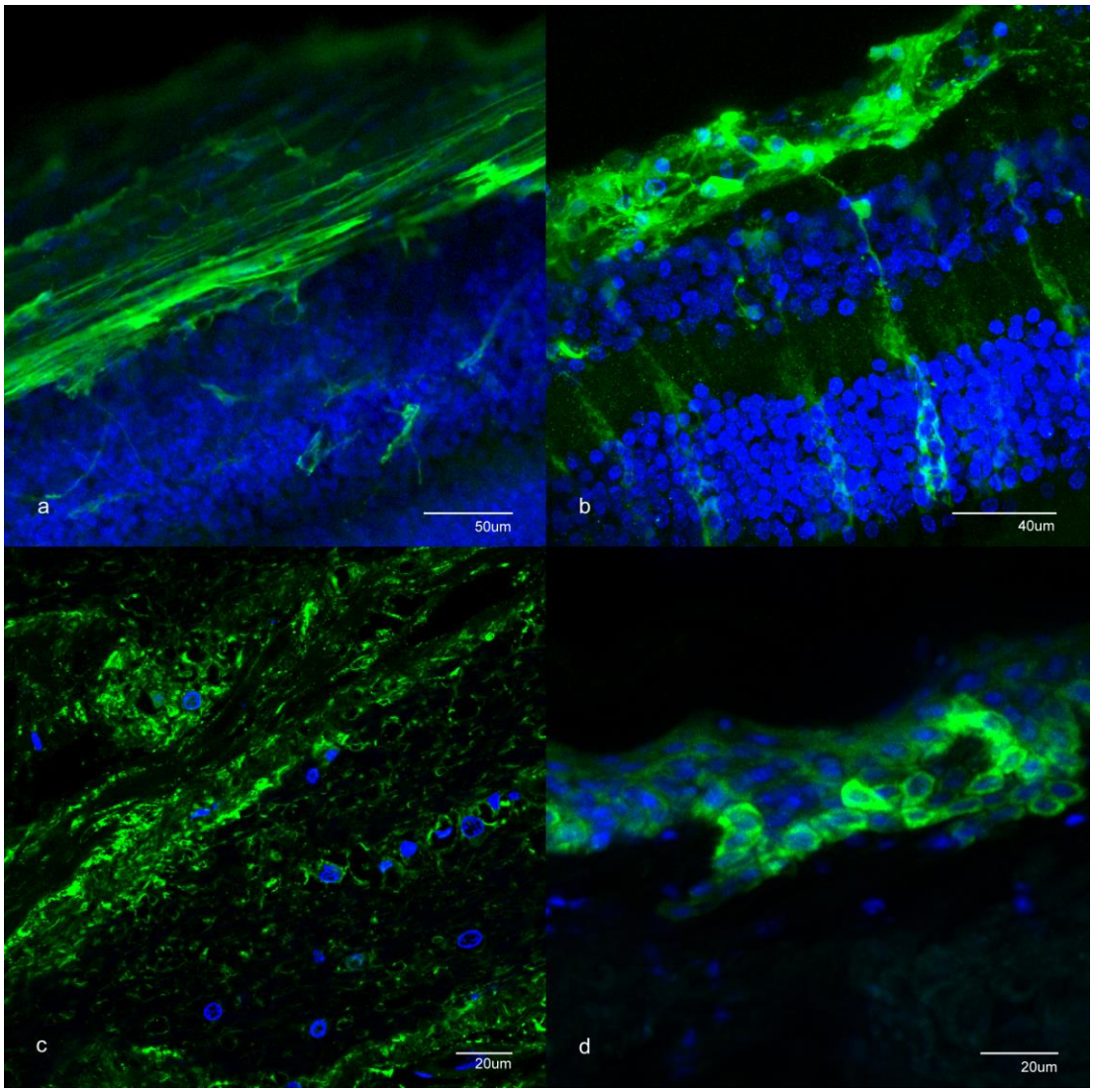

Figure 6-6 Positive control: S100B

Confocal micrographs demonstrating: (a) retinal nerve fibre layer (x20), (b) retinal astrocytes (x31.5), (c) optic nerve (x31.5), (d) epidermis (x31.5).

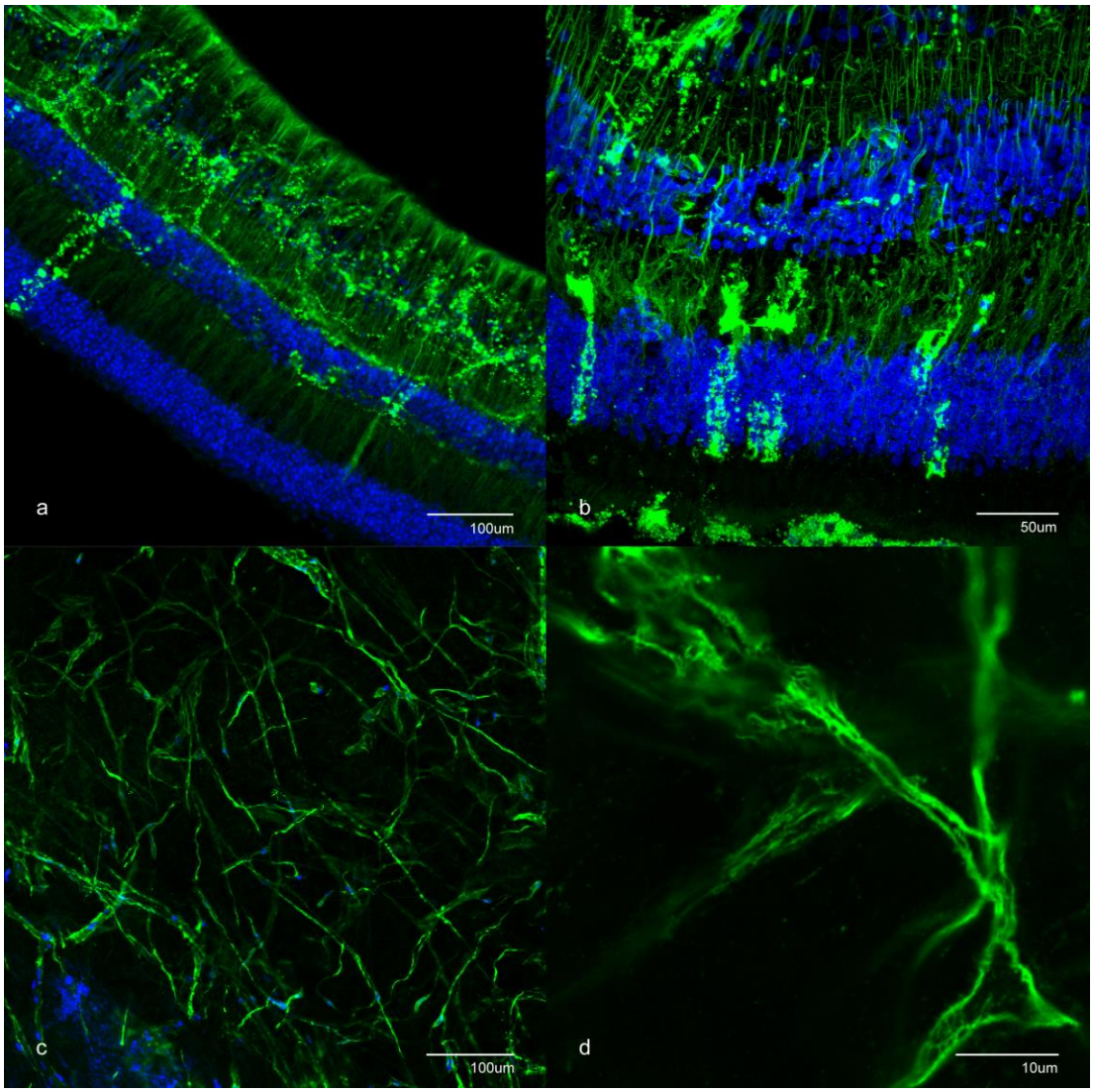

Figure 6-7 Positive control: vimentin

Confocal micrographs demonstrating: (a) retinal astrocytes and their orientation towards the internal limiting membrane (x10), (b) maximum image projection of retinal astrocytes spanning the inner and outer plexiform layers of the retina (x52), (c) and (d) optic nerve fibres (x10, x126 respectively).

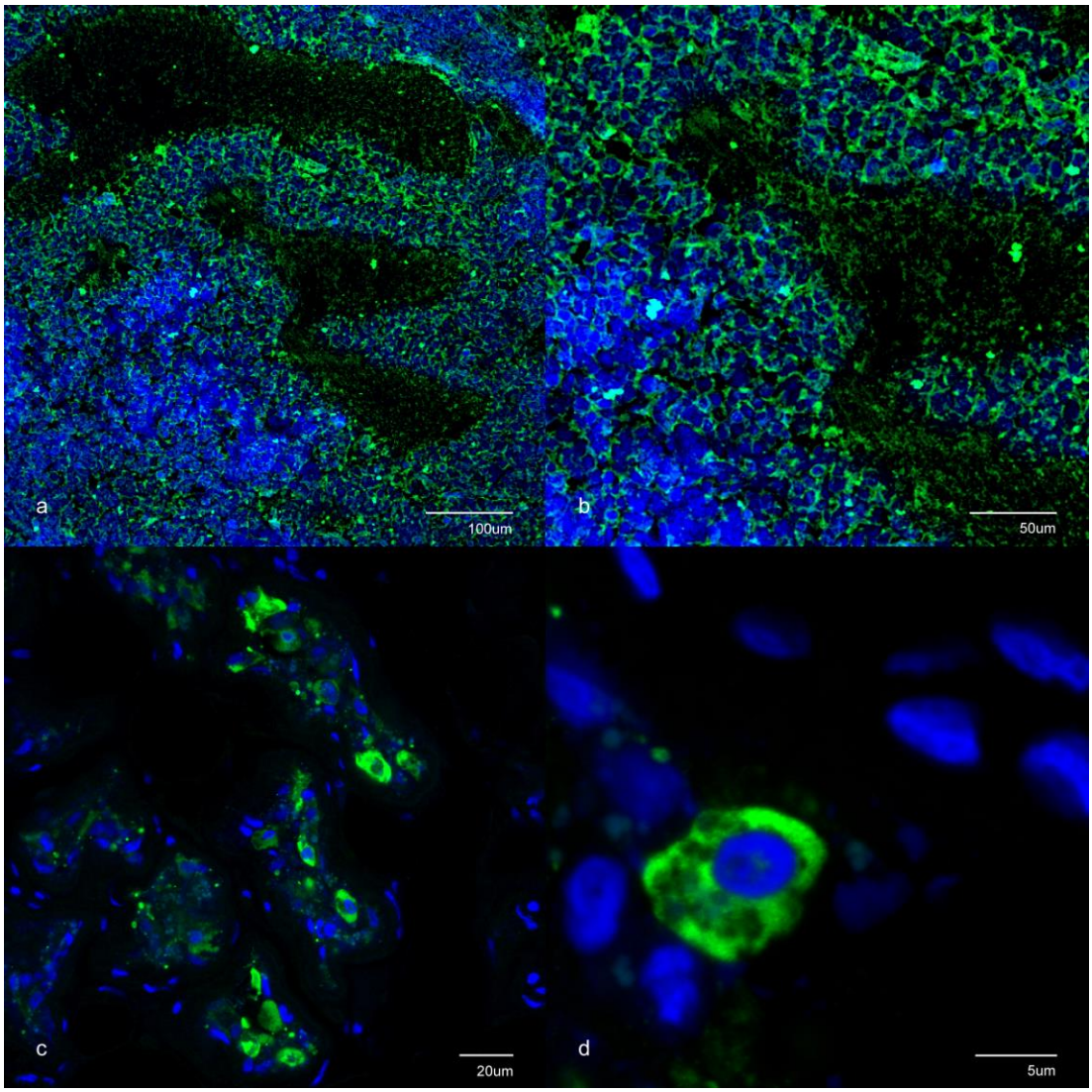

Figure 6-8 Positive control: mouse monoclonal anti-MHC Class II antibody

Confocal micrographs demonstrating: (a) and (b) tonsil macrophages (x10, x20 respectively), (c) and (d) dermal macrophages (x31.5, x189 respectively).

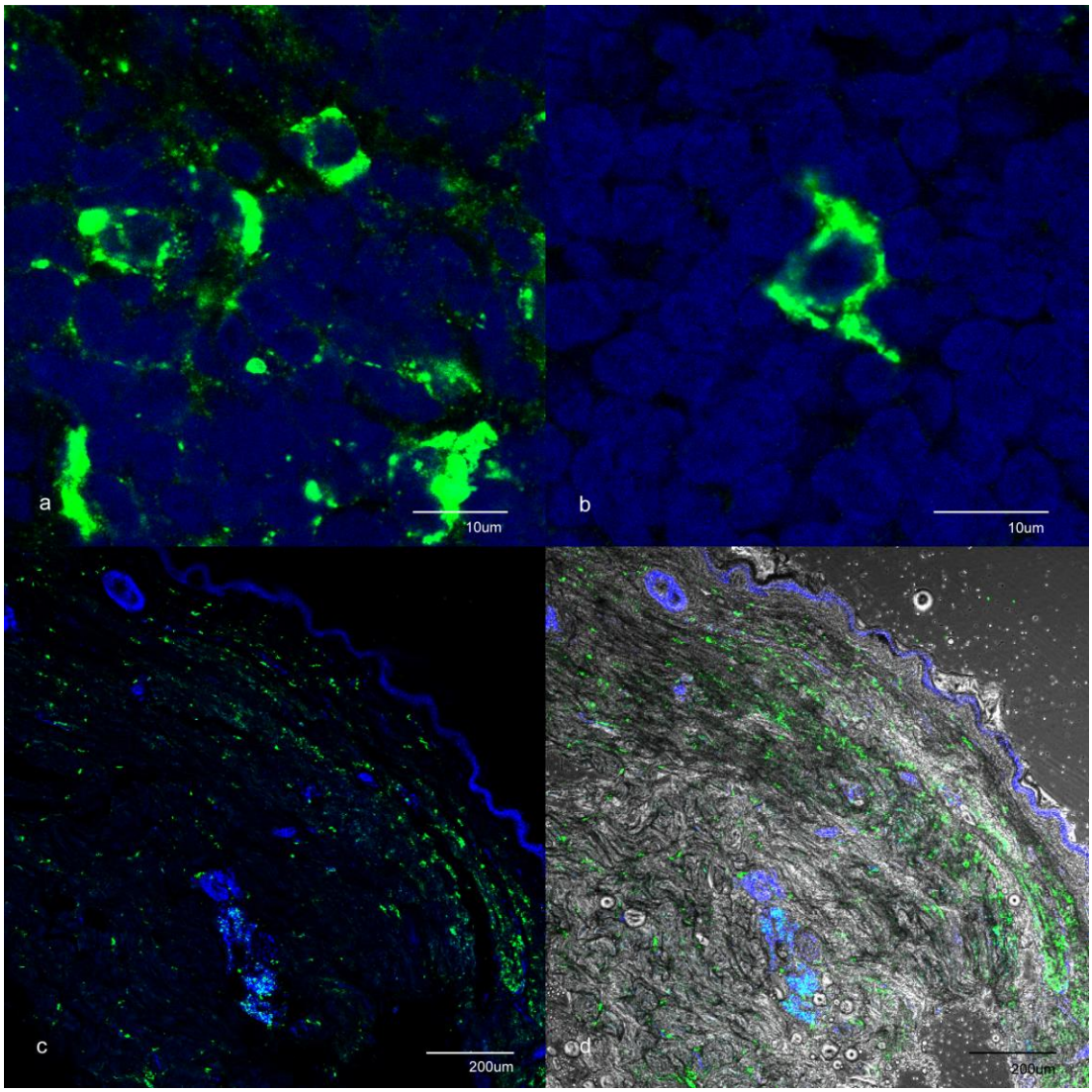

Figure 6-9 Positive control: CD68

Confocal micrographs demonstrating: (a) tonsil macrophages (x100), (b) tonsil interdigitating cell (x120), (c) and (d) dermal macrophages represented with and without phase contrast overlay respectively (x5).

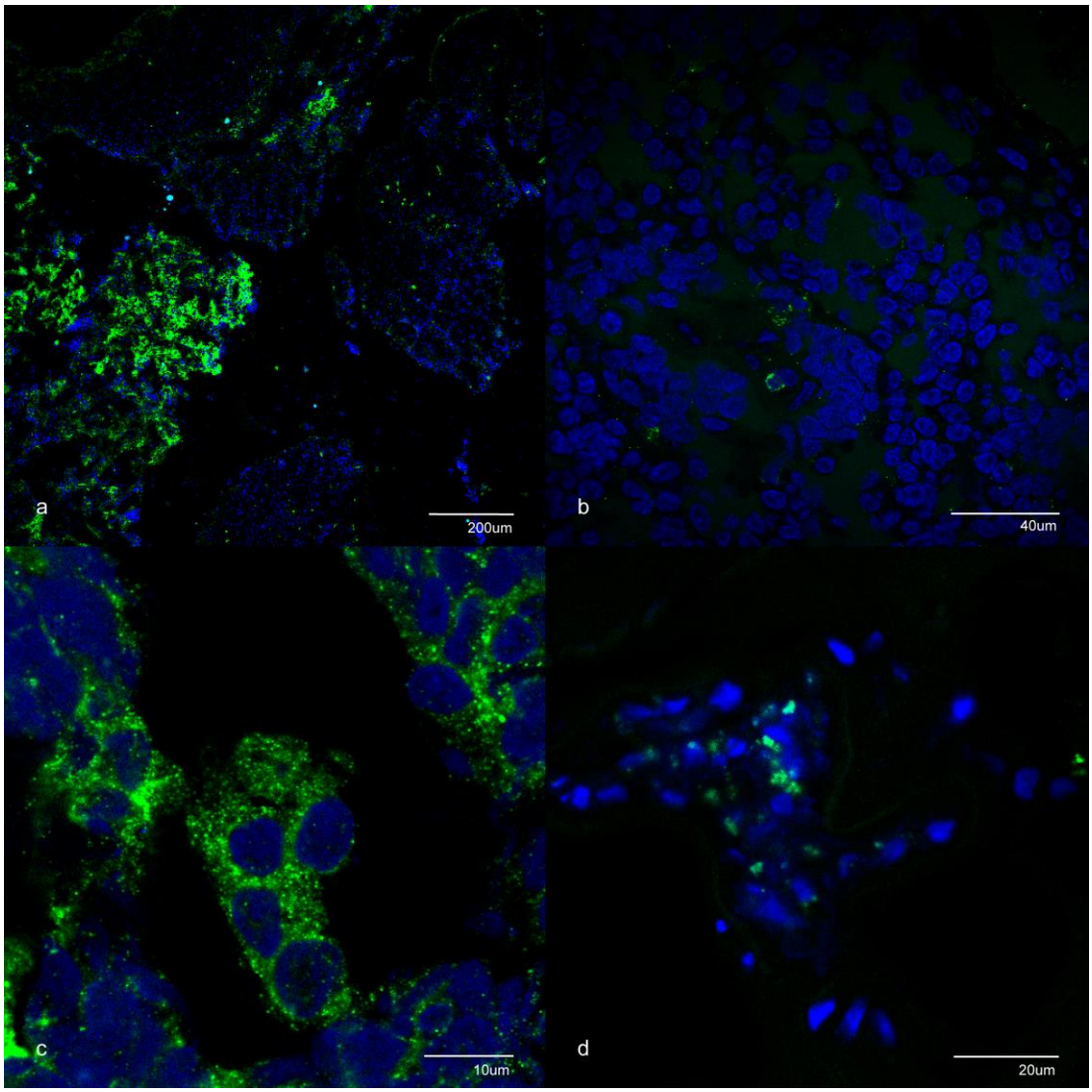

Figure 6-10 Positive control: CD11

Confocal micrographs demonstrating: (a), (b) and (c) tonsil macrophages (x5, x31.5, x100.8 respectively), (d) dermal macrophages (x63).

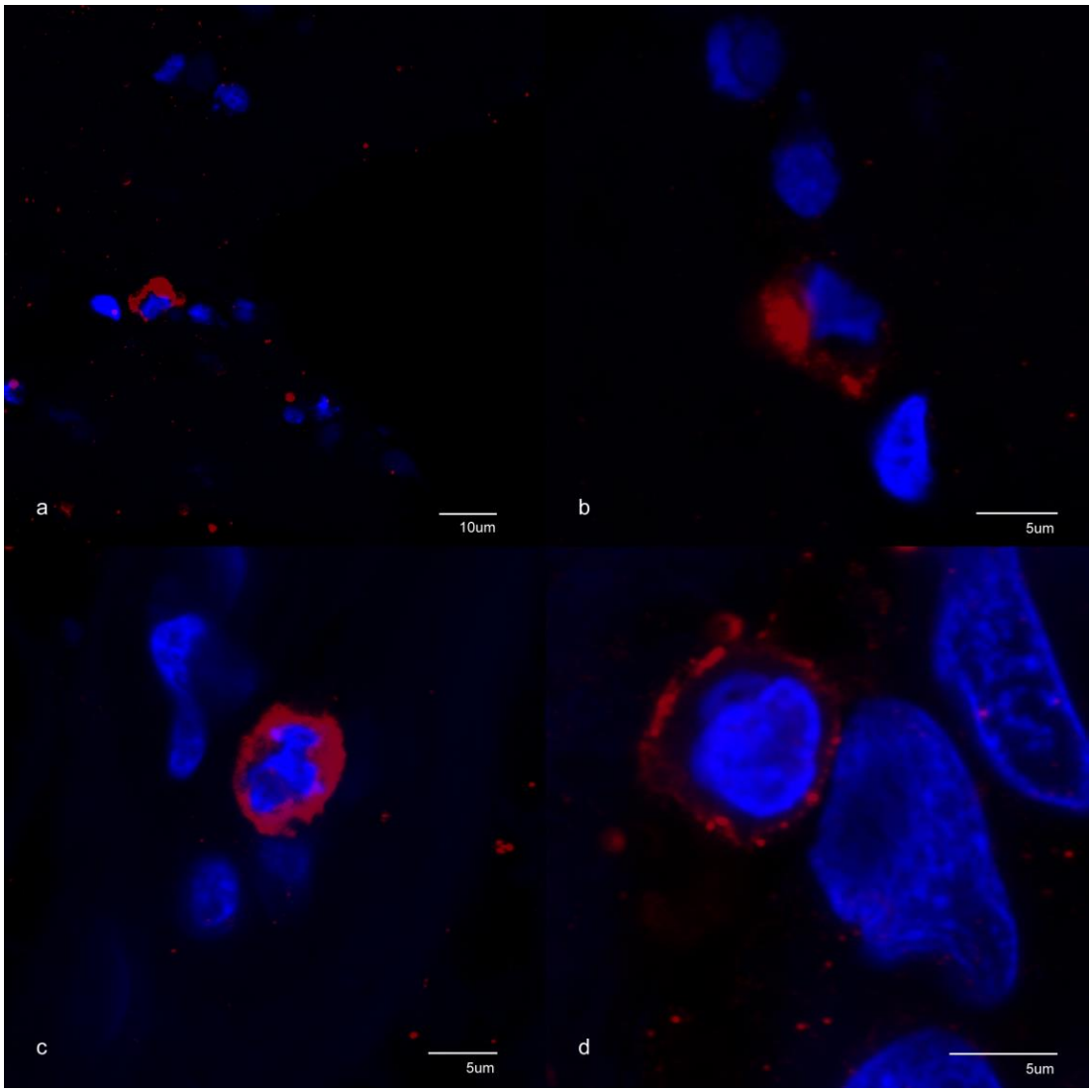

Figure 6-11 Positive control: Iba1

Confocal micrographs demonstrating: (a) and (b) frontal lobe cortex microglia (x63, x189 respectively), (c) and (d) optic nerve microglia (x163.8, x245.7).

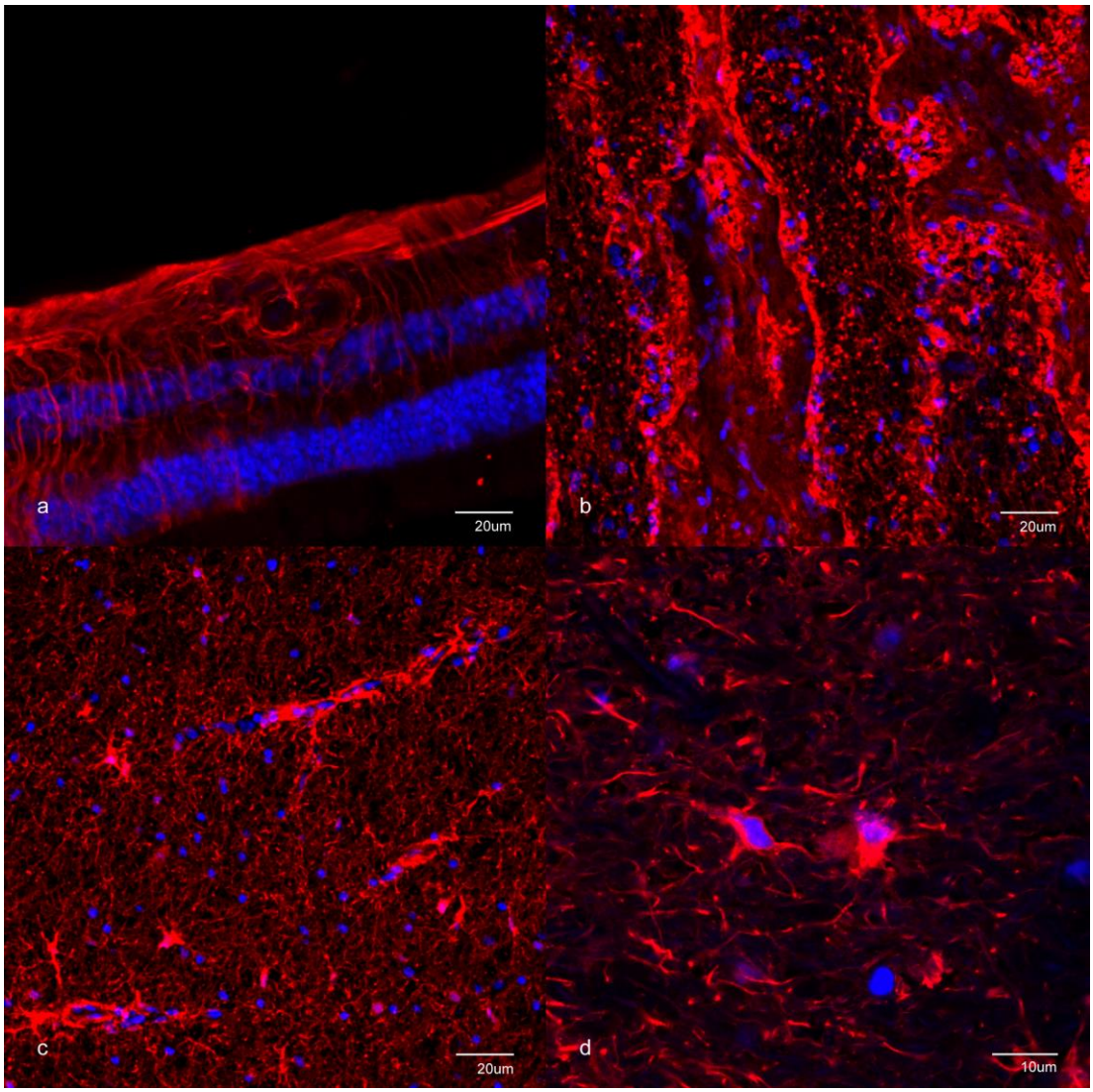

Figure 6-12 Positive control: GFAP (rabbit polyclonal)

Confocal micrographs demonstrating: (a) retina (x20), (b) optic nerve (x20), (c) and (d) frontal lobe cortex (x20, x63 respectively).

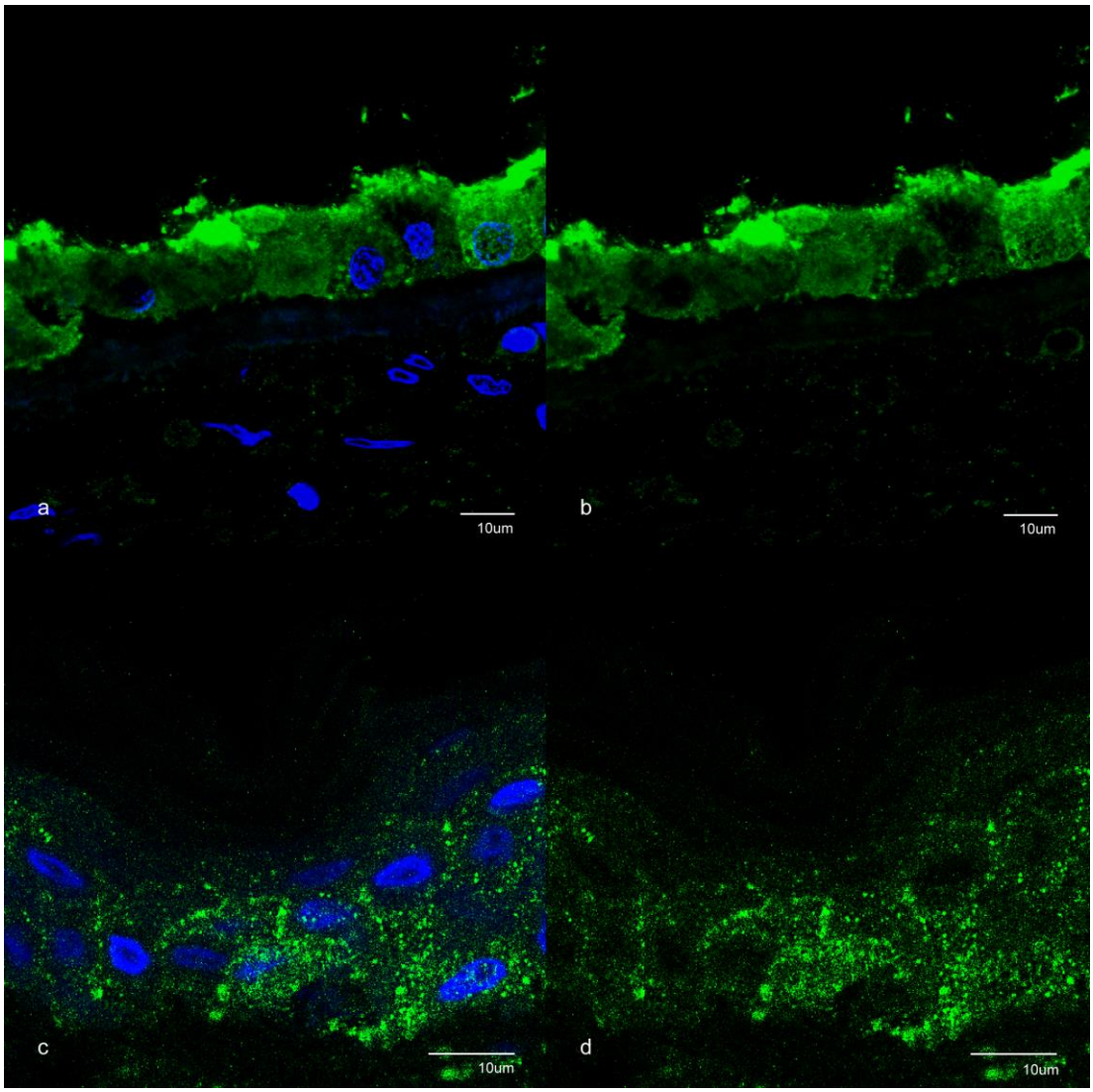

Figure 6-13 Positive control: ezrin

Confocal micrograph demonstrating: (a) and (b) retinal pigment epithelium with and without DAPI nuclear staining respectively (note nuclear void in (b) demonstrating stain specificity) (x63), (c) and (d) epidermis with and without DAPI nuclear staining respectively (note nuclear void in (d) demonstrating stain specificity) (x107.1).

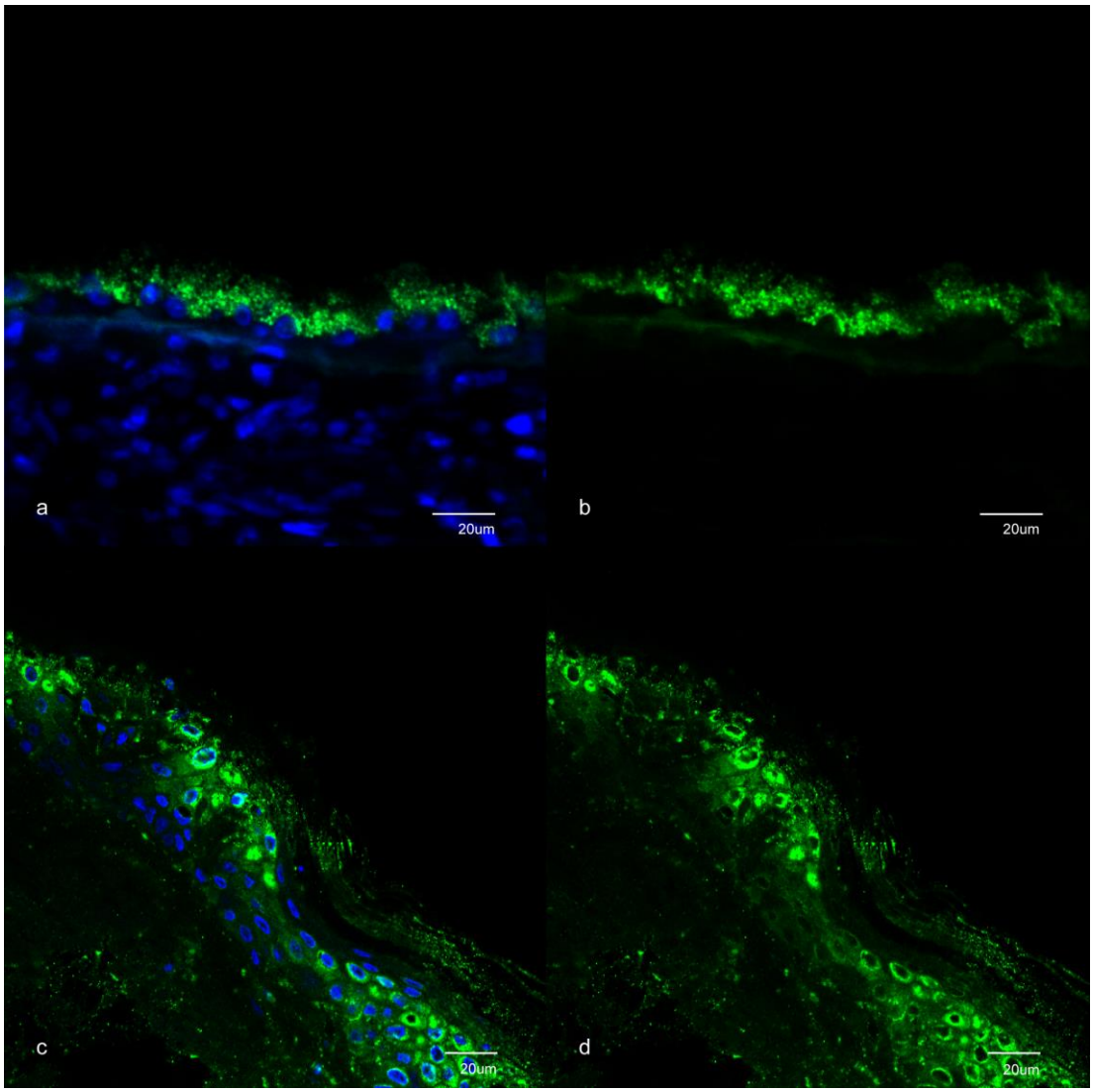

Figure 6-14 Positive control: cytokeratin

Confocal micrograph demonstrating: (a) and (b) retinal pigment epithelium with and without DAPI nuclear staining respectively (note nuclear void in (b) demonstrating stain specificity) (x37), (c) and (d) epidermis with and without DAPI nuclear staining respectively (note nuclear void in (d) demonstrating stain specificity) (x31.5).

6.2 Negative controls

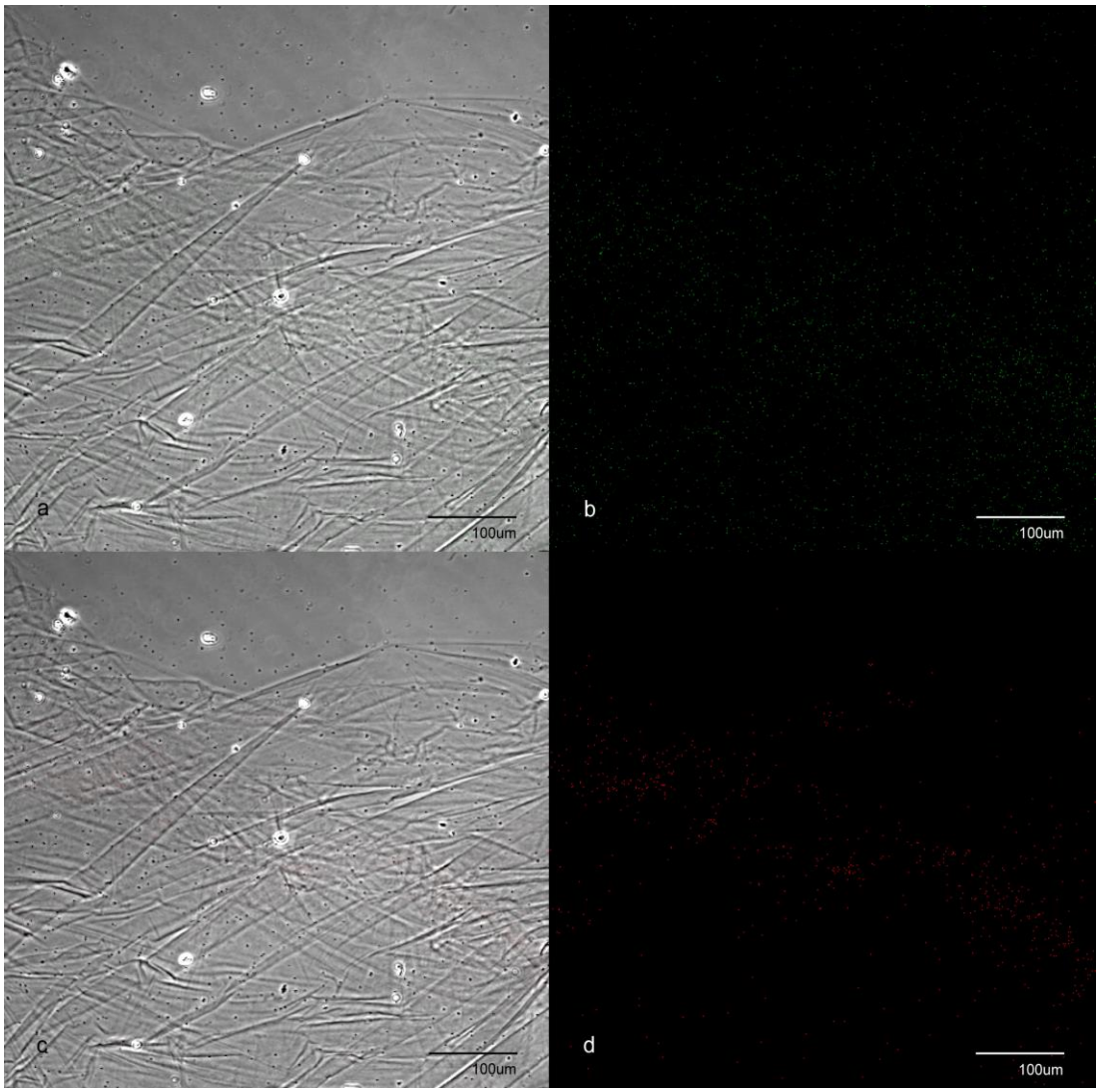

Figure 6-15 Negative control: posterior hyaloid membrane

Posterior hyaloid membrane confocal micrographs demonstrating: (a) and (b) donkey anti-mouse antibody conjugated to Alexa Fluor® 488, with and without phase contrast overlay respectively (x10), (c) and (d) donkey anti-rabbit antibody conjugated to Alexa Fluor® 568, with and without phase contrast overlay respectively (x10).

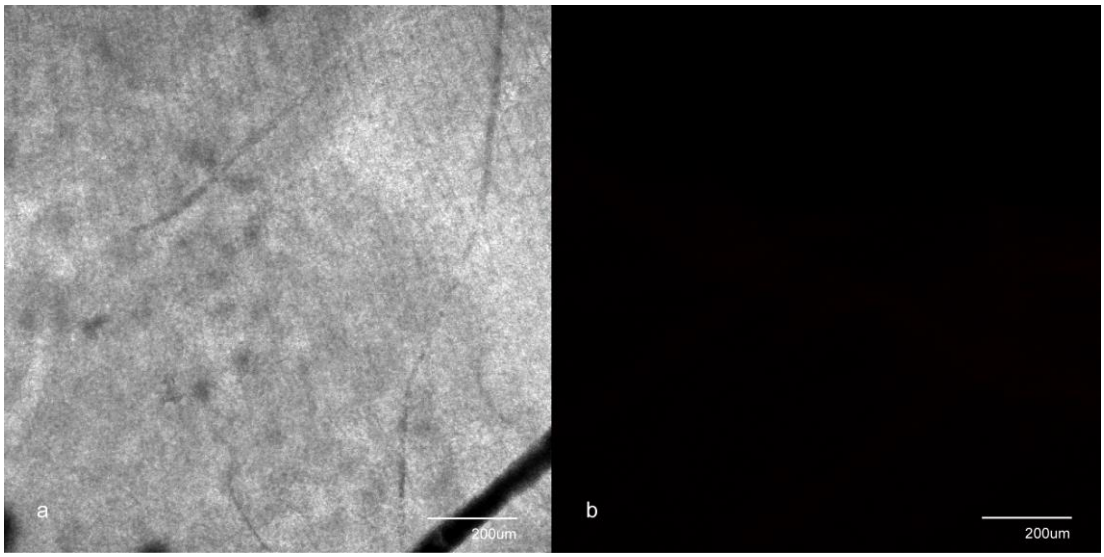

Figure 6-16 Negative control: retinal flat mount

Retinal flat mount confocal micrographs demonstrating: (a) and (b) donkey anti-rabbit antibody conjugated to Alexa Fluor® 568, with and without phase contrast overlay respectively (x5).

Note: retinal microvascular detail lost on phase contrast imaging due to density of multi-layered retina.

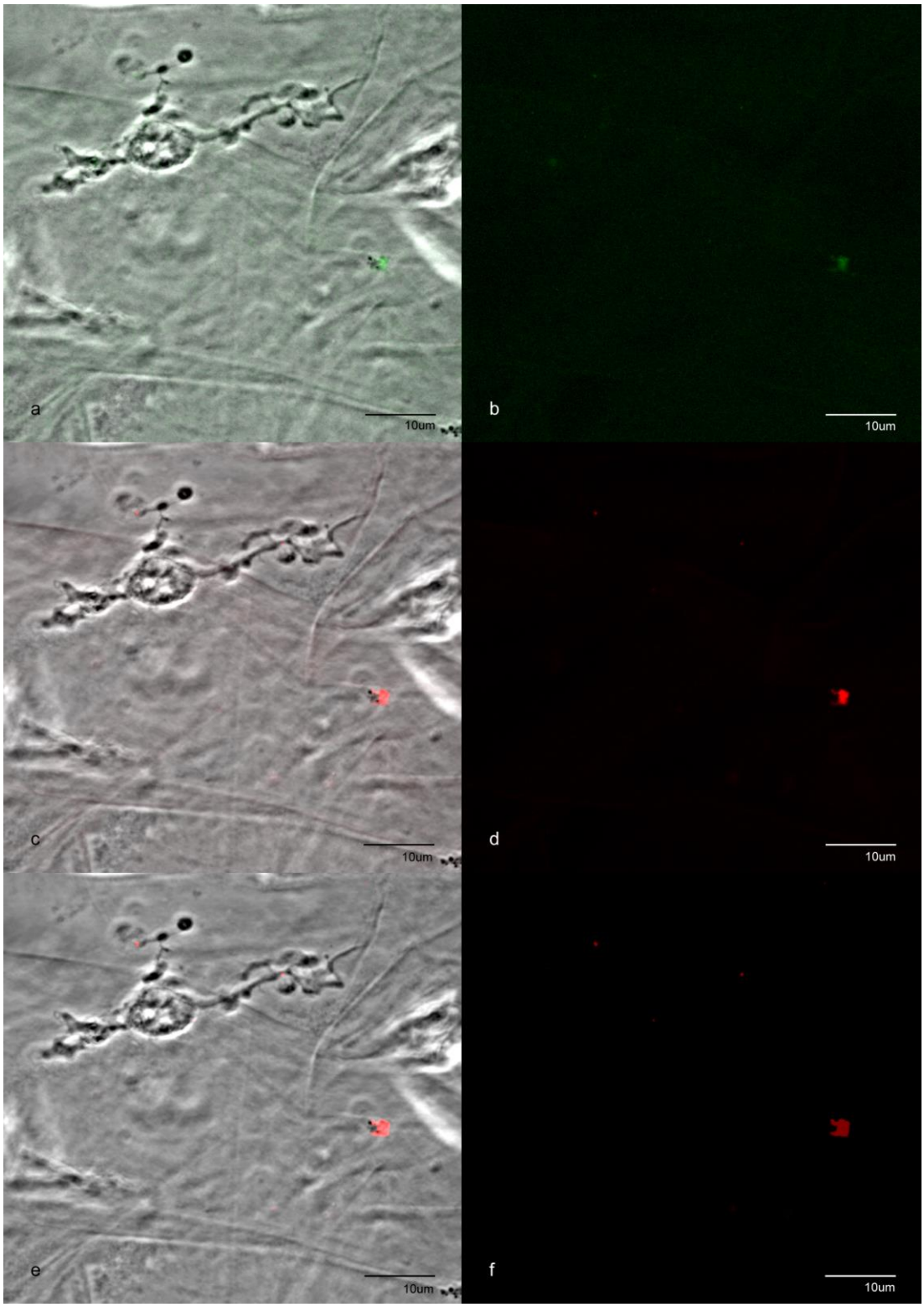

Figure 6-17 Negative control: laminocyte

Please turn over for figure legend

Figure 6-17 Negative control: laminocyte

Laminocyte confocal micrographs demonstrating: (a) and (b) donkey anti-mouse antibody conjugated to Alexa Fluor® 488, with and without phase contrast overlay respectively (x126), (c) and (d) donkey anti-rabbit antibody conjugated to Alexa Fluor® 568, with and without phase contrast overlay respectively (x126), (e) and (f) donkey anti-goat antibody conjugated to Alexa Fluor® 647, with and without phase contrast overlay respectively (x126).

7 Prizes

Prizes awarded for the presentation of:

‘The prevention of retinal detachment in type 1 Stickler syndrome: the Cambridge Prophylactic Cryotherapy protocol.’

- The Oxford Ophthalmological Congress: Ian Fraser Cup winner (July 2013)
- Royal Society of Medicine, Ophthalmology section: Dermot Pierse Prize winner (June 2013)
- The East of England Deanery specialist registrar meeting: John Cairns Memorial Prize (December 2012)

8 Publications

Fincham, G.S., Pasea. L, Carroll, C., McNinch, A.M., Poulson, A.V., Richards, A.J., Scott, J.D., Snead, M.P. (2014) Prevention of Retinal Detachment in Stickler Syndrome: the Cambridge Prophylactic Cryotherapy Protocol. Ophthalmology. 121(8), 1588-97

PMID: 24793526